UNIVERSIDAD AUTONOMA DE MADRID

Facultad de Ciencias

Departamento de Biología Molecular

POLYMERASES SPECIALIZED IN DAMAGE TOLERANCE AND DNA DOUBLE-STRAND BREAK REPAIR

DOCTORAL THESIS

GUILLERMO SASTRE MORENO

Madrid, 2016

Departamento de Biología Molecular
Facultad de Ciencias
Universidad Autónoma de Madrid

Polymerases specialized in damage tolerance and DNA double-strand break repair

Guillermo Sastre Moreno
BSc, Biochemistry

The work presented in this Doctoral Thesis has been carried out at the Centro de Biología Molecular "Severo Ochoa" (CBMSO) under the direction and supervision of Professor Luis Blanco Dávila and Dr. José Francisco Ruiz Pérez.

Madrid, 2016

CSIC
CONSEJO SUPERIOR DE INVESTIGACIONES CIENTÍFICAS

UAM
UNIVERSIDAD AUTONOMA DE MADRID

CENTRO DE BIOLOGÍA MOLECULAR "SEVERO OCHOA"

Professor **Luis Blanco Dávila**, group leader from the Centro de Biología Molecular "Severo Ochoa" (CBMSO), and Dr. **José Francisco Ruiz Pérez** from the University of Seville and the Centro Andaluz de Biología Molecular y Medicina Regenerativa (CABIMER)

CERTIFY:

That the Doctoral Thesis titled "**Polymerases specialized in damage tolerance and DNA double-strand break repair"** developed by Mr Guillermo Sastre Moreno, BSc, MSc was carried out under our direction in the Centro de Biología Molecular "Severo Ochoa" (CBMSO), and that we authorize its presentation to the tribunal. This Doctoral Thesis meets all the requirements to obtain the degree of Doctor of Philosophy (PhD) in Molecular Biology and, with the aforementioned objective, it will be defended at the Universidad Autónoma de Madrid.

We hereby issue this certification in Madrid in April 28th, 2016.

Luis Blanco Dávila, PhD
PhD Thesis Director

José Francisco Ruiz Pérez, PhD
PhD Thesis Co-director

Luis Blanco, PhD
Research Professor of the Spanish Research Council (CSIC)
Centro de Biología Molecular "Severo Ochoa"
c/ Nicolás Cabrera 1
Campus Universidad Autónoma
Cantoblanco
28049 Madrid
Spain

José Francisco Ruiz Pérez, PhD
Investigador Ramón y Cajal
Universidad de Sevilla, Sevilla
Centro Andaluz de Biología Molecular y Medicina Regenerativa (CABIMER)
Avda. Americo Vespucio s/n
41092. Sevilla
Spain

A mi hermana Irene

A mis padres

A Isabel

“El éxito no es definitivo, el fracaso no es fatídico.
Lo que cuenta es el valor para continuar”

Winston Churchill

“Each solution still gives rise to a new question as difficult as the foregoing, and leads us on to farther enquiries”

David Hume, *An Enquiry Concerning Human Understanding*, Section IV, Part II

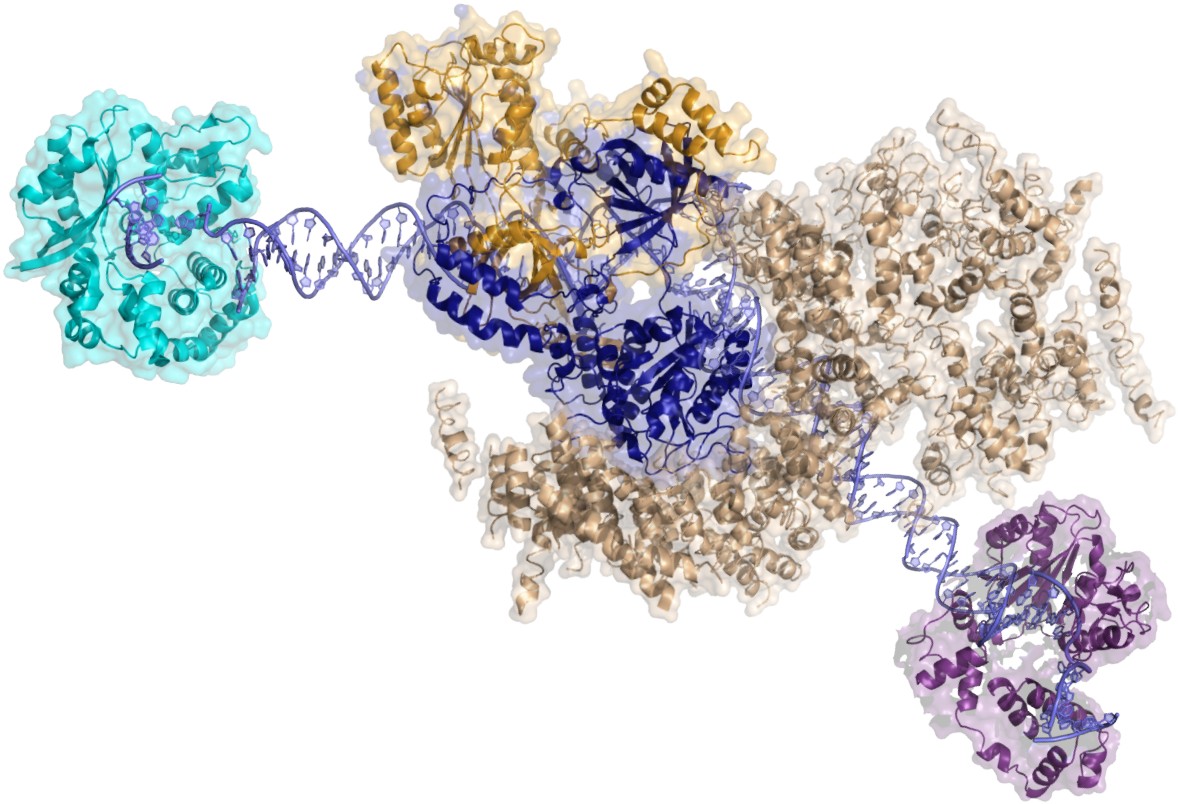

Index

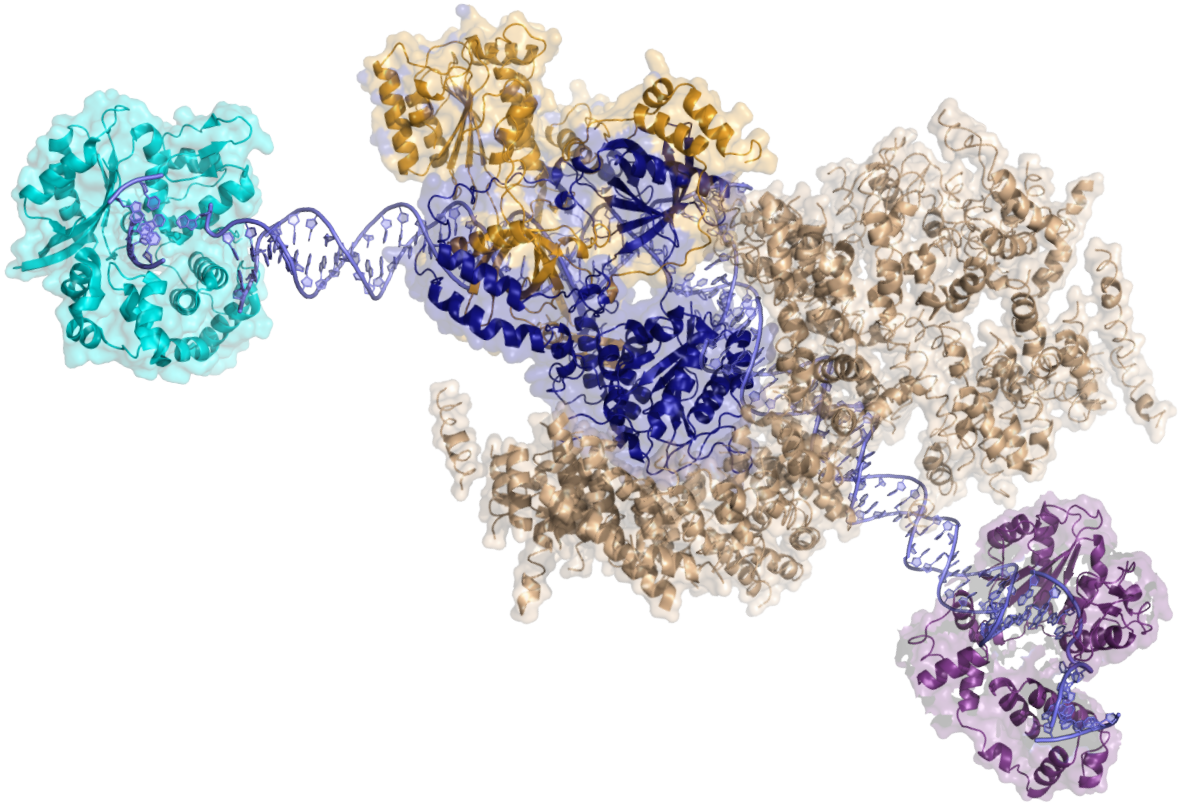

Resumen

A pesar de que todas las DNA polimerasas catalizan la misma reacción química, todas poseen propiedades únicas que les permiten adaptarse a sintetizar DNA de la manera más eficiente en los distintos mecanismos en los que participan. En esta Tesis Doctoral hemos estudiado las DNA polimerasas humanas Polλ y Polμ y su ortólogo en levaduras Pol4, que están especializadas en la reparación de roturas de doble cadena (DSBs), así como PrimPol, una DNA primasa/polimerasa humana especializada en la tolerancia de daños en el DNA. En este trabajo hemos querido comprender mejor la función de estas DNA polimerasas, las bases estructurales de su adaptación a dichas funciones y la regulación de su actividad.

Pol4 es el único miembro de la familia X de DNA polimerasas (PolX) presente en levaduras, recibiendo el nombre de *Sp*Pol4 en *S. pombe*. En este trabajo demostramos que la baja capacidad de discriminación por azúcar de *Sp*Pol4 es relevante durante la tolerancia de la pre-mutagénica lesión oxidativa 8oxodG. *Sp*Pol4 incorpora preferentemente ATP, el ribonucleótido más abundante, frente a 8oxodG, también durante la reparación de DSBs. Aunque esta actividad conlleva la generación de un par de bases con un error de base y azúcar, no es problemática puesto que el ribonucleótido es posteriormente reparado por el mecanismo de reparación por excisión de ribonucleótidos, que mostramos estar asociado a la incorporación de del nucleótido correcto, dCTP, frente a 8oxodG.

Utilizando también como modelo las levaduras, demostramos que *Sc*Pol4, la única PolX de *S. cerevisiae*, es fosforilada por la quinasa Tel1/ATM en respuesta a daño. Esta evidencia nos empujó a evaluar la regulación por fosforilación de su ortólogo humano más cercano, Polλ, y de este modo, demostramos que Polλ es fosforilada por DNA-PK, la quinasa reguladora de la vía de reparación de DSBs por reunión de extremos no homólogos (NHEJ), modulando su actividad al estimular la interacción en respuesta a daño con el factor Ku80. Por otro lado, también hemos caracterizado dos variantes tumorales de la otra PolX humana implicada en NHEJ, Polμ, y demostramos que dichas variantes disminuyen la eficiencia y fidelidad de Polμ al reducir su dependencia de molde durante NHEJ *in vitro*.

Finalmente, hemos profundizado en las propiedades de PrimPol demostrando que posee capacidad de transpolimerización a través de moldes discontinuos, incluso cuando molde e iniciador no poseen complementariedad. También mostramos como los cofactores metálicos Mg^{2+} y Mn^{2+} modulan las propiedades de translesión de PrimPol, proporcionando un buen balance entre fidelidad y eficiencia, pero sugerimos que su centro activo está adaptado a usar con máxima eficiencia el Mn^{2+}.

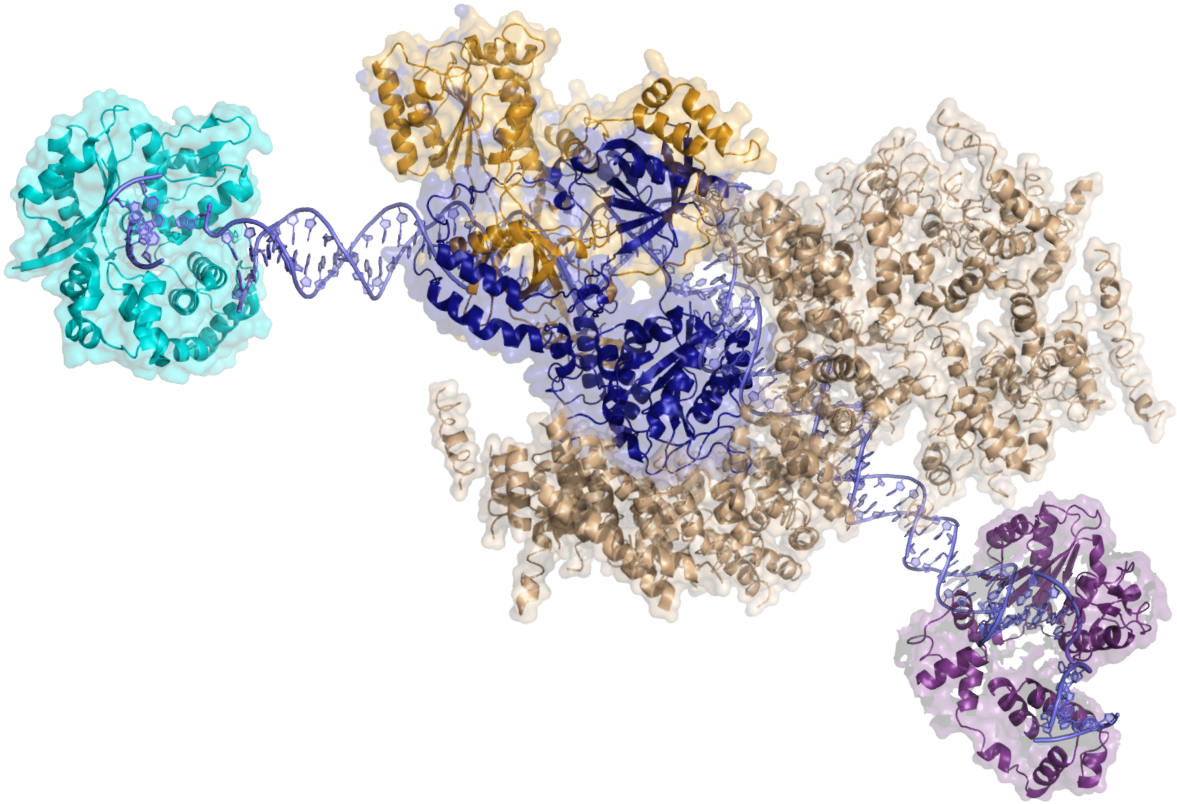

Abstract

In spite of the fact that all DNA polymerases catalyse the same chemical reaction, they all harbour unique properties that suit them to synthesize DNA as efficiently as possible in the different mechanisms in which they are involved. In this Doctoral Thesis we have studied the human DNA polymerases Polλ and Polμ and their ortholog in yeast Pol4, which are specialized in double-strand break (DSB) repair, and also PrimPol, a human DNA primase/polymerase specialized in damage tolerance. In this work we have attempted to further understand the function of these DNA polymerases, the structural bases of their adaptation to those functions and the regulation of their activity.

Pol4 is the only member of the family X of DNA polymerases (PolX) found in yeast, and it is named *Sp*Pol4 in *S. pombe*. In this work we show that the low sugar discrimination property of *Sp*Pol4 is relevant during the tolerance of the pre-mutagenic lesion 8oxodG. *Sp*Pol4 incorporates ATP, the most abundant ribonucleotide, preferably opposite 8oxodG, also during DSB repair. Although this activity leads to the generation of a base pair with both a sugar and base errors, it is not problematic since the ribonucleotide can be later repaired by the ribonucleotide excision repair mechanism, which we show to be coupled to the incorporation of the correct nucleotide, dCTP, opposite 8oxodG.

Using also yeast as model, we demonstrate that *Sc*Pol4, the only PolX in *S. cerevisiae*, is phosphorylated by the Tel1/ATM kinase in response to DNA damage. This evidence prompted us to evaluate the regulation by phosphorylation of its closest human ortholog, Polλ, and hence, we demonstrate, that Polλ is phosphorylated by DNA-PK, the kinase that regulates the non-homologous end joining pathway (NHEJ), modulating its activity by stimulating the interaction with Ku80 in response to DNA damage. On the other hand, we have also characterized two tumour variants of the other human PolX specialized in NHEJ, Polμ, and we demonstrate that both tumour variants decrease the efficiency and fidelity of Polμ by diminishing its template dependence during NHEJ *in vitro*.

Finally, we have gained further insight into the properties of PrimPol by demonstrating that it is endowed with the ability to transpolymerize across discontinuous templates, even when the primer and template have no complementarity. We also show how the metal cofactors Mg^{2+} and Mn^{2+} modulate the previously described translesion properties of PrimPol, providing a good balance between fidelity and efficiency, although we suggest that its active site is adapted to use Mn^{2+} with maximum efficiency.

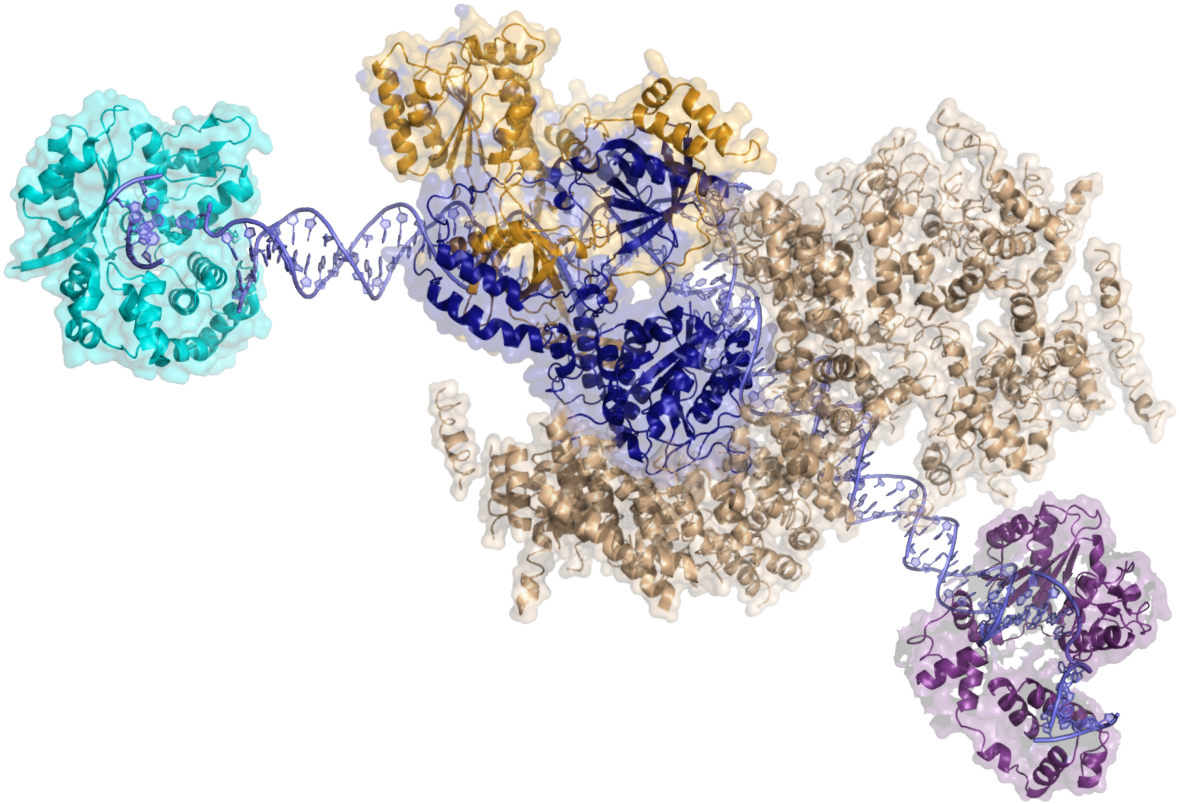

Abbreviations

8oxoG	7,8-dihydro-8-oxoguanine
8oxodG	8-oxodeoxyguanosine
AEP	Archaeo-eukaryotic primase
a-NHEJ	Alternative non-homologous end joining
bp	Base pair
BER	Base excision repair
BRCT	BRCA1 C-terminal
BSA	Bovine Serum Albumin
DMEM	Dulbecco's modified Eagle's medium
dRP	deoxyribose phosphate
DSB	Double-strand break
DTT	Dithiothreitol
EDTA	Ethylenediaminetetraacetic acid
EMM	Edimburgh minimal medium
HEK	Human embryonic kidney
HhH	Helix-hairpin-helix
HR	Homologous recombination
ICL	Interstrand cross-link
KO	Knock-out
MEF	Mouse embryonic fibroblast
MMEJ	Microhomology-mediated end joining
MMR	Mismatch repair
NER	Nucleotide excision repair
NHEJ	Non-homologous end joining
nt	Nucleotide
P	Phosphate
PIKK	Phosphatidylinositol-3 kinase-related kinase
PMSF	Phenylmethylsulfonyl fluoride
PolX	X-family DNA polymerase
RER	Ribonucleotide excision repair
TLS	Translesion synthesis
WCE	Whole cell extract

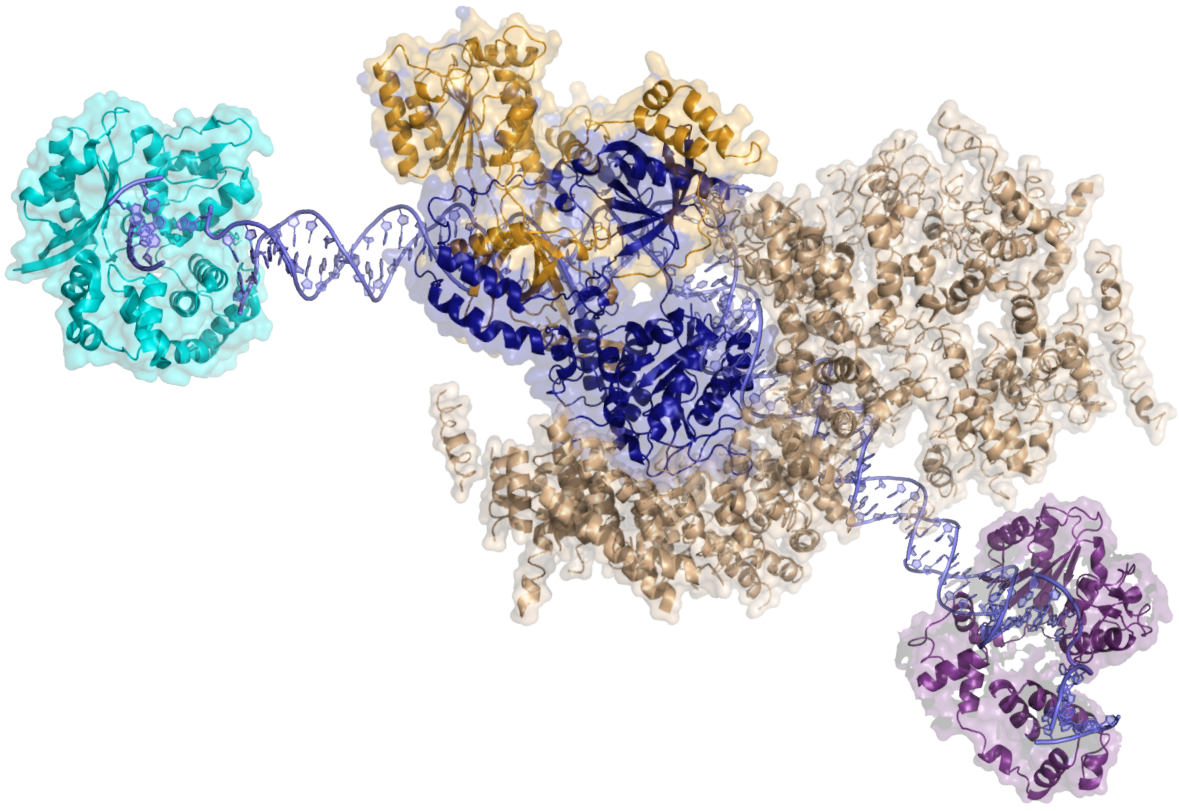

Introduction

1. DNA polymerases

DNA polymerases are the enzymes that catalyse DNA synthesis and therefore, they are essential for the replication and maintenance of the stability of the genetic information, stored in most organisms in the form of DNA. Kornberg and colleagues were the first to identify an enzymatic activity capable of catalysing DNA synthesis, when they first described DNA polymerase I from *Escherichia coli* (Lehman et al., 1958). Since then several DNA polymerases have been identified in most organisms leading to the understanding that all DNA polymerases share common properties and are probably evolutionary related.

In this regard, all DNA polymerases share a common two-metal ion mechanism of catalysis (Steitz, 1999), consequent with the fact that they all catalyse the same reaction: the nucleotidyl-transfer reaction between a dNTP and the 3' hydroxyl (OH) group from the terminus of a DNA molecule referred to as primer. The proposed mechanism of nucleotydil-transfer by Polβ, depicted in Figure 1, was one of the first structural evidence of the two-metal ion mechanism showing that the chemical reaction requires two divalent metal ions (most commonly Mg^{2+}) that are coordinated by 3 carboxylates (Pelletier et al., 1994). Additionally, in order to catalyse synthesis DNA polymerases generally require a pre-existent DNA primer, as they cannot initiate synthesis *de novo*, and also the presence of a template DNA molecule to direct nucleotide incorporation through Watson-Crick base pairing (Johnson, 2010, 2008).

Structural analyses also argue in favour of an evolutionary relationship between all DNA polymerases. Since the first resolution of the structure of a DNA polymerase (Ollis

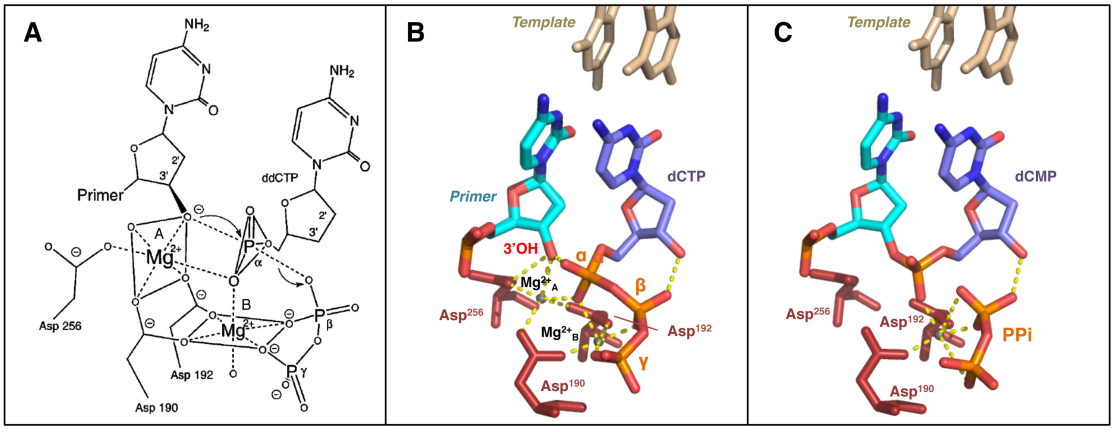

Figure 1. Proposed nucleotidyl-transfer mechanism for Polβ. Three aspartic residues (Asp^{190}, Asp^{192} and Asp^{256}) coordinate two Mg^{2+} ions, named A and B, required for catalysis. Metal A interacts with the 3'OH of the primer DNA lowering its pK_a to facilitate nucleophilic attack on the α–phosphate of the incoming dNTP. Metal A and B together stabilize the structure and charges of the pentacovalent transition state of the reaction. Metal B interacts with the β– and γ–phosphates of the dNTP to facilitate the release of the PPi (A) Schematic representation of the two-metal ion mechanism, adapted from (Sawaya et al., 1997). (B) Snapshot 10s after initiation of Polβ-mediated catalysis of dCTP incorporation, only showing the reactants (PDB ID 4KLE). (C) Product state after 11h of the initiation of the catalysis by Polβ (PDB ID 4KLM).

et al., 1985), 3-dimensional structures of multiple DNA polymerases have been solved (Figure 2), demonstrating that DNA polymerases share a common structural organization, which consists of a polymerase domain that comprises three characteristic subdomains: palm, fingers and thumb. These subdomains are arranged in conformation that resembles a right hand (Steitz, 1999).

Importantly, analysis of the resolved structures of DNA polymerases also reveals significant variability. The length and the shape of the three subdomains are diverse among polymerases of the different families (Figure 2), but also among members of the same family. These differences, even the subtlest, often account for different properties, as they affect processivity, fidelity and substrate specificity. Significant variability is also evident taking into consideration other aspects of DNA polymerases such as size and domain composition. DNA polymerase size is highly variable and ranges in mammals from as small as Polβ (38 kDa) to as large as Polζ (353 kDa)

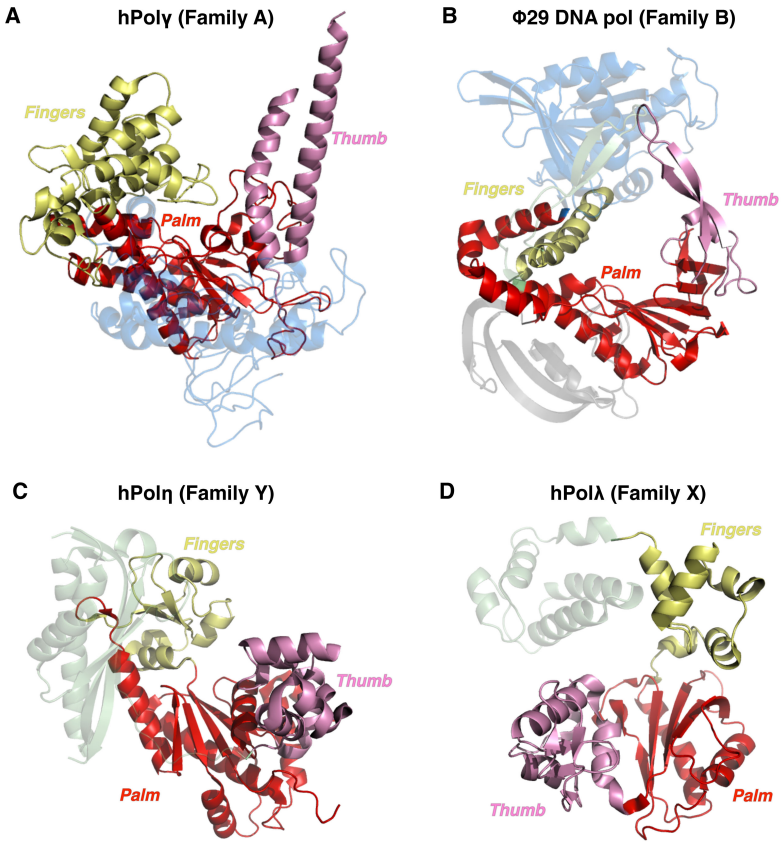

Figure 2. 3D structure of representative DNA polymerases. Structure of DNA polymerases is comprised of 3 subdomains: palm, thumb and fingers. The palm subdomain is essential for catalysis, as it harbours the three catalytic residues that coordinate the two divalent metal ions required for polymerization. The fingers subdomain is relevant for the interaction with the incoming deoxynucleoside triphosphate (dNTP) and with the templating base. The thumb subdomain takes part in positioning of the duplex DNA and in translocation. Palm, fingers and thumb subdomains are coloured in red, yellow and pink respectively. (A) Human Polγ holoenzyme (PDB ID 3IKM), MLS and spacer subdomains are not shown for simplicity. (B) DNA polymerase of bacteriophage ϕ29 (PDB ID 1XHX). (C) Human Polη (PDB ID 3MR2). (D) Human Polλ (PDB ID 1XSN).

(Table 1). Moreover, catalytic subunits of most DNA polymerases can include additional domains that can harbour other enzymatic activities (Table 1). The exonuclease domain of replicative polymerases is a relevant example; it is responsible for the 3'-5' exonuclease activity found in these enzymes, also known as proofreading activity, which excises misincorporated nucleotides thereby increasing fidelity of synthesis. Other domains, although not enzymatically active, are necessary for establishing interactions with the DNA or with other proteins. Protein-protein interactions are essential for the function and regulation of most polymerases, as some polymerases require coupling of multiple protein subunits that may modulate the properties and interactions of the catalytic subunit.

Understanding of all these different properties and also of the fact that most organisms possess several DNA polymerases, has led to the realization that DNA polymerases have become highly specialized through evolution in various vital processes such as DNA replication, damage tolerance and DNA repair (reviewed in Bebenek and Kunkel, 2004; Garcia-Diaz and Bebenek, 2007).

2. The need for specialized DNA polymerases

Analyses of the biological roles of polymerases and of their primary sequence led to a classification of polymerases in at least 6 families: A, B, C, D, X and Y (Burgers et al., 2001). Table 1 shows the DNA polymerases found in higher eukaryotes and their homologs in yeast, which belong to only 4 of the 6 canonical families: A, B, X and Y. All these DNA polymerases are highly specialized to take part in different pathways of DNA replication, DNA repair or damage tolerance (Figure 3) (Bebenek and Kunkel, 2004; Garcia-Diaz and Bebenek, 2007), and are classified accordingly. In addition to these polymerases, some eukaryotic organisms may possess other specialized polymerases that do not belong to the 6 canonical families, including a retro-transcriptase, named telomerase, which is specialized in telomere maintenance (Autexier and Lue, 2006), and a Primase-Polymerase named PrimPol that belongs to the archaeo-eukaryotic primase (AEP) super-family (Iyer et al., 2005) and that is specialized in damage tolerance and reinitiation of stalled forks (García-Gómez et al., 2013; Mourón et al., 2013).

As mentioned earlier, the specialization of these DNA polymerases is a consequence of their primary sequence and structural differences that translate in different properties and substrate specificity. Moreover, high specialization is the reason why most organisms have several polymerases (especially higher eukaryotes

Family	HUGO name	Greek name	Human catalytic subunit gene	Proposed function	Catalytic subunit size and domain structure	*S. cerevisae* gene	*S. pombe* gene
A	POLG	Polγ (gamma)	*POLG*	Replication/Repair of mtDNA	Polγ (140 kDa)	*MIP1*	*pog1*
	POLQ	Polθ (theta)	*POLQ*	MMEJ	Polθ (290 kDa)	-	-
	POLN	Polν (nu)	*POLN*	ICL repair	Polν (100 kDa)	-	-
B	POLA	Polα (alpha)	*POLA1*	DNA replication/HR	Polα (166 kDa)	*POL1*	*pol1*
	POLD1	Polδ (delta)	*POLD1*	DNA replication/ MMR/HR/NER	Polδ (124 kDa)	*POL3*	*cdc6*
	POLE	Polε (epsilon)	*POLE*	DNA replication/ MMR/HR/NER	Polε (262 kDa)	*POL2*	*cdc20*
	POLZ	Polζ (zeta)	*REV3L*	TLS	Polζ (353 kDa)	*REV3*	*rev3*
X	POLB	Polβ (beta)	*POLB*	BER/Meiosis	Polβ (38 kDa)	-	-
	POLL	Polλ (lambda)	*POLL*	NHEJ//BER/ Meiosis/V(D)J	Polλ (63 kDa)	*POL4*	-
	POLM	Polμ (mu)	*POLM*	NHEJ/V(D)J	Polμ (55 kDa)	-	*pol4*
	TDT	-	*DNTT*	V(D)J	TdT (58 kDa)	-	-
Y	POLH	Polη (eta)	*POLH*	TLS	Polη (78 kDa)	*RAD30*	*eso1*
	POLI	Polι (iota)	*POLI*	TLS	Polι (83 kDa)	-	-
	POLK	Polκ (kappa)	*POLK*	TLS	Polκ (99 kDa)	-	*kpa1*
	REV1	-	*REV1*	TLS	Rev1 (138 kDa)	*REV1*	*rev1*
RT	TERT	-	*TERT*	Elongation of telomeric DNA	Telomerase Reverse Transcriptase (127 kDa)	*EST2*	*trt1*
AEP	PRIMPOL	-	*CCDC111*	Repriming of stalled forks, TLS	PrimPol (64 kDa)	-	-

List of Domains: Exonuclease, Polymerase, Helicase, 8 kDa, BRCT, S/P rich, Reverse transcriptase, RNA binding, AEP

Table 1. Eukaryotic DNA polymerases. BER: base excision repair; ICL: interstrand cross-link; HR: homologous recombination; MMEJ: microhomology-mediated end joining; MMR: mismatch repair; NER: nucleotide excision repair; NHEJ: non-homologous end joining; TLS: translesion synthesis

that have at least 17) but nevertheless, this also poses the intriguing question of why organisms require DNA polymerases to be so highly specialized.

Specialization of DNA polymerases provides the maximal efficiency during DNA synthesis to the mechanisms in which they are involved. DNA replication is a relevant example, as it is arguably the best characterized function of DNA polymerases (Bell and Dutta, 2002; Masai et al., 2010). In eukaryotic cells, nuclear DNA replication requires the faithful synthesis of a large amount of DNA and consequently DNA polymerases specialized in nuclear replication, such as B-family Polδ and Polε (Byrnes et al., 1976; Wintersberger and Wintersberger, 1970), are highly processive rendering them well suited to synthesize long tracks of DNA, and are also very accurate due to the high nucleotide selectivity of their active sites and to their inherent 3'-5' exonuclease activity that can remove misincorporated nucleotides (Bebenek and Kunkel, 2004). These properties, in particular their processivity that is enhanced by interaction with the sliding clamp PCNA (Moldovan et al., 2007), are highly convenient to nuclear DNA replication as they allow Polδ and Polε to synthesize DNA very rapidly and accurately. Moreover, these polymerases are further specialized to have complementary roles during replication: Polδ synthesizes the lagging-strand and Polε

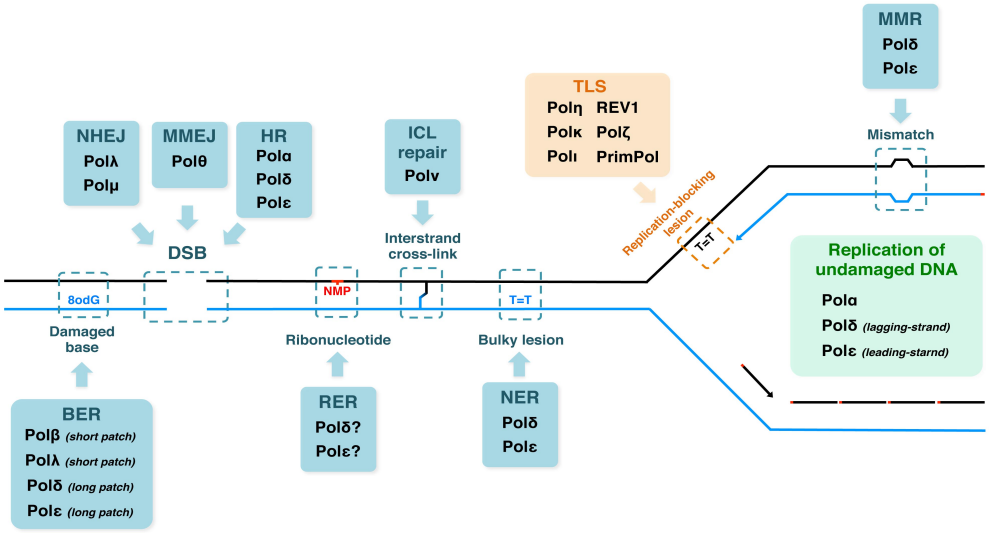

Figure 3. Functions of mammalian DNA polymerases. BER: base excision, ICL: interstrand cross-link; HR: homologous recombination; MMEJ: microhomology-mediated end joining; MMR: mismatch repair; NER: nucleotide excision repair; NHEJ: non-homologous end joining; RER: ribonucleotide excision repair; TLS: translesion synthesis.

the leading-strand (Miyabe et al., 2011; Nick McElhinny et al., 2008). Interestingly, eukaryotic mitochondrial DNA replication is a similar scenario whereby, although the exact mode of replication is still under intense debate (Clayton, 1991; Falkenberg et al., 2007; Holt, 2009), replication is performed by Family A Polγ (Foury, 1989; Ropp and Copeland, 1996), another processive and faithful polymerase endowed with 3'-5' proofreading exonuclease activity.

Most eukaryotic DNA repair mechanisms require DNA synthesis steps that are also performed by DNA polymerases. However, it is quite remarkable to note that only some of them require specialized DNA polymerases fully devoted to that pathway. In fact most of them take advantage of replicative polymerases, including those that repair mismatches (mismatch repair (MMR), (Jiricny, 2006; Peña-Diaz and Jiricny, 2012)), bulky DNA destabilizing lesions (Nucleotide excision repair (NER), (Marteijn et al., 2014)) and misincorporated ribonucleotides (ribonucleotide excision repair (RER), (Sparks et al., 2012)). Simplistically, all these pathways are initiated by recognition of the lesion that drives either incision or excision of the damaged DNA. Subsequently they all require the synthesis of a large track of DNA and even in some cases displacement of the parental strand. Polδ and Polε are well suited to perform these tasks, and hence, they are involved in these mechanisms by synthesizing the excised DNA prior to ligation (Bebenek and Kunkel, 2004).

Other DNA repair pathways also require DNA synthesis, although less extensive. Double-strand break (DSB) repair is a hazardous scenario in which the substrates to

be repaired require connection and template annealing, as both DNA strands are broken. The high processivity and fidelity of replicative polymerases comes with the cost of not being able to handle these kinds of substrates, and only a DNA polymerases highly specialized in using these unconventional substrates can be active. Replication of damaged DNA is another specialization-demanding scenario, as replicative polymerases have narrow and highly selective active sites that cannot accommodate damaged DNA. Consequently they are mostly inactive when facing lesions in the DNA template that can therefore compromise DNA replication.

Highly specialized DNA polymerases capable of using discontinuous or damaged templates were likely needed early in evolution to overcome the problems of DNA synthesis during DSB repair and across damaged bases, which are arguably the most difficult contexts.

3. DNA polymerases specialized in DSB repair

DSBs are lesions generated when the two strands of the DNA helix are broken in close proximity. DSBs are arguably the most harmful lesion as they can lead to genomic rearrangements and even to cell death if they are not properly repaired. Due to these harmful potential consequences, defects in DSB repair correlate with human diseases such as neurological disorders and cancer (Khanna and Jackson, 2001; McKinnon, 2009). Exogenous agents such as ionizing radiation (IR) can drive DSB formation, yet DSB can also arise from endogenous sources including collapsed DNA replication forks (Mehta and Haber, 2014). DSB are also generated physiologically at programmed contexts (via specific nucleases) with the purpose of generating genomic variability at immune receptor genes or during meiosis (Mehta and Haber, 2014).

Mammalian cells possess two major pathways for DSB repair: homologous recombination (HR) and non-homologous end joining (NHEJ) (Chapman et al., 2012). Recently, the existence of another mechanism involved in DSB repair, dubbed microhomology-mediated end joining (MMEJ), has become well established (Deriano and Roth, 2013). DSB repair pathway choice has been intensively studied and is partly mediated by the cell cycle context, which modulates end resection at the break, a divergent early step of DSB repair (Ceccaldi et al., 2016). Homologous recombination (HR) is highly conserved through evolution, and in mammalian cells it is the dominant DSB repair mechanism during the mid-S cell cycle stage (Karanam et al., 2012). Different subpathways of HR have been described (Krejci et al., 2012; Sung and Klein, 2006), and given that most of them rely on using the sister chromatid as a back-up

template for DNA synthesis, HR is considered as an error-free pathway. This characteristic is really relevant as it circumvents the problem of template discontinuity inherent to a DSB. However, this characteristic also restricts HR to operate only during the S and G2 cell cycle phases (Chapman et al., 2012), and requires large resection of the DSB ends to allow strand invasion, which in turn implies the synthesis of large tracks of DNA. The need for a lengthy DNA synthesis on a continuous DNA template, implies that HR does not require DNA polymerases devoted to the pathway and that it can take advantage of the major replicative polymerases Polδ or Polε for DNA synthesis (Bebenek and Kunkel, 2004; Holmes and Haber, 1999).

Microhomology-mediated end joining (MMEJ), also referred to as alternative NHEJ (a-NHEJ), was discovered as a mechanism capable of repairing DSBs in cells deficient for critical factors of "classical" NHEJ (Boulton and Jackson, 1996; Liang and Jasin, 1996). MMEJ was initially considered simply as a back up mechanism, but it was soon realized that it is a relevant physiological pathway that operates also in NHEJ-proficient cells (Deriano and Roth, 2013). Although MMEJ is known to operate independently of the NHEJ core factors, its precise mechanism is not well understood. Experimental data suggest that MMEJ is initiated by resection of the 5' ends of the DSB that proceeds until regions with microhomology (5-25 nt) are exposed. Subsequently, the 3' ssDNA ends are annealed at the microhomologies and the ends are processed to remove the non-complementary DNA flaps and to fill the gaps generated upon hybridization (McVey and Lee, 2008). The exact role and the possible specialization of DNA polymerases in MMEJ are not fully understood and is a hot topic in the field. In yeast, apparently, there are no polymerases fully specialized in MMEJ as several polymerases have been associated with the pathway (Decottignies, 2007; Lee and Lee, 2007). Conversely, recent data suggest that in human cells there is a polymerase specialized in MMEJ, Polθ, which is not conserved in yeast. Polθ specialization in MMEJ relies on its ability to bridge dsDNA molecules with long 3' protruding ends (which mimic MMEJ intermediates) and accordingly, Polθ has been clearly linked to MMEJ in mammalian cells (Hogg et al., 2012; Kent et al., 2015; Mateos-Gomez et al., 2015). Polθ exact mechanism of action in MMEJ is not yet clear, although structural analyses indicate that it dimerizes to promote MMEJ of DSBs (Zahn et al., 2015) similarly to bacterial NHEJ polymerases (Brissett et al., 2007).

In contrast to other DSB repair pathways, NHEJ operates by directly rejoining broken DNA ends that harbour little or no microhomology (0-5 nt) (Figure 4) (Lieber, 2010, 2008; Waters et al., 2014). This characteristic allows NHEJ to be active

throughout the cell-cycle (Chapman et al., 2012), rendering NHEJ the major DSB repair pathway in mammalian cells. The ends of a physiological DSB are generally imperfect, thus, it is likely that they cannot be ligated after their synapsis and require processing, which usually includes DNA synthesis to fill the gaps generated upon annealing (Figure 4). DNA synthesis coupled to NHEJ implies that short tracks of DNA need to be synthesized under extreme circumstances in which the template is discontinuous and, if the ends are not complementary, where the primer may not even be hybridized to the template. This necessarily requires a highly specialized DNA polymerase capable of bridging broken ends with short protrusions (even if they are non-complementary) and of filling the DNA gaps generated after microsynapsis. DNA synthesis coupled to NHEJ is clearly beneficial given that it avoids extensive resection of the DNA, in clear contrast to MMEJ. However due to the low sequence redundancy that NHEJ exploits, it comes with the cost of high error-proneness as it frequently leads to deletions. DSB are commonly associated with other kinds of damage, including oxidized bases, which are often found at the broken ends

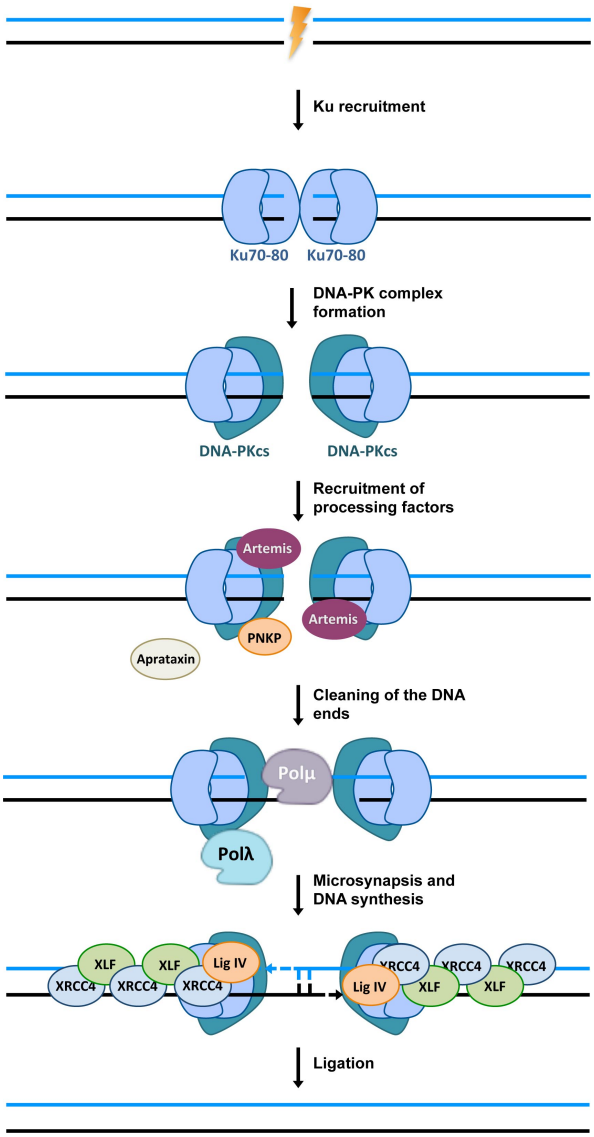

Figure 4. NHEJ in mammalian cells. Ku70/80 binding to the broken ends initiates NHEJ in mammals. This recruits the DNA-PKcs that forms a complex with Ku70/80 named DNA-PK. The formation of the DNA-PK complex also promotes the synapsis of the ends. The DNA-PK complex is essential for regulation of the NHEJ pathway through phosphorylation by its kinase subunit. After synapsis, the imperfectly aligned ends may be directly ligated due to the fact that the NHEJ machinery can efficiently tolerate mismatches at the ligation step. However, it is much more likely that after synapsis the ends cannot be ligated and require processing prior to ligation. End processing involves several enzymes such as Artemis, aprataxin, APLF and the polynucleotide kinase/phosphate (PNKP), that are recruited by the DNA-PK complex and whose participation depends on the nature of the ends. Processing also involves a PolX, either Polλ or Polμ, which promote microsynapsis of the ends and fill the gaps formed after alignment. Finally, the XLF/XRCC4/ligIV complex seals the nicks.

and that can interfere with the repair process (Schipler and Iliakis, 2013). Moreover, direct annealing of the ends during NHEJ can also result in mismatches in addition to gaps (Waters et al., 2014). For this reason, NHEJ requires DNA polymerases with the ability not only to fill the gaps but also to tolerate lesions and imperfectly aligned ends to overcome these problems.

In eukaryotes, the members of the X family are the polymerases specialized in NHEJ as they harbour all these extraordinary abilities.

3.1 DNA polymerases specialized in NHEJ: The X family

DNA polymerases from the X family (PolXs) are small monomeric polymerases specialized in filling small DNA gaps either during NHEJ or base excision repair (BER). PolX adaptation to filling small gaps implies that these enzymes polymerize DNA not in a processive but in a distributive fashion, in clear contrast to replicative polymerases. PolXs adaptation to NHEJ arises from having flexible actives site capable of stabilizing discontinuous templates. This characteristic, together with their lack of exonuclease proofreading activity (Moon et al., 2007a), renders these enzymes significantly less faithful during DNA synthesis than replicative polymerases. PolX promiscuity is a relevant property as PolXs play an important role in the generation of variability at immune system receptors during V(D)J recombination, a specialized form of NHEJ. Several PolXs are also characterized by displaying low sugar discrimination, as they can incorporate both dNTPs and NTPs to the DNA. This is also a distinctive characteristic of PolXs in comparison with replicases, and it is also shared with some bacterial polymerases specialized in NHEJ that do not belong to the X family (Pitcher et al., 2007).

PolXs are highly conserved through evolution from bacteria to higher eukaryotes (Uchiyama et al., 2009). Higher eukaryotes possess the widest diversity having several and highly specialized members, whereas lowers organisms posses fewer less specialized PolXs probably more closely related to the ancestors of the family. In this regard, mammalian cells are endowed with four PolXs members: Polβ, Polλ, Polμ and the terminal deoxynucleotidyl transferase (TdT), whereas budding and fission yeast have only one PolX named Pol4 (Figure 5).

PolXs have a common structural organization consisting of a Polβ-core that comprises a catalytic C-terminal polymerase domain and an 8 kDa domain (Figure 5) (Ramsden and Asagoshi, 2012; Ramsden, 2011). The polymerase domain in turn comprises the three typical subdomains found among DNA polymerases: the fingers,

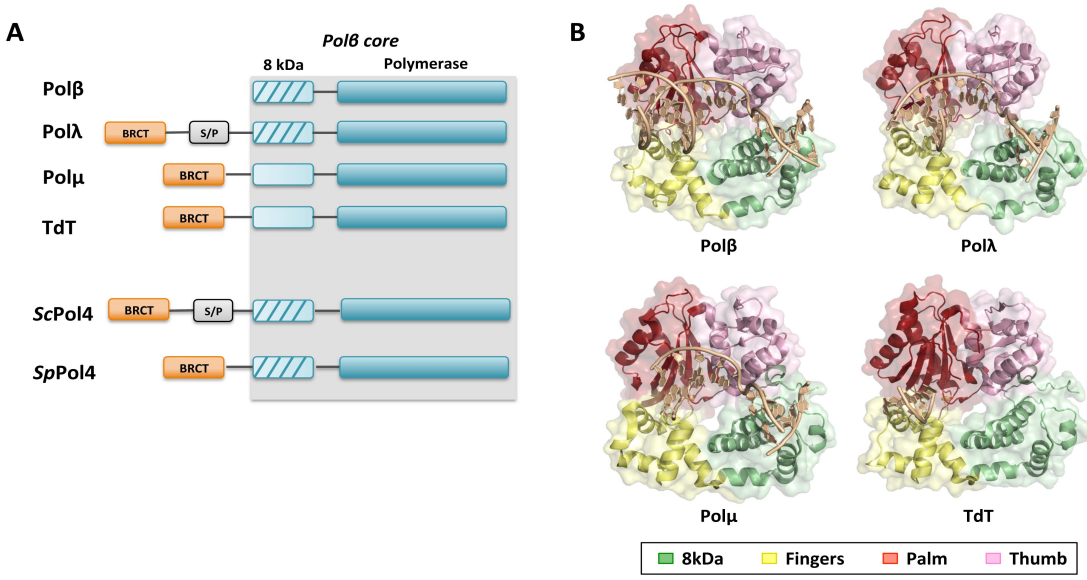

Figure 5. PolX structural organization. (A) Schematic representation of the domains found and structure of human and yeast PolXs. (B) Crystal structures of the Polβ-core of human Polβ (PDB ID 1BPY), Polλ (PDB ID 1XSN) and Polμ (PDB ID 4M04) and murine TdT (PDB ID 1KEJ).

the palm and the thumb (Figure 5). The 8 kDa is a pivotal domain for PolXs being key for their specialization in filling small gaps as it provides PolXs with the ability to interact with the downstream molecule of a DNA gap. The 8 kDa domain is endowed with one or more helix-hairpin-helix motifs (HhH) that interact with the DNA in a nonspecific manner, and also with a positively charged pocket that can specifically bind the 5'-phosphate group of the downstream DNA molecule (Moon et al., 2007a). These interactions are more prominent in Polβ and Polλ than in Polμ, and are almost inexistent in TdT (Ramsden and Asagoshi, 2012). Importantly, in several members of the PolX family including Polβ, Polλ and Pol4, the 8 kDa domain harbours 5'-deoxyribose phosphate (5'dRP) lyase activity (Bebenek et al., 2005; García-Díaz et al., 2001; González-Barrera et al., 2005; Matsumoto and Kim, 1995).

Unlike Polβ, most PolXs have an N-terminal domain termed BRCT (BRCA 1 C-terminal) in addition to the polymerase and 8 kDa domains (Figure 5). The BRCT domain is commonly found in proteins involved in DNA repair, and in the case of PolXs, it was demonstrated to be an essential adaptation to NHEJ as it is strictly required for the physical interaction with the NHEJ factors Ku70/80 and XRCC4/Ligase IV (Davis et al., 2008; Fan and Wu, 2004; Lee et al., 2004; Ma et al., 2004; Mahajan et al., 2002; Mueller et al., 2008; Nick McElhinny et al., 2005; Tseng and Tomkinson, 2002). In fact, the presence of a BRCT is sufficient to categorize a PolX as specialized in NHEJ. The BRCT domain from all the mammalian PolXs has been resolved, yet only independently of the other domains revealing in the case of Polλ and Polμ that they

have somewhat different interaction surfaces (Davis et al., 2008; Mueller et al., 2008). It is also worth noting that some PolX members, only Polλ in mammals, have a serine/proline-rich domain (S/P) that links the BRCT domain with the rest of the protein. This domain is likely quite disordered as to date its structure has never been solved. Its function also remains unknown, but it probably contributes to the post-translational regulation of these polymerases.

3.1.1 Eukaryotic PolXs specialized in NHEJ

Polλ

Polλ and Polμ were demonstrated to be the mammalian polymerases specialized in NHEJ, which posed the intriguing question of why do mammals require two polymerases for the same task. Exhaustive research led to the realization that Polλ and Polμ are tailored to repair ends of different complementarity. Polλ is specialized in repairing DSBs breaks in which the broken ends have at least 1 complementary bp, whereas Polμ is adapted to non-complementary ends (Nick McElhinny et al., 2005; Pryor et al., 2015). Moreover, Polλ is uniquely effective in filling gaps longer than one 1nt (Garcia-Diaz et al., 2009; Pryor et al., 2015), a particularly difficult task for most PolXs given that they interact simultaneously with the primer-terminus and the 5'-P of the downstream molecule limiting the DNA gap, and for this reason they can be particularly inefficient if they are distant (as is in the case of gaps longer than 1 nt). Polλ ability to "scrunch" the template molecule overcomes this problem by keeping extrahelical the "yet to be-copied" template bases (Garcia-Diaz et al., 2009). Extrahelical bases are stabilized in a pocket formed by three residues: Leu^{277}, His^{511} and Arg^{514} (Figure 6A).

Blanco and colleagues first identified Polλ and demonstrated its high expression in mouse testis, suggesting a role in DNA repair associated to meiosis (García-Díaz et al., 2000). Polλ possess different biochemical properties from Polμ, including proficient sugar discrimination and dRP lyase activity (García-Díaz et al., 2001). Polλ has high propensity to induce frameshift errors (Bebenek et al., 2003), partly due to its aforementioned striking ability to stabilize extrahelical bases (Garcia-Diaz et al., 2006). Although NHEJ is Polλ major role *in vivo*, Polλ can also back up Polβ in BER (Braithwaite et al., 2010, 2005; Tano et al., 2007). Polλ is also pivotal in the tolerance of the damaged base 8-oxoguanine (8oxoG). 8oxoG, commonly found in the DNA as 8-oxodeoxyguanosine (8oxodG), is one of the most frequent damaged bases and arises in the DNA as a consequence of guanine oxidation caused by reactive oxygen species

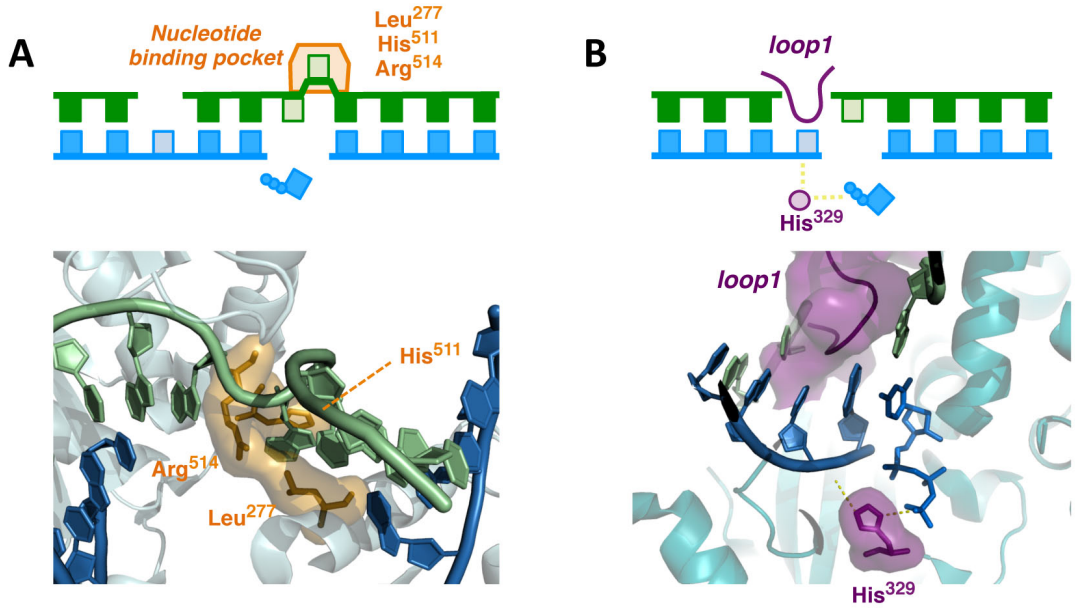

Figure 6. Structural elements of Polλ and Polμ required for their specific NHEJ roles. (A) Polλ stabilizes extrahelical bases in a pocket comprised of 3 residues in order to fill gaps longer than 1 nt (PDB ID 3HWT). (B) Polμ loop1 and His329 are indispensable for NHEJ of non-complementary ends, its preferred substrate. The loop1 is highly flexible and has not been crystalized. Herein, Polμ loop1 modelled to TdT loop1 (PDB ID 4I27) (SWISS model software (http://swissmodel.expasy.org/), (Arnold et al., 2006)) is shown superimposed to Polμ structure (PDB ID 4M04).

(ROS) (Valko et al., 2004). 8oxodG has been extensively studied due to its ability to stably match with adenine, leading to dC:dG to dA:dT transversion mutations (Moriya, 1993; Moriya et al., 1991). Polλ is stimulated by RPA and PCNA to incorporate dCTP efficiently and almost exclusively opposite 8oxodG after removal of misincorporated dAMPs, preventing mutagenesis (Maga et al., 2007; van Loon and Hubscher, 2009).

Development of Polλ-null mouse models has been one of the approaches to address its possible redundancy with Polμ. Mouse embryonic fibroblasts (MEFs) defective for Polλ are not radiosensitive (Bertocci et al., 2006; Vermeulen et al., 2007), and Polλ deficiency does not affect B-cell development, although it impairs NHEJ of DSB intermediates during V(D)J recombination at the immunoglobulin heavy chain loci (Bertocci et al., 2006). Over-expression of a dominant negative Polλ or of a mutator variant associated with cancer was shown to interfere with NHEJ (Capp et al., 2006; Terrados et al., 2009), although the most clear evidence on Polλ specific function in NHEJ was obtained using a NHEJ cellular system derived from MEFs defective in both Polλ and Polμ (Pryor et al., 2015), which confirmed Polλ adaptation to filling gaps when DSB ends are complementary, especially if the gaps have a length of 2 nt.

Polμ

Blanco and colleagues identified Polμ as a new human PolX with high homology to TdT (41% identity), preferentially expressed in secondary lymphoid tissues

(Domínguez et al., 2000). Polμ, likewise TdT, can catalyse template-independent incorporation of nucleotides although, with less efficiency (Domínguez et al., 2000), partly due to the limitation imposed by a single arginine in Polμ (Arg^{387}) (Andrade et al., 2009). Importantly, Polμ can also catalyse template-dependent DNA synthesis, in fact, more efficiently than independently of the template (Andrade et al., 2009). Polμ is well suited to take part in NHEJ due to its unique effectiveness in extending protruding primer termini that are unpaired to a template. In fact, Polμ can synthesize DNA *in vitro* using non-complementary broken ends in a template-dependent fashion either in complex with some NHEJ core factors (Davis et al., 2008; Nick McElhinny et al., 2005) or even alone (Andrade et al., 2009). In this context, Polβ and Polλ are inactive, and only TdT can also operate although only by randomly incorporating dNTPs (Ramsden and Asagoshi, 2012). Polμ can also function when the primer is paired to the template, although less accurately than Polλ. Taking into consideration the substrate requirements described for the mammalian PolXs, these enzymes can be ordered in a gradient of template dependency (Nick McElhinny et al., 2005) (Figure 7).

Several studies have addressed some of the molecular basis underlying Polμ ability to utilize non-complementary ends for synthesis. In this regard, two key structural elements have been identified in human Polμ: the loop1 and the residue His^{329}, which are both conserved only in TdT (Figure 6B). Loop1 is a mobile and flexible motif in Polμ that has been shown to be strictly required for terminal transferase activity and NHEJ of non-complementary ends (Juárez et al., 2006; Nick McElhinny et al., 2005). The structure of TdT loop1 suggests that this motif may operate in both TdT and Polμ as a pseudo-template that stabilizes the unpaired primer terminus (Figure 6B). His^{329} is also relevant for NHEJ of incompatible ends by Polμ by coordinating the incoming nucleotide with the unpaired primer terminus (Figure 6B) (Moon et al., 2007b). The different substrate specificity of Polμ and Polλ renders their roles mainly non-overlapping during NHEJ (Pryor et al., 2015). Moreover, unlike Polλ, Polμ can efficiently incorporate NTPs to the DNA (Nick McElhinny and Ramsden, 2003; Ruiz et al., 2003), substrates that increase its fidelity during NHEJ (Martin et al., 2013a). Polμ deficiency in mice affects B-cell development due to excessive deletion during NHEJ of V(D)J recombination intermediates (Bertocci et al., 2003). Interestingly, Polμ deficiency specifically affects immunoglobulin light-chain recombination (Bertocci et al., 2006). Polμ-defective MEFs are mildly radiosensitive, have delayed repair of radiation induced breaks and are more prone to senescence (Chayot et al., 2010; Lucas et al., 2009). Polμ can efficiently tolerate damage in the DNA (Zhang et al., 2002), although it can be

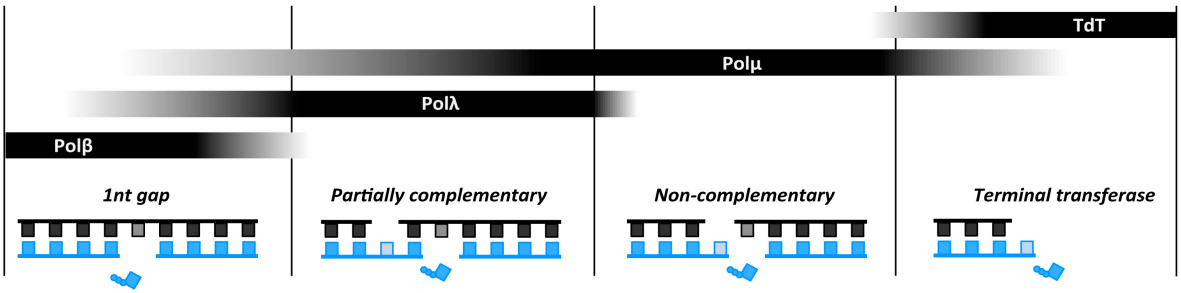

Figure 7. Template dependency of mammalian PolXs. Polβ, Polλ, Polμ and TdT different template dependency is depicted as a gradient from high (left) to low/none (right). Adapted from (Ramsden and Asagoshi, 2012).

highly error-prone, which could possibly related to the fact that Polμ-deficient aged mice have maintained learning abilities (Lucas et al., 2013).

Pol4

Both *Saccharomyces cerevisiae* and *Schizosaccharomyces pombe* have a single PolX, named *Sc*Pol4 and *Sp*Pol4 respectively. Based on primary sequence similarity, *Sc*Pol4 is more closely related to human Polλ and *Sp*Pol4 to human Polμ. *Sc*Pol4 and *Sp*Pol4 have similar biochemical properties including the aforementioned dRP-lyase activity and low sugar discrimination (Bebenek et al., 2005; González-Barrera et al., 2005). *Sp*Pol4 ability to incorporate NTPs is remarkable among PolXs, as it incorporates both dNTPs and NTPs to the DNA with roughly the same efficiency (González-Barrera et al., 2005). *Sc*Pol4 and *Sp*Pol4 are well suited to participate in NHEJ, in part thanks to their BRCT domain that in the case of *Sc*Pol4 was shown to interact with NHEJ core factors (Tseng and Tomkinson, 2002). Both polymerases can also efficiently tolerate mismatches near the primer termini, a frequent hallmark of NHEJ substrates *in vivo* (Ramsden and Asagoshi, 2012). In fact, both *Sc*Pol4 and *Sp*Pol4 were demonstrated to perform gap-filing DNA synthesis during NHEJ *in vivo* (Li et al., 2012; Wilson and Lieber, 1999).

3.1.2 PolXs role in NHEJ: unaddressed questions

Although it is now clear that Polλ and Polμ have complementary non-redundant roles in NHEJ, which rely on their adaptation to ends of different complementary, the mechanism that mediates the final decision between the two during NHEJ remains unclear. Regulation of enzymatic action during NHEJ is not fully understood, but the kinase activity of DNA-PK complex is thought to be is essential for regulation through phosphorylation by its kinase subunit (Lieber, 2008). Therefore, it is likely that Polλ and Polμ participation during NHEJ may not just depend on their affinity to broken ends of

different nature but also on post-translational modifications. Reciprocal regulation could be essential to avoid superfluous competition, especially at substrates where both polymerases can be active (Figure 7). Both Polλ and Polμ were shown to be phosphorylated by CDK-cyclin complexes, which stabilize and inactivate Polλ and Polμ respectively during S-phase, a somehow complementary regulation (Esteban et al., 2013; Frouin et al., 2005; Wimmer et al., 2008). However, it remains unknown whether Polλ and Polμ could be more precisely regulated during NHEJ through phosphorylation by DNA-PK, or even by other DNA damage response kinases from the same family such as ATM (Shiloh, 2003). Moreover, two other aspects regarding PolX regulation during NHEJ are intriguing, first, whether the possible mechanism of regulation by phosphorylation could be conserved in PolXs form lower eukaryotes such as Pol4, and second whether Polλ and Polμ could be dysregulated in cancer. Interestingly, defects of function of both Polλ and Polβ caused by single amino acid mutations have been linked to increased genomic instability and tumourigenesis respectively (Sweasy et al., 2005; Terrados et al., 2009), but nothing is known about Polμ on this regard.

Low sugar discrimination is a highly conserved characteristic of several PolX, such as Pol4 and Polμ (Bebenek et al., 2005; González-Barrera et al., 2005; Nick McElhinny and Ramsden, 2003; Ruiz et al., 2003). Polymerases specialized in NHEJ belonging to other families, such as some bacterial AEP members, also incorporate ribonucleotides very efficiently (Pitcher et al., 2007), suggesting that this property might be very relevant for NHEJ. Ribonucleotide concentration is much higher than that of deoxynucleotides (Traut, 1994), especially in cell-cycle phases other than the S-phase, when NHEJ prevails over HR (Chapman et al., 2012), which could render them useful substrates and could explain why some NHEJ PolX incorporate them so efficiently. Although ribonucleotide incorporation is undesirable, due to their high propensity to hydrolysis (Li and Breaker, 1999), one would speculate that their incorporation to DNA is a low price to pay during NHEJ due to the hazardous consequences of unrepaired DSBs and the fact that single incorporated ribonucleotides are efficiently targeted by RNase H2, which initiates their repair (Cerritelli and Crouch, 2009; Sparks et al., 2012). The relevance of ribonucleotide incorporation during NHEJ and how they are repaired after the completion of the process is not fully understood.

Efficient tolerance of DNA lesions is another common characteristic of several PolXs (Maga et al., 2007; Zhang et al., 2002), and also of bacterial NHEJ polymerases (Pitcher et al., 2007), and is thought to be consequent with the fact that DNA lesions are often associated with DSBs. The importance of damage tolerance during NHEJ by

PolXs is also somewhat unclear and so is whether ribonucleotides could be relevant for tolerarting DNA lesions. Polλ role in the tolerance of 8oxodG is known to be very relevant in mammals (Maga et al., 2007; van Loon and Hubscher, 2009), however the conservation of this role in lower eukaryotic homologs such as Pol4 is unknown. This could be particularly relevant is *S. pombe*, where the glycosylase that excises 8oxodG from the DNA, OGG1, is not conserved, suggesting persistence of the lesion.

3.2 Other specializations of PolXs:

V(D)J Recombination

The genes that code for immunoglobulins (Igs) and T cell receptors (TCR), exist in a non-functional state in the germline, in which the portion that codes for the antigen binding site is arranged as an array of variable (V), diversity (D) and joining (J) genes segments (Schatz and Ji, 2011). V(D)J recombination is an specialized form of NHEJ that assembles these segments individually in a single V(D)J exon (Bassing et al., 2002; Schatz and Ji, 2011). Generation of diversity during the process relies on the multiple options of combination of the segments and on the addition of random nucleotides by a PolX. V(D)J recombination occurs only in developing B or T lymphocytes and it is a site specific process initiated by the RAG recombinase (Swanson, 2004). The RAG complex cleaves the DNA at the recombination signal sequences (RSS) that flank each V, D, and J segments generating DSBs that are repaired by NHEJ to arrange the V, D and J segments in a single exon.

Although, as mentioned before, Polλ and Polμ can take part in V(D)J recombination (Bertocci et al., 2006), TdT is the only mammalian polymerase fully devoted to this process. TdT is highly specialized in generating variability by randomly incorporating nucleotides to DSB intermediates during V(D)J recombination to increase variability (Desiderio et al., 1984). TdT adaptation to the process has several implications, including being inactive on substrates with recessed primers and catalysing DNA synthesis strictly in a template-independent fashion (Figure 7) (Kato et al., 1967). Likewise Polμ, TdT is endowed with a prominent Loop1 motif that produces the steric exclusion of templating bases, and whose deletion can confer TdT certain template-dependency (Romain et al., 2009). Also similarly to Polμ, TdT is rather promiscuous as it can incorporate dNTPs, NTPs and several non-nucleotide triphosphates with high efficiency (Arzumanov et al., 2000; Boulé et al., 2001). Given its promiscuity, TdT expression is highly regulated and it is mainly restricted to pre-B and pre-T lymphocytes but not during light-chain recombination in late developing pre-

B lymphocytes in adult mice. TdT-deficient mice are viable and fertile but they have a defective immune adaptive response (Gilfillan et al., 1993). Although TdT is fully devoted to V(D)J recombination, Polμ plays a more relevant role in this process during embryogenesis (Gozalbo-López et al., 2009).

Base excision repair

Base excision repair (BER) is a highly conserved mechanism that repairs damaged bases arising from oxidative damage, alkylation and deamination (Dianov and Hübscher, 2013; Robertson et al., 2009). Two different BER mechanisms have been described: short-patch BER, that replaces only 1 nt, and long-patch BER that replaces a track of at least 2 nt by taking advantage of replicative enzymes. Irrespective of the subpathway, BER is always initiated by a damage-specific DNA glycosylase that recognizes the lesion and cleaves the N-glycosylic bond between the damaged base and the sugar phosphate backbone, generating an apurinic/apyrimidinic (AP) site (Krokan et al., 1997). Processing of the AP site, which may involve several enzymes, generates a gap suitable for synthesis and ligation harbouring a 5'P and 3'OH. Polβ is specialized in filling this small gap during both short-patch and long-patch BER. In the long-path scenario after Polβ fills the 1nt gap Polδ performs strand-displacement synthesis (Podlutsky et al., 2001), generating a flap of 2 to 12 nt that is cut off by FEN1 and sealed by ligase I (Klungland and Lindahl, 1997).

BER has been suggested to be an specialization of single-strand break (SSB) repair (Caldecott, 2008), and the involvement of PolXs in the process suggests that is also related to NHEJ, being in line with the fact that in both processes small DNA gaps have to be filled. In fact, likewise other PolXs, Polβ is highly active on small DNA gaps, especially if they are flanked by a 5'P group (Prasad et al., 1994). However, unlike other PolXs, Polβ is not suited to take part in NHEJ as it lacks the BRCT domain and cannot tolerate discontinuities in primer/template base-pairing (Ramsden and Asagoshi, 2012). Polβ is well adapted to BER also thanks to its and dRP lyase activity that involves Polβ in processing of the ends after cleavage of the AP site (Matsumoto and Kim, 1995). In fact, Polβ DNA polymerase and dRP lyase activity are both essential to BER (Podlutsky et al., 2001; Sobol et al., 2000). Likewise other PolXs, Polβ lacks proofreading activity, although it is generally more faithful than the other mammalians members of the family (Bebenek et al., 2003; Zhang et al., 2001). Polβ is more closely related to Polλ and similarly to this polymerase, Polβ does not incorporate NTP efficiently to the DNA. In agreement with Polβ lower promiscuity and with its

essential role in BER, Polβ is expressed in all tissues. Polβ null mice die immediately after birth due to extensive apoptosis in the nervous system, supporting a relevant role for Polβ in DNA repair *in vivo* (Sugo et al., 2000).

4. DNA polymerases specialized in translesion synthesis

In spite of the efficacy of the DNA repair mechanisms described in eukaryotes, it is likely that some lesions remain unrepaired before the initiation of DNA replication. Replicative DNA polymerases are specialized in synthesizing DNA with incredibly high efficiency and fidelity, but that comes with the cost of not being able to accommodate damaged bases in their active sites. Hence, unrepaired lesions can interfere and stall DNA replication, a potentially cytotoxic scenario, as the DNA must be fully replicated before mitosis. Moreover, blocking DNA replication is also hazardous since stalled replication forks also lead to the generation of DSBs. Different strategies have arisen through evolution to overcome this problem that rely in either tolerating or avoiding the damage (Friedberg, 2005). Damage avoidance utilizes the replicative machinery and avoids copying the damaged template through at least two different mechanisms: post-replication recombinational repair and replication-fork regression. Damage tolerance is arguably the most frequently used strategy in mammalian cells and relies in specialized low stringency polymerases that synthesize DNA past the lesion, a process known as translesion synthesis (TLS) (Lehmann et al., 2007; Sale et al., 2012).

TLS is an error-prone process that may proceed by the direct incorporation of nucleotides either opposite or beyond the lesion. In mammalian cells TLS is performed by the Y family polymerases Polη, Polι, Polκ and Rev1, and also by Polζ from the B family (Lehmann et al., 2007; Sale et al., 2012). In clear contrast to replicative polymerases, these polymerases share certain properties such as low processivity, lack of proofreading activity and a loose active site that, all together, render these enzymes poorly faithful. Despite their similarities, mammalian TLS polymerases have different specializations. Polη is uniquely effective in synthesizing DNA past cyclopyrimidine dimers (CPDs), the major UV photoproduct. Polη can tolerate this damage by preferably incorporating two adenines as efficiently as opposite an undamaged template (Masutani, 2000; McCulloch et al., 2004). Accordingly, Polη deficiency causes the variant form of *xeroderma pigmentosum* (XP-V), a disease characterized by high incidence of sunlight-induced skin cancer (Johnson et al., 1999; Masutani et al., 1999). Interestingly, Polη cannot bypass the other major UV-induced lesion the pyrimidine(6-4)pyrimidone photoproducts (6-4PPs) (Lehmann et al., 2007).

Polι is capable of tolerating certain damages and was identified as a highly error-prone polymerase (Tissier et al., 2000). No clear phenotype has been identified in mice deficient for Polι and its exact function remains unknown (McDonald et al., 2003). Polκ-deficiency in mice does not correlate with any pronounced phenotype either, in spite of the fact that Polκ is specialized in tolerating benzo[a]pyrene-guanine and other adducts in the N^2 position of guanine both *in vitro* and *in vivo* (Avkin et al., 2004; Jarosz et al., 2006; Ogi et al., 2002). Strictly, Rev1 is not a DNA polymerase but a dCMP transferase that can incorporate this nucleotide opposite dG and AP sites (Nelson et al., 2000). Polζ is a heterodimer consisting of the Rev7 regulatory subunit and the Rev3 B family catalytic subunit. Rev1 and Rev3 have been shown to be relevant for bypassing abasic sites and 6-4PP in yeast (Gibbs et al., 2005; Nakajima et al., 2004; Nelson et al., 2000; Otsuka et al., 2005). Interestingly, Rev1 and Polζ deficiency in mice have severe phenotypes and display growth retardation and embryonic lethality respectively (Bemark et al., 2000; Esposito et al., 2000; Jansen et al., 2006; Wittschieben et al., 2000).

4.1 PrimPol, a novel human primase-polymerase

Blanco and collaborators have recently described a novel DNA polymerase specialized in TLS in human cells (García-Gómez et al., 2013). The enzyme harbours polymerase and primase activities that rely in the same active site and was consequently named PrimPol. Other enzymes combining those activities have been previously described in archaea and bacteria (Bocquier et al., 2001; Sanchez-Berrondo et al., 2012), suggesting that PrimPols are an archaic solution to the “priming problem”, which is defined by the fact that DNA polymerases, unlike RNA polymerases, cannot initiate DNA synthesis *de novo*. In fact, most DNA polymerases require a pre-existing DNA primer to operate, which is generated by either a break in the DNA or by another DNA polymerase. DNA replication is a remarkable scenario whereby eukaryotes have circumvented the priming problem by developing an specialized RNA polymerase, termed primase (Kuchta and Stengel, 2010), that generates a short RNA molecule used as a primer, and specialized DNA polymerase (Polα) that extends the RNA by synthesizing DNA (Bebenek and Kunkel, 2004). These specialized primase and polymerase operate together as a complex (Conaway and Lehman, 1982; Hübscher, 1983; Kaufmann and Falk, 1982; Yagura et al., 1982), in a way resembling PrimPols.

Human PrimPol is a different solution to the priming problem as it can initiate synthesis *de novo* using dNTPs, unlike conventional primases that generate only RNA

molecules. PrimPol is thus a DNA primase, the first described in mammalian cells (García-Gómez et al., 2013). PrimPol incorporates preferably dNTPs during priming and regular polymerization reactions, although it is not a proficient sugar discriminator, as it can also use ribonucleotides (García-Gómez et al., 2013; Martínez-Jiménez et al., 2015). PrimPol is endowed also with polymerase activity and polymerizes DNA in a distribute manner. PrimPol overall activity is highly stimulated by the use of Mn^{2+} as cofactor and it is a relatively error-prone polymerase that lacks proofreading activity (García-Gómez et al., 2013; Martínez-Jiménez et al., 2015; Zafar et al., 2014).

In silico analyses indicate that PrimPol belongs to the archaeo-eukaryotic primase (AEP) super-family a heterogeneous family of enzymes (Iyer et al., 2005). PrimPol contains the typical A, B and C motifs found among AEP members and a Zinc Finger domain (Wan et al., 2013; García-Gómez et al., 2013), shown to be indispensable for primase but not for polymerase activity (Mourón et al., 2013, Keen et al., 2014). PrimPol has been shown to localize to both nucleus and mitochondria of human cells, being thus the first primase and second polymerase known to operate in the latter (García-Gómez et al., 2013). PrimPol is particularly efficient when tolerating DNA lesions and is specialized in TLS operating in three ways (Figure 8): 1) PrimPol can efficiently incorporate nucleotides opposite certain lesions such as 8oxodG (García-Gómez et al., 2013; Martínez-Jiménez et al., 2015; Zafar et al., 2014), 2) PrimPol can realign primers ahead of unreadable lesions such as the 6-4PP to continue DNA synthesis (Martínez-Jiménez et al., 2015), 3) PrimPol can prime ahead of lesions to allow fork progression during DNA replication (Mourón et al., 2013). PrimPol primase activity was shown to be pivotal for fork reinitiation at UV damage sites, most likely in the leading strand during nuclear replication (Mourón et al., 2013). Due to the lack of polymerases specialized in TLS in mitochondria, and the higher efficiency in 8oxodG bypass displayed by PrimPol in comparison to the mitochondrial replicase Polγ (García-Gómez et al., 2013), it is likely that PrimPol polymerase activity may be more relevant in mitochondria.

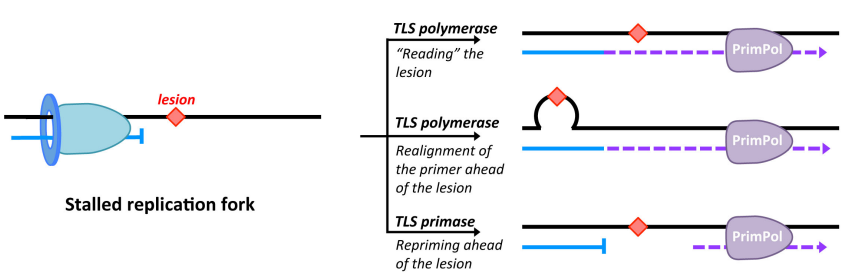

Figure 8. Model of PrimPol mechanisms of action. PrimPol can function as a TLS polymerase to copy the lesion or realign the primer ahead to continue synthesis. PrimPol can also assist stalled forks as a TLS primase and reinitiate replication ahead of the lesion.

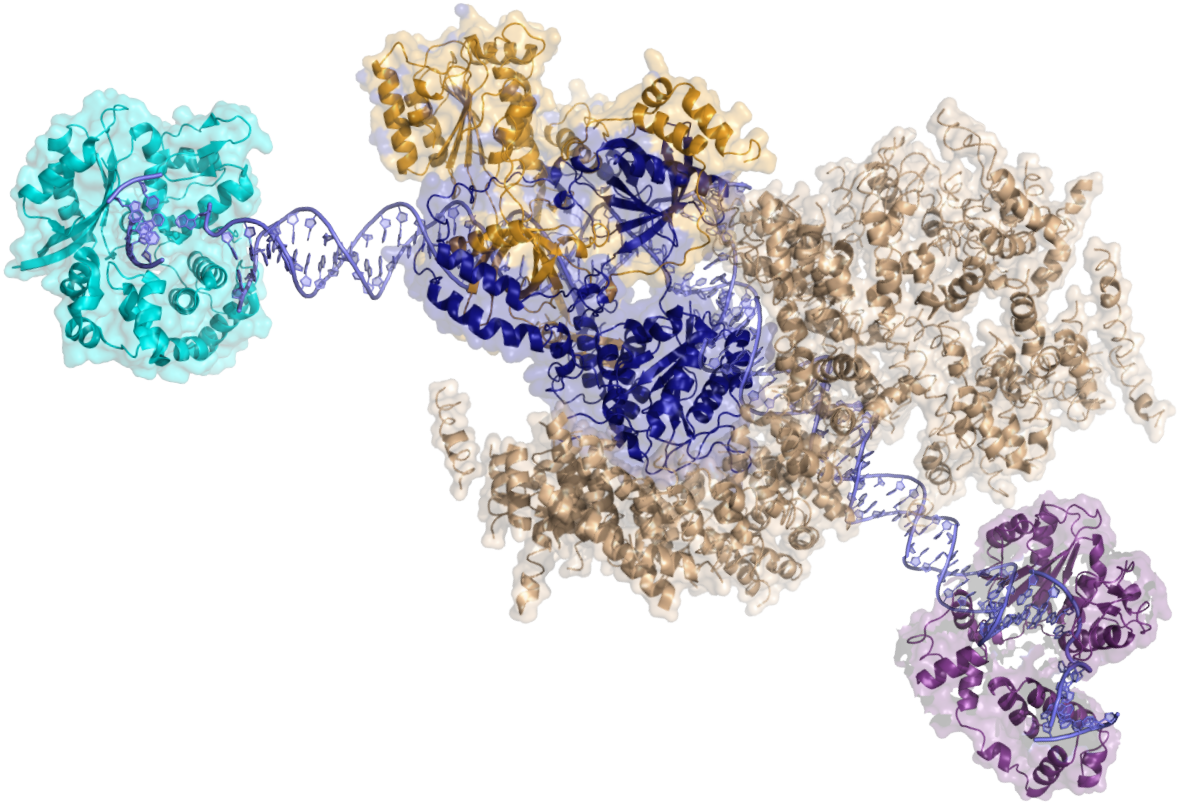

Objectives

During the course of this Doctoral Thesis we set the following objectives:

1. Evaluate the ability of *Sp*Pol4 to tolerate the oxidative lesion 8oxodG during regular gap-filling reactions and NHEJ *in vitro* by using both the purified polymerase and *S. pombe* whole cell extracts. Taking into account the low sugar discrimination capacity of *Sp*Pol4 and the dual capacity of 8oxodG to pair with either cytosine of adenine, determine the preferred substrate of incorporation opposite 8oxodG by *Sp*Pol4 considering the nucleotide physiological concentrations.
2. Explore the conservation of the ribonucleotide excision repair mechanism in *S. pombe* by using whole cell extracts to test whether RNase H2 can initiate this mechanism at ribonucleotides paired to 8oxodG. Additionally, evaluate the fidelity and efficiency of 8oxodG bypass of the polymerase activity coupled to the RNase H2 activity in *S. pombe* whole cell extracts.
3. Evaluate the capacity of *Sp*Pol4 to incorporate the oxidized nucleotides 8oxo-dGTP and 8oxo-GTP in comparison to undamaged nucleotides.
4. Test the possible phosphorylation in response to DNA damage of DNA polymerases from the X family using as model *Sc*Pol4 and kinase Tel1/ATM in *S. cerevisiae* and Polλ and DNA-PKcs kinase in human cells.
5. Determine the effect of DNA-PKcs-mediated phosphorylation of Polλ during NHEJ in human cells by assessing the catalytic activity of Polλ during the process and its interaction with NHEJ core factors before and after phosphorylation.
6. Characterize two tumour-associated point mutations of human Polμ: Evaluate the effect of these mutations in the efficiency and fidelity of Polμ during NHEJ *in vitro* and *in vivo*; determine their effect on Polμ-mediated gap-filling of 2nt gaps.
7. Evaluate the transpolymerization capacity of human PrimPol across discontinuous templates. Study the influence of short vs long protruding DNA ends and the requirement of primer/template homology in these *in vitro* reactions by PrimPol.
8. Explore the effect of the concentration and combination of the metal cofactors Mn^{2+} and Mg^{2+} in the fidelity and efficiency of human PrimPol during *in vitro* translesion synthesis of 8oxodG and during template dislocation reactions. Evaluate the possible involvement of the PrimPol metal binding motif in metal cofactor selection during these processes.

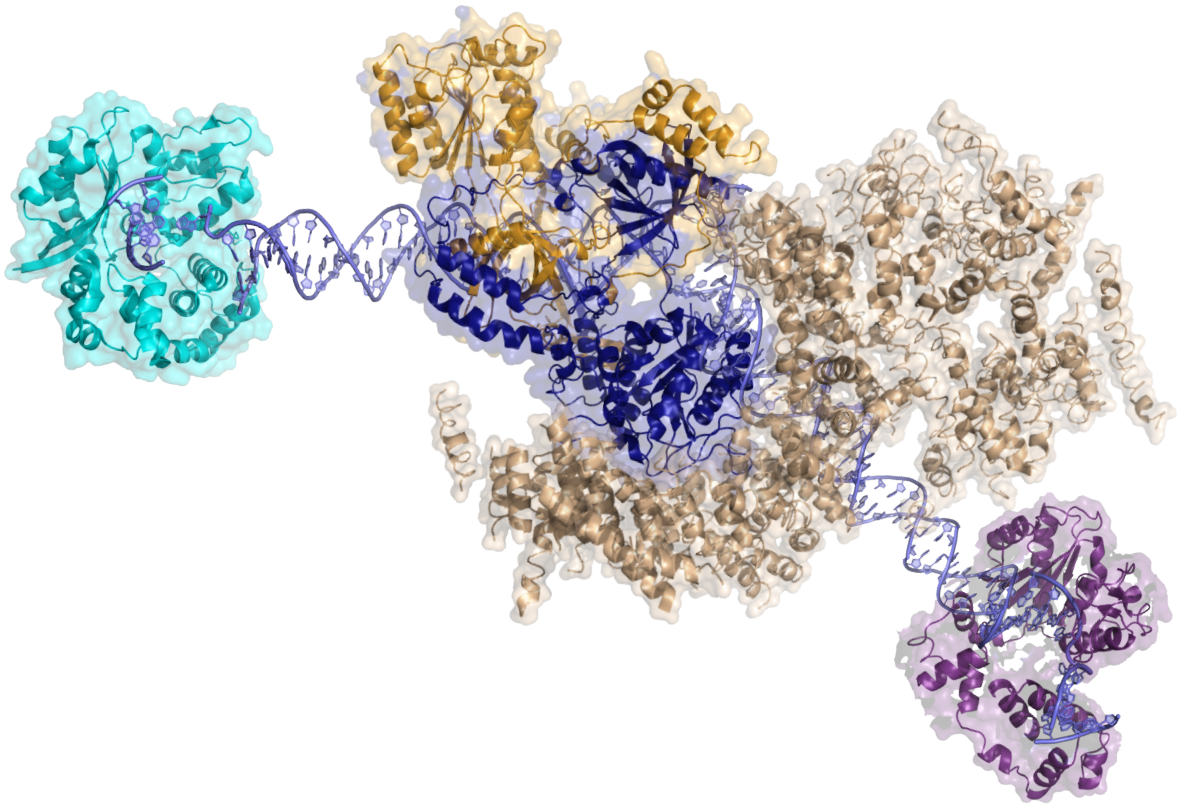

Materials and Methods

1. DNA and proteins

GST-tagged *Sp*Pol4 (GST-*Sp*Pol4) was purified as previously previously described (González-Barrera et al., 2005). Full-length *Sc*Pol4 DNA coding sequences were obtained by PCR amplification with primers CT-P4s (5'-CTATGAatcgatATGTCTCTAAAGGGTAAAT-3') and CT-P4as (5'-TTGATCgcggccgcTTATGCAGTTTTTTTTTCCCATTCG-3'), which had *ClaI* and *NotI* cleavage sites, respectively. *Sc*Pol4 overexpression plasmids were obtained by cloning the corresponding *ClaI-NotI* PCR fragments under the Tet-promoter into the pCM184 plasmid. *Sc*Pol4 single (T64A, T540A) and double (T64A,T540A) mutations were obtained in the pCM184 plasmid by site-directed mutagenesis using the T64As (5'-ATGCATTTGGCTCAGAAAGAT-3'), T64Aas (5'-ATCTTTCTGAGCCAAATGCAT-3'), T540As (5'-TTCAAGCTTGCACAACACGGT-3') and T540Aas (5'-CCGTGTTGTGCAAGCTTGAA-3') primers. Wild-type and mutant (T64A, T540A, T64A-T540A) *Sc*Pol4 versions were also fused to 6xHis-tag epitope by subcloning the corresponding *BamHI-NotI* fragments from pCM184 into the pET28c(**+**) vector (Novagen). Recombinant His-tagged wild-type *Sc*Pol4 and the T64A, T540A and T64A-T540 mutants were partially purified using Ni-NTA agarose (Qiagen) following manufacturer's instructions.

Wild-type Polλ gene (POLL) cDNA was amplified with oligonucleotides sBglII (5´-TTGATCAGATCTTATGGATCCCAGGGGTATCTTG-3') and asXbaI (5´-TTGATCTCTAGATAACCAGTCCCGCTC-3') and cloned in the p3xFLAG-Myc-CMV Expression Vector (Sigma). The Polλ-T204A phospho-dead mutant was generated by site-directed mutagenesis starting from the wild-type construct and using oligonucleotides T204As (5´-GGGGAAGAAGCCCAGGTTAGTGC-3') and T204Aas (5´-GCACTAACCTGGGCTTCTTCCCC-3'). For the construction of human Polλ mutant versions for protein purification, T204A, T188A, T188A-T204A and T204E Polλ mutants were obtained by site-directed mutagenesis using the plasmid pET22b-Polλ as a template (Garcia-Diaz et al., 2004) and with T204As, T204Aas, T188As (5'-GCACCAAACGCCCAAGCCCAGCC-3'), T188Aas (5'-GGCTGGGCTTGGGCGTTTGGTGC-3'), T204Es (5´-GATGATGAAGCCAGTGATGGGGAAGAAGAGCAGGTTAGTGCAGCTGATCTGGAAGCC-3') and T204Eas (5´-GGCTTCCAGATCAGCTGCACTAACCTGCTCTTCTTCCCCATCACTGGCTTCATCATC-3') primers. Over-expression and purification of wild-type and mutant versions of

Polλ was carried out in *E. coli* BL21-pRIL as previously described (Martin et al., 2013b). Human Polβ was purified as described in (Martin et al., 2012).

Human wild-type Polμ and G174S and R175H mutants were purified as described in (Martin et al., 2013b). G174S and R175H were devised by site-directed mutagenesis on the over-expressing construct pRSET-hPolμ (Domínguez et al., 2000), using the QuickChange Site-Directed Mutagenesis Kit (Stratagene) and the following synthetic oligonucleotides as primers: G174Ss (5'-GAAGGCAGTGAGAGCCGCCTCCTCACC-3') and G174Sas (5'- GGTGAGGAGGCGGCTCTCACTGCCTTC-3') in the case of the G174S mutant, and R175Hs (5'-GGCAGTGAGGGCCACCTCCTCACCTTC-3') and R175Has (5'-GAAGGTGAGGAGGTGGCCCTCACTGCC-3') in the case of the R175H mutant.

Wild-type PrimPol and the E116D mutant were purified as described in (García-Gómez et al., 2013). E116D was devised by site-directed mutagenesis in the Doctoral Thesis of Dr. Sara García Gómez using E116Ds (5'-GTGCAAGCTTTATTTTGATTTGGCATTTAACAAACCTGCCAACCC-3') and E116Das (5'-GGGTTGGCAGGTTTGTTAAATGCCAAATCAAAATAAAGCTTGCAC-3') primers.

DNA oligonucleotides for site-directed mutagenesis were purchased from Sigma-Aldrich. Synthetic DNA oligonucleotides used for the DNA polymerization assays were purchased from either Isogen or Sigma-Aldrich, except for the ones containing 8oxodG that were acquired from Eurogentec. Oligonucleotides used for DNA polymerization assays were purified by 8 M urea-20% polyacrylamide gel electrophoresis (PAGE). Synthetic oligonucleotides used as primers in the polymerization assays were radiolabelled using [γ-^{32}P]ATP (3000Ci/ mmol) (Perkin-Elmer) and T4 polynucleotide kinase (New England Biolabs) for 45 min at 37 °C. Hybridizations were performed in 1X hybridization buffer (50 mM Tris-HCl pH 7.5, 0.3M NaCl) for 10 min at 80°C. Unlabelled ultrapure dNTPs were supplied by GE Healthcare. 8oxo-dGTP and 8oxo-GTP were purchased from TriLink Biotechnologies.

2. DNA polymerization assays

2.1 *Sp*Pol4

For the analysis of gap-filling activity, a 5'[^{32}P]-labelled 15-mer DNA primer (5'-GATCACAGTGAGTAC-3') was hybridized to a 28-mer template (5'-AGAAGTGTATCTNGTACTCACTGTGATC-3', where N = dA, dC, dG, dT or 8oxodG) and to a 12-mer downstream oligonucleotide harbouring a 5'P (5'P-AGATACACTTCT-3) to generate a dsDNA molecule with a 1nt-gap. The reactions were performed by

incubating the labelled DNA substrate (2.5 nM) with purified GST-*Sp*Pol4 (35 nM) in a final volume of 20 μl that also contained 1X reaction buffer (50 mM Tris-HCl/ pH 7.5, 1 mM DTT, 4% glycerol and 0.1 mg/ml BSA), the indicated concentration of the NTPs or dNTPs and 2.5 mM $MgCl_2$. Reactions were incubated for 15 min at 30 °C and stopped by adding gel loading buffer (95% (v/v) formamide, 10 mM EDTA, 0.1% (w/v) xylene cyanol and 0.1% (w/v) Bromophenol Blue). Primer extension was analysed by 8 M urea/20% PAGE. After electrophoresis, extended products were detected either by autoradiography or using a BAS-1500 phosphorimager (Fujifilm). When indicated, band intensities were determined by densitometry.

For the NHEJ polymerization assays, a 5'[^{32}P]-labelled 16-mer DNA primer (5'-CCCTCCCTCCGCGGCC-3') was hybridized to the 11-mer oligonucleotide (5'-CGGAGGGAGGG-3'), to generate a labelled dsDNA primer with a 3'-protrusion of 5 nt. A 21-mer oligonucleotide (5'-CGCGCACTCACGTCCCNGGCC-3', where N = dG or 8oxodG) was hybridized to the 16-mer oligonucleotide (5'-GGGACGTGAGTGCGCG-3'), which harboured a 5'P when indicated, to generate an unlabelled dsDNA template molecule with a 3'-protrusion of 5 nt, which was used in the assays only when indicated. For the assays, the dsDNA primer molecule (5nM) was incubated with the unlabelled DNA template molecule (12.5 nM) and with purified GST-*Sp*Pol4 (200 nM). The reaction was carried out for 1 h at 30°C in a final volume of 20 μl and also contained variable concentrations of NTPs, 1X reaction buffer and 1 mM $MnCl_2$. Trans-directed primer extension was analysed as described above. When indicated, the percentage of primers extended with a given nucleotide was quantified by densitometry of the autoradiographs.

To study gap-filling activity present in cell extracts, 2.5 nM of the indicated 1nt-gapped dsDNA molecule, prepared as described above, was incubated with 20 μg of the whole cell extract (WCE). The reaction mixture (20 μl), contained 1X reaction buffer, 1 mM $MnCl_2$ and variable concentrations of NTPs or dNTPs. Reactions were incubated for 20 min at 30 °C, and primer extension was analysed as described previously.

For the NHEJ reactions with cell extracts, we used the 3'-protruding dsDNA substrates described above. The labelled 3'-protruding dsDNA (5 nM) was incubated with the unlabelled 3'-protruding dsDNA (12.5 nM) and with 30 μg of the WCE. The reaction mixture (20 μl), contained 1X reaction buffer, the indicated concentrations of dNTPs/NTPs and 1 mM $MnCl_2$. Reactions were performed during 30 min at 30°C, and primer extension was analysed as described above.

2.2 Polλ

For 1 nt DNA gap-filling assays, a 5'[^{32}P]-labelled 15-mer DNA primer (5'-GATCACAGTGAGTAC-3') was hybridized to a 28-mer DNA template (5'-AGAAGTGTATCTCGTACTCACTGTGATC-3') and to a 12-mer DNA downstream molecule harbouring a 5'-phosphate group (5'-AGATACACTTCT-3'). Purified Polλ (50 nM) was incubated with 2.5 nM of the labelled 1 nt gapped-DNA in a reaction mixture (20 µl) containing $MgCl_2$ (2.5 mM), increasing concentrations of ddGTP (0.1, 0.25, 0.5, 1, 2.5 nM) and 1X of reaction buffer. Following 30 min of incubation at 30°C, reactions were stopped by adding loading buffer and the products were separated by 8M urea-20% PAGE. After electrophoresis, extension products were analysed as described previously and gel band intensities determined by densitometry.

For *in vitro* NHEJ assays, a 5'[^{32}P]-labelled 15-mer DNA primer (5'-CCCTCCCTCCGCGGC-3') was hybridized to an 11-mer DNA oligonucleotide (5'-CGGAGGGAGGG-3') to generate a labelled primer dsDNA molecule with a 3'-overhang. A 21-mer DNA template (5'-CGCGCACTCACGTCCCTCGCC-3') was hybridized to a 16-mer DNA oligonucleotide (5'-GGGACGTGAGTGCGCG-3') harbouring a 5'-phosphate group when indicated, to generate a 3'-protruding dsDNA template molecule. The labelled primer molecule (5 nM) was incubated with, the template molecule (12.5 nM), purified Polλ (500 nM), $MnCl_2$ (0.1 mM), and either increasing concentrations of dGTP (10, 25, 50, 100 and 500 nM) for efficiency assays, or 500 nM of the indicated dNTPs for fidelity assays. In each case, the final reaction volume (20 µl) contained 1X reaction buffer and was incubated at 30°C for 60 min. Reactions were stopped by the addition of loading buffer and extension products were also analysed as described above.

2.3 Polµ

For 1nt gap-filling assays, a 5'[^{32}P]-labelled 15-mer DNA primer (5'-GATCACAGTGAGTAC-3') was hybridized to a 28-mer template (5'-AGAAGTGTATCTCGTACTCACTGTGATC-3') and to a 12-mer downstream oligonucleotide harbouring a 5'P (5'P-AGATACACTTCT-3) to generate a dsDNA molecule with a 1nt-gap. DNA (2.5 nM) was incubated with purified Polµ (25 nM) and the indicated amounts of dGTP for 30 min at 30°C. The reaction mixture (20 *µ*l) contained 2.5 mM $MgCl_2$ and 1X reaction buffer. After incubation reactions were stopped by addition of loading buffer and primer extension was analysed as described previously.

For 2nt gap-filling assays, a 5'[^{32}P]-labelled 15-mer DNA primer (5'-TCTGTGCAGGTTCTT-3') was hybridized to a 32-mer template (5'-TGAAGTCCCTCTCGACGAAGAACCTGCACAGA-3) and to a 15-mer downstream oligonucleotide harbouring a 5'P (5'P-TCGAGAGGGACTTCA-3') to generate a 2nt-gapped dsDNA. Reactions were performed as described above for the 1nt gap-filling experiments but using the indicated concentrations of either dCTP or dGTP. After 30 min of incubation at 30°C, primer extension was analysed as described previously.

To test the ability of Polμ to perform the NHEJ of compatible ends *in vitro*, a 5'[^{32}P]-labelled 13-mer DNA (5'-CCCTCCCTCCCGT-3') was hybridized to an 11-mer oligonucleotide (5'-GGGAGGGAGGG-3') to generate a labelled dsDNA primer molecule with a 3'-protruding end. Additionally, a 15-mer oligonucleotide (5'-GCACTCACGTCCCCA-3') was hybridized to a 13-mer oligonucleotide harbouring a 5'P (5'P-GGGACGTGAGTGC-3') to generate an unlabelled dsDNA molecule with a 3'-protruding end that will be recognised mainly a as a template by Polμ due to the presence of a 5'P group flanking the protrusion. Reactions were performed by incubating the labelled DNA (7 nM) with the unlabelled DNA (18 nM), in the presence of 200 nM of purified Polμ. The reaction mixture (20 μl) also contained 2.5 mM of $MgCl_2$, 1X reaction buffer and the indicated amounts of dGTP. After 30 min of incubation at 30°C, primer extension was analysed as described previously.

To assess the effect of the mutations on the NHEJ of non-compatible ends *in vitro*, a 5'[^{32}P]-labelled 12-mer DNA primer (5'-CCCTCCCTCCCN-3', where N = dA or dC) was hybridized to the 11-mer oligonucleotide (5'-GGGAGGGAGGG-3'), to generate a labelled dsDNA primer with a 3'-protrusion of 1nt. A 14-mer oligonucleotide (5'-GCACTCACGTCCCN-3', where N = dA or dC) was hybridized to the 13-mer oligonucleotide harbouring a 5'P (5'P-GGGACGTGAGTGC-3') to generate an unlabelled dsDNA template molecule with a 3'-protrusion of 1nt, which was used in the assays only when indicated. Reactions were performed as described above for the *in vitro* assays of compatible end NHEJ using the indicated amounts of dGTP to test efficiency of template directed insertions, the indicated amounts of dATP to test efficiency of incorporation of incorrect nucleotides, or 5 μM of each individual dNTP to test the fidelity of the reactions. After incubation for 30 min at 30°C, primer extension was analysed as described previously.

Terminal transferase activity of Polμ was assayed by incubating 5 nM of a 5'[^{32}P]-labelled 21-mer polydT with 600 nM of purified Polμ and 100 μM of each individual dNTP. The reaction mixture (20 μl) also contained 1 mM of $MnCl_2$ and 1X reaction

buffer. After 30 min of incubation at 37°C, reactions were stopped with loading buffer as described previously. Primer extension was also analysed as described above.

2.4 PrimPol

To evaluate the ability of PrimPol to polymerize across discontinuous templates, 5'[^{32}P]-labelled 13-mer (5'-CCCTCCCTCCCGT-3'), 20-mer (5'-CGCGCACTCACGTCCCCGCC-3'), 40-mer (5'-GGCCACGCAATGTTGACGTTTTTCGACAAGACCTCAGTAT-3') oligonucleotides or a 5'[^{32}P]-labelled 21-mer polydT were incubated with purified PrimPol when indicated. The reaction mixture contained 5 nM of the indicated labelled ssDNA, 400 nM of PrimPol, 1 mM $MnCl_2$, 100 μM of the indicated dNTPs or NTPs, and 1X reaction buffer in a final volume of 20 μl. The reactions were incubated for 60 min at 30ºC and were stopped by addition of loading buffer**.** Samples were resolved by 8 M urea-20% PAGE and extended products analysed as described previously.

The activity of PrimPol on dsDNA with 3'-protrusions was evaluated by incubating 400 nM of purified PrimPol with 5 nM of different 5'[^{32}P]-labelled oligonucleotides of distinct length: 20-mer (5'-CGCGCACTCACGTCCCCGCC-3'), 23-mer (5'-CGCGCACTCACGTCCCCGCCAAG-3'), 26-mer (5'-CGCGCACTCACGTCCCCGCCAAGTCC-3') or 29-mer (5'-CGCGCACTCACGTCCCCGCCAAGTCCGAG-3'), which were all individually hybridized to a 16-mer oligonucleotide (5'-GGGACGTGAGTGCGCG-3') to generate a labelled dsDNA with a 3'-protrusion of either 4 nt, 7 nt, 10 or 13 nt respectively. When indicated 12.5 nM of an unlabelled 15-mer oligonucleotide (5'-CCCTCCCTCCGCGGC-3') hybridized when indicated to a 11-mer oligonucleotide (5'-CGGAGGGAGGG-3'), which in turn harboured a 5'P group also when indicated, were added to the reaction. The reaction mixture (20 μl) also contained 1 mM $MnCl_2$, 1X reaction buffer and 100 μM of the indicated dNTPs. After 60 min of incubation at 30ºC, reactions were stopped and analysed as described above.

To evaluate the effect of metal cofactors Mn^{2+} and Mg^{2+} on the ability of PrimPol to polymerize across discontinuous templates, purified PrimPol (400 nM) was incubated with the 5'[^{32}P]-labelled 20-mer oligonucleotide (5 nM) for 60 min at 30ºC. The reaction mixture (20 μl) also contained 100 μM of dGTP and the indicated amounts of Mn^{2+}, Mg^{2+}, or of Mn^{2+} combined with 5 mM Mg^{2+}. Reactions were stopped by addition of loading buffer and primer extension was analysed as described above.

For *in vitro* analysis of 8oxodG tolerance, a 5'[^{32}P]-labelled 15-mer DNA primer (5'-CTGCAGCTGATGCGC-3') was hybridized to a 34-mer DNA template (5'-

GTACCCGGGGATCCGTAC8GCGCATCAGCTGCAG-3'), and incubated with purified PrimPol (200 nM) in the presence of the indicated concentrations of dNTPs/NTPs and the indicated concentrations metal cofactors Mg^{2+} or Mn^{2+}. The reaction mixture (20 μl) contained 1X reaction buffer and 2.5 nM of the template/primer DNA. After 60 min of incubation at 30ºC reactions were stopped and analysed as described previously, band intensities were quantified by densitometry.

PrimPol primer realignment capacity was evaluated by incubating purified PrimPol (200 nM) with a 5' [^{32}P]-labelled 14-mer DNA primer (5'- CACTGACTGTATGATG-3') hybridized to a 30-mer DNA template (5'-CTCGTCAGCATGTTCATCATACAGTCAGTG-3'). The reaction mixture contained 2.5 nM of the labelled DNA, 1X reaction buffer, 10 μM of either dATP or dCTP and the indicated concentrations of Mn^{2+} or Mg^{2+}. After 60 min of incubation at 30°C, primer extension was analysed as described previously.

3. Steady-state kinetics assays

Kinetic parameters of 1nt gap-filling reactions mediated by *Sp*Pol4 were analysed as described previously (Creighton et al., 1995). For these analyses, a 5'[^{32}P]-labelled 15-mer DNA primer (5'- GATCACAGTGAGTAC-3') was hybridized to a 28-mer template (5'-AGAAGTGTATCTNGTACTCACTGTGATC-3', where X= dA, dC, dG or 8oxodG) and to a 12-mer downstream oligonucleotide harbouring a 5'P (5'P-AGATACACTTCT-3) to generate a dsDNA molecule with a 1nt-gap. The reaction mixture (20 μl) contained 1X reaction buffer (50 mM Tris-HCl pH 7.5, 1 mM DTT, 4% glycerol, 0.1 mg/ml BSA), 0.2 μM of the gapped DNA substrate and 2-8 nM of purified *Sp*Pol4. Reactions were initiated by adding the nucleotide at different concentrations ranging from 0.01 to 25 μM, except for dCTP incorporation opposite 8oxodG and 8oxoGTP incorporation opposite dA where the concentrations used ranged from 0.1 to 250 μM and dGTP incorporation opposite dC where the concentrations used ranged from 0.001 to 2.5 μM. After incubation for 5 min at 30°C, reactions were stop by adding loading buffer. Primer extension was analysed by 8 M urea/20% PAGE and gel band intensities were quantified using a BAS reader 1500 (Fujifilm). The observed rate of nucleotide incorporation (extended primer) was plotted as a function of nucleotide concentration and the data were fit to the Michaelis-Menten equation using non-linear regression to determine the apparent K_m and V_{max} parameters. The relative insertion efficiency (f^eins) was determine using the following equation $f^e\text{ins} = (k_{cat}/K_m)_{damaged}/(k_{cat}/K_m)_{undamaged}$, where $k_{cat} = V_{max}/[\text{enzyme}]_{total}$.

4. Electrophoretic mobility shift assays

Electrophoretic mobility shift assays were performed using a 5'[γ^{32}-P] labelled 13-mer oligonucleotide (5'-CCCTCCCTCCCGT-3') hybridized to a 11-mer oligonucleotide harbouring a 5'P group (5'P- GGGAGGGAGGG-3'). Purified Polμ (either 200, 400 or 600 nM) was incubated with 14 nM of the labelled DNA and 1X reaction buffer in a final volume of 10 μl. After 10 min of incubation at 30°C samples were mixed with 3 μl of 30% glycerol and subsequently resolved by native 4% polyacrylamide (w/v) gel electrophoresis. After electrophoresis the gels were dried and the labelled DNA was detected by either autoradiography or using a BAS-1500 phosphorimager (Fujifilm).

5. Ribonucleotide excision assays

To analyse RNase H2 activity present in WCE, a 5' [^{32}P]-labelled 28-mer oligonucleotide (5'-GATCACAGTGAGTACNAGATACACTTCT-3', where N = dA, dC, rC or rA) was hybridized to a 28-mer oligonucleotide (5'-AGAAGTGTATCTNGTACTCACTGTGATC-3', where N = dG, dT or 8oxodG) to generate a labelled dsDNA molecule. The labelled dsDNA (2.5 nM) was incubated with 30 μg of the WCE in 20 μl of reaction mixture containing 1X reaction buffer (50 mM Tris-HCl/ pH 7.5, 2.5 mM $MgCl_2$, 1 mM DTT, 4% glycerol and 0.1 mg/ml BSA) for the indicated times at 30°C. DNA incision by RNase H2, was analysed by 8 M urea/20% PAGE and detected by either autoradiography or using a BAS-1500 phosphorimager (Fujifilm). The labelled 15-mer product was quantified by densitometry.

To study the subsequent polymerization after RNase H2 incision, 2.5 nM of a 5' [^{32}P]-labelled 28 mer oligonucleotide (5'-GATCACAGTGAGTACrAAGATACACTTCT-3'), hybridized to a 28-mer oligonucleotide (5'-AGAAGTGTATCT8GTACTCACTGTGAT-3') was incubated with 30 μg of the WCE. The reaction mixture (20 μl) contained 1X reaction buffer, the indicated amounts of NTPs and/or dNTPs. Samples were incubated for 30 min at 30°C. Incision of the DNA and the subsequent extension was analysed as described above.

6. Extrachromosomal NHEJ repair assay

To evaluate wild-type Polλ and mutant T204A, the extrachromosomal substrate preparation and NHEJ repair assays were carried out as described previously (Pryor et al., 2015). Briefly, 285-bp linear DNA fragments were generated by PCR amplification with primers (5´-CAAGTGGTCCACCGTCATGGCTTAGCTGTATAG and 5´-G CCGACCAGCGTCATGGCACACCCATCTCA), digested with BstXI (New England Biolabs) to generate GACG3' overhangs and purified using a Qiaquick PCR purification

kit (Qiagen). This purified substrate (20 ng), together with 600 ng of pMAX-GFP plasmid (Lonza), was introduced into $2x10^5$ Polμ-Polλ double-deficient mouse embryonic fibroblasts (MEFs) in a 10 μl volume by electroporation (Neon, Invitrogen) using a 1350 V-30 ms pulse. Following electroporation, cells were incubated at 37 °C for 1h in fresh media, washed with PBS to remove untransfected substrate, and the total cellular DNA was harvested using a QIAamp DNA mini kit (Qiagen). Complementation of MEF cells with purified proteins were carried out as described above but with the inclusion of 0.1–0.5 ng of purified proteins. Cells lacking both polymerases were used to ensure that all of the products of synthesis could be unambiguously attributed to activity of the introduced protein (Pryor et al., 2015). Repair accuracy was characterized by PCR amplification of the repair products using Cy-5 labelled PCR primers (5´-CTTACGTTTGATTTCCCTGACTATACAG-3' and 5´-GCAGGGTAGCCAGTCTGAGATG-3') and digestion with enzyme AatII (New England Biolabs). Digestion products were resolved on a 5% (wt/vol) native polyacrylamide gel, visualized using a Typhoon Imager (GE Healthcare) and quantified using ImageJ.

Extrachromosomal repair assays to evaluate wild-type Polμ and mutants G174S and R175H were carried out as described in above. In this case, substrates were assembled by ligation of ~15 bp double-stranded DNA caps containing the desired overhang sequence to a 280 bp core fragment digested with Bsai-HF (NEB) at a ratio of 3:1 (cap:core). The primers used to generate the caps were the following: C3' cap1 (5'-ACGTCACCCATCTCA-3' and 5'-AGTCTGAGATGGGTGACGTC-3'), C3' cap2 (5'-ACGTCCTTAGCTGTATA-3' and 5'-TGACTATACAGCTAAGGACGTC-3'), GCG3' cap1 (5'-TGGCACACCCATCTCA-3' and 5'-AGTCTGAGATGGGTGTGCCAGCG-3') GCG3' cap2 (5'-TGGCTTAGCTGTATA-3' and 5'-TGACTATACAGCTAAGCCAGCG-3') GACG3' cap1 (5'-GTGGCACCCATCTCA-3' and 5'-AGTCTGAGATGGGTGCCACGACG-3') and GACG3' cap2 (5'-GTGGGCTTAGCTGTATA-3' and 5'-TGACTATACAGCTAAGCCCACGACG-3'), where the asterisk (*) denotes 5'-phosphorylation. Substrates were then purified using a Qiaquick PCR purification kit (Qiagen), and resolved on a native acrylamide gel to ensure substrates preparations were free of unappended core and excess cap. Protein complementation was carried out as above with the addition of purified protein (10 or 100 ng) to the substrate transfection solution immediately before electroporation. Repair junctions were amplified also as described previously using Cy-5 labeled PCR primers and characterized by restriction enzyme digests. The restriction enzymes used for each substrate were as follows: SalI for the +G junctions of the C3′ substrate,

*Hpy166*II for the +X junctions of the C3' substrate, AfeI for the +C junctions of the GCG3′ substrate, MluI for the +C products of the GACG3' substrate, or AatII for the +TC products of the GACG3′ substrate. Digestion products were resolved, visualized and quantified as described above.

7. *In vitro* kinase assays

7.1 *Sc*Pol4

Tel1-HA was immunoprecipitated from cells previously transformed with plasmid pKR5, which encodes an HA-tagged *TEL1* gene (Mallory and Petes, 2000). Control non-transformed cells were assayed in parallel to obtain HA-immunoprecipitates without HA-Tel1 enrichment that were used as a negative control in kinase assays. Both transformed and non-transformed cells were grown to exponential phase and broken using glass-beads in lysis buffer (25 mM MOPS pH 7.2, 15 mM EGTA, 0.1% NP-40, 150 mM KCl, 1 mM DTT, protease inhibitor cocktail (Sigma), 1 mM phenylmethylsulfonyl fluoride). Extracts were clarified by centrifugation and HA-tagged Tel1 was immunoprecipitated from soluble fractions with anti-HA antibodies (Roche). Immunocomplexes were collected with Protein G-coupled DynaBeads (Life Technologies) and used in kinase assays as described previously (Mallory and Petes, 2000) to test the phosphorylation of recombinant partially-purified *Sc*Pol4.

7.2 Polλ

Recombinant wild-type Polλ and phospho-dead mutants (T204A, T188A and T188A-T204A) were expressed and purified as described above. These purified proteins were phosphorylated *in vitro* using human DNA-PK complex (Promega) in kinase reaction buffer (50 mM Tris-HCl pH 7.5, 10 mM $MgCl_2$, 0.1 mM EDTA, 2 mM DTT) supplemented with 200 µM of ATP and 100 ng of double-stranded DNA. Radiolabelling assay was performed in the presence of [γ-^{32}P]ATP (3000 Ci/mmol) (PerkinElmer). All reaction mixtures were incubated at 30ºC for 30 min and boiled in Laemmli sample buffer for 5 min. Radioactive samples were separated by 4-20% gradient SDS-PAGE gels (Biorad), dried and detected by phosphor-imaging using a BAS-1500 phosphorimager (Fujifilm). Quantification of relative band intensities was carried out using ImageJ software.

For kinase assay on peptide-scanning arrays, N-terminal acetylated overlapping dodecapeptides covering the N-terminal domains of human Polλ were generated by automated spot synthesis onto an amino-derivatized cellulose membrane (CNB Proteomics Core Facility, Proteored, Spain). Peptides were immobilized by their C-

termini via a polyethylene glycol spacer. Overlapping peptides were spotted onto membrane so that they shared 10 amino acids with its adjacent peptide on the array, corresponding to a change of two amino acids per peptide. The incubation of the peptide-array with human purified DNA-PKcs (a gift of Dr. Susan Lees-Miller) and [γ-^{32}P]ATP was performed as described above.

8. Thermal shift and partial proteolysis assays

For protein thermal shift experiments, purified human Polλ proteins (2 μg each sample) were mixed with PTS-Dye (Applied Biosystems) and melting profiles were obtained within a range of 25–99ºC using a ramping rate of 0.05ºC s^{-1} and an acquisition of 20 data points per degree celsius in a ViiA™7 Real-Time PCR System (Applied Biosystems). Data was analysed using the Protein Thermal Shift™ Software v1.0 (Applied Biosystems). Data was corrected for the background signal of the buffer conditions and presented as units of fluorescence with respect to temperature. Melting temperatures (T_m) were determined according to the Boltzmann model. Error bars represent S.D. from n=4 independent replicates.

For proteolysis assays purified human Polλ proteins (5 μg each sample) were incubated at 37ºC for 120 min with 0.2 μg trypsin (Promega) in a buffer containing 25 mM MOPS pH 7.0, 20 mM Tris pH 8.0, 5 mM $MgCl_2$, 8% glycerol, 80 mM NaCl and 2 mM DTT. Reactions were stopped and boiled in Laemmli buffer for 5 min at 95ºC and resolved by 10% SDS-PAGE and Coomassie blue staining.

9. *S.pombe* growth conditions and whole cell extract (WCE) preparation

9.1 Strains and growth conditions

Fission yeast cells were grown and manipulated according to standard protocols in either yeast extract (YES) or minimal medium (EMM) (Moreno et al., 1991). Appropriate amino acids were added to the medium when required to a final concentration of 250 mg/l. The strains involving Pol4 deletion (*Δpol4*) carried the construction pol4::KanMX6, as previously described in (González-Barrera et al., 2005).

To over-produce GST:*Sp*Pol4, the *h$^-$ ura4-D18 pDS473(GST)*:Pol4 and *h$^-$ ura4-D18 pDS473(GST)* strains were generated by transforming the *h- ura4-D18 Δpol4* strain by the lithium acetate protocol (Norbury and Moreno, 1997) with pDS473(GST) control plasmid or the pDS473(GST):*pol4* plasmid, in which *pol4* is under the control of the thiamine-repressible *nmt* promoter (15 μM of thiamine were added for full repression). These strains were grown exponentially in EMM medium containing thiamine (15 μM). Subsequently, the cells were washed three times and resuspended

in the same medium without thiamine. After 18 h of overproduction, $3x10^8$ cells were collected to obtain samples for cell extracts.

The *h⁻ ura4-D18 leu1-32 ade6-M26* (provided by Dr. A. Pastink (Leiden University Medical Center)) and the *h⁺ ura4-D18 leu1-32 ade6-704 Δrnh201:kanMX* (provided by Prof. Antony Carr (Univ. of Sussex, GDSC)) strains were used to study RNase H2 mediated removal of ribonucleotides paired to 8oxodG. The strains were grown in EMM supplemented with the appropriated amino acids until logarithmic phase (0.6-0.8 $O.D_{595nm}$) and a sample of $3x10^8$ cells was collected.

To induce cell cycle arrest in G1 phase, the thermosensitive strains *cdc10-129* (provided by Dr. S. Moreno (Institute of Functional Biology and Genomics, Spain)) and *cdc10-129 Δpol4* were grown in EMM until they reached logarithmic phase (0.6-0.8 $O.D_{595nm}$). Subsequently, cells were arrested at the restrictive temperature of 36°C during 4 h and samples of each culture were collected to obtain whole cell extracts (WCE). To obtain samples from cells arrested in G2 phase, the thermosensitive *cdc25-22* (provided by Prof. Juan Jiménez (Univ. Pablo de Olavide, Spain)) strain was used following the same protocol described for *cdc10-129* mutants.

To induce arrest in mitosis, the thermosensitive *nda3KM-311 leu1-32* ((provided by Dr. S. Moreno (Institute of Functional Biology and Genomics, Spain)) strain was grown exponentially in YES medium until it reached logarithmic phase (0.6-0.8 $O.D_{595nm}$). Cells were subsequently arrested at the restrictive temperature of 19°C for 6 h and a sample from the culture was collected.

9.2 *S. pombe* WCE preparation

Samples of $3x10^8$ cells of each culture in asynchronous and arrest conditions were collected and washed with stop buffer (NaCl 150 mM, NaF 50 mM, EDTA 10 mM and NaN_3 1 mM, pH 8). Pellets were kept at -80°C. The frozen cells were thawed on ice and resuspended in 50 µl of cold lysis buffer (PBS, NaF 50 mM, EDTA 2mM pH 8, NP-40 1%, p-NH_2-benzamidine 1.3 mM, phenylmethylsulfonyl sulfate (PMSF) 1 mM and a protease inhibitor cocktail (Roche)). Cells were broken using 750 mg of glass beads (0.4 mm, Sigma) for 15 seconds (x3) in a Fast-prep machine (Bio101 Inc.) and the crude extract was recovered with 0.2 ml of lysis buffer. After centrifugation (30 min, 15000 rpm) the soluble fraction was collected and kept at -80°C. Protein concentration was determined by BCA protein assay kit (Thermo Scientific Pierce).

10. Immunoprecipitation

10.1 *Sc*Pol4

Wild-type *Sc*Pol4 and T540A mutant were tagged with the Flag epitope by PCR amplification using primers CT-P4s (5'-CTATGAATCGATATGTCTCTAAAGGGTAAAT-3') and p4FLAGnot-as (5'-TTGATCGCGGCCGCTTAGATGTTGTCATCGTCATCTTTATAATCTAATGCAGTTTTTTTTTC-3'), together with the aforementioned pCM184-[*POL4*] plasmids as a template. The different PCR products were digested with *ClaI* and *NotI* and then cloned into the pCM184 plasmid. The constructs were transformed in either *Δpol4* (*MATa-inc ade2-1 can1-100 his3-11,15 leu2**Δ**::SFA1 trp1-1 ura3-1 ade3::GAL-HO lys2**Δ**::GAL1p-ISCEI ACT1**Δ**i ChrIII-GAL1p::leu2**Δ**3´::ACT1-i**Δ**3´::ISceI::URA3 ChrXV-HYG::HO::ACT1-i**Δ**5´::leu2**Δ**5´ pol4**Δ**::natMX4*) or *Δpol4Δtel1 (MATa-inc ade2-1 can1-100 his3-11,15 leu2**Δ**::SFA1 trp1-1 ura3-1 ade3::GAL-HO lys2**Δ**::GAL1p-ISCEI ACT1**Δ**i ChrIII-GAL1p::leu2**Δ**3´::ACT1-i**Δ**3´::ISceI::URA3 ChrXV-HYG::HO::ACT1-i**Δ**5´::leu2**Δ**5´ pol4**Δ**::natMX4 tel1**Δ**::kanMX4) S. cerevisiae* strains, which were isogenic to W303 and generated from the strain (*MATa-inc ade2-1 can1-100 his3-11,15 leu2**Δ**::SFA1 trp1-1 ura3-1 ade3::GAL-HO lys2**Δ**::GAL1p-ISCEI ACT1**Δ**i ChrIII-GAL1p::leu2**Δ**3´::ACT1-i**Δ**3´::ISceI::URA3 ChrXV-HYG::HO::ACT1-i**Δ**5´::leu2**Δ**5´*) by PCR-based gene replacement and confirmed by PCR and Southern analyses following standard procedures.

The cells were grown up to the exponential phase and were then synchronized at G1 by addition of α-factor. DSBs were induced by addition of 100 μg/ml Zeocin (Invitrogen). After 1 h incubation, cells were broken using glass-beads in lysis buffer (20 mM Hepes-KOH pH 7.5, 150 mM NaCl, 10% glycerol, 0.1% Tween-20, 1 mM phenylmethylculphonyl fluoride, Complete protease inhibitor cocktail (Roche), PhosSTOP phosphatase inhibitor cocktail (Roche)) for 20 min at 4°C. Extracts were clarified twice by centrifugation. Flag-*Sc*Pol4 proteins were immunoprecipitated from supernatants with anti-Flag M2 antibody (Sigma) coupled to Protein G Sepharose 4 Fast Flow (GE Healthcare) in lysis buffer overnight at 4°C on a rotating wheel. Sepharose-bound proteins were centrifuged, washed extensively with lysis buffer and eluted in Laemmli buffer.

10.2 Polλ

For immunoprecipitations, $2x10^5$ human HEK293T cells were seeded per well in 6-well dishes, cultured for 24 h and transfected with p3xFLAG-Myc-CMV expression vector containing either wild-type POLL or POLL-T204A phospho-dead mutant.

Twenty-four hours later, cells were either mock-irradiated or irradiated with 10 Gy of IR. When indicated, cells were pre-incubated with 10 μM DNA-PKcs inhibitor Ku7441 (Tocris) for 1 h. At the indicated times post-irradiation, asynchronous cultured cells were washed with cold-phosphate buffered saline (PBS) and collected by low speed centrifugation. Cells were lysed in 500 µl lysis buffer (20 mM Tris-HCl pH 7.5, 150 mM NaCl, 10% glycerol, 2 mM EDTA, 1% NP-40, 1 mM PMSF, protease and phosphatase inhibitor cocktails (Sigma) and 1 mM DTT) homogenized and incubated on ice for 30 min. Lysates were cleared by centrifugation at 13,000 rpm for 20 min at 4ºC and input (whole cell extract) samples saved for subsequent analysis. Remaining supernatants were incubated with FLAG M2 monoclonal antibody (Sigma) overnight at 4ºC. Immuno-complexes were then incubated with Protein G-coupled Dynabeads (Life Technologies) for 4 h with end-to-end mixing at 4°C. Beads were washed two times in lysis buffer and bound immuno-complexes were eluted by boiling in Laemmli buffer at 95ºC for 5 min.

11. Western blotting

Proteins were resolved by 10% SDS-PAGE. When indicated, 25 μM Phos-tag (Wako) was included in the acrylamide/bisacrylamide solution (Sigma). In Phos-tag-containing gels proteins were resolved by 6% SDS-PAGE. Western blot analyses were performed by standard techniques using the following primary antibodies: mouse monoclonal anti-FLAG M2 (Sigma), mouse anti-tubulin (Sigma), mouse anti-GST (Sigma), rabbit anti-Ku80 (Santa Cruz), rabbit anti-DNA-PK (Santa Cruz), and rabbit anti-phospho (Ser/Thr) ATM/ATR substrate (Cell Signaling). Quantification of relative band intensities was carried out using ImageJ software.

12. Generation of a phosphospecific antibody to Polλ Thr^{204}

Antibodies against Polλ phosphorylated at threonine 204 were generated in rabbit using pT204-containing peptides coupled to KLH according to standard immunization protocols. The phosphospecific antibodies for pT204 were partially purified from serum by two sequential steps using aldehyde-activated cross-linked beaded agarose columns (Thermo Scientific) coupled to either the synthetic non-phosphopeptide or phosphopeptide (Thermo Scientific) according to the manufacturer protocol. Antibodies were eluted using 200 mM glycine pH 2.5, neutralized with Tris 1M pH 8 and concentrated with centrifugal filters (Centricon 3,000 NMWL Ultracel YM, Millipore). Phospho-specific antibodies were incubated with the non-phosphorylated T204-containing peptide (5 μg/ml) during Western blot experiments.

13. Cell culture

Human embryonic kidney 293 cells (HEK293T) and human osteosarcoma cells (U2OS) cells were cultured in DMEM medium (Sigma) supplemented with 10% fetal bovine serum (Sigma), 2 mM L-glutamine and antibiotics (100 units/ml penicillin, 100 μg/ml streptomycin; Sigma) at 37°C in a humidified atmosphere containing 5% CO_2. Mouse embryonic fibroblast cells were cultured as previously described (Pryor et al., 2015). Transient transfections of plasmids were performed with Gene Juice (Novagen) according to manufacturer instructions.

14. Immunofluorescence

For standard immunofluorescence studies approximately 2×10^5 U2OS cells were seeded onto sterile glass coverslips in each well of a four-well dish, cultured for 24h and transfected with FLAG-Polλ constructs as described above. Twenty-four hours later, cells were either mock-irradiated or irradiated with 10 Gy of IR and allowed to recover for the indicated time. Cells were fixed with 4% paraformaldehyde in PBS at room temperature, permeabilized with PBS supplemented with 0.2% Triton X-100 for 2 min and blocked in PBS-5% BSA for 30 min. Then, cells were incubated with mouse monoclonal anti-FLAG M2 (Sigma) and rabbit polyclonal anti-53BP1 (Santa Cruz) diluted in PBS-5% BSA. After washes with PBS-0.1% Tween20, cells were incubated with the corresponding Alexa Fluor-conjugated secondary antibodies (Jackson) and washed again as described above. Finally, they were counterstained with 4,6 diamidino-2-phenylindole (DAPI 1 μg/ml; Sigma) and mounted using Vectashield mounting medium (Vector Laboratories). 53BP1 foci were manually (double-blind) counted in 40 cells from each experimental condition using a Leyca DM6000B fluorescence microscope with a HCX PL APO 63x/NA 1.40 oil immersion objective.

For proximity ligation assays (PLA) U2OS cells were grown on sterile glass coverslips and transfected as described above. After 48h cells were exposed or not to 2 Gy of IR and allowed to recover for 1 h. Then, cells were fixed and permeabilized as previously described. The PLA assay was performed with the Duolink PLA kit (Sigma) following manufacturer's instructions, and using mouse anti-FLAG M2 (Sigma) and either rabbit anti-Ku80 (Santa Cruz) or rabbit anti-DNA-PKcs (Santa Cruz) primary antibodies. After final wash step cells were counterstained with DAPI and mounted as described above. Images were captured using a Leyca DM6000B fluorescence microscope with a HCX PL APO 63x/1.40 oil immersion objective. Images were taken at *z*-sections (10 sections) of 0.5-μM intervals using the 594-nm (Alexa 594) and 405-nm (for DAPI) lasers. Co-localization foci counting was performed blindly.

15. Primary sequence alignments and 3D protein structure visualization

Multiple alignments of amino acid sequences were performed using the MULTALIN server (Corpet, 1988) (http://multalin.toulouse.inra.fr/multalin/). 3D structural images were created with the PyMol Molecular Graphics System (Version 1.2r2, Schrödinger), using the following PDB IDs: 4LZD for human apoenzyme Polμ, 4M04 for human Polμ ternary pre-catalytic complex (Moon et al., 2014), 1BPY for human Polβ complexed with a gapped DNA and ddCTP (Sawaya et al., 1997), and 1XSN for Polλ in complex with a 1 nt-gapped DNA and ddTTP (Garcia-Diaz et al., 2005).

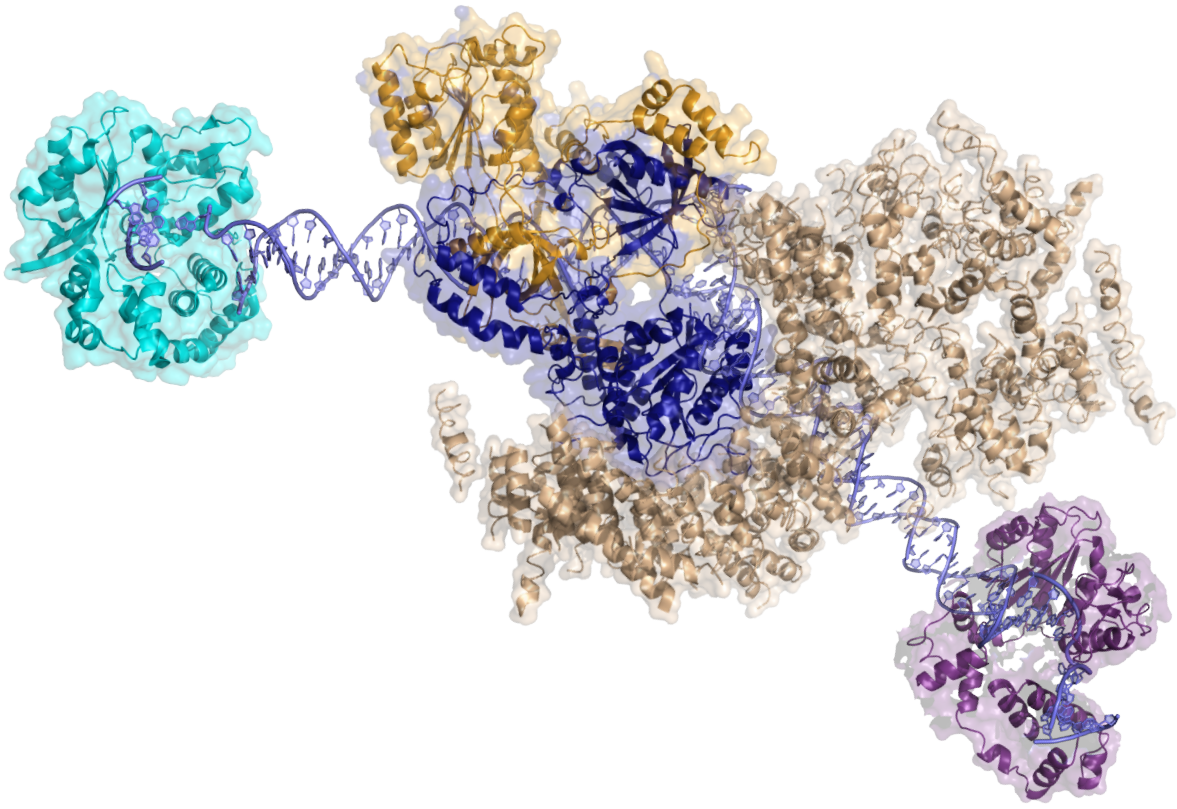

Results

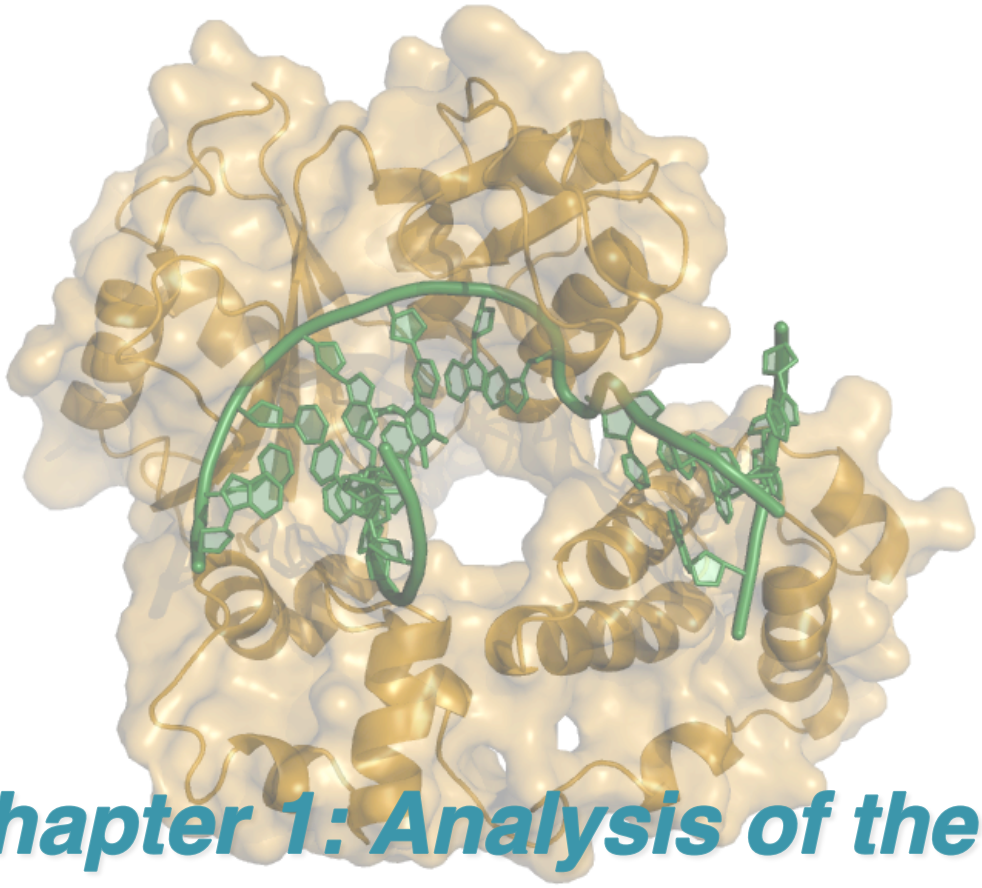

Chapter 1: Analysis of the role of SpPol4 in the tolerance of oxidative damage

Figure: SpPol4 structure modelled to human Polλ (PDB ID 1XSN)

Reactive oxygen species (ROS) arise during cellular aerobic metabolism and through the action of exogenous agents such as ionizing radiation or H_2O_2 (Valko et al., 2004). ROS accumulation can damage diverse cellular components, and is responsible for one of the most common threats to genetic stability: DNA oxidation (Lindahl, 1993). The most frequent DNA lesion generated by oxidation is 7,8-dihydro-8-oxoguanine (8oxoG), reaching steady-state levels of about 10^3 to 10^4 lesion per mammalian cell (Beckman and Ames, 1997; Helbock et al., 1998). As mentioned in the introduction section, 8oxoG is commonly found in DNA as a deoxyribonucleoside form (8oxodG) that is highly pre-mutagenic, because it does not block DNA synthesis and replicative DNA polymerases can efficiently insert the wrong dA opposite the lesion. The pre-mutagenicity of 8oxodG indeed relies on its pairing alternatives: with dC, when it adopts the regular *anti* conformation (Oda et al., 1991), and with dA, when it adopts a *syn* conformation (Kouchakdjian et al., 1991), which can eventually lead to dG:dC to dT:dA transversion mutations (Moriya, 1993; Moriya et al., 1991). The mutagenic potential of 8oxodG together with the association of ROS with carcinogenesis, aging and neurodegenerative diseases make the study of how cells deal with this lesion especially relevant (Ames, 1983; Harman, 1981; Radak et al., 2011).

Cells have developed multiple mechanisms to reduce ROS toxicity and to eliminate 8oxodG (Valko et al., 2004), being base excision repair (BER) the principal pathway that repairs this lesion. In *Escherichia coli* a three-component mechanism, referred to as GO system, prevents 8oxodG mutagenicity (Michaels and Miller, 1992). It comprises two DNA glycosylases, MutM and MutY, and also an 8oxo-dGTPase named MutT. MutM removes 8oxodG preferentially paired to dC in DNA, but if it fails to repair the damage, 8oxodG can promote dA misincorporation, probably during DNA replication. At this point, MutY excises dA from the 8oxodG:dAMP mispair to provide a second opportunity to restore the original sequence. MutT hydrolyses 8oxo-dGTP and 8oxo-GTP from the oxidized nucleotide pool to prevent their incorporation into DNA. The GO system is highly conserved through evolution from bacteria to higher eukaryotes. Mammalian cells feature homologs of MutM, MutY and MutT named OGG1, MYH and MTH1, respectively (Mo et al., 1992; Russo et al., 2007). However, despite the relevance of the GO system in the maintenance of genetic stability, some of these enzymes have not been identified in yeast. The budding yeast *Saccharomyces cerevisiae* displays two MutM homologs, Ogg1 and Ogg2, but lacks MutY and MutT homologs (Boiteux et al., 2002). The fission yeast *Schizosaccharomyces pombe* lacks MutM and MutT homologs. Little is known about how 8oxoG is repaired in *S. pombe*

but in the absence of a MutM homolog –a crucial enzyme to eliminate 8oxodG from DNA- persistence of this lesion should promote a more frequent misincorporation of dATP. To combat this threat, the MutY homolog glycosylase is conserved in fission yeast (*Sp*MYH) (Lu and Fawcett, 1998).

Also as mentioned in the introduction section, human Polλ is pivotal in 8oxodG tolerance, since after dA removal from the 8oxodG:dA mispair by MYH, Polλ is specialized in incorporating the correct dCTP opposite 8oxodG with high efficiency when the reaction is modulated by RPA and PCNA (Maga et al., 2007). Additionally after tolerating the lesion, Polλ efficiently extends the correct base pair (8oxodG:dCMP) formed (Picher and Blanco, 2007). This evidence, together with the possible persistence of 8oxodG is *S. pombe*, prompted us to analyse whether *Sp*Pol4, a Polλ ortholog and the only PolX in fission yeast, could be involved in the repair and tolerance of 8oxodG lesions, both during gap-filling and NHEJ reactions. Our results suggest that ATP is transiently inserted opposite 8oxodG by *Sp*Pol4, but readily eliminated by RNase H2 and substituted for dCTP. Moreover, analysis of 8oxo-dGTP and 8oxo-GTP incorporation suggests that *Sp*Pol4 may not contribute significantly to their accumulation in the DNA.

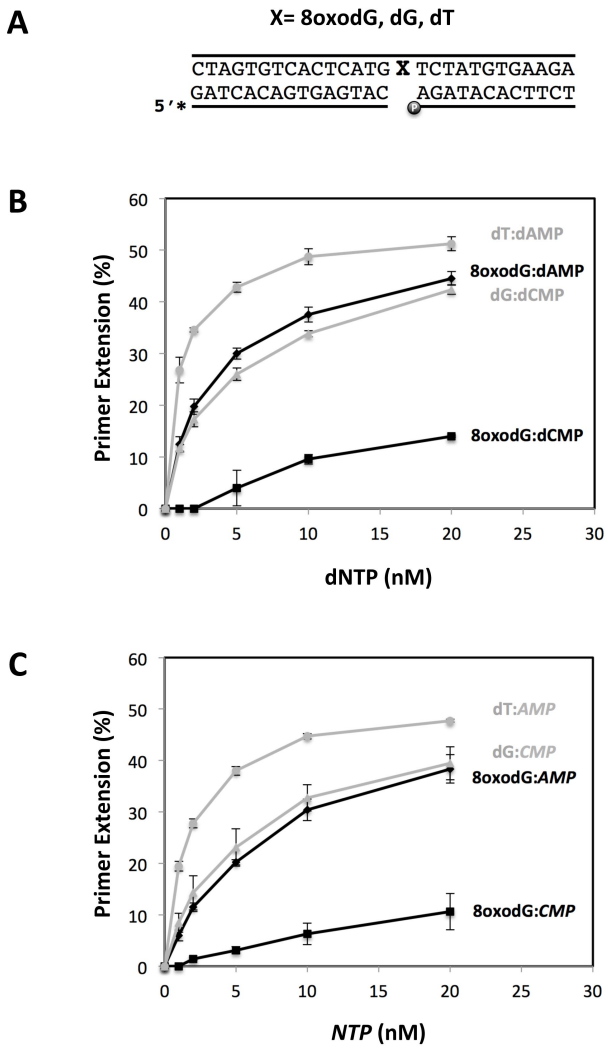

Figure 9. Error-free *vs* error-prone incorporation opposite 8oxodG by *Sp*Pol4 *in vitro*. (A) Scheme of the labelled substrates used to determine the gap-filling activity of *Sp*Pol4 *in vitro*. The molecules contained a 1nt-gap (X) with 8oxodG, dG or dT in the gap position and a recessive 5'-phosphate flanking the gap (B) Primer extension (gap-filling) by purified GST-*Sp*Pol4 (35 nM), templated either by 8oxodG, dT or dG, with the indicated amounts of dCTP or dATP (n=3). After incubation at 30°C for 15 min, samples were processed as described in Materials and Methods. (C) The same gap-filling analysis performed in (B) but using the indicated amounts of either ATP or CTP (n=3).

1. *Sp*Pol4 tolerates 8oxodG, preferably in an error-prone manner

To elucidate a possible role of *Sp*Pol4 in the tolerance of 8oxodG, we first evaluated its efficiency and

Table 2. Steady-state kinetic parameters of insertion opposite dG and 8oxodG by purified *Sp*Pol4

Template	dNTP/NTP	K_m (μM)	k_{cat} (min^{-1})	k_{cat}/K_m (min^{-1} μM^{-1})	f°_{ins}
dG	dCTP	0.36 ± 0.15	3.93 ± 0.69	10.92	1
8oxodG	dCTP	10.01 ± 1.04	3.94 ± 0.54	0.39	0.04
8oxodG	dATP	0.64 ± 0.16	7.34 ± 1.50	11.47	1.05
8oxodG	*ATP*	0.97 ± 0.18	6.78 ± 1.32	6.99	0.64

Data are means (±standard error) from at least three different experiments

preference of incorporation of dNTPs opposite the lesion. For this, purified *Sp*Pol4 was assayed on a 1nt-gapped DNA molecule either with dG, 8oxodG, or dT in the gap position (X in Figure 9A). This DNA molecule, that mimics BER and NHEJ intermediates, has a recessive 5´phosphate flanking the gap, which increases the efficiency of DNA polymerization by purified *Sp*Pol4 (González-Barrera et al., 2005). As shown in figure 9B, *Sp*Pol4 could incorporate dCTP and dATP opposite 8oxodG but, strikingly, it performed the error-prone reaction (8oxodG:dAMP) with much higher efficiency. Moreover, incorporation of dATP opposite 8oxodG was only around 3-fold less efficient than opposite dT, and similar to the insertion of dCTP opposite dG. Likewise other PolXs, such as Pol*μ* and TdT, *Sp*Pol4 has the extraordinary ability to incorporate NTPs to a DNA primer (González-Barrera et al., 2005). Remarkably, *Sp*Pol4 could tolerate 8oxodG using NTPs (Figure 9C), and as efficiently as using dNTPs. Again, *Sp*Pol4 displayed a similar preference for the error-prone reaction (8oxodG:AMP), that also reached the efficiency of CTP incorporation opposite an undamaged dG (dG:CMP; Figure 9C).

To further confirm these conclusions, we performed kinetic analysis of the gap-filling reactions opposite 8oxodG under steady-state conditions. As shown in table 2, the catalytic efficiency of dATP insertion opposite 8oxodG was 29-fold higher than dCTP, as *Sp*Pol4 displayed much lower affinity (higher K_m) for this nucleotide, and as efficient as dCTP insertion opposite an undamaged dG. As expected, the catalytic efficiency of ATP insertion was very similar to dATP (only 1.6 fold lower) and 18-fold higher than dCTP insertion opposite the lesion. All together, these results demonstrated that *Sp*Pol4 preferably tolerates 8oxodG in an error-prone manner using either dNTPs or NTPs, and that this lesion does not impair *Sp*Pol4 gap-filling efficiency compared to an undamaged template dG.

*2. Sp*Pol4 tolerates 8oxodG by using physiological concentrations of ATP

Cellular concentrations of NTPs significantly exceed those of dNTPs, being the levels of ATP particularly elevated. In both budding yeast and human cells,

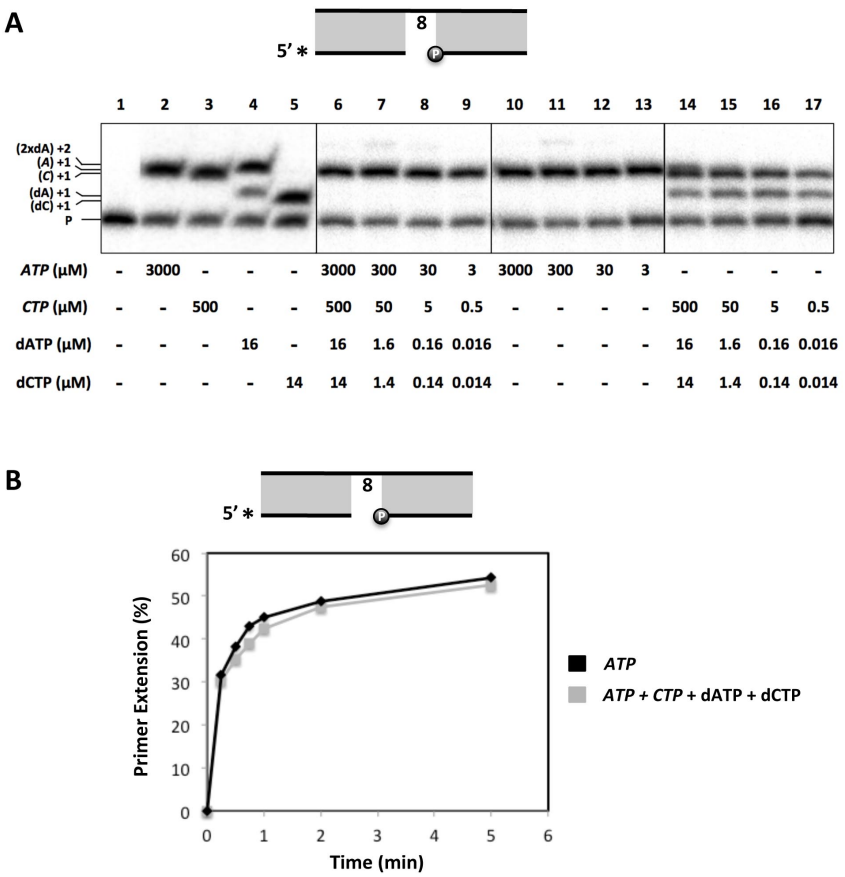

Figure 10. *In vitro* tolerance of 8oxodG by *Sp*Pol4 using physiological concentrations of nucleotides. (A) Purified GST-*Sp*Pol4 (35 nM) was incubated with the 8oxodG-gapped substrate (2.5 nM), and the indicated combination and concentration of ribo and deoxynucleotides. After incubation at 30°C for 15 min, primer extension was analysed as described in the Materials and Methods. (B) Kinetics of ATP incorporation opposite 8oxodG by purified GST-*Sp*Pol4 (35 nM), using a physiological concentration of ATP (3000 µM) either in alone or in the presence of CTP (500 µM), dATP (16 µM) and dCTP (14 µM). After incubation at 30°C for the indicated times, samples were processed as described in Materials and Methods.

concentration of nucleotide pools is very similar (Nick McElhinny et al., 2010; Traut, 1994), but in *S. pombe* it has not been precisely determined, although some studies have estimated dNTP concentrations as a percentage of either total NTP concentration (Håkansson et al., 2006) or ATP concentration (Fleck et al., 2013). Remarkably these studies demonstrate that, likewise in *S. cerevisiae*, dATP and dCTP concentrations are very similar in *S. pombe*, and represent around only 0.4% of the total ATP concentration (Fleck et al., 2013). Thus, 8oxodG tolerance by *Sp*Pol4 was evaluated using the gapped DNA molecule previously used (Figure 9) and the nucleotide concentrations described for *S. cerevisiae in vivo*. Competitive incorporation of NTPs versus dNTPs could be evaluated since they have different molecular weights, and the different +1 extended primers can be separated by gel electrophoresis, as shown in figure 10A (first panel). Therefore, when a mix of ATP, CTP, dATP and dCTP was provided at their putative physiological concentrations (3 mM ATP; 0.5 mM CTP; 16 µM

dATP; 14 μM dCTP), or at lower but proportional concentrations, *Sp*Pol4 generated only one product (Figure 10A, second panel) whose electrophoretic mobility was compatible with the incorporation of a ribonucleotide, perhaps ATP, according to the specific mobility of each independent +1 product (see Figure 10A, first panel). In fact, when ATP was provided alone, *Sp*Pol4 generated the same polymerization product, even with an ATP concentration as low as 3 μM (Figure 10A, third panel). Conversely, when ATP was removed from the nucleotide mix, *Sp*Pol4 generated 3 distinct products (Figure 10A, fourth panel), two of them corresponding to the incorporation of CTP and dATP, and a minor band likely corresponding to the incorporation of two dATP units (see also Figure 10A first panel) occurring through strand-displacement, due to the presence of a dT templating base contiguous to the 8oxodG lesion (Figure 11); interestingly, no band corresponding to incorporation of dCTP was observed, perhaps suggesting a strong and direct competition with CTP. In the presence of all the nucleotides (ATP, CTP, dATP and dCTP) at the physiological concentrations, only ATP appeared to be incorporated, suggesting that all the alternative nucleotides were outcompeted (see also Figure 12).

We next evaluated the kinetics of ATP incorporation opposite 8oxodG, at the

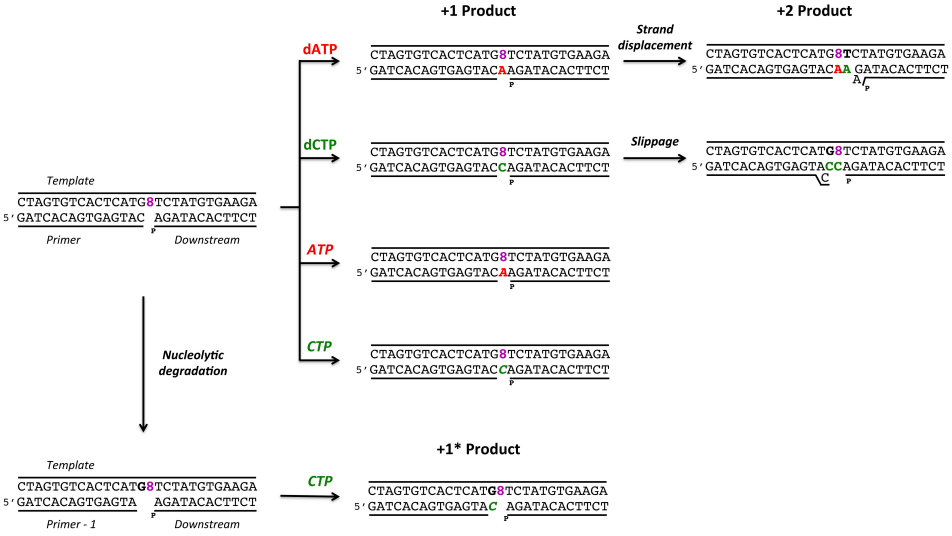

Figure 11. Extension products generated by purified *Sp*Pol4 or WCE during gap-filling opposite 8oxodG. Purified *Sp*Pol4 and other polymerases present in the cell extracts can incorporate two subsequent dATPs when the 8oxodG-containing DNA gap was provided; the first incorporation occurs opposite 8oxodG, and the second is directed by the adjacent dT, thus requiring strand displacement. Purified *Sp*Pol4 can tolerate 8oxodG incorporating only one dCTP, but other polymerases present in the cell extracts can incorporate dCTP twice, both opposite 8oxodG, and the second after realigning the primer one position backwards. *Sp*Pol4 was inefficient extending ribonucleotides, and produced mainly +1 extension products using either ATP or CTP as substrates. Given that the WCE could degrade the primer terminus, a 1 nt-deleted primer could be extended using CTP, generating a band (denoted as +1*, and detectable in Figure 13B) with slightly slower migration than the original primer.

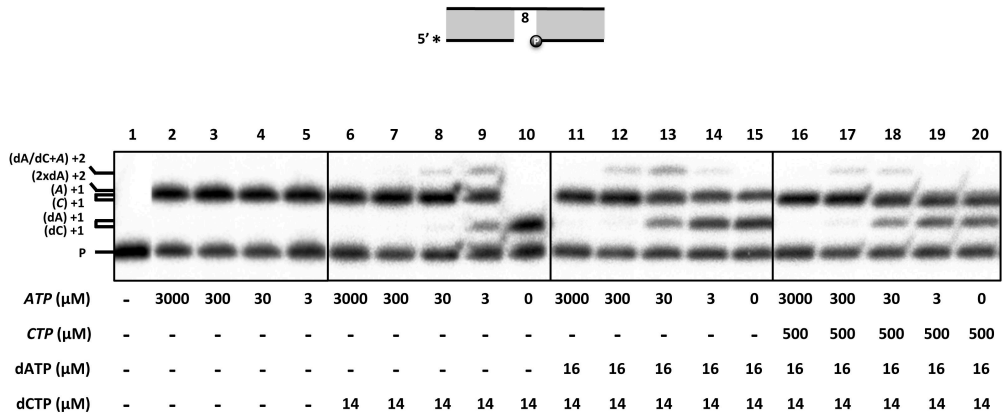

Figure 12. Incorporation of ATP opposite 8oxodG by *Sp*Pol4 in competition with physiological concentration of nucleotides. GST-*Sp*Pol4 (35 nM) was incubated with the 8oxodG-containing DNA gap, and serial dilutions of ATP (3000, 300, 30 or 3 μM) and physiological concentrations of dCTP (14 μM), dATP (16 μM) and CTP (500 μM) were added to the reaction as indicated. **Panel 1**: *Sp*Pol4 was able to insert ATP opposite 8oxodG even at the lowest concentration tested (3 μM; see panels 2-5). **Panel 2**: *Sp*Pol4 could not incorporate dCTP when ATP was provided either at 3000 μM, at 300 μM and even at 30 μM, but it was incorporated when ATP was either 1000-fold reduced to 3 μM or was not added (lanes 6-10). **Panel 3**: In agreement with our previous data, a physiological concentration of dATP (16 μM) further added to the experiment precluded any dCTP insertion, as the +1 band observed corresponds to the mobility of a primer extended (+1) with dA (lanes 13-15, and panel 4 lanes 18-20). Moreover, a 10-fold reduction of the physiological concentration of ATP (300 μM) was sufficient to outcompete completely dATP (lane 12); however, *Sp*Pol4 could efficiently incorporate dATP with 30 μM ATP (lanes 13), and outcompete 3 μM ATP, on the basis of the slightly different mobility between the (2xdA)+2 *versus* (A)+1 products (lane 14; the origin of this +2 product has been described in Figure 11). **Panel 4**: Addition of a physiological CTP concentration (500 μM) can compete ATP (note the different mobility of the (A)+1 and (C)+1 products), but only when ATP concentration is at least 100-fold reduced (30 μM; panel 4, see lanes 18-20). The slowest migrating band appearing in panels 2-4, denoted as (dA/dC+A)+2, corresponds to a first extension of the primer using either dA or dC, and a subsequent extension using ATP, mediated through strand-displacement and mimicking the described for two subsequent dATPs incorporations (Figure 11). All together, these data indicate that under physiological conditions *Sp*Pol4 will tolerate 8oxodG incorporating ATP almost exclusively, as ribonucleotides are the most abundant substrates and that even CTP can not outcompete ATP when both are provided at physiological concentrations.

physiological concentration of 3 mM. The gap-filling reaction performed by *Sp*Pol4 was very efficient and became saturated after 1 min of incubation (Figure 10B), although about 50% of the primers could not be extended, possibly due to incomplete hybridization. As expected, the kinetics of primer extension with ATP was not affected by the addition of physiological concentrations of CTP, dATP and dCTP (Figure 10B). All together, these results demonstrated that *Sp*Pol4 tolerates 8oxodG by incorporating ATP almost exclusively.

3. Error-prone incorporation of ATP opposite 8oxodG is *Sp*Pol4-specific in *S. pombe* cell extracts

To further evaluate the contribution of *Sp*Pol4 to 8oxodG tolerance *in vivo*, we tested the gap-filling activity of *S. pombe* whole cell extracts (WCE) either containing or lacking *Sp*Pol4, and using the same 8oxodG-containing gap described above. It has been demonstrated that NHEJ is the predominant DSB repair mechanism during G1

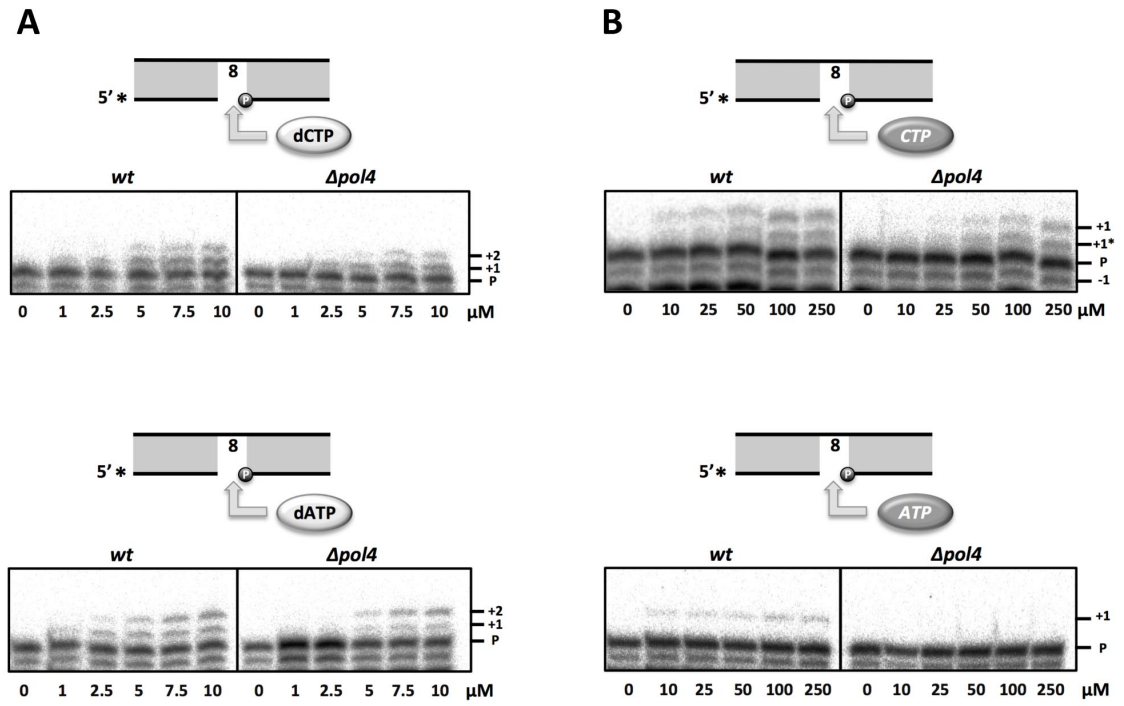

Figure 13. Incorporation of nucleotides opposite 8oxodG by *S. pombe* cell extracts. (A) Gap-filling activity by WCE derived from either wild-type or *Δpol4 S. pombe* synchronized in G1. 20 µg of each extract were incubated with the 8oxodG-gapped substrate (2.5 nM), and the indicated amounts of either dCTP (upper panel) or dATP (lower panel). (B) Gap-filling experiments were performed as in (A) but using the indicated amounts of either CTP or ATP. After incubation at 30°C for 20 min, primer extension was analysed as described in Materials and Methods.

phase in fission yeast (Ferreira and Cooper, 2004); thus, given the possible implication of *Sp*Pol4 in this pathway (González-Barrera et al., 2005; Li et al., 2012), we used G1-synchronized wild-type or *Sp*Pol4-defective (*Δpol4*) extracts. Extracts from each strain could incorporate dCTP opposite 8oxodG (Figure 13A, top), and a second dCTP incorporation mediated by primer slippage (see also Figure 11); however, *Sp*Pol4 contribution was not scored at any concentration (Figure 13A, top; compare *wt* and *Δpol4* panels). The wild-type WCE also catalysed the incorporation of dATP opposite 8oxodG (Figure 13A bottom), and a subsequent dATP incorporation mediated by strand-displacement (see also Figure 11); however, *Δpol4* WCE failed to promote misinsertion of dATP opposite 8oxodG at low concentrations (1-2.5 µM), supporting an *Sp*Pol4 contribution (Figure 13A bottom).

Incorporation of CTP by both extracts also produced two different bands (Figure 13B top): the slower migrating band (+1) corresponded to a direct insertion opposite 8oxodG, and the faster migrating band (+1*), which corresponds to its insertion opposite an undamaged dG (preceding the 8oxodG lesion) occurring onto partially degraded (-1) primer molecules (see also Figure 11). Similarly to dATP, CTP

incorporation opposite 8oxodG (+1 product) was not detected with *Δpol4* WCE when using low CTP concentrations (10-25 μM; Figure 13B top), supporting an *Sp*Pol4 contribution when reading the 8oxodG lesion; conversely, and mimicking the situation with dCTP, we could not detect an *Sp*Pol4 contribution to the +1* product (inserted opposite an undamaged dG templating base) at any concentration. Remarkably, incorporation of ATP opposite 8oxodG produced a single product, which was completely *Sp*Pol4-specific at any concentration tested, as it was undetectable in the WCE lacking *Sp*Pol4 (Figure 13B bottom).

These results suggest that *in vivo*, other polymerases in addition to *Sp*Pol4 may tolerate 8oxodG by incorporating dATP/dCTP and even CTP. However, *Sp*Pol4 appears to be quite efficient and specific to read the 8oxodG lesion with ATP, an error-prone outcome favouring transversion mutations.

4. *Sp*Pol4 inserts ATP opposite 8oxodG during NHEJ

DSBs are frequently associated with other kinds of lesions such as abasic sites, dRP residues and also damaged bases like 8oxodG (Harrison et al., 1999). Thus, damage tolerance associated to DSB repair can be essential to overcome this dangerous form of DNA damage. Firstly, we wanted to know whether *bona-fide* NHEJ could be performed *in vitro* by *Sp*Pol4 with NTPs, and in the absence of core factors, as recently shown for human Pol*μ* (Martin et al., 2013a). For that we used two different dsDNA molecules with 3'-protruding, partially complementary ends. After microsynapsis of the two ends, if bridged by the NHEJ polymerase, these molecules would form two 1 nt-gaps, one of which contains a templating dG adjacent to a connection of 4 bps of complementarity (Figure 14A). Based on previous work with human Pol*μ* and Polλ (Andrade et al., 2009), we could anticipate that a recessive 5'-phosphate exclusively present in the unlabelled DNA molecule, flanking the dG-containing gap, would orient *Sp*Pol4 to extend the labelled primer with CTP.

In these conditions, we observed an efficient +1 extension of the labelled primer only when CTP was provided, as expected from a *bona fide* NHEJ reaction (Figure 14B top left, and 14Ca). Under the same reaction conditions, when dCTP was added at similar concentrations, the efficiency of NHEJ was comparable (Figure 15A). Thus, the nearly complete lack of sugar discrimination described for *Sp*Pol4 during gap-filling (González-Barrera et al., 2005) is also valid during NHEJ.

As anticipated, this preferred insertion of CTP was drastically reduced if a 5´P was not present at the unlabelled (template) DNA end (Figure 14B, top right). As a control to

evaluate the existence of some terminal transferase activity with NTPs, that could explain the minor extension obtained with GTP and UTP, only the labelled end (acting as primer) was provided in the presence of each NTP at 0.5 μM. In this case, *Sp*Pol4 did not incorporate ATP or UTP, but catalysed some GTP and CTP incorporation (Figure 14B, bottom left). Although some terminal transferase activity cannot be formally discarded, we favour that the incorporation of GTP could have occurred as a NHEJ event in which two labelled molecules form two 1nt-gaps with a dC directing the insertion (Figure 14Cb). On the other hand, the lower background with CTP observed

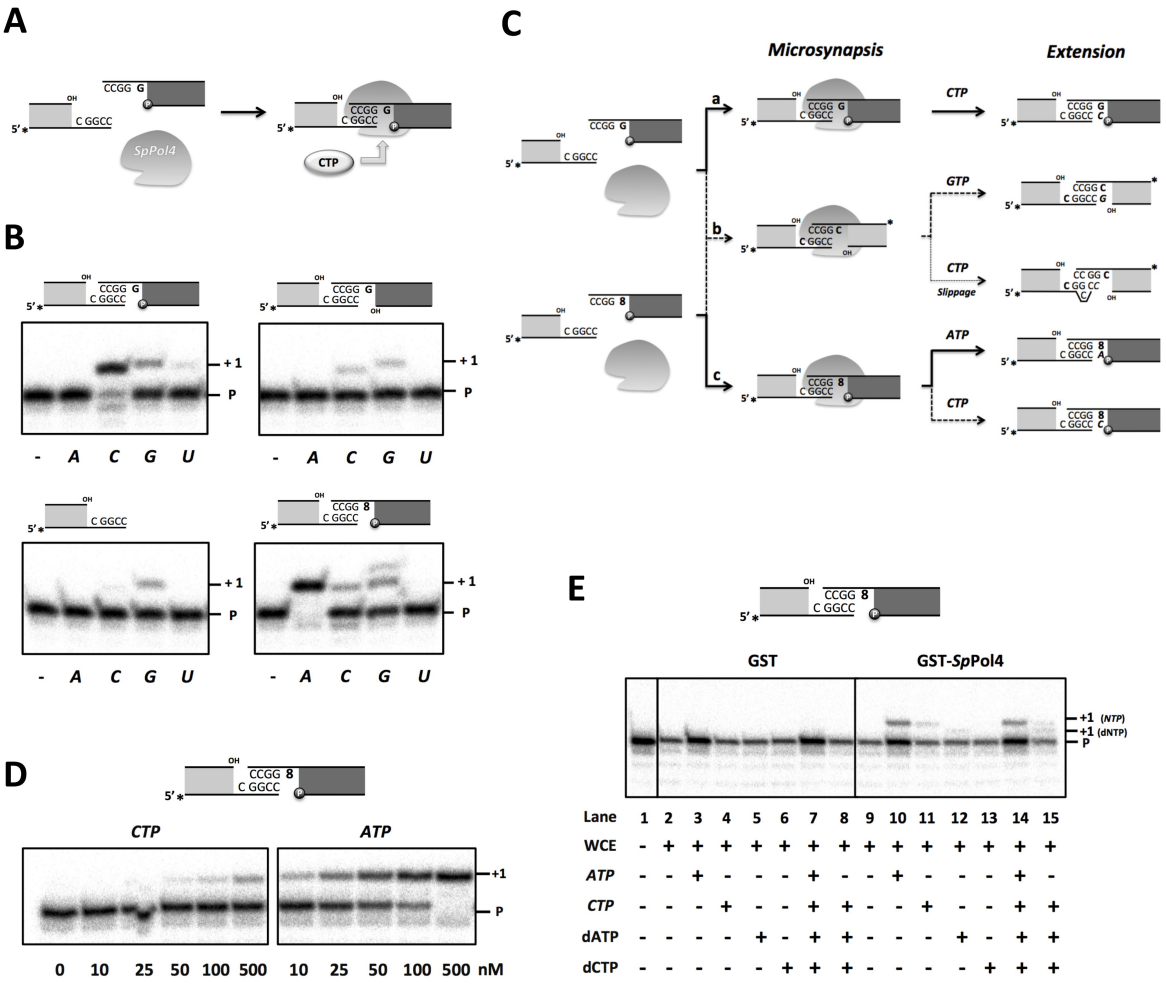

Figure 14. NHEJ coupled to 8oxodG tolerance by *Sp*Pol4. (A) Scheme of *Sp*Pol4 bridging two 3'-protruding DNA molecules used for NHEJ experiments. (B) NHEJ by GST-*Sp*Pol4 (200 nM) using a labelled 3'-protruding primer molecule (5 nM) either alone or with a set of different 3'-protruding cold template molecules (12.5 nM). ATP, CTP, GTP or UTP (500 nM) were added to the reaction when indicated. After incubation at 30°C for 60 min, NHEJ was analysed as described in Materials and Methods (C) Schematic representation of the different outcomes of the NHEJ experiments shown in (B). (D) Nucleotide insertion opposite 8oxodG during NHEJ, analysed as in (B), but using the indicated amounts of either CTP or ATP. The relative efficiency of incorporation of ATP *versus* CTP opposite 8oxodG (20-fold higher) was quantified as described in Materials and Methods. (E) Tolerance of 8oxodG during NHEJ using asynchronous WCE overexpressing either GST or GST-*Sp*Pol4 (30 μg) and physiological concentrations of ATP (3000 μM), CTP (500 μM), dATP (16 μM) and dCTP (14 μM), added as indicated. After incubation at 30°C for 30 min, NHEJ was analysed as described in the Materials and Methods. Ribonucleotides are denoted in italics.

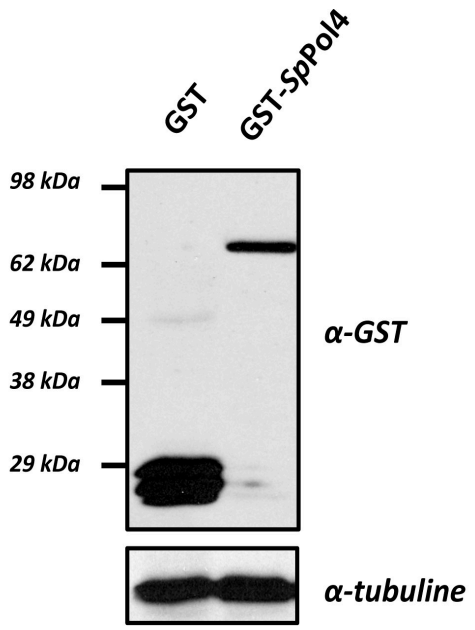

Figure 16. Western-blot analysis of GST-*Sp*Pol4 over-expression. GST-tagged *Sp*Pol4 and control GST-over-expressing *S. pombe* cell extracts (50 μg) were resolved by SDS-polyacrylamide gel electrophoresis. Over-expression of the proteins was demonstrated by western-blot analysis using anti-GST antibodies.

by providing only the primer supports the *bona-fide* NHEJ reaction shown in figure 14B (top left), but it could be also due to a NHEJ event involving two identical (labelled) ends and misalignment of the connected primer (Figure 14Cb).

To evaluate whether *Sp*Pol4 could tolerate 8oxodG during NHEJ, we performed the same experiment, but using a template molecule bearing an 8oxodG in the gap position. Under these conditions *Sp*Pol4 preferentially incorporated ATP, and much less CTP and GTP (Figure 14B, bottom right, and Figure 14Cc). The lack of any background with ATP in the previous experiments supports a *bona-fide* NHEJ reaction where 8oxodG is preferentially recognized by *Sp*Pol4 in the *syn* conformation, directing insertion of ATP. It is also worth noting that most of the incorporated CTP in this experiment is likely templated by 8oxodG, by comparison with the experiment shown in figure 14B (bottom left). Further analysis at different nucleotide concentrations demonstrated that *Sp*Pol4 tolerates 8oxodG during NHEJ by incorporating ATP with about 20-fold higher efficiency than CTP (Figure 14D). On the other hand, GTP incorporation was similar to the background detected in all the previous experiments, which again suggests that it is occurring through the synapsis of two labelled primer molecules (Figure 14Cb). The very same conclusions can be obtained when the incorporation of dATP and dCTP opposite 8oxodG was tested during NHEJ: dATP was favoured over dCTP (Figure 15B), but it can be predicted that ATP would be the preferred nucleotide inserted opposite 8oxodG given the physiological concentration of each of these substrates.

Endogenous levels of *Sp*Pol4 were insufficient to study NHEJ reactions using WCE (data not shown). Thus, to gain further insights on the 8oxodG tolerance reactions carried out by *Sp*Pol4 during NHEJ in the presence of other core factors, we obtained asynchronous WCE derived from cells overexpressing GST-tagged *Sp*Pol4 (Figure 16). These extracts were incubated with the same 3´-protruding DNA molecules

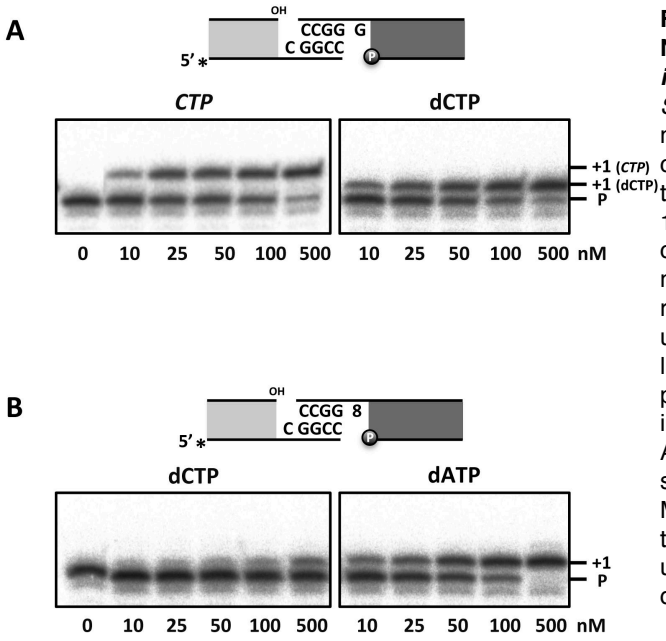

Figure 15. *Sp*Pol4 incorporates dNTPs and NTPs with similar efficiency during NHEJ *in vitro*. For the analysis of NHEJ *in vitro* by *Sp*Pol4 we used two different dsDNA molecules with 3'-protruding, partially complementary ends. After microsynapsis of the two ends, these molecules would form two 1 nt-gaps, adjacent to a connection of 4 bps of complementarity (see schemes) that require nucleotide insertion, and further ligation for full repair. (A) NHEJ by GST-*Sp*Pol4 (200 nM) using the labelled end acting as primer (5 nM; light grey), the cold end (12,5 nM; dark grey) providing a templating dG at the gap, and the indicated amounts of either dCTP or CTP. After 60 min of incubation at 30°C, the samples were processed as described in Materials and Methods. (B) NHEJ involving a templating 8oxodG, performed as in (A) but using the indicated amounts of dCTP and dATP.

described before, and physiological concentrations of ATP, CTP, dATP or dCTP, either alone or in combination. These WCE tolerated 8oxodG during NHEJ using ATP, CTP or dATP, but only if GST-*Sp*Pol4 was over-expressed (Figure 14E, lanes 10-12). In agreement with our *in vitro* data, *Sp*Pol4 preferably incorporated ATP during the repair process (Figure 14E, lane 10), when other NHEJ repair factors provided by the extract were also present. Moreover, *Sp*Pol4 incorporated ATP almost exclusively in the presence of physiological concentrations of CTP, dATP and dCTP (Figure 14E, compare lanes 14 and 15).

All together, these data indicate that *Sp*Pol4 (either in the absence or presence of NHEJ core factors) can perform *bona-fide* NHEJ and tolerate 8oxodG preferentially with ATP.

5. RNase H2 present in *S. pombe* cell extracts efficiently targets 8oxodG:AMP mispairs

The high cellular concentrations of NTPs make these nucleotides valuable substrates for DNA repair and tolerance reactions; however, their persistence in the genome is undesirable as it renders DNA more susceptible to hydrolysis. In eukaryotic organisms, RNase H2 initiates the removal of single NMPs embedded within a DNA sequence (Cerritelli and Crouch, 2009); however, whether RNase H2 or other enzymes can initiate ribonucleotide repair of 8oxodG:AMP base pairs has not been reported yet. To evaluate this hypothesis, labelled dsDNA molecules containing a single dT:dAMP, dT:AMP, 8oxodG:dAMP or 8oxodG:AMP base pair in a central position were incubated

with *S. pombe* cell extracts, corresponding to synchronized G1, G2 or M cell-cycle phases. None of the extracts incised the dsDNA at the central position corresponding to either dT:dAMP or 8oxodG:dAMP (Figure 17A; first and second panels), despite a reported *Sp*MYH-like activity that could eliminate dA paired to 8oxodG (Lu and Fawcett, 1998). Conversely, the extracts efficiently incised the labelled strand, at the 5' side of the ribo-adenosine (*A* in the figure), similarly in both DNA substrates containing either dT:AMP or 8oxodG:AMP base pairs (Figure 17A, third and fourth panels). Remarkably, the 15-mer incised product was better detectable in the G1 extract than in both G2 and

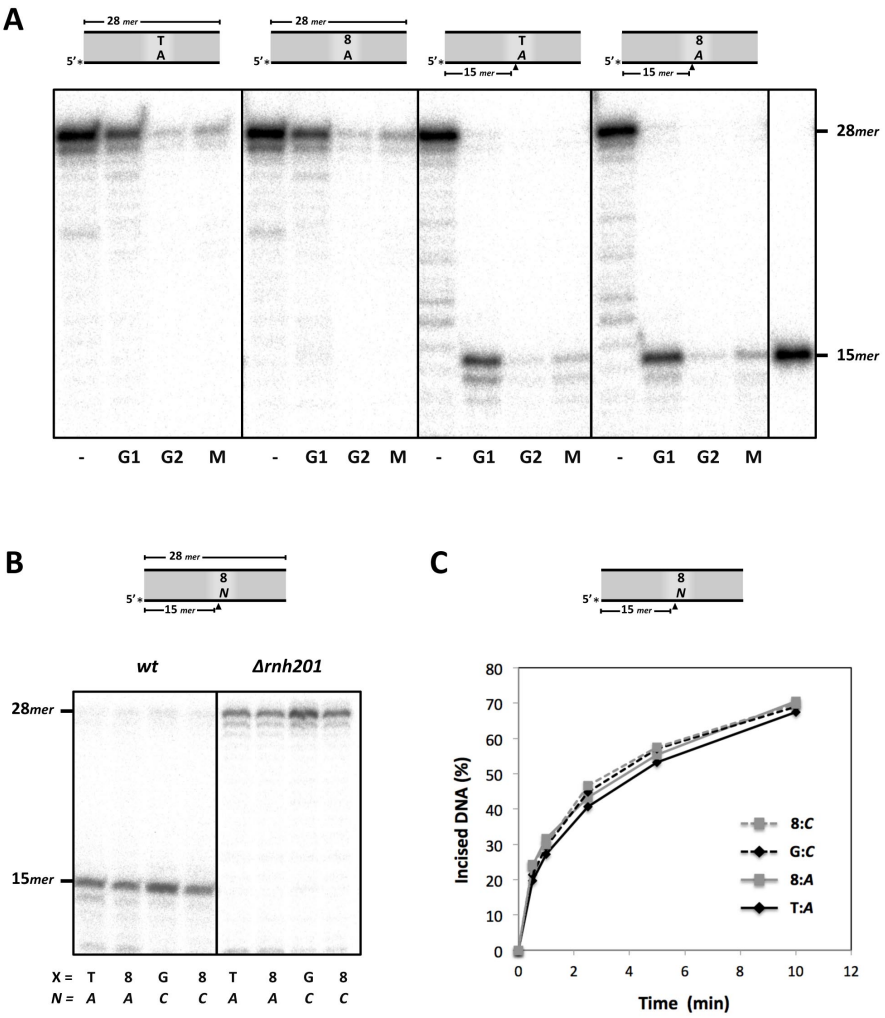

Figure 17. RNase H2 mediated 5'-incision of ribonucleotides paired to 8oxodG. (A) Ribonucleotide incision experiments performed with labelled dsDNA molecules (2.5 nM; 28*mer*) containing dT:dAMP, 8oxodG:dAMP ,dT:AMP or 8oxodG:AMP bases pairs that were incubated separately with WCE synchronized in G1, G2 or M (30 μg). These molecules were also incubated without WCE (-), to be used as a marker of the intact substrate. A labelled oligonucleotide (Sp1C; 15*mer*) was used as an appropriate molecular marker. After 30 min of incubation at 30°C, incision of the DNA was analysed as described in Materials and Methods (B) Wild-type and RNH201 null (*Δrnh201*) asynchronous WCE were incubated with labelled dsDNA molecules (2.5 nM) containing either dT:AMP, 8oxodG:AMP, dG:CMP or 8oxodG:CMP base pairs embedded, and processed as in (A). (C) Kinetics of ribonucleotide incision by RNase H2 present in wild-type G1 WCE (30 μg), performed as in (A). The percentage of 15*mer* product generated by RNase H2 is designated as incised DNA (%). Ribonucleotides are denoted in italics.

M extracts, possibly due to higher unspecific nuclease activity in the latter.

Those incised products on DNA molecules containing either dT:AMP or 8oxodG:AMP could be also obtained when using asynchronous wild-type cell extracts, and also when the DNA molecules contained either dG:CMP or 8oxodG:CMP (Figure 17B). RNase H2 is a heterotrimeric enzyme composed of 2 regulatory subunits (RNase H2 B and RNase H2 C) and a catalytic subunit (RNase H2 A), the latter named RNH201 in yeast (Cerritelli and Crouch, 2009). When using RNH201 deficient (*Δrnh201)* asynchronous extracts, no incision was detected in all cases (Figure 17B), demonstrating that RNase H2 targets not only single ribonucleotides present in dsDNA, but also those paired to the 8oxodG lesion. Quantitative analysis of the incision kinetics demonstrated that RNase H2 can remove the ribonucleotides paired to 8oxodG as efficiently as when paired to an undamaged base (Figure 17C).

6. Elimination of AMP mispaired to 8oxodG triggers specific error-free bypass in *S. pombe* cell extracts

Ribonucleotide excision repair (RER), reconstituted *in vitro* with enzymes purified from *S. cerevisiae,* requires several steps: RNase H2 incision (5' of the ribonucleotide), strand displacement-mediated DNA polymerization by Polδ and PCNA, and finally flap excision and DNA ligation performed by FEN1 and DNA ligase I, respectively (Sparks et al., 2012). In an attempt to reproduce the steps of RER that could be excising ribonucleotides inserted opposite 8oxodG lesions, and could require *Sp*Pol4 activity, we used the dsDNA molecule containing an 8oxodG:AMP base pair (Figure 18; see scheme), physiological concentrations of selected nucleotides, and either wild-type or *Δpol4* WCE (synchronized in G1). Following the activity of RNase H2, some ATP could be incorporated by the wild-type extract but barely by the *pol4*-deficient (Figure 18, lanes 2 versus 10), demonstrating again that although this reaction is limited, it is *Sp*Pol4-dependent; however, if ATP is reinserted during RER, it would be unproductive, as it would restore the excised ribonucleotide. Neither CTP nor dATP (two valid *Sp*Pol4 substrates to be inserted opposite 8oxodG, as shown *in vitro*) were incorporated by the extracts (Figure 18 lanes 3-4 and 11-12). Remarkably, dCTP was inserted as efficiently as ATP opposite 8oxodG, but irrespective of the presence of *Sp*Pol4 (Figure 18 lanes 5 and 13), demonstrating that the excised ribonucleotide can be substituted by dC, thus triggering error-free tolerance of this lesion.

On the other hand, when ATP, CTP, dATP and dCTP were provided together, 2 polymerization products were generated by both WCE (Figure 18 lanes 6 and 14). The

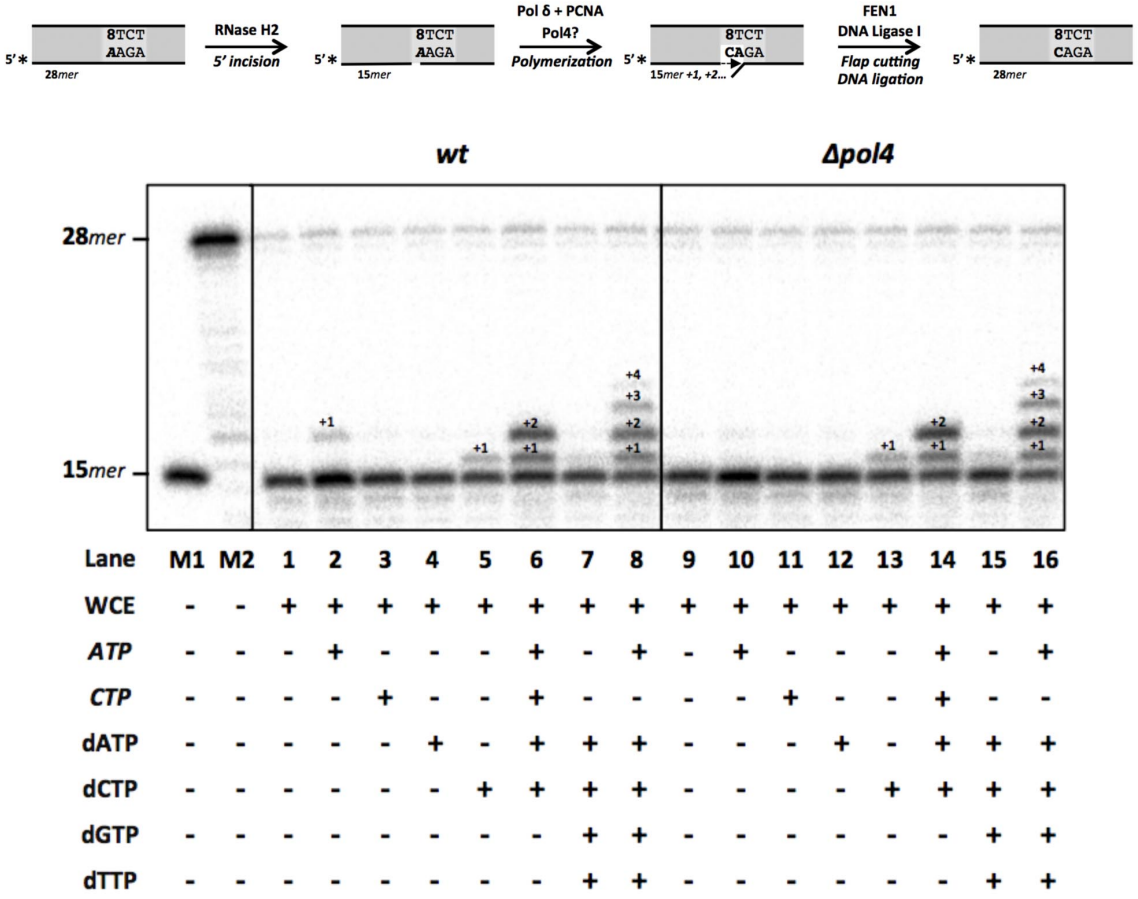

Figure 18. Ribonucleotide excision repair and error-free bypass of 8oxodG using *S. pombe* cell extracts. The top scheme shows the DNA substrate used, and the order of events compatible with the ribonucleotide excision repair (RER) pathway. Wild-type and *Δpol4* WCE synchronized in G1 (30 μg) were incubated with the labelled dsDNA molecule containing the 8oxodG:AMP base and. ATP (3000 μM), CTP (500 μM), dATP (16 μM), dCTP (14 μM), dGTP (12 μM) or dTTP (30 μM) were added to the reaction when indicated. After 30 min at 30°C, incision and further extension was analysed as described in Materials and Methods. M1, labelled oligonucleotide (Sp1C; 15*mer*) used as a molecular marker. M2, labelled dsDNA molecule (28*mer*) used as substrate for RER. In the figure, ribonucleotides are denoted in italics.

mobility of the upper band (+2) is not compatible either with an ATP incorporation after a dC first insertion, or with a first ATP incorporation, given its intensity and its *Sp*Pol4-independence; therefore, the +2 product likely corresponds to the consecutive insertion of dC and dA, the latter templated by the dT base following the 8oxodG lesion.

Remarkably, no elongation products were observed in the presence of the 4 dNTPs (Fig 18, lane 7 and 15). However, +1, +2, +3 and +4 products were observed when the 4 dNTPs were supplemented with ATP (Figure 18 lanes 8 and 16), in agreement with its need for PCNA loading, and further strand-displacement during RER process (Sparks et al., 2012).

Taken together these data demonstrated that AMP paired to 8oxodG is efficiently removed and substituted by dCMP (error-free tolerance), in a process similar to regular RER.

7. 8oxo-dGTP and 8oxo-GTP are inefficient substrates during *in vitro* polymerization by *Sp*Pol4

ROS can oxidize the cellular pools of nucleotides generating 8oxodGTP and 8oxoGTP, which may abound in *S. pombe* due to the absence of a MutT homolog and could be wrongly incorporated opposite dA. In fact, as 8oxodGTP is in *syn* configuration in solution (Jang et al., 2002), it is ready to be misrecognized (as dTTP) for most DNA polymerases. Given the flexibility of *Sp*Pol4 active site, which allows both ribo and deoxynucleotide substrates and efficiently tolerates 8oxodG template lesions, we evaluated whether *Sp*Pol4 could use 8oxo-dGTP/8oxo-GTP as nucleotides for DNA polymerization. For this, purified *Sp*Pol4 was incubated with a 5' labelled 1nt-gapped DNA molecule with either dC or dA in the gap position and variable concentrations of either 8oxo-dGTP or 8oxo-GTP. Interestingly, *Sp*Pol4 incorporated 8oxo-dGTP with

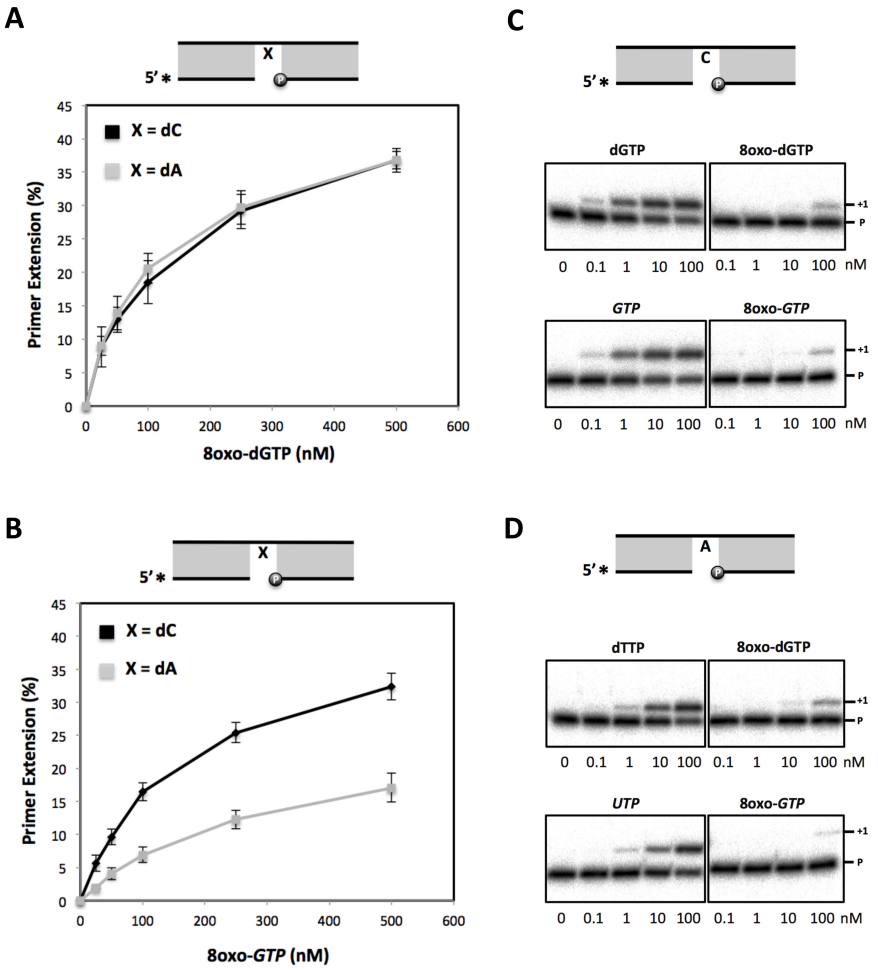

Figure 19. 8oxo-dGTP and 8oxo-GTP incorporation by *Sp*Pol4 *in vitro*. (A) Primer extension (gap-filling) by purified GST-*Sp*Pol4 (35 nM) opposite templates dC or dA using the indicated concentrations of 8oxodGTP (n=3). After incubation at 30°C for 15 min, primer extension was analysed as described in the Materials and Methods. (B) The same gap-filling experiment described in (A) was carried out using 8oxo-GTP (n=3). (C) Comparative incorporation of 8oxo-dGTP/8oxo-GTP *versus* undamaged dGTP/GTP by purified GST-*Sp*Pol4 (35 nM) opposite the dC-gapped molecule, performed as in (A). (D) As in (C) but using dTTP and UTP as undamaged nucleotides and template dA.

Table 3. Steady-state kinetic parameters of 8oxo-dGTP and 8oxo-GTP incorporation by purified *Sp*Pol4

Template	dNTP/NTP	K_m (μM)	k_{cat} (min^{-1})	k_{cat}/K_m (min^{-1} μM^{-1})	f°_{ins}
dC	dGTP	0.018 ± 0.001	1.87 ± 0.11	103.89	1
dC	8oxo-dGTP	3.76 ± 1.86	0.93 ± 0.14	0.25	2.41×10^{-3}
dC	*8oxo-GTP*	9.17 ± 1.73	1.16 ± 0.28	0.13	1.25×10^{-3}
dA	dTTP	0.22 ± 0.09	1.47 ± 0.34	6.68	1
dA	8oxo-dGTP	1.90 ± 0.49	0.52 ± 0.15	0.27	4.04×10^{-2}
dA	*8oxo-GTP*	24.34 ± 3.08	0.38 ± 0.07	0.016	2.40×10^{-3}

Data are means (±standard error) from at least three different experiments

similar efficiency opposite templates dC or dA (Figure 19A), and 8oxo-GTP opposite template dC better than opposite dA, but similarly to the incorporation of 8oxodGTP (Figure 19B). Thus, it is tempting to speculate that the 2'OH group of the ribose is limiting polymerization specifically in the *syn* conformation. To better understand the incorporation of 8oxodGTP and 8oxoGTP by *Sp*Pol4 during gap-filling reactions, and obtain quantitative data, we evaluated the kinetics of their insertion under steady-state conditions. This analysis demonstrated that the catalytic efficiency of 8oxodGTP insertion was very similar opposite either template dA or dC (Table 3). Moreover, the catalytic efficiency of 8oxoGTP incorporation opposite dC was similar to 8oxodGTP insertion and 8-fold more efficient than opposite dA (Table 3).

Once we determined that they are valid substrates, an important question is how these oxidized nucleotides compete with the cognate normal substrates (dGTP/GTP; dTTP/UTP). Remarkably, when copying a template dC, *Sp*Pol4 incorporated undamaged dGTP/GTP with much higher efficiency than 8oxo-dGTP and 8oxo-GTP (Figure 19C). Furthermore a detailed kinetic analysis demonstrated that *Sp*Pol4 showed a low affinity for 8oxodGTP and 8oxoGTP, being incorporated opposite dC 440-fold and 800-fold less efficiently than dGTP (Table 3). When copying a template dA, *Sp*Pol4 also preferred the undamaged nucleotides dTTP and UTP (Figure 19D), being the incorporation of 8oxo-dGTP and 8oxo-GTP 25-fold and 418-fold less efficient than dTTP, respectively (Table 3). Therefore, we can conclude that 8oxo-dGTP and 8oxo-GTP are inefficient substrates for *Sp*Pol4.

8. Specificity of the incorporation of 8oxo-dGTP and 8oxo-GTP by *Sp*Pol4 in *S. pombe* cell extracts

The incorporation of 8oxo-dGTP and 8oxo-GTP by wild-type and *Δpol4* G1 WCE was evaluated using the 1nt-gapped molecules with either dC or dA in the gap position.

The error-free incorporation of 8oxo-dGTP (opposite template dC) was very specific for *Sp*Pol4 activity at any concentration (0.5-25 μM), as incorporation was barely detectable in the *Δpol4* extracts (Figure 20A top). Conversely, other polymerases present in the WCE incorporated 8oxo-dGTP very efficiently opposite dA, precluding the detection of *Sp*Pol4 possible contribution, if any (Figure 20A, bottom). In agreement with *Sp*Pol4 unique ability to use NTPs, the incorporation of 8oxo-GTP opposite both template dC and template dA was completely *Sp*Pol4-dependent at all the concentrations tested (Figure 20B). It is worthy to note that in contrast to our previous data (Figure 19B), *Sp*Pol4 incorporated 8oxo-GTP more efficiently opposite template dA than opposite dC.

All together, these data demonstrate that *Sp*Pol4 can incorporate 8oxo-GTP and 8oxo-dGTP to the DNA in cell extracts, and that among fission yeast polymerases, *Sp*Pol4 is the only able to incorporate 8oxoGTP as a valid substrate, both opposite dC and dA. Moreover, incorporation of 8oxo-dGTP opposite dC also appears to be *Sp*Pol4-dependent.

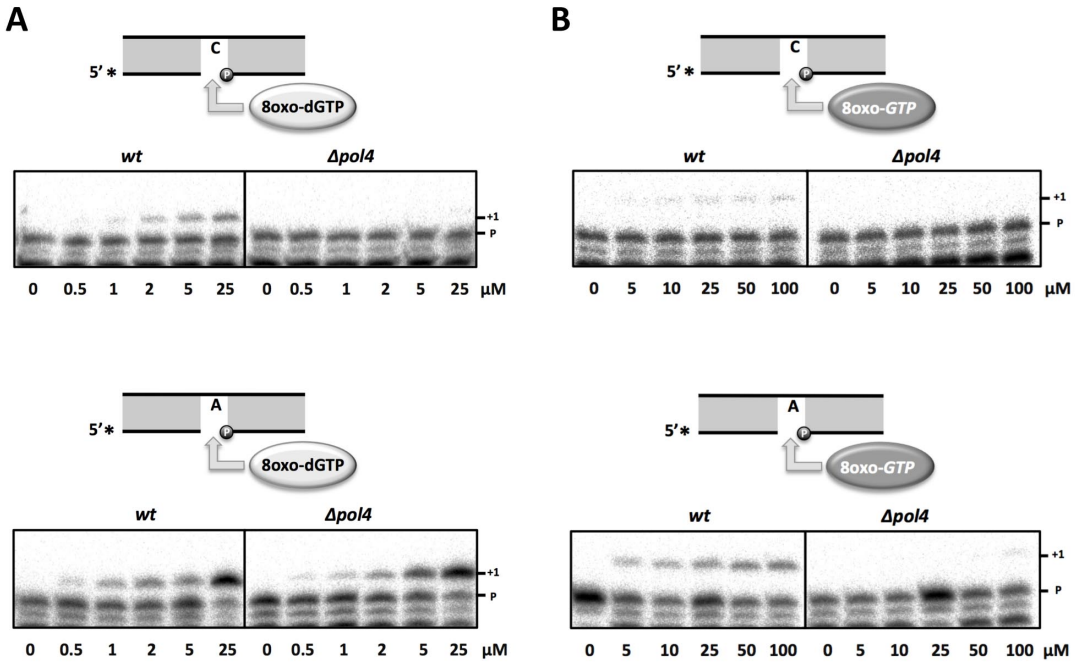

Figure 20. Analysis of 8oxo-dGTP and 8oxo-GTP incorporation by cell extracts. (A) Wild-type and *Δpol4* G1 cell extracts (20 μg) were incubated with 1nt-gapped molecules with either a dC or dA template (2.5 nM) and the indicated concentrations of 8oxo-dGTP. After incubation at 30°C for 20 min, primer extension was analysed as described in the Materials and Methods. (B) Gap-filling reactions performed as in (A) but using the indicated concentrations 8oxo-GTP.

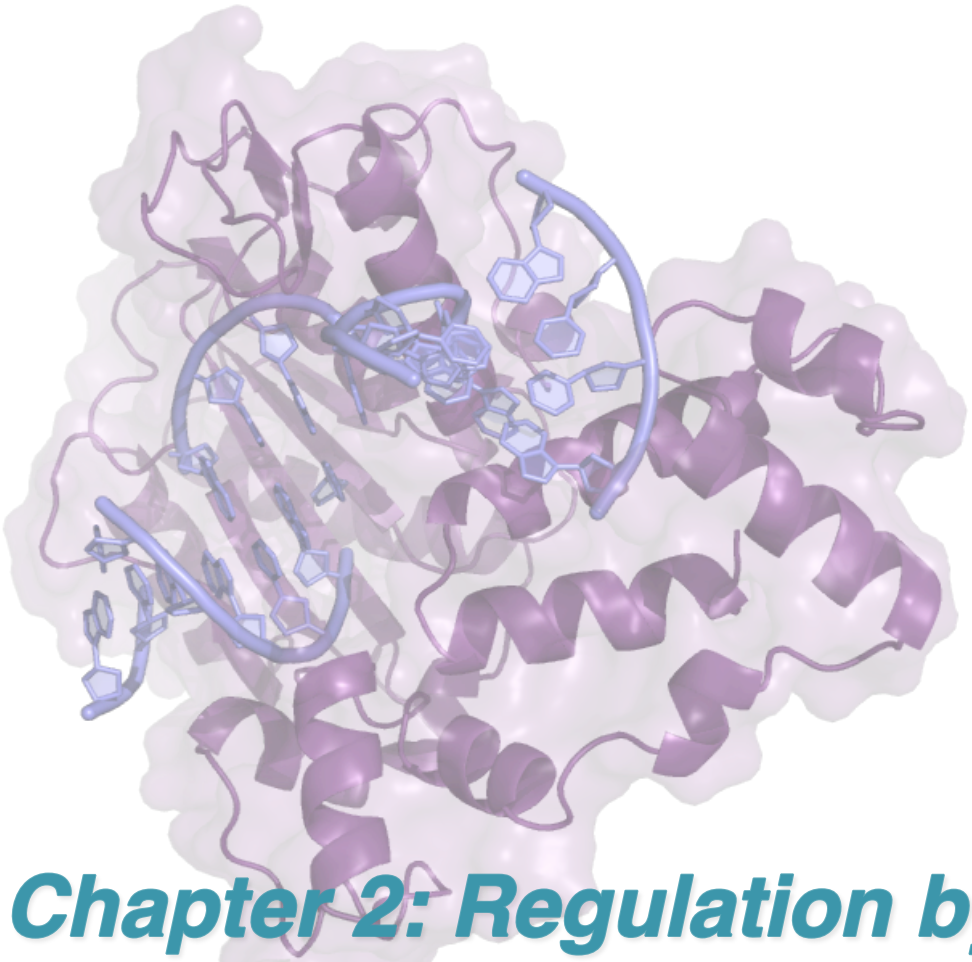

Chapter 2: Regulation by phosphorylation of PolXs in response to DNA damage

Figure: Ternary complex of human Polλ bound to 2nt-gapped DNA (PDB ID 3HWT)

One of the most relevant unaddressed questions regarding the family X of DNA polymerases is the possible regulation of their function in response to DNA damage. Given that they are specialized in filling small DNA gaps only during DNA repair, one would speculate their activity to be regulated so that they function only during those repair events, especially in the case of the members specialized in DSB repair, which are usually error-prone DNA polymerases. This possible regulation could be mediated by several mechanisms, at either a translational or post-translational level, but among them, phosphorylation by DNA damage-responsive kinases could be the most direct regulation mechanism. In this chapter we took advantage again of yeast, in this case of the budding yeast *S. cerevisiae*, as a model organism to address this question. This way, we demonstrate that Tel1 kinase, the yeast homolog of ATM, phosphorylates *Sc*Pol4, the only PolX in *S. cerevisiae*, in response to DNA damage. This finding prompted us to evaluate the possible regulation by phosphorylation of the closest homolog of *Sc*Pol4 in human cells, Polλ, and hence, in this chapter we also show that Polλ is indeed regulated by phosphorylation by DNA-PK kinase.

1. *Sc*Pol4 is phosphorylated by Tel1

Yeast Tel1 (homolog of mammalian ATM), is a serine/threonine protein kinase from the phosphatidylinositol-3 kinase-related kinase (PIKK) family that is recruited and activated by DSBs. Given that DNA-PK, another kinase from the PIKK family and the main mediator of NHEJ in mammalian cells is not conserved in *S. cerevisiae*, Tel1 is likely the main regulator of the NHEJ pathway in this organism. Thus, we sought to determine whether *Sc*Pol4, specialized in NHEJ, could be a target of Tel1/ATM during NHEJ-mediated DSB repair. We first searched for potential Tel1 phosphorylation sites in the amino acid sequence of *Sc*Pol4, and we found two threonine residues (Thr^{64} and Thr^{540}) within [S/T]Q consensus sites, which have been defined for all PIKK-kinases, including Tel1 (Figure 21A). Interestingly, among these two sites, only the $T^{540}Q$ motif is highly conserved in different *Saccharomyces* species, probably suggesting a functional relevance (Figure 21A). To evaluate whether Tel1 can phosphorylate Thr^{64} and/or Thr^{540} we partially purified His-tagged wild-type and mutant *Sc*Pol4 phospho-dead variants in which Thr^{64} and Thr^{540} were mutated to nonphosphorylatable alanines (Figure 22A). We tested their phosphorylation *in vitro* using HA-Tel1-enriched immunoprecipitates obtained as previously described in (Mallory and Petes, 2000) (Figure 21B and Figure 22B). Control immunoprecipitates from cells that were not transformed with the HA-Tel1-encoding plasmid were also used to detect the possible

activities of other kinases. By performing a kinase assay we observed that *in vitro* phosphorylation of *Sc*Pol4 was clearly higher using Tel1-enriched immunoprecipitates than with those obtained from non-transformed cells (Figure 22B).

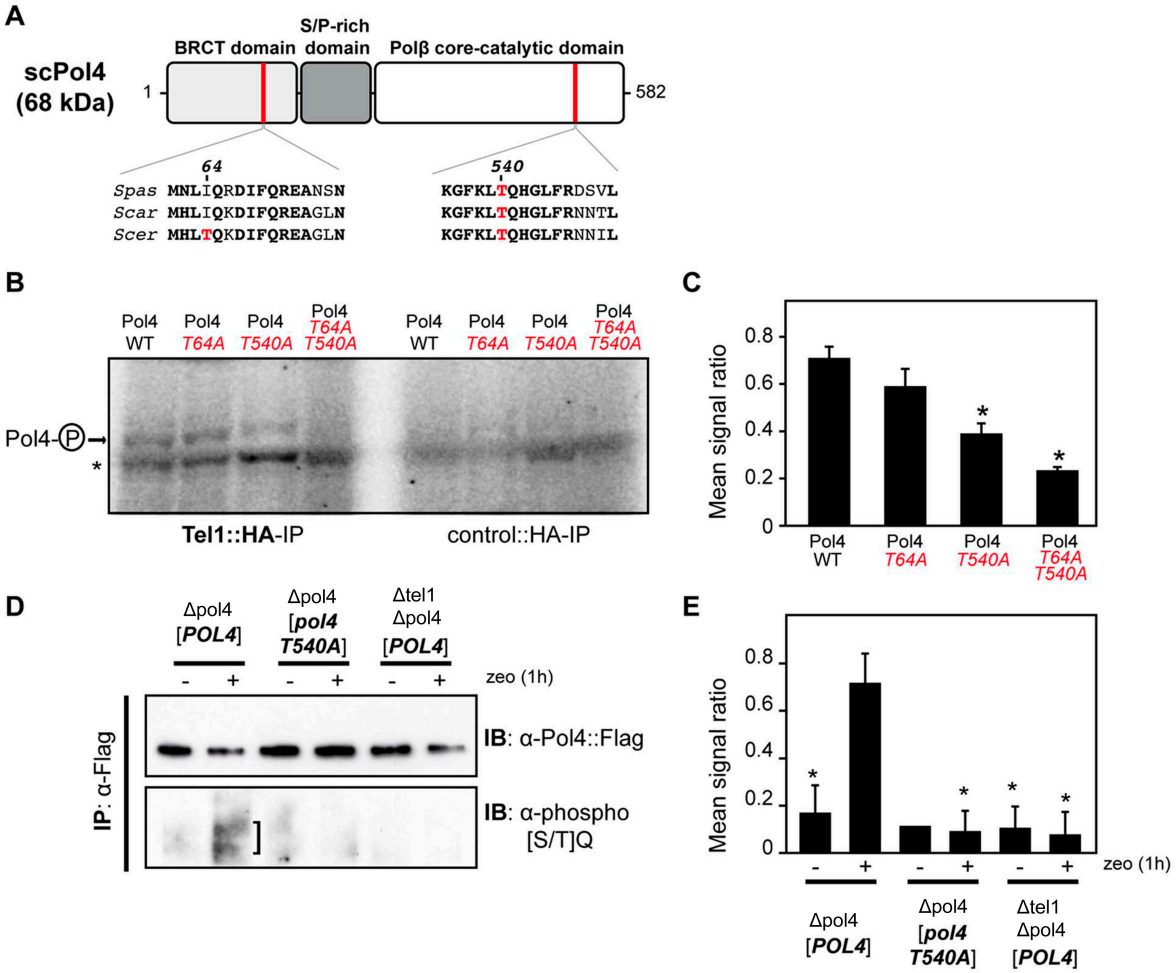

Figure 21. *Sc*Pol4 phosphorylation by the Tel1 kinase. (A) *Sc*Pol4 structural and functional domains. The location of the two *Sc*Pol4 [S/T]Q consensus motifs for Tel1 kinase activity is indicated. Amino acid alignment of these motifs in three different *Saccharomyces* species is shown at the bottom. Thr^{64} and Thr^{540} amino acid residues are marked in red. *Spas*, *Saccharomyces pastorianus*; *Scar*, *Saccharomyces cariocanus*; *Scer*, *Saccharomyces cerevisiae.* (B) *In vitro* kinase assay. Partially purified *Sc*Pol4 proteins were subjected to kinase assays using HA-immunoprecipitates obtained from yeast cells either transformed (Tel1::HA-IP, *left*) or non-transformed (control::HA-IP, *right*) with a *TEL1::HA*- encoding plasmid. Phosphorylated Pol4 proteins are indicated with an arrow. A contaminant protein, showing basal levels of phosphorylation in all samples, is marked with an asterisk. (C) Quantitative measurement of *Sc*Pol4 phosphorylation *in vitro* by immunoprecipitated Tel1. Quantification data are represented as ratio averages between phosphorylated Pol4 and phosphorylation of the contaminant protein. Error bars represent standard deviations (SD). Statistical analysis was carried out using unpaired *t*-test with Welch's correction, compared to wild-type *Sc*Pol4 phosphorylation (p values expressed as *p,0.05 were considered significant). (D) Detection of *Sc*Pol4 phosphorylation *in vivo*. Flag-tagged Pol4 proteins were immunoprecipitated from G1-synchronized cells in the absence (2) or presence (+) of zeocin (zeo) to induce DSBs. After immunoprecipitation with anti-Flag antibodies, Flag-tagged proteins were detected with either anti-Flag antibodies (*upper panel*) or specific antibodies recognizing phosphorylated [SQ/TQ] motifs (*bottom panel*). Damage-induced SQ/ TQ phosphorylation corresponding to Pol4 is indicated with a vertical bar. IB, immunoblotting; IP, immunoprecipitation. (E) Quantitative measurement of Tel1-mediated *Sc*Pol4 phosphorylation *in vivo*. Quantification data are represented as ratio averages between Pol4 phosphorylation signals from the anti-phospho [SQ/TQ] immunoblotting and Pol4 signals from the anti-Flag immunoblotting. Error bars represent SD. Statistical analysis was carried out using unpaired *t*-test with Welch's correction compared to Pol4 phosphorylation obtained in *Δpol4* [*POL4*] cells treated with zeocin (p values expressed as *p,0.05 were considered significant).

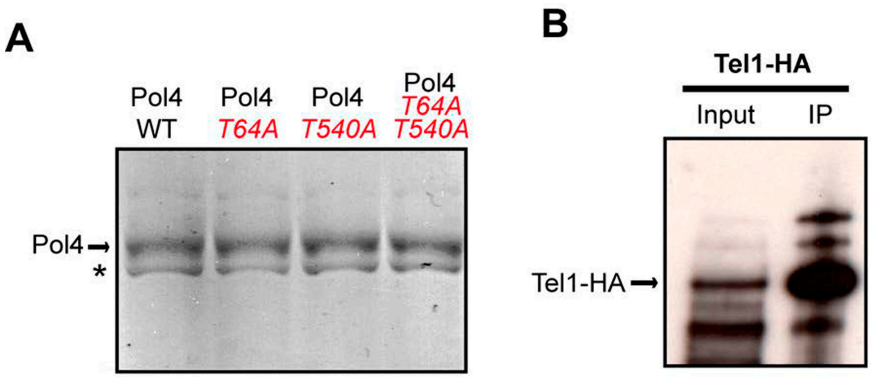

Figure 22. Partial purification of *Sc*Pol4 and Tel1. (A) Purification of *Sc*Pol4 proteins. His-tagged Pol4 proteins were partially purified using Ni-NTA agarose, separated in 8% SDS-PAGE and Coomassie stained. A 70-kDa main product corresponding to the expected electrophoretic mobility of Pol4 proteins is indicated. A smaller contaminant protein, marked with an asterisk, was co-purified in all samples. (B) Immunoprecipitation of Tel1 from yeast. HA-tagged yeast Tel1 kinase was immunoprecipitated with anti-HA antibodies from cells transformed with a plasmid encoding *TEL1::HA*, as previously described (Mallory and Petes, 2000). Immunoprecipitated HA-Tel1 was immunodetected by Western using anti-HA antibodies and is indicated with an arrow.

As deduced from quantification of phosphorylation signals, wild-type *Sc*Pol4 and the *Sc*Pol4-*T64A* mutant were similarly phosphorylated by Tel1 (Figure 21C). However, a significant decrease of phosphorylation was observed in the *Sc*Pol4-*T540A* mutant, which was more pronounced in the *Sc*Pol4-*T64A,T540A* double mutant (Figure 21C). These results indicated that *Sc*Pol4-Thr^{540} residue is the most efficiently phosphorylated by Tel1 *in vitro*.

Next, we sought to determine whether *Sc*Pol4 phosphorylation could also take place *in vivo* in response to DSBs. For this, Flag-tagged wild-type and *T540A Sc*Pol4 proteins were overexpressed in *Δpol4* cells in which we simultaneously induced DSBs with zeocin (Figure 21D). To favour NHEJ-mediated repair of the DSBs, they were induced in G1-arrested cells, a cell-cycle phase when NHEJ prevails over HR. Flag-tagged *Sc*Pol4 proteins were immunoprecipitated with anti-Flag antibodies and subsequently immunodetected using both anti-Flag antibodies and antibodies that specifically recognize phosphorylated SQ/TQ motifs. As shown in Figure 21D, a damage-induced SQ/TQ phosphorylation signal was specifically observed in cells over-expressing *Sc*Pol4 (*Δpol4* [*POL4*] cells), which was detected as a slower migrating protein with respect to *Sc*Pol4 molecular mass. Importantly, this phosphorylation was barely detected when the *Sc*Pol4-*T540A* phosphomutant was overexpressed in the same experimental conditions (*Δpol4* [*pol4-T540A*] cells), (Figure 21D). To evaluate whether the observed phosphorylation signal was dependent on Tel1, wild-type *Sc*Pol4 was overexpressed in a *Δtel1 Δpol4* double mutant. Interestingly, damage-induced SQ/TQ phosphorylation in this condition was again much weaker than that obtained in

the *Δpol4* [*POL4*] cells, demonstrating its dependence on Tel1 (Figure 21D). As deduced from the quantification of phosphorylation signals, the decrease of damage-induced *Sc*Pol4 phosphorylation either in the *Δpol4* [*pol4-T540A*] cells or in the absence of the Tel1 kinase was statistically significant (Figure 21E).

Altogether, these data suggest that *Sc*Pol4 is phosphorylated on the Thr^{540} residue by Tel1 *in vitro* and also in response to DNA damage *in vivo*. Interestingly, these results were part of a report in which the effect of the Tel1-mediated *Sc*Pol4 phosphorylation was evaluated *in vivo* (Ruiz et al., 2013). Those results showed that the phosphorylation of *Sc*Pol4 Thr^{540} stimulated its activity during NHEJ *in cis*, although it also enhanced NHEJ-dependent translocations, demonstrating that *Sc*Pol4 can contribute to those error-prone events (Ruiz et al., 2013). Importantly, these data prompted us to evaluate whether the closest homolog of *Sc*Pol4 in humans, Polλ, could also be regulated by phosphorylation in response to DNA damage.

2. Polλ is phosphorylated by DNA-PKcs *in vitro*

In the NHEJ pathway, after the recognition of the DSB by the Ku70/80 complex, the DNA-dependent protein kinase catalytic subunit (DNA-PKcs) is the first protein recruited to the break where, together with the Ku heterodimer, forms the DNA-PK complex (Lieber, 2008). This activates its kinase activity; that is known to be essential for the precise coordination of the NHEJ machinery. However, although activated DNA-PKcs are known to phosphorylate a number of NHEJ factors following DSBs induction (Mahaney et al., 2009), there is little evidence regarding the physiological relevance of this activity in higher eukaryotes. Given that Polλ is the closest ortholog to budding yeast *Sc*Pol4 and that the DNA-PKcs is the main kinase operating during NHEJ, we sought to determine whether PolX phosphorylation is conserved in human cells by evaluating phosphorylation of human Polλ by DNA-PKcs.

For this purpose, we first performed a kinase assay using purified human Polλ and DNA-PK complex, which showed that Polλ is efficiently phosphorylated by DNA-PKcs *in vitro* (Figure 23A). Interestingly, Polλ phosphorylation mainly relied on its N-terminal region, since a mutant protein lacking the BRCT and S/P-rich domains was barely phosphorylated (Figure 23A). In agreement with this finding, phosphorylation of Polβ, a close homolog of Polλ in human cells that lacks these N-terminal domains, was barely detectable in this assay (Figure 23A). Remarkably, western blot analysis using a phospho-antibody specific of phosphorylated [S/T]Q sites, the consensus sites for DNA-PKcs activity, confirmed that Polλ is phosphorylated by this kinase *in vitro* (Figure

23B). In this experiment, we also observed a significant decrease in phosphorylation in the presence of a specific DNA-PKcs inhibitor and a complete absence of phosphorylation following phosphatase treatment (Figure 23B), further confirming DNA-PKcs-mediated *in vitro* phosphorylation of Polλ. Analysis of the amino acid sequence of

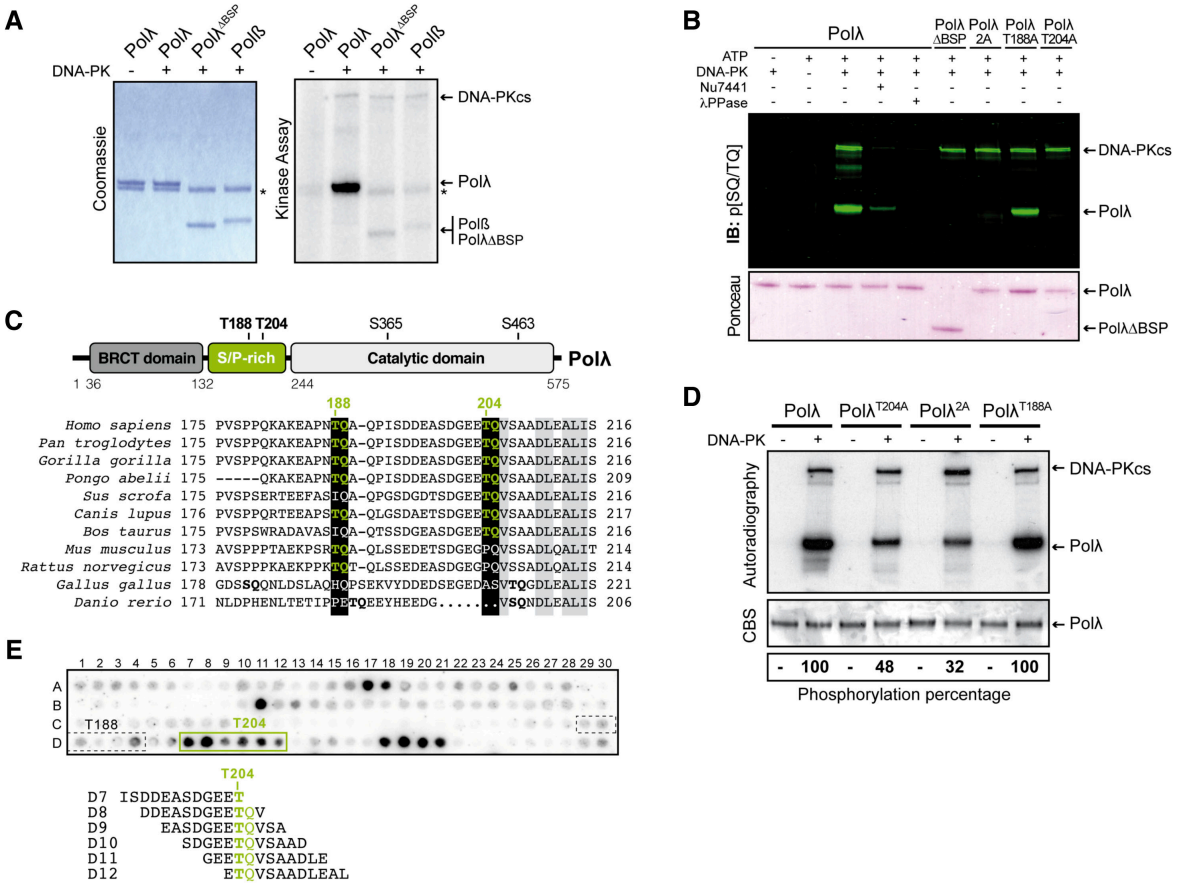

Figure 23. Human Polλ is phosphorylated by DNA-PKcs *in vitro*. (A) Kinase assay using DNA-PK complex and purified recombinant Polλ proteins. Proteins were incubated with [γ-^{32}P]ATP with (+) or without (-) purified DNA-PK as indicated and samples were analysed by SDS-PAGE followed by Coomassie staining (*left*) and autoradiography (*right*). The position of the proteins used in the assay is indicated on the right. Polλ$^{\Delta BSP}$ indicates a Polλ deletion mutant lacking the two amino terminal domains (BRCT and S/P-rich). Autophosphorylated DNA-PKcs on the autoradiogram is indicated as an internal control in the assay. Polβ is shown as a control of Polλ phosphorylation specificity. Asterisks mark the position of bovine serum albumin. (B) Kinase assay and analysis of DNA-PKcs-mediated Polλ phosphorylation by Western blot using anti-phosho[S/T]Q specific antibodies. The indicated purified Polλ proteins were incubated with DNA-PK, ATP, DNA-PKcs inhibitor Nu7441 and λ-phosphatase, as indicated, and then analysed by SDS-PAGE followed by Western blot using a specific antibody for phosphorylated [S/T]Q sites. The position of phosphorylated Polλ and autophosphorylated DNA-PKcs are indicated. Ponceau staining indicating the purified proteins used in the assay is shown. (C) Schematic of human Polλ domain organization with main PIKK-dependent phosphorylation sites indicated. Residues located in the S/P-rich domain are marked in bold; *Bottom:* Sequence alignment of the 175–216 amino acid region of Polλ highlighting the conservation of PIKK consensus sites across species (green over black background). Threonine residues that are part of these PIKK consensus sites are indicated, so are residues conserved in all species (grey boxes). (D) Single and double threonine (T) to alanine (A) Polλ phospho-dead mutants were generated by mutations at Thr^{188} and Thr^{204} as indicated, and *in vitro* kinase assay with purified DNA-PK was performed as described in A). *Upper panel:* autoradiography showing phosphorylated Polλ and autophosphorylated DNA-PKcs. *Lower panel:* Coomassie blue staining (CBS). Phosphorylation of the mutants is represented as the percentage of phosphorylation of wild-type Polλ (*bottom*). (E) Kinase assay on peptide-scanning arrays covering N-terminal BRCT and S/P-rich domains using purified DNA-PKcs. Peptides containing Thr^{204} are shown (green boxes) and their sequence is listed below the array.

human Polλ with specialized software for the detection of phosphorylation sites (Obenauer et al., 2003) identified four sites matching the [S/T]Q consensus motif common for all PIKKs involving the following phosphorylatable residues: Thr^{188}, Thr^{204}, Ser^{365} and Ser^{463}. Interestingly, the fact that Thr^{188} and Thr^{204} localize in the N-terminal S/P-rich domain (Figure 23C), which we previously observed to be involved in the phosphorylation of Polλ by DNA-PKcs (Figure 23A&B), made us anticipate that the could be the main targets of phosphorylation. In fact, the S/P-rich domain has been already suggested to be involved in the regulation of Polλ (García-Díaz et al., 2000), in which some cyclin-dependent kinase (CDK)-mediated phosphorylations have been identified (Frouin et al., 2005). Additionally, the [S/T]Q consensus motifs corresponding to Thr^{188} and Thr^{204} are highly conserved amongst orthologs, particularly in mammals, which also suggests their possible functional relevance (Figure 23C). Hence, to identify the target site for DNA-PKcs-mediated phosphorylation of Polλ, we devised the phospho-dead T188A and T204A mutant proteins, in which the Thr^{188} and Thr^{204} residues were mutated to non-phosphorylatable alanine residues. Interestingly, both western blot analysis with [S/T]Q phospho-specific antibodies (Figure 23B) and *in vitro* kinase assays (Figure 23D) using these purified phospho-dead mutant proteins showed a pronounced decrease in phosphorylation only in the case of the T204A mutant, demonstrating that the Thr^{204} residue is the principal target among the two for DNA-PKcs-mediated phosphorylation. *In vitro* kinase assays on a peptide-array of human Polλ covering its N-terminal (BRCT and S/P-rich) domains also confirmed this finding (Figure 23E). Taken together, these results demonstrate that human Polλ is phosphorylated *in vitro* by DNA-PKcs, with Thr^{204} being a relevant target for such modification.

3. DNA-PKcs phosphorylates Polλ Thr^{204} *in vivo*

Next we sought to determine whether the newly identified phosphorylation of Polλ by DNA-PKcs could also occur *in vivo*. To determine this, we compared the electrophoretic mobility of FLAG-tagged Polλ in human HEK293T cells, both with and without DSBs induction by treatment with ionizing irradiation (IR). FLAG-Polλ was immunoprecipitated and analysed by SDS-PAGE and Western blotting in the presence of the phosphate-binding agent Phostag™ (Kinoshita, 2005). In these experimental conditions, a slower migration form of FLAG-Polλ, representing a phosphorylated protein, appeared specifically in response to IR (Figure 24A). Notably, when these cells were pre-treated with a specific DNA-PKcs inhibitor prior to irradiation, the slow

migration form was reduced, indicating that in this experiment DNA-PKcs was the main kinase responsible for Polλ phosphorylation after DNA damage (Figure 24A). A similar decrease of the slower migration band was observed when a FLAG-tagged Polλ-T204A mutant protein was analysed under the same experimental conditions (Figure

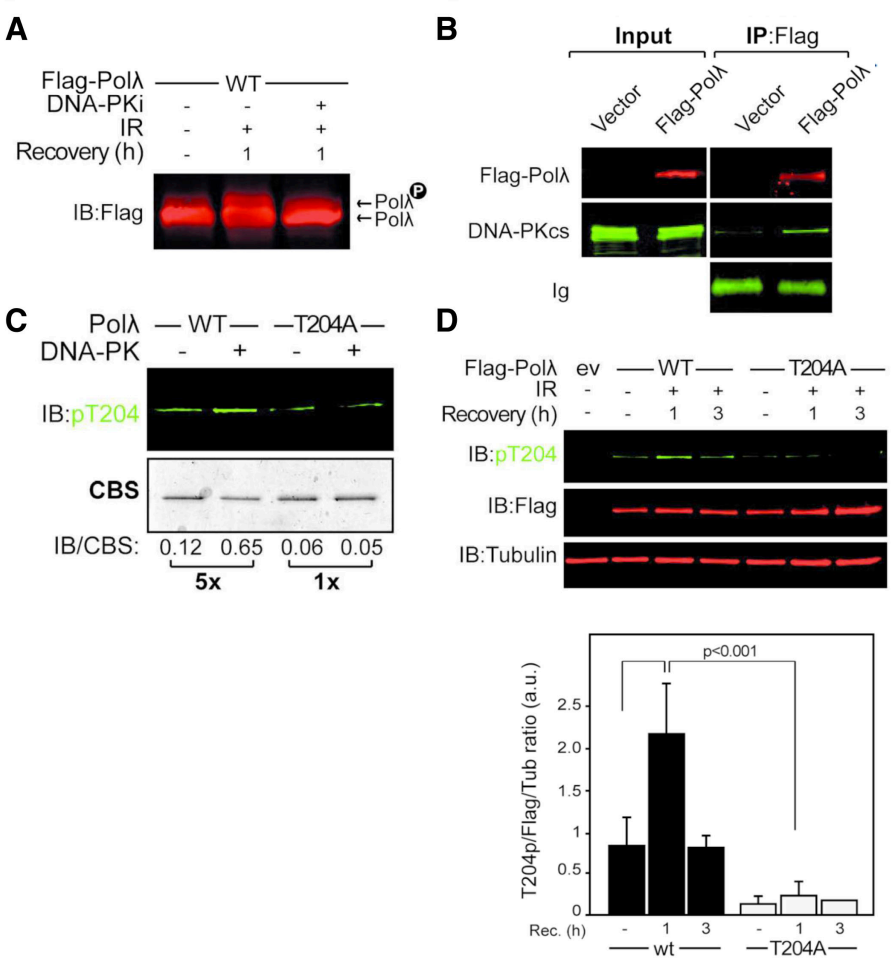

Figure 24. Human Polλ is phosphorylated by DNA-PKcs in human cells at Thr^{204}. (A) HEK293T cells transfected with FLAG-POLL^{WT} plasmid were mock irradiated or irradiated with 10 Gy of IR and collected 1h post-irradiation. When indicated, cells were pre-treated with 10 μM DNA-PK specific inhibitor (Nu7441) for 1h prior to irradiation. Cell extracts were analysed by SDS-PAGE containing Phostag (20 μM) and immunoblotted with anti-FLAG antibody. (B) Polλ-DNA-PKcs interaction analysed by co-immunoprecipitation. HEK293T cells transfected either with FLAG-empty or FLAG-POLL^{WT} plasmid were irradiated as in (A). FLAG-Polλ was immunoprecipitated with anti-Flag antibody (IP) and immunoblotted (IB) with the indicated antibodies. Rabbit IgGs are shown as an immunoprecipitation control. Input samples are 20% (v/v) with respect to IP samples. (C) Characterization of a phospho-specific antibody to phosphorylated Thr^{204}. Purified Polλ and Polλ-T204A proteins (125 ng) were assayed for DNA-PKcs kinase activity *in vitro*. Phosphorylation was detected with a rabbit polyclonal serum enriched in phospho-specific antibodies against phosphorylated Thr^{204} (pT204). Phosphorylated Thr^{204} visualized in the immunoblot (IB) and total protein visualized in the Coomassie blue staining (CBS) were quantified by densitometry. The ratio IB/CSB for each sample and the fold increase of Thr^{204} phosphorylation is indicated. (D) HEK293T cells transfected either with FLAG-empty (ev), FLAG-POLL^{T204A} or FLAG-POLL^{WT} plasmid were treated as in (A) and collected at indicated times post-irradiation. Cell extracts were analysed by SDS-PAGE and Western blotting for the indicated proteins. A representative experiment is shown. *Bottom:* Quantification of Thr^{204} phosphorylation observed in two independent experiments. Band intensities were quantified using ImageJ and phosphorylated Thr^{204} (pT204) is represented as pT204/FLAG/total protein ratios. Statistical significance was determined with one-tailed Mann-Whitney test; p<0.001 compared either to FLAG-POLL^{WT} transfected cells without irradiation or to FLAG-POLL^{T204A} transfected cells 1h post-irradiation.

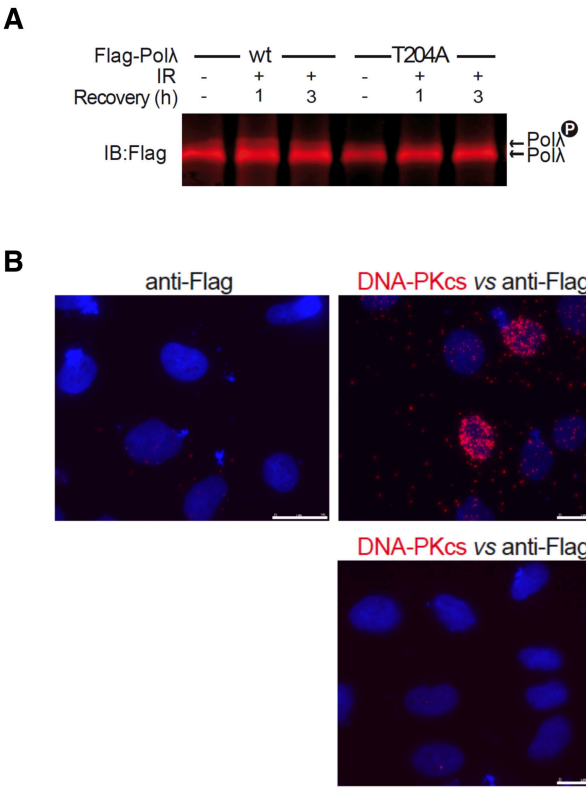

Figure 25. Electrophoretic mobility of the T204A mutant and proximity ligation assay. (A) HEK293T cells overexpressing either FLAG-Polλ or FLAG-PolλT204A were irradiated with 10 Gy of IR to induce nonspecific DSBs and collected at the indicated times. Whole cellular protein extracts were obtained and run on Phos-tag-containing (25 μM) SDS-PAGE gels and immunoblotted with anti-FLAG antibody. Electrophoretic mobilities of both phosphorylated- and non-phosphorylated Polλ are indicated. (B) Polλ interaction with DNA-PKcs as determined by proximity ligation assay (PLA). U2OS cells transfected with either FLAG-empty or FLAG-POLL plasmid were irradiated with 2 Gy of IR and examined for PLA foci of FLAG (for Polλ) and DNA-PKcs (right panels) by immunofluorescence 1h post-irradiation. Control immunofluorescence analysis using anti-FLAG antibody alone is also shown (left panel). The nuclei were counterstained with DAPI and the PLA signals (in red) were visualized in a fluorescence microscope (scale bars=25 μm).

25A), suggesting that Polλ Thr^{204} is phosphorylated *in vivo*. In line with these previous data, we detected interaction of Polλ and DNA-PKcs *in vivo* following DSB induction both by co-immunoprecipitation and proximity ligation assays (PLA) (Figure 24B and Figure 25B). To further determine whether Polλ Thr^{204} is phosphorylated by DNA-PKcs in human cells, we also performed Western blot assays using a polyclonal rabbit serum enriched in phospho-specific antibodies against phosphorylated Thr^{204} (pT204), which we show to specifically detect Thr^{204} phosphorylation of Polλ *in vitro* (Figure 24C). We irradiated HEK293T cells that overexpressed either wild-type FLAG-Polλ or FLAG-PolλT204A and analysed Thr^{204} phosphorylation with the pT204 antibody at several times following irradiation. As shown in Figure 24D, a significant increase in Thr^{204} phosphorylation was observed only in cells overexpressing wild-type Polλ after irradiation, but not with the T204A phospho-dead mutant, either in the absence or presence of DSB induction (Figure 24D). Altogether, these results demonstrate that Polλ is phosphorylated at Thr^{204} by DNA-PKcs after DSB induction *in vivo*.

4. Thr^{204} phosphorylation is required for efficient NHEJ *in vivo*

We subsequently sought to determine the physiological role of Polλ-Thr^{204} phosphorylation by DNA-PKcs during NHEJ *in vivo*, but first we comparatively studied the *in vitro* polymerase activity of purified wild-type Polλ and the T204A phospho-dead

mutant, in an attempt to rule out any catalytic defects possibly caused by this mutation. Remarkably, both proteins showed similar DNA polymerization activity on a labelled 1nt gap-containing dsDNA substrate (Figure 26A), which resemble BER and NHEJ repair intermediates, the two main pathways in which Polλ is involved, suggesting that the T204A mutation does no affect *in vitro* DNA polymerization by Polλ. Next, we evaluated the possible effect of the T204A mutation on NHEJ substrates that mimicked those preferentially managed by Polλ *in vivo* (Figure 26B) (Pryor et al., 2015). These substrates are two dsDNA molecules with partially compatible 3'-protruding ends

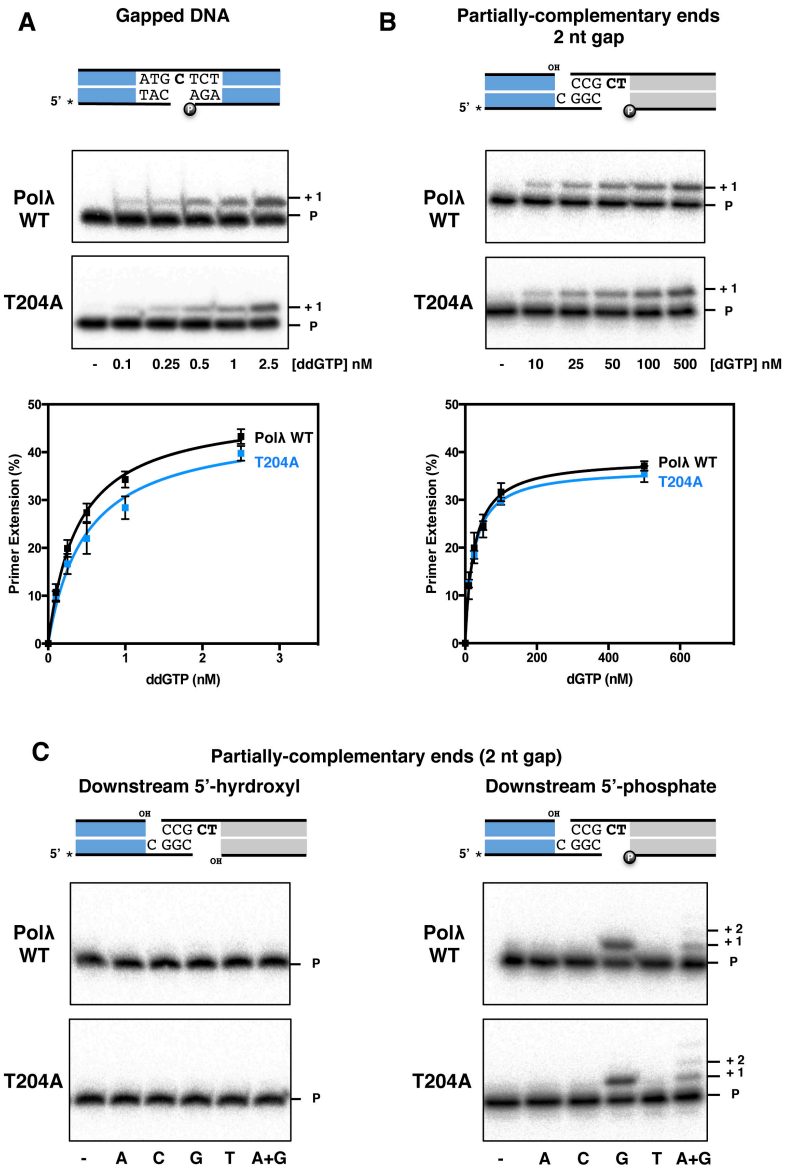

Figure 26. *In vitro* characterization of the T204A mutant. (A) Analysis of the gap-filling activity of either purified wild-type Polλ or the T204A mutant on a labelled 1nt-DNA gap. Data in the graph correspond to the means from 3 independent experiments ± SD. (B) Evaluation of the effect of the T204A mutation on the efficiency of *in vitro* NHEJ of compatible ends with a 2nt gap by Polλ. Data in the graph represent the means from 3 independent experiments ± SD. (C) Fidelity of purified wild-type Polλ or the T204A mutant during *in vitro* NHEJ at a 2nt gap, either in the absence (*left*) or presence (*right*) of a 5'P flanking the 2nt-gap.

(Figure 26B, depicted in blue and grey), which form 2 gaps upon Polλ-induced annealing of their ends, one of which has a length of 2 nts. Polλ activity is pronouncedly directed to this 2nt-gap due to the presence of a 5'P adjacent to the gap. Importantly, when using these dsDNA substrates, the T204A mutation did not have detectable effect on the efficiency of the incorporation by Polλ of the nucleotide complementary to the first nucleotide of the 2nt-gap (Figure 26B). Additionally, compared to wild-type Polλ, the T204A mutation did not affect whatsoever neither fidelity of these NHEJ *in vitro* reactions nor the requirement for downstream 5'-P flanking the 2nt gap in the assay (Figure 26C). Altogether, these results indicate that the T204A mutation did not have deleterious effects on the polymerase activity of Polλ *in vitro*, suggesting that Thr^{204} is not directly involved in catalysis.

Having confirmed that the T204A mutation was not disadvantageous for Polλ-mediated *in vitro* DNA synthesis, we investigated the role of Polλ Thr^{204} in DSB repair *in vivo* by following the time course of 53BP1 foci disappearance after DSB induction in human U2OS cells overexpressing either wild-type Polλ or the T204A mutant (Figure 27A). 53BP1 is an important positive regulator of NHEJ-mediated DSB repair (Panier and Boulton, 2014), and, since the number of 53BP1 foci correlates well with the number of breaks, their quantification following DSB induction constitute a well-established procedure for monitoring NHEJ-mediated repair *in vivo*. Under these experimental conditions, we observed that cells overexpressing the mutant Polλ-T204A showed significantly higher persistence of residual 53BP1 foci than cells overexpressing wild-type Polλ (Figure 27A), which suggests a delay in the repair of DSBs due to the lack of Thr^{204} phosphorylation, given that Thr^{204} is not relevant for DNA synthesis *per se* (Figure 26). It is also worthy to note that overexpression of wild-type Polλ generated a delay in the disappearance of 53BP1 foci with respect to control cells (Figure 27A), suggesting a dominant negative effect of the overexpression of Polλ proteins. To further evaluate the role of Thr^{204} phosphorylation in the repair of DSBs, in collaboration with Dr. Dale A. Ramsden (University of North Carolina, USA), we took advantage of a recently described cellular assay to measure accurate NHEJ-mediated repair of DSB substrates with defined end structures *in vivo* (depicted in Figure 27B) (Pryor et al., 2015). This assay relies on the co-electroporation of a DNA substrate mimicking a DSB and a purified polymerase into MEFs deficient in both Polλ and Polμ. In agreement with the high degree of specialization of Polλ in filling 2nt gaps during NHEJ, DNA substrates with broken ends whose alignment generates 2 nt gaps are repaired with low accuracy by polymerase-independent means in this $Pol\lambda^{-/-}Pol\mu^{-/-}$ MEF

cells, but the ability to perform accurate repair is recovered upon complementation with wild-type Polλ (Figure 27C) (Pryor et al., 2015). Significantly, the Polλ-T204A protein was 3-fold less effective than the wild-type protein in the complementation of these deficient MEFs (Figures 27C and 27D), which again, given that the T204A mutant is catalytically competent (Figure 26), suggests that efficient NHEJ by Polλ requires

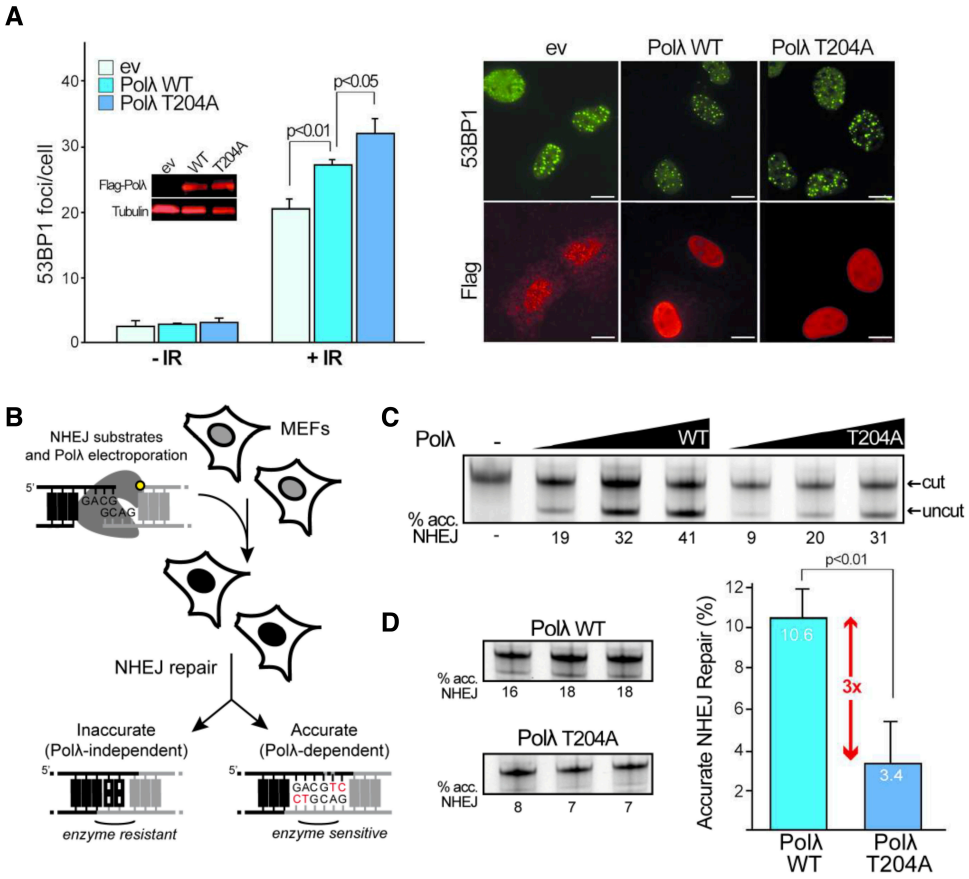

Figure 27. Thr^{204} phosphorylation modulates Polλ activity during NHEJ *in vivo*. (A) Determination of 53BP1 foci in U2OS cells transiently overexpressing either FLAG-empty, FLAG-Polλ or FLAG-PolλT204A and exposed to 10 Gy of IR. Twelve hours after treatment, cells were fixed and co-stained for 53BP1 and FLAG-Polλ. The absolute number of 53BP1 foci was scored in FLAG-positive cells. The plot represents the mean and standard error of the mean (SEM) of three independent experiments, with at least 40 cells being scored for each sample and treatment condition. Statistical significance was determined using the repeated measures one-Way ANOVA test with a Bonferroni's post-test correction. Western blot analysis of FLAG-tagged proteins expressed in U2OS cells is shown. *Right:* Representative images of the immunofluorescent identification of FLAG-positive cells and scored 53BP1 foci is shown (scale bars, 10 μm). (B) Scheme of the extrachromosomal NHEJ assay. A linear DNA fragment with GACG3' overhangs that can align to generate a 2-nt gap (described in cartoon) was introduced into Polμ-Polλ double-deficient mouse embryonic fibroblasts (MEFs) that were complemented with varying amounts of purified wild-type or T204A variant Polλ proteins. Repair products were recovered and amplified. Amplified products were subjected to restriction enzyme digestion using an enzyme diagnostic for accurate repair (*AatII*). (C) The GACG3' NHEJ substrates were introduced into the polymerase-deficient MEFs together with 0, 0.1, 0.2, and 0.5 ng of purified Polλ or Polλ-T204A proteins. The percentage of junctions formed after Polλ-mediated accurate synthesis is indicated. (D) The same experiment was performed in triplicate with 0.1 ng of protein. The percentage of junctions formed after Polλ-mediated fill-in of the 2 nt gap is indicated. The quantification of these experiments in shown in the plot. Mean recovery efficiencies were assessed as significantly different with confidence p<0.01 using one-tailed Mann-Whitney test.

Thr^{204} phosphorylation *in vivo*. Collectively, these results indicate that the inability to phosphorylate Polλ at Thr^{204} results in less efficient Polλ-dependent gap-filling DNA synthesis during NHEJ *in vivo*.

5. Thr^{204} phosphorylation stimulates Polλ and Ku80 interaction after DSB induction *in vivo*

To further understand the role of Thr^{204} phosphorylation during NHEJ, we evaluated protein-protein interactions between Polλ and NHEJ core factors. Recent proteomic analyses have identified both Ku80 and DNA-PKcs as the main partners of Polλ in human cells (Xing et al., 2015), a finding in clear agreement with previous results demonstrating the interaction of Polλ with Ku:DNA complexes *in vitro* (Ma et al., 2004; Nick McElhinny et al., 2005). We performed anti-FLAG immunoprecipitation (IP) assays in HEK293T cells overexpressing FLAG-Polλ that were subjected to IR to induce DSBs. As shown in Figure 28A, in the experiment we detected an efficient co-precipitation of Ku80 together with FLAG-Polλ demonstrating that they interact, either directly or indirectly, under conditions of DSB induction *in vivo*. This Ku80-Polλ association was strictly dependent on the presence of a functional BRCT domain in Polλ (Figure 28B). Additionally, the interaction between Ku80 and Polλ was sensitive to ethidium bromide, which disrupts DNA-protein interactions (Lai and Herr, 1992),

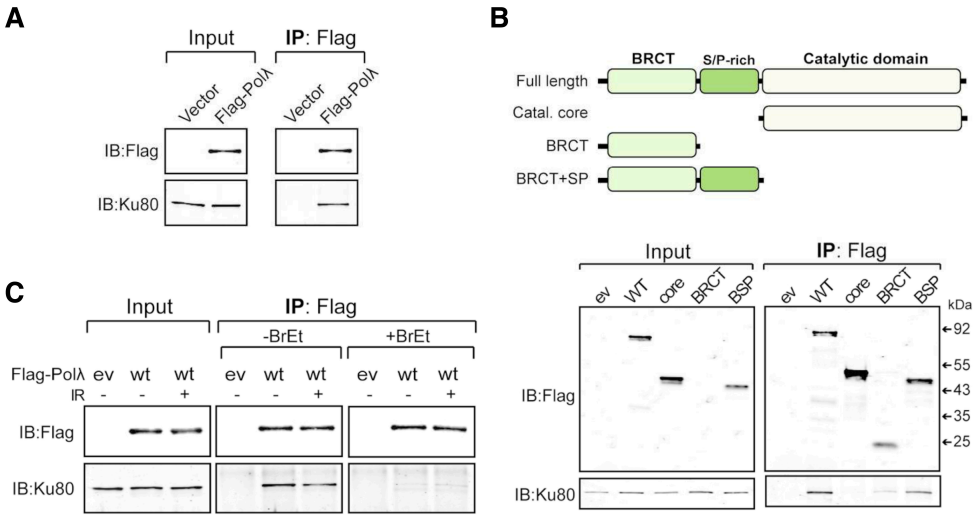

Figure 28. Polλ interacts with Ku80. (A) HEK293T cells overexpressing either FLAG-empty or FLAG-tagged Polλ were irradiated with 10 Gy of IR to induce nonspecific DSBs. One hour later, FLAG-tagged proteins were immunoprecipitated (IP) with anti-FLAG antibody and immunoblotted (IB) as indicated. Input samples are 10% (v/v) with respect to IP samples. (B) HEK293T cells overexpressing either FLAG-empty or FLAG-tagged variants of Polλ (a scheme is shown at top) were treated as in (A). FLAG-tagged proteins were immunoprecipitated (IP) with anti-FLAG antibody and immunoblotted (IB) as indicated. Input samples are 10% (v/v) with respect to IP samples. (C) HEK293T cells overexpressing either FLAG-empty or FLAG-tagged Polλ were treated with or without IR and processed an in (A). When indicated 100 μg/ml ethidium bromide were added to disrupt DNA-mediated protein-protein interactions.

indicating the involvement of dsDNA molecules present in the lysates (Figure 28C).

Importantly, we also detected Ku80 and Polλ interaction in non-irradiated cells (Figure 28C, 29A), and in those non-damage conditions it was comparable between cells overexpressing either the T204A mutant or wild-type Polλ (Figures 29A). Remarkably, following DSB induction with IR, the interaction of Ku80 with the Polλ-T204A mutant was significantly reduced compared to that observed in cells overexpressing wild-type Polλ (Figure 29A). A similar decrease was also observed when cells overexpressing wild-type Polλ were pre-treated with a specific DNA-PKcs inhibitor prior to irradiation (Figure 29A), demonstrating that this kinase modulates the

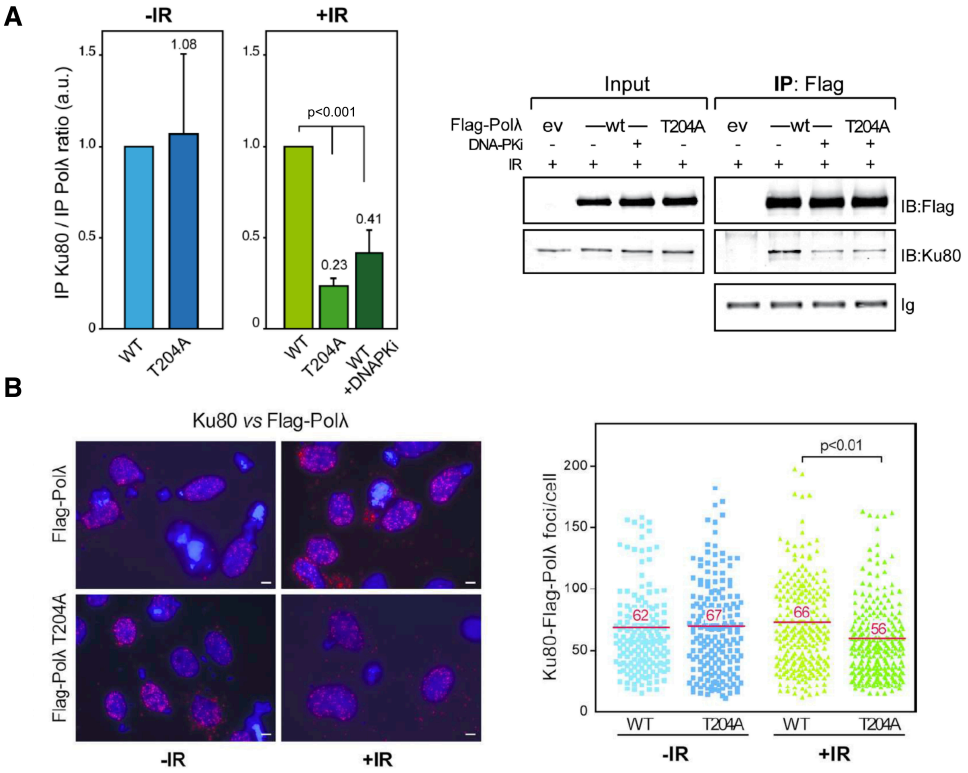

Figure 29. Thr^{204} phosphorylation mediates the interaction of Polλ with Ku80 after DSB induction. (A) HEK293T cells overexpressing either FLAG-Polλ or FLAG-PolλT204A were treated with or without 10 Gy of IR. FLAG-tagged proteins were immunoprecipitated (IP) with anti-FLAG antibody and immunoblotted (IB) with anti-Ku80 antibody. When indicated, cells were pre-treated with 10 μM DNA-PK specific inhibitor (Nu7441) for 1 hour before irradiation. The plot shows the quantification of co-immunoprecipitated Ku80 observed *in vivo* in three independent experiments in the absence or presence of IR. Statistical significance was determined with one-tailed Mann-Whitney test; p<0.001 compared to cells transfected with FLAG-POLL^{WT} plasmid. *(Right)* Shown is a representative co-immunoprecipitation experiment with irradiated cells as described in (A). (B) U2OS cells overexpressing either FLAG-Polλ or FLAG-Polλ-T204 were treated with (2 Gy) or without IR and examined for PLA foci of FLAG (for Polλ) and Ku80 by immunofluorescence 1h post-irradiation. Nuclei were counterstained with DAPI and the PLA signals (red) were visualized in a fluorescence microscope (scale bars, 7.5 μm). The plot shows quantification of PLA signals/nucleus from at least 150 cells (n = 3; lines denote mean values) and representative images are shown. Statistical analysis was performed first with Kolmogorov-Smirnov test, which indicates the non-parametric distribution of samples, and with Kruskal–Wallis One-Way test and Dunn´s post-test correction. p<0.001 compared to wild-type Polλ transfected cells.

interaction between Polλ and Ku80. To corroborate these findings, we performed PLA assays in human U2OS cells, a technique that allows the visualization of physically associated proteins in physiological conditions (*in cell*). In agreement with our previous results, by using this technique we detected robust signals of Ku80 and Polλ in cells in the absence of DNA damage (Figure 29B), suggesting that both proteins localize in close proximity before the induction of DSBs. These signals were similar in cells overexpressing either wild-type Polλ or the Polλ-T204A mutant (Figure 29B), which is also in agreement with our previous data. However, following irradiation, we again observed a significant reduction in the co-localization of Ku80 and Polλ specifically in cells overexpressing the T204A mutant, but no changes in those overexpressing wild-type Polλ (Figure 29B). Hence, altogether these results indicate that Thr^{204} phosphorylation is required for the maintenance of Ku80-Polλ interaction after DBSs *in* vivo, thereby suggesting that this modification is relevant to achieve optimal NHEJ repair. However, the fact that we detected similar level of interaction between Polλ wild-type and Ku80 regardless of induction of DSBs is quite intriguing and be will later discussed.

6. The T204E phospho-mimetic mutation modifies Polλ conformation

The finding that Thr^{204} phosphorylation is required for the optimal interaction between Ku80 and Polλ after DNA damage prompted us to gain further insight into the effect of this modification in Polλ and on how it could affect this interaction. In the absence of DNA damage, the T204A mutant interacted with Ku80 as proficiently as its wild-type counterpart with Ku80 suggesting that the Thr^{204} residue is not directly involved in the interaction, which is in agreement with previous finding demonstrating that this interaction is not mediated by the S/P-rich domain (where Thr^{204} localizes) but by the BRCT domain (Ma et al., 2004; Mueller et al., 2008; Nick McElhinny et al.,

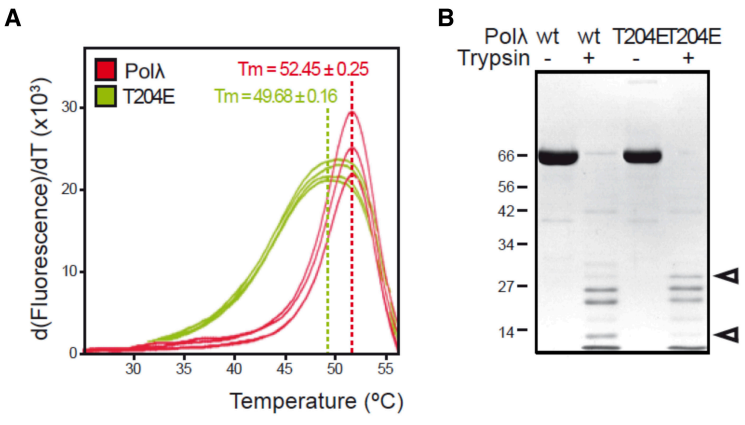

Figure 30. The T204E phospho-mimetic mutation induces conformation changes in Polλ. (A) Thermal denaturation curves obtained by differential scanning fluorimetry of recombinant wild-type Polλ (solid red line) and Polλ-T204E (solid green line). Results are displayed as the differential of the fluorescence in arbitrary units divided by the differential of the temperature, plotted against temperature. (B) Partial proteolysis assay. Recombinant wild-type Polλ and the phospho-mimetic mutant Polλ-T204E were subjected to a partial proteolysis with trypsin.

2005). Hence we speculated that phosphorylation at Thr^{204} by DNA-PKcs kinase could modify the conformation of Polλ to facilitate the interaction after DSB induction. To test this hypothesis, we devised the phospho-mimetic mutant T204E, in which Thr^{204} was replaced by a glutamic acid, thereby mimicking a phosphorylated threonine, and subjected both this mutant to a thermal shift assay, which measures the thermal denaturation of proteins. Interestingly, the experiment showed that the T204E mutation decreased the melting temperature of Polλ (Figure 30A), suggesting that the Thr^{204} phosphorylation could lead to a more open conformation. We also performed partial proteolysis assays to test a possible change in conformation, which showed that in the T204E mutant displayed a different pattern of proteolysis (Figure 30B), again suggesting a change in conformation induced by the phospho-mimetic mutation. Taken together, these results strongly suggest that phosphorylation of Thr^{204} modifies the conformation of Polλ to facilitate interaction after the induction of DSBs.

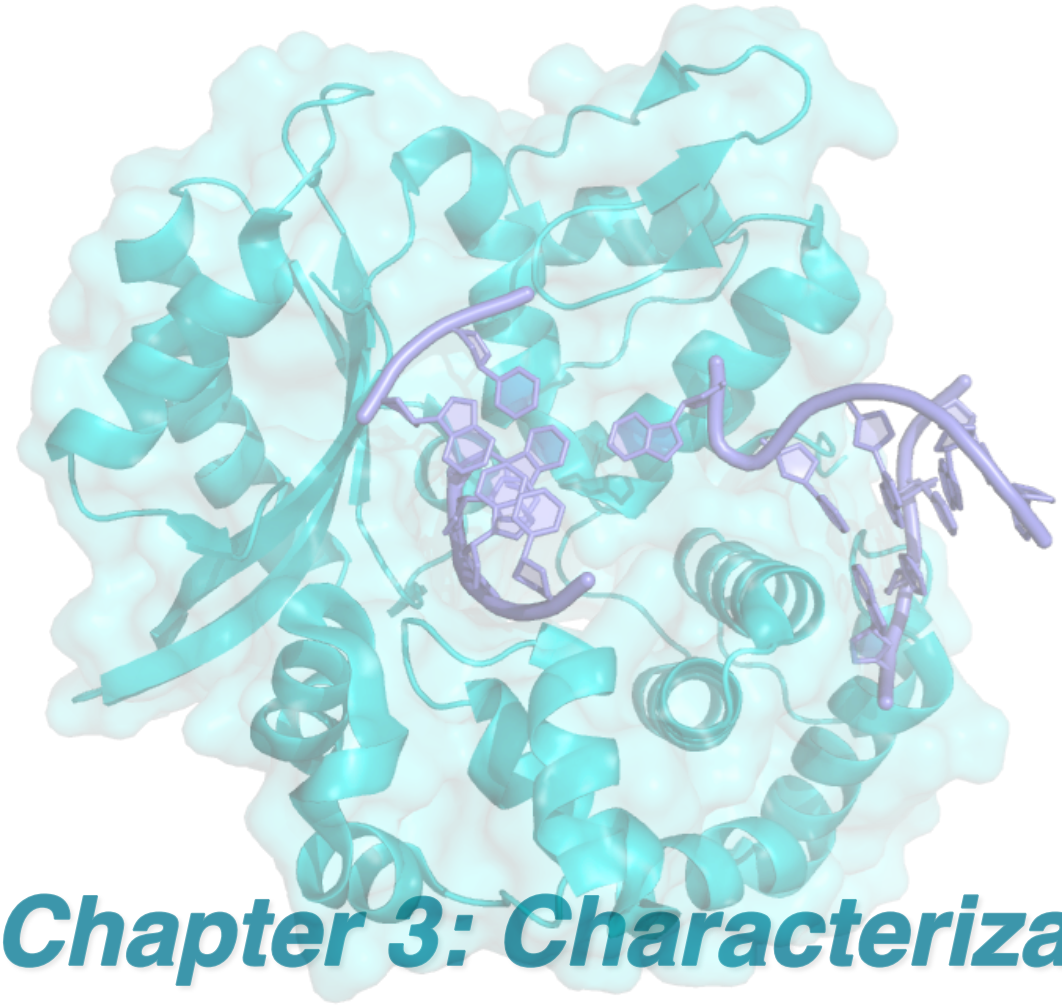

Chapter 3: Characterization of Polμ tumour variants

Figure: Ternary pre-catalytic complex of human Polμ (PDB ID 4M04)

In this chapter we have evaluated whether the alteration or deregulation of the activity of Polμ, one of the two human PolXs specialized in NHEJ, could be associated to a certain extent to tumourigenesis, a relevant pathological scenario. We focused in human Polμ because, in contrast to Polβ and Polλ, whether Polμ mutations found in tumours could alter the properties of this enzyme has never been studied. Additionally, instead of considering post-translational modifications, we sought to characterize tumour variants affecting residues directly involved in catalysis for mainly two reasons: 1) although previous studies have clearly supported Polμ specialization in the NHEJ of non-complementary DSBs and identified some of the structural elements of Polμ required for this complex task, there are still some aspects of this adaptation that remain unknown, and 2) analyses of Polβ and Polλ tumour variants demonstrated that some point mutations can alter the function of these polymerases and helped to identify residues relevant for their activity (Dalal et al., 2005; Lang et al., 2004; Sweasy et al., 2005; Terrados et al., 2009). Hence, this chapter describes the characterization of two tumour variants of Polμ, G174S and R175H, involving two adjacent residues Gly^{174} and Arg^{175}, and demonstrates that both mutations pronouncedly decrease the efficiency and fidelity of Polμ during NHEJ *in vitro* and *in vivo*.

1. Structural analysis and evolutionary conservation of Polμ Gly^{174} and Arg^{175}

Previous studies compiled in the COSMIC database (http://cancer.sanger.ac.uk/cosmic) (Forbes et al., 2008), have identified two human Polμ point mutations, G174S and R175H, described in a skin and ovary carcinomas respectively (Bell et al., 2011; Durinck et al., 2011). These tumour mutations affect two adjacent residues, Gly^{174} and Arg^{175}, located within the 8 kDa and in close proximity to the downstream and template strands limiting a DNA gap (Figure 31A). Gly^{174} is positioned near the template base that is paired to 5' end-terminal base of the downstream strand flanking the gap (Figure 31A). Interestingly, Polβ and Polλ harbour a histidine (His^{34}) or a tryptophan (Trp^{274}) respectively at that position (Figure 31B & C), that can perform stacking interactions with the template base ring moiety and are highly evolutionary conserved in Polβ and Polλ from vertebrates (Figure 32A & B). Conversely, the small size of Gly^{174} minimizes interaction with the DNA, which could suggest a minimal interference with sporadic distortions of the template molecule. As previously reported, Arg^{175} directly interacts with the 5'P group of the downstream strand when Polμ is bound to a DNA gap (Figure 31A; Moon et al., 2007b). Analysis of the structure of Polμ suggests that Arg^{175} may be the most relevant ligand of the 5'P

group compared to the other ligand, His^{208}. Accordingly, mutation of Arg^{175} to alanine pronouncedly diminishes Polμ activity during NHEJ (Davis et al., 2008). The recently solved structures of the catalytic cycle of human Polμ show that Arg^{175} is mobile when Polμ is not bound to the DNA and consequently its side chain is not visible in this context (Figure 31D left panel); however, the 5'P of a DNA strand fixes its conformation (Figure 31D), supporting a relevant role for Arg^{175} in DNA binding.

Primary sequence alignment of Polμ homologs shows that both Gly^{174} and Arg^{175} are highly conserved in vertebrates (Figure 31C), supporting their functional relevance.

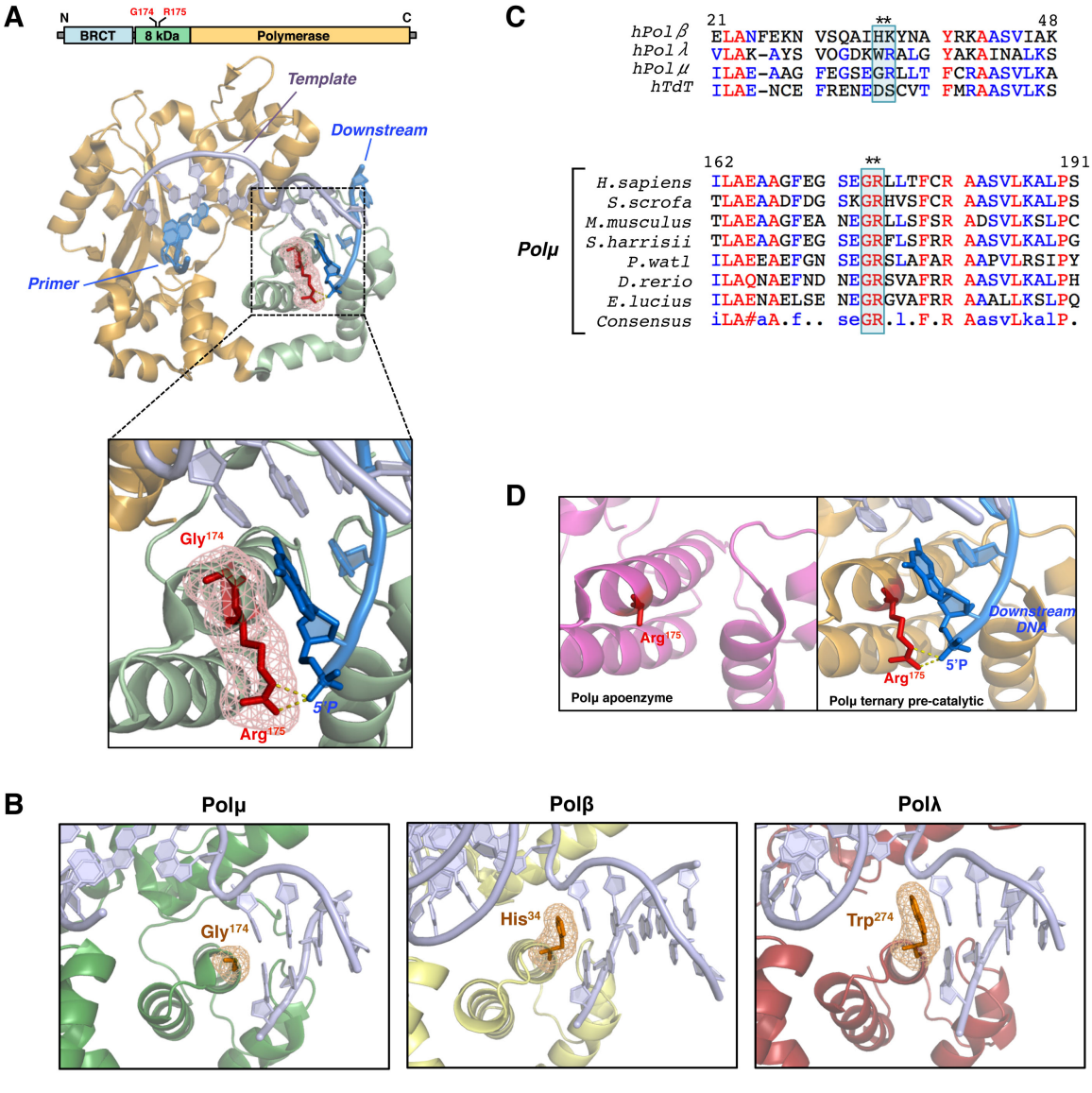

Figure 31. Structure and conservation of human Polμ Gly^{174} and Arg^{175}. (A) Structure of the ternary pre-catalytic complex of human Polμ (PDB ID: 4M04) showing Gly^{174} and Arg^{175} structure and localization. (B) Structural comparison of human Polμ, human Polβ and human Polλ (PDB IDs: 4M04, 1BPY and 1XSN respectively). (C) Primary sequence alignments of the human PolX members and of the indicated vertebrate Polμ homologs. (D) Comparison Arg^{175} in the structures of apoenzyme Polμ (PDB ID: 4LZD) and the ternary pre-catalytic complex of Polμ.

A more exhaustive alignment showed that Arg[175] is more strictly conserved than Gly[174], that can be changed to other residues such as cysteine, valine and alanine, in a few Polμ homologs (Figure 33). However, most of these other residues are likewise glycine small and nonpolar (Figure 33), hence, mutation of Gly[174] to serine in Polμ (as in the tumour variant G174S) could have functional implications, as serine is a small but polar residue. The R175H mutation might also affect the optimal function of Polμ given that histidine interaction with a 5'P may be weaker than that of arginine, given that at a physiological pH, histidines are generally not positively charged, unlike arginines. The possible relevance of Polμ Arg[175] is also supported by its invariance in Polλ (Arg[273]) and by the presence of a conservative substitution in Polβ (Lys[33]) (Figure 32A, B) the two other human PolXs that strongly bind the 5'P of the downstream strand flanking the a gap (García-Díaz et al., 2002; Prasad et al., 1994; Singhal and Wilson, 1993). Interestingly, both Gly[174] and Arg[175] are not conserved in human TdT, possibly suggesting that these residues and this area of the 8 kDa domain are especially important for template-dependent reactions. In fact, the important variability observed at these corresponding positions in TdT

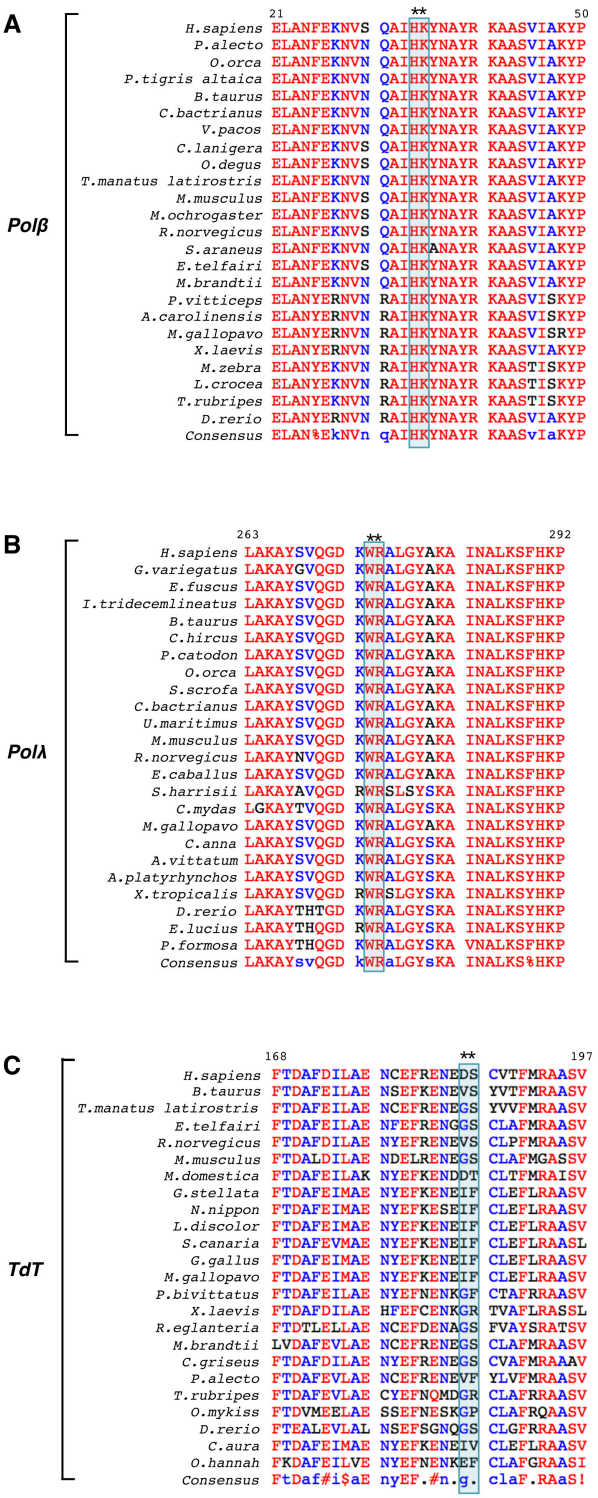

Figure 32. Primary sequence alignments of Polβ, Polλ and TdT homologs. Primary sequence alignments of the homologs of (A) Polβ, (B) Polλ or (C) TdT, from the indicated vertebrates were performed using the MULTALIN server (http://multalin.toulouse.inra.fr/multalin/). The highlighted residues are the amino acids located in the equivalent position of human Polμ Gly[174] and Arg[175] (See Figure 31C). These highlighted residues are highly conversed through evolution in both Polβ and Polλ, but not in TdT.

among vertebrates also supports this idea (Figure 32C).

2. The G174S and R175H mutations limit the efficiency of accurate NHEJ by Polμ both *in vitro* and *in vivo*

To determine the effect of the G174S and R175H mutations on the activity of human Polμ, we devised the mutants by site-directed mutagenesis and purified the recombinant proteins. First, the ability of the mutants to fill a 1nt-gap was tested by incubating the purified proteins with a 5'-labelled dsDNA containing a 1nt gap flanked by a 5'P (Figure 34A see scheme), a group known to stimulate the activity of Polμ *in vitro*. The R175H mutation did not alter the efficiency of Polμ during gap-filling of a 1nt-gap compared to its wild-type counterpart (Figure 34A), in clear contrast to what was described for the R175A mutation, which was partially defective in the filling of 1nt-gaps (Davis et al., 2008). This suggests that, although Arg^{175} is necessary for optimal gap-filling activity, a histidine can replace this residue for this task. Conversely, the G174S mutation reduced Polμ gap-filling efficiency, but very mildly (roughly 1.5-fold) (Figure 34A), suggesting that Gly^{174} is also not strictly required for this reaction. Next, after demonstrating that the tumour variants are active proteins and proficient in gap-filling *in vitro*, we sought to test the possible effect of these mutations on NHEJ, the major role of Polμ *in vivo*. For this, we used two dsDNA molecules, one labelled (Figure 34B, depicted in blue) and the other unlabelled (Figure 34B, depicted in grey), and that are endowed with 3'-protruding ends that have a complementarity of 1nt. Likewise in similar experiments previously shown in this

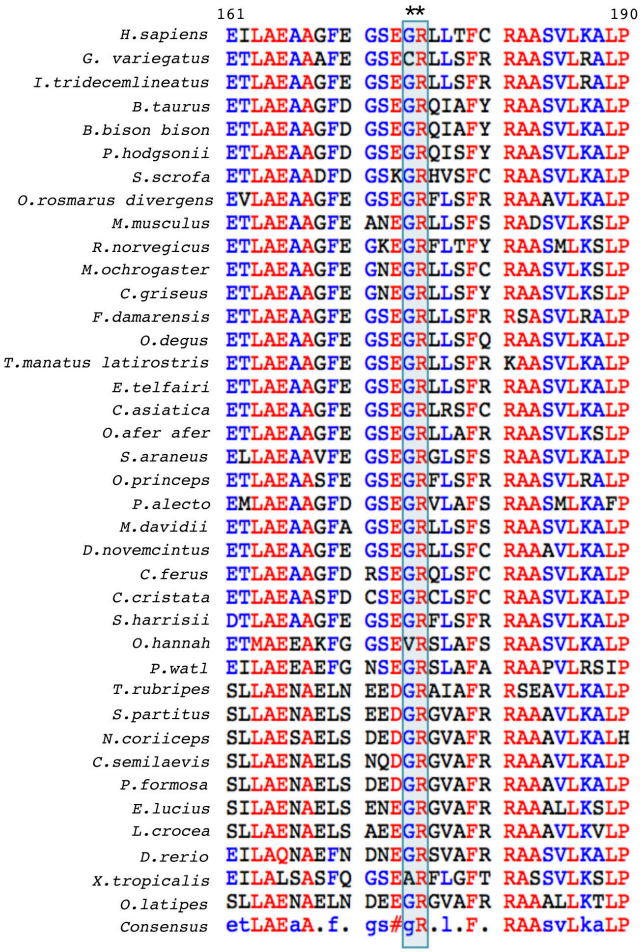

Figure 33. Primary sequence alignment of Polμ homologs. Primary sequence alignment of Polμ homologs corresponding to the indicated vertebrates were performed using the MULTALIN server. The position of human Polμ Gly^{174} and Arg^{175} and the aligning residues is highlighted. The alignment shows that both residues are highly conserved, although Arg^{175} more strictly.

Thesis, after annealing of the complementary ends, which is induced by the polymerase, two 1nt-gaps are formed, having both a template dC. Importantly, the presence of a gap-flanking 5'P only in the unlabelled molecule, stimulates Polμ to preferably use this molecule as template and the 3'-protruding end of the labelled molecule as primer. In this NHEJ assay, both the R175H and G174S mutations decreased Polμ efficiency of incorporation of dGTP, the template directed nucleotide (Figure 34B), approximately 2.5-fold and 5-fold respectively, suggesting that Arg^{175} and Gly^{174} are required for optimal NHEJ of complementary ends *in vitro*. Next, we evaluated the effect of the tumour mutations G174S and R175H on the NHEJ of non-complementary ends, the most specific role of Polμ *in vivo* (Pryor et al., 2015). We performed a similar NHEJ *in vitro* assay but using dsDNA molecules with 3'-protruding non-complementary ends (Figure 34C, see scheme). The experiment showed that both R175H and G174S mutations markedly decreased Polμ NHEJ efficiency when using non-complementary ends *in vitro* (Figure 34C), approximately 7- and 15-fold respectively, thus more pronouncedly that during the NHEJ of compatible ends (Figure 34B). Hence, these results demonstrate that the G174S and R175H tumour variants are defective in accurate NHEJ *in vitro*, more markedly when the broken ends are non-complementary, the most specific context of Polμ action. These results also support a relevant role for human Polμ Gly^{174} and Arg^{175} in NHEJ, already demonstrated for the latter (Davis et al., 2008), but completely unknown in the case of the former.

The pronounced defect caused by the mutations on NHEJ *in vitro*, prompted us to validate these conclusions in a physiological context. For this purpose, in collaboration with Dr. Dale A. Ramsden (University of North Carolina, USA), we took advantage of a recently described NHEJ extrachromosomal system (Pryor et al., 2015). As described in previous chapters, this system operates through the co-electroporation of purified polymerases and apporpriate DNA substrates into Polμ- and Polλ-deficient MEFs (Figure 34D). After electroporation, DNA substrates mimicking a DNA DSB are repaired by NHEJ inside the MEFs, and the accuracy of repair by NHEJ is monitored by restriction digestion of the substrate recovered from the cells (Figure 34D). Additionally, the fact that the recipient cells lack endogenous Polμ and Polλ implies that this accurate repair, which is mediated by gap-filling and does not require nuclease processing of the ends, completely relies on the co-electroporated purified DNA polymerases (Pryor et al., 2015). First, we used a DNA substrate mimicking a DSB with 3'-protruding ends with 2nt of complementarity (Figure 34E). Accurate repair of the substrate generates a product, referred to as +C junctions, that is monitored by

AfeI restriction. When no protein was coelectroporated with the DNA, +C junctions were barely detectable an only accounted for roughly 2% of the total DNA junctions recovered (Figure 34E). Co-electroporation of Polμ wild-type clearly stimulated the level of detectable +C junctions, demonstrating that accurate NHEJ is enhanced by Polμ-mediated gap-filling (Figure 34E). Conversely, co-electroporation of either R175H or G174S mutants only produced a slight increase in accurate NHEJ efficiency compared to the non co-electroporated protein condition, and led to 5-fold lower percentage of +C junction recovery compared to the wild-type protein (Figure 34E). According to our *in vitro* data, we expected a less pronounced defect in the case of the R175H mutant compared to the G174S mutant; however, the decrease in efficiency

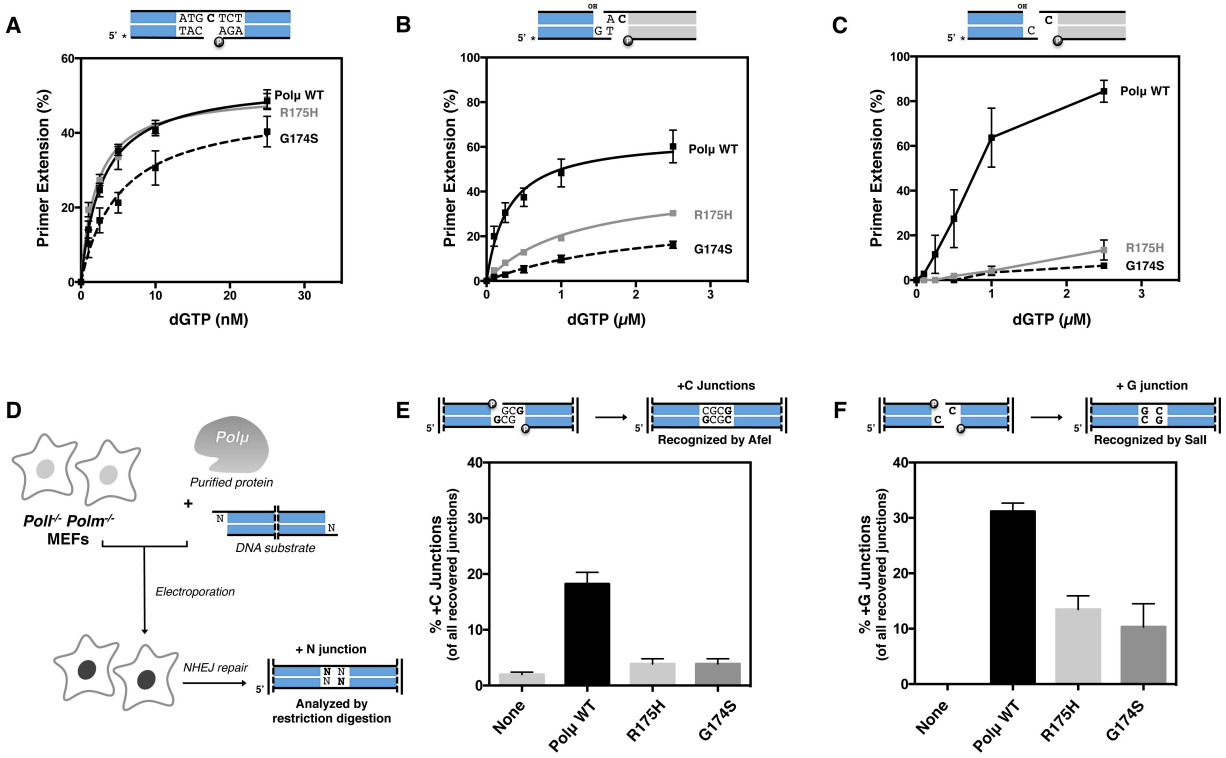

Figure 34. The effect of the G174S and R175H mutations on the efficiency of accurate NHEJ. (A) Analysis of the activity of either wild-type Polμ or the G174S and R175H mutants on a 1nt gapped DNA. Data represented are means of at least 3 independent times and the error bars correspond to the SD. (B) Kinetic analysis of the effect of the mutations on the efficiency of accurate NHEJ of complementary ends *in vitro*. Data are represented as in (A) and correspond to at least 3 independent experiments. (C) *In vitro* kinetic analysis of the efficiency of accurate NHEJ of non-complementary ends by Polμ and the G174S and R175H tumour variants *in vitro*. Data are represented as in (A) and correspond to at least 3 independent experiments. (D) Schematic representation of the extrachromosomal NHEJ cellular system. DNA substrates mimicking different types of DSBs and purified Polμ were electroporated into MEFs deficient for Polλ (*Pol*$^{-/-}$) and Polμ (*Polm*$^{-/-}$). Accurate NHEJ could be monitored by reconstitution of a restriction site in the DNA substrates. (E) Study of the effect of the G174S and the R175H mutation on accurate NHEJ in the extrachromosomal cellular system using DNA substrate mimicking a DSB with complementary ends. Protein complementation was carried out using 10 ng of the purified proteins and accurate NHEJ of the substrates was analysed by measurement the generation of the +C junction repair product, in which the restriction site of the AfeI enzyme was reconstituted by Polμ activity (n=3). (F) Effect of the mutations on the NHEJ of non-complementary ends in the cellular system. Protein complementation was carried out using 10 ng of the purified proteins and accurate NHEJ by Polμ generated the +G junction productions that were detected by digestion of the recovered DNA with the Sal I restriction enzyme (n=3).

caused by the mutations *in vivo* is overall similar to that observed *in vitro* when using a comparable substrate (Figure 34B), further confirming that these tumour variants are defective in NHEJ. Next, we performed a similar experiment electroporating a DNA molecule that mimicks a non-complementary DSB. Faithful repair by NHEJ of the molecule could be monitored by digestion of the recovered with SalI restriction enzyme (Figure 34E). As previously described, these events of faithful repair, that we named +G junctions, were completely Polμ-dependent, as they are undetectable when this polymerase was not electroporated (Figure 34F) (Pryor et al., 2015). Remarkably, when Polμ wild-type was co-electroporated with the DNA into the MEFs, +G junctions were detectable and accounted for 30% of the total repair events (Figure 34F). Electroporation of either R175H or G174S tumour variants significantly reduced the percentage of +G junctions compared to the wild-type protein (roughly 3-fold in both cases) (Figure 34F), again suggesting that the mutations reduce the ability of Polμ to perform accurate NHEJ efficiently. Interestingly, it is worthy to note that the defect caused by the mutations in the cellular system was less pronounced in the case of substrate with non-complementary ends compared to the DNA with complementary ends (Figure 34E), in clear contrast to our *in vitro* data. In fact, this defect on the NHEJ of non-complementary ends was also less pronounced than that detected *in vitro* experiment when using a comparable substrate (Figure 34C), which could suggest that the presence of other NHEJ factors could alleviate the defect caused by the mutations specifically during NHEJ of non-complementary ends, which is Polμ's most specific task *in vivo*. In any case, overall, our data unambiguously indicate that the R175H and G174S tumour variants fail to perform accurate NHEJ efficiently *in vivo*.

3. The G174S and R175H mutations lead to decreased fidelity during NHEJ

Once demonstrated that the G174S and R175H mutations hamper the efficiency of accurate NHEJ, we wanted to evaluate whether this phenotype could impact their overall fidelity. For this purpose, either the tumour variants or the wild-type control were incubated with the dsDNA molecules mimicking a DSB with non-complementary ends and 5μM of each of the 4 dNTPs, which were added to the mix independently. Wild-type Polμ incorporated dGTP, the template directed nucleotide, much more efficiently than incorrect nucleotides (Figure 35A, left graph); as a control, incorporation of dGTP required the presence of the unlabelled molecule with the 5'P to be efficient (Figure 35A, compare dGTP incorporation in both left and right graphs). Importantly, when the molecule harbouring the 5'P was not present in the assay, dGTP incorporation,

although much less efficient, was still detectable, most likely do to the fact that Polμ can simultaneously bind two of the labelled molecules, which also have 3' protruding dCs, and use one of them as a template (Figure 35B). Interestingly, wild-type Polμ could also catalyse the incorporation of the 3 incorrect nucleotides, and with comparable efficiency irrespectively of the presence of the molecule with the 5'P group (Figure 35A). Furthermore, in the absence of the DNA ends with the 5'P, incorrect nucleotides were incorporated as efficiently as dGTP, suggesting that when the phosphate group that flanks the template base is absent, the templating base dC cannot be "read" correctly by Polμ, probably due to defective binding and/or orientation of the two DNA ends (Figure 35B). In fact, we speculate that these events of catalysis are due to the terminal transferase activity of Polμ (Juárez et al., 2006), known to be limited by the presence of 5'P groups (Andrade et al., 2009), and therefore, they may not necessarily involve simultaneous binding of two DNA molecules. In agreement with our previous results, the G174S and R175H variants incorporated dGTP less efficiently than wild-type Polμ when the two kinds of DNA molecules were present (Figure 35A left panel). The G174S variant incorporated dGTP with similar efficiency either in the presence or absence of the dsDNA molecule with the 5'P (Figure 35A, left & right graphs) and overall similarly to incorrect nucleotides (Figure 35A), but strikingly, with comparable efficiency to the wild-type protein in the absence of the dsDNA molecule with the 5'P (Figure 35A, right graph). The fact that incorporation of the template directed dGTP by the Polμ variants less stimulated by presence of a 5'P group flanking the template base compared to their wild-type counterpart suggests that they either cannot correctly bind or orientate template DNA molecules (Figure 35B). It is worthy to note this phenotype was particularly more pronounced in the G174S mutant, which could not incorporate dGTP more efficiently that incorrect nucleotides in any scenario (Figure 35A). In line with this, the experiments also demonstrated that incorrect nucleotides were incorporated with similar efficiency by the mutants and wild-type Polμ (Figure 35A), and that overall, these proteins behaved similarly in the absence of a 5'P flanking the template base (Figure 35A right graph), indicating that the mutations do not affect catalysis but specifically hamper incorporation of template directed nucleotides, which occurs through bona-fide NHEJ reactions requiring a 5'P to flank the template base (Figure 35B).

Kinetic analyses of the incorporation of dATP opposite under these conditions further confirmed that the G174S and R175H mutations did not affect incorporation of non-templated nucleotides during NHEJ of non-complementary ends, which again took place similarly either in the absence of presence of a 5'P flanking the template base (Figure 35C), further confirming that this reaction does not occur via bona-fide NHEJ. Interestingly, in addition to phosphate groups, certain sequence contexts have also been shown to impact Polμ activity during NHEJ. For instance, certain bases, such as dA, are poor templates during Polμ-mediated NHEJ of non-complementary ends *in*

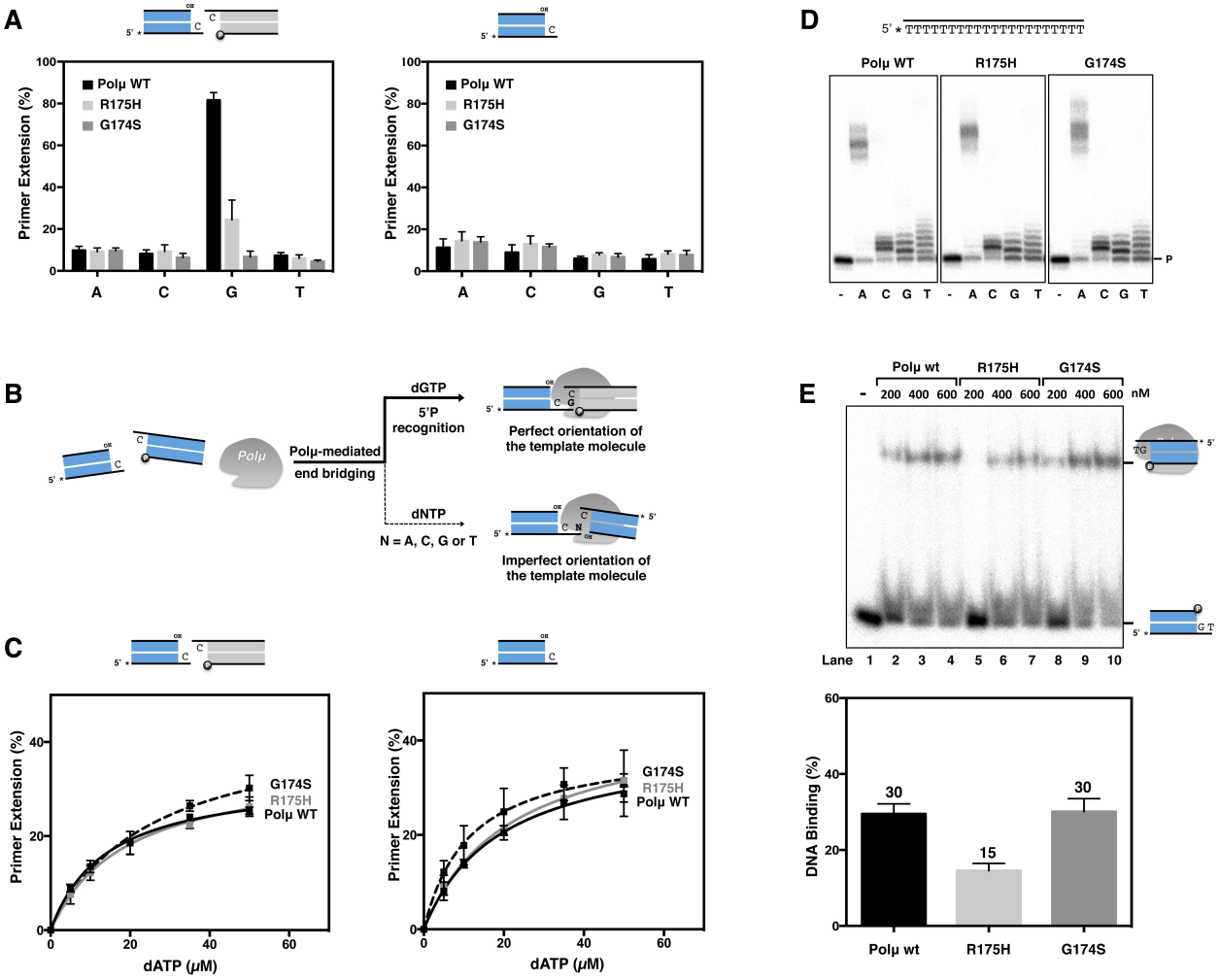

Figure 35. Decreased fidelity caused by the G174S and R175H mutations on NHEJ *in vitro*. (A) Purified Polμ and the G174S and R175H mutants (200 nM) were incubated with 5 μM of each individual dNTP and the two DNA molecules mimicking a DSB with non-complementary ends to test the fidelity of these reactions (*left graph*). The effect of the 5'P group flanking the template base on the fidelity of NHEJ was evaluated by repeating the experiment in the absence of the unlabelled 3'-protruding DNA molecule (*right graph*). The data represented in the graphs are of at least 3 independent experiments and the error bars correspond to the SD. (B) Schematic representation of Polμ-mediated end-bridging of the DNA molecules used in (A) explaining template dependent and template independent incorporations of nucleotides. (C) Kinetic analysis of template independent nucleotide incorporation by Polμ at DSBs with non-complementary ends, measured by dATP insertion, by Polμ and the G174S and R175H mutants. Data are the means of at least two independent experiments and the SD is represented in the error bars. (D) Analysis of the terminal transferase activity of Polμ on homopolymeric DNA. (E) Effect of the G174S and R175H mutation on DNA binding monitored by of electrophoretic shift assays. The graph represents means of triplicate experiments using 400 nM of either Polμ wild-type or the G174S and R175H mutants, and the error bars show the SD.

vitro (Martin et al., 2013a). In agreement with our previous data, the tumour variants showed a similar rate of incorporation of all dNTPs compared to wild-type Polμ in this error-prone sequence context (Figure 36), confirming that the mutants show a specific defect in template-directed NHEJ reactions. As mentioned earlier, we speculate that the incorporation of template-independent nucleotides during NHEJ is due to the terminal transferase activity of Polμ. Also in line with our previous results, the G174S and R175H mutations did not affect the terminal transferase activity of Polμ measured by incorporation of dNTPs on a homopolymeric ssDNA molecule (Figure 35D).

Taken together, our results demonstrate that the G174S and R175H mutations specifically decrease Polμ efficiency to incorporate template-directed nucleotides during NHEJ of non-complementary ends. The mutations on the other hand, do not impact whatsoever the incorporation of incorrect dNTPs at DSBs, which likely occurs through terminal transferase-like reactions. Hence, these results indicate that these tumour mutations will impact the fidelity of Polμ during NHEJ via interfering with template-dependent selection of nucleotides *in vivo*. Given that the residues affected by the mutations localize in the 8 kDa domain, which is involved in binding the template/downstream junction at a gap, the low efficiency of bona-fide NHEJ caused by the mutations could be consequence of a defect in binding/orientatopn of the templating base, either directly or indirectly caused by defective 5'P recognition. Electrophoretic mobility shift assays indicate that the R175H variant, but not the

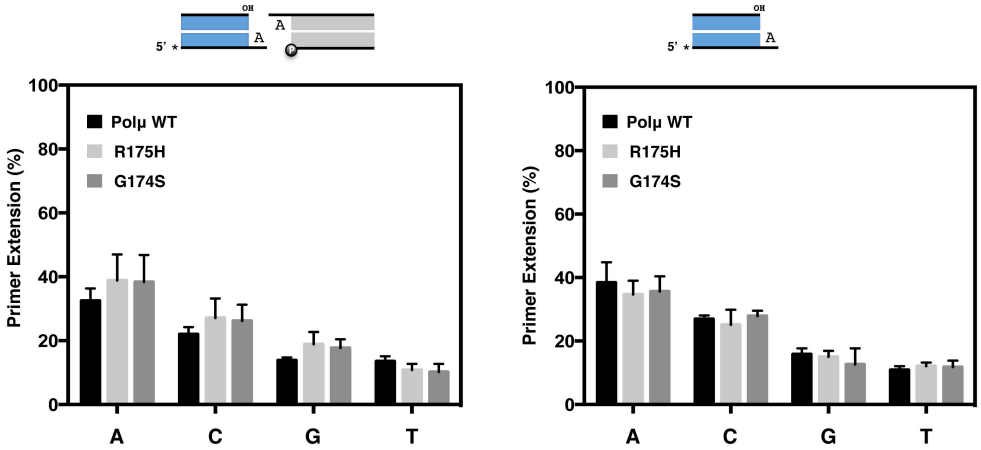

Figure 36. Analysis of the effect of the G174S and R175H mutations on the fidelity of NHEJ in an error-prone sequence context. Certain template bases such as dA, cannot faithfully direct nucleotide incorporation by Polμ. Accordingly, the experiment showed that Polμ could not incorporate the template-directed nucleotide, dTTP in this sequence context, more efficiently than the incorrect nucleotides, unlike what was observed in the comparable non-complementary NHEJ experiment using a different sequence context (Figure 35A). Additionally, and also unlike in the other sequence context, Polμ behaved similarly irrespective of the presence of a 5'P flanking the template base, confirming that in this experiment Polμ preferably incorporates nucleotides in a template-independent fashion. Interestingly, in this assay both the G174S and R175H mutations displayed a similar rate of incorporation of all dNTPs compared to the wild-type control, causing no detectable effect.

G174S, bound defectively to a 3'-protruding DNA substrate harbouring a 5'P next to the protrusion (Figure 35E). This suggests that defective NHEJ by R175H is thus a consequence of impaired DNA binding in agreement with the fact that Arg^{175} is the main ligand of the 5'P group. However, this experiment could also indicate that although R175H and the G174S variants lead to a similar phenotype, they might affect NHEJ differently, as the G174S mutation apparently does not impair binding of the DNA. We speculate that this mutation might affect proper orientation of the templating base that is likely facilitated by the small and flexible Gly^{174}.

4. The G174S and R175H mutations impact alternatively 2nt gap-filling by Polμ

The adaptation of the members of the PolX family to filling small DNA gaps -a common DNA transaction in both BER and NHEJ- was achieved in part thanks to the development of the 8 kDa domain, which allows these polymerases to interact not only with the 3'end of the primer, like a regular polymerase, but also with the 5' end of the downstream strand of the gap. Consequently, PolXs can be particularly ineffective if these ends are too distant. In fact, a recent study demonstrated that in mammalian NHEJ, PolX activity is mainly restricted in mammalian NHEJ mainly to the filling of 1nt and 2nt gaps *in vivo* (Pryor et al., 2015). However, 2nt gaps are already a challenging scenario for most PolXs, where Polμ was demonstrated to be ineffective (Moon et al., 2015; Pryor et al., 2015). Whereas Polλ can accurately fill 2nt gaps due to its unique ability to scrunch the template (Garcia-Diaz et al., 2009), Polμ lacks this capacity and is both less efficient and more error-prone in this context (Moon et al., 2015; Pryor et al., 2015). In fact, when dealing with 2nt gaps, Polμ was shown to preferably copy the template base closer to 5' end of the downstream strand, rather than the first template base, a reaction termed skipping-ahead that potentially leads to frameshift mutations (Ruiz et al., 2004; Juárez et al., 2006; Martin et al., 2012; Moon et al., 2015; Pryor et al., 2015). Due to the specific role of the 8 kDa in interacting with the 5' end of the downstream DNA strand, this domain has already been anticipated to possibly influence Polμ's error-proneness during the filling of 2nt gaps (Moon et al., 2015). Moreover, one would also speculate that the lack of stacking interactions with the base pair flanking the gap, a stark difference between Polμ and Polλ, could also have an influence on how differently these enzymes behave on 2nt gaps. Hence, we decided to address the role of the Gly^{174} and Arg^{175} residues on the filling of 2nt gaps by Polμ by analysing the effect of the G174S and R175H mutations. For this, we used a 5'-labelled dsDNA molecule harbouring a 2nt gap in which incorporation opposite the first template

base and opposite the second template base could be monitored by incorporation of dCTP and dGTP respectively (Figure 37A). As expected, under these conditions, Polμ was clearly more efficient (roughly 7-fold) using the second template base to direct nucleotide incorporation (dGTP in this case) rather than the first, although it could use either of them for catalysis (Figure 37B, note the scale of nucleotide concentration). Strikingly, the R175H mutation pronouncedly decreased the overall efficiency of Polμ in both reactions, so markedly that incorporation of the nucleotide complementary to the first template base (dCTP) was not detected in the experiment (Figure 37B). Consequently, these data indicate that Arg^{175} is indispensable for the filling of 2nt gaps by Polμ, and that a histidine cannot replace it for this task, similarly to what was observed in the NHEJ experiments (Figure 34). Conversely, this result contrasts that obtained in a 1nt gap-filling assay (Figure 34A), where the R175H had no detectable defect, suggesting that the 2nt gap is a more challenging scenario, likely more dependent on optimal interaction with the 5'P of the downstream strand. Conversely, the G174S mutation improved (roughly 2.5-fold) the incorporation of the nucleotide complementary to the

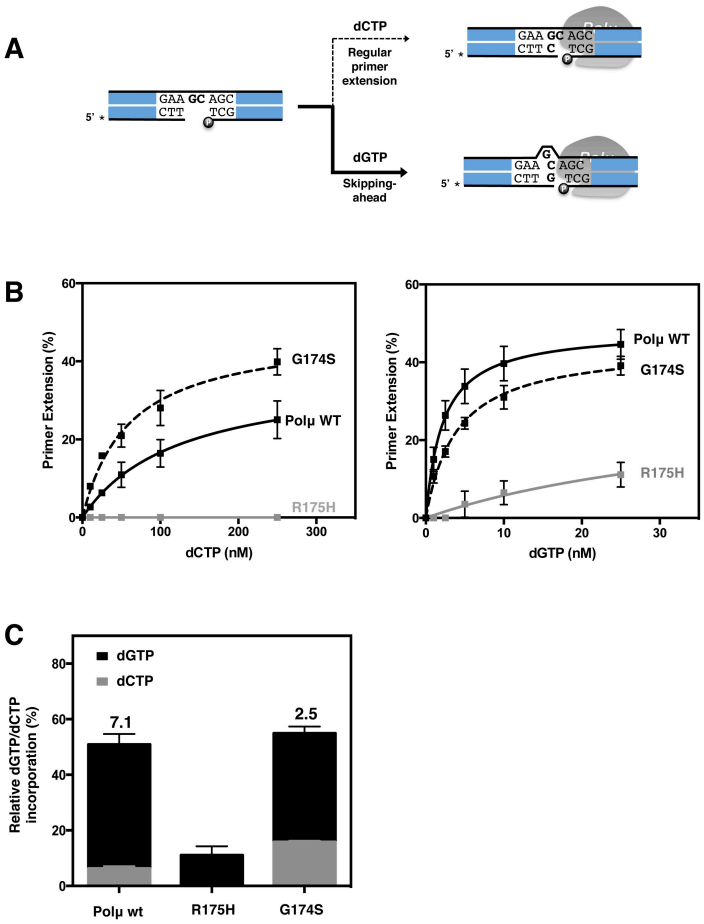

Figure 37. Analysis of the effect of the G174S and R175H mutation on 2nt gap-filling by Polμ *in vitro*. (A) Schematic representation of incorporation of the nucleotide complementary to the first template base (regular primer extension) and to the second template base (skipping-ahead) mediated by Polμ. (B) Effect of the G174S and R175H mutations on the efficiency of both reactions measured by dCTP and dGTP incorporation respectively. Data represent means of triplicate experiments and the error bars the SD. (C) Representation of the incorporation of 25 nM of dGTP and dCTP shown in B, relative to each other. The total length of the bar corresponds to the summed incorporation of both nucleotides. The fraction represented in black corresponds to the incorporation of dGTP whereas the grey fraction corresponds to dCTP incorporation. The number above the Polμ wild-type and the G174S bar was calculated by dividing primer extension with dGTP by primer extension with dCTP. This kind of analysis was not performed in the case of the R175H mutant because no dCTP incorporation could be detected by this mutant at any concentration.

first template base (Figure 37B), and led only to a moderate decrease in efficiency (1.5-fold approximately) in the skipping-ahead reaction compared to wild-type Polμ (Figure 37C). Hence, although the G174S mutants still showed a clear preference for the skipping-ahead reaction, our data indicate that it performed this reaction only 2.5-fold more efficiently than the incorporation of nucleotides opposite the first template base, in contrast to wild-type Polμ that skipped-ahead 7.1-fold higher efficiency (Figure 37C). Overall, these data suggest that Gly^{174} and Arg^{175} have different roles on 2nt gap-filling by Polμ; while Arg^{175} is required for any reaction mediated by Polμ involving a 2nt gap, Gly^{174} limits nucleotide incorporation opposite the first template base. Additionally, analyses in our cellular NHEJ system indicate that both the G174S and the R175H mutants decreased similarly (2-fold) the ability of Polμ to perform skipping-ahead reactions on 2nt gaps during NHEJ, consequent with their effect on these reactions and their overall limitation during NHEJ (Figure 38). However, likewise Polμ, the mutants could not fill the 2nt gap by incorporating 2 nucleotides and extending the primer normally, suggesting that, although Gly^{174} favours normal primer extension at 2nt-gaps *in vitro*, its mutation to serine may not be sufficient to perform accurate 2nt gap-filling *in vivo*.

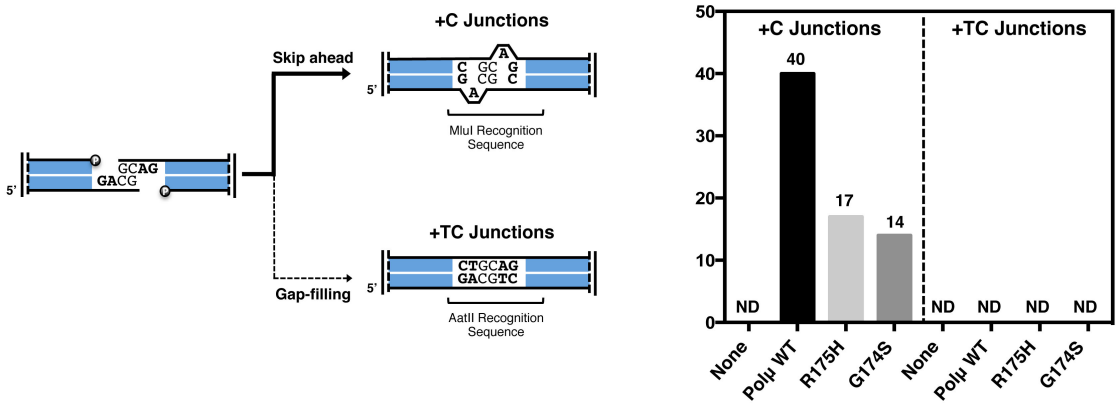

Figure 38. 2nt gap-filling coupled to NHEJ *in vivo*. A DNA substrate mimicking a DSB with 2nt gaps was electroporated into the cell together with the 100 ng of the purified enzymes, as described in the materials and methods section. The substrate allowed monitoring of both the complete filling of the 2nt gap (+TC junctions) and the skipping-ahead phenomenon (+C junctions) by reconstitution of the AatII and MluI restriction sites respectively. The experiment showed that neither wild-type Polμ nor the mutants could correctly fill the 2nt gap, suggesting that despite the effect of the mutations on 2nt gap-filling *in vitro* on a 2nt gap-containing dsDNA it is not sufficient for this reaction to take place during NHEJ. Moreover, the mutants performed the skipping-ahead reaction during NHEJ *in vivo* less efficiently than the wild-type control, in agreement with their defect in skipping ahead *in vitro* and their overall deficient ability to perform NHEJ.

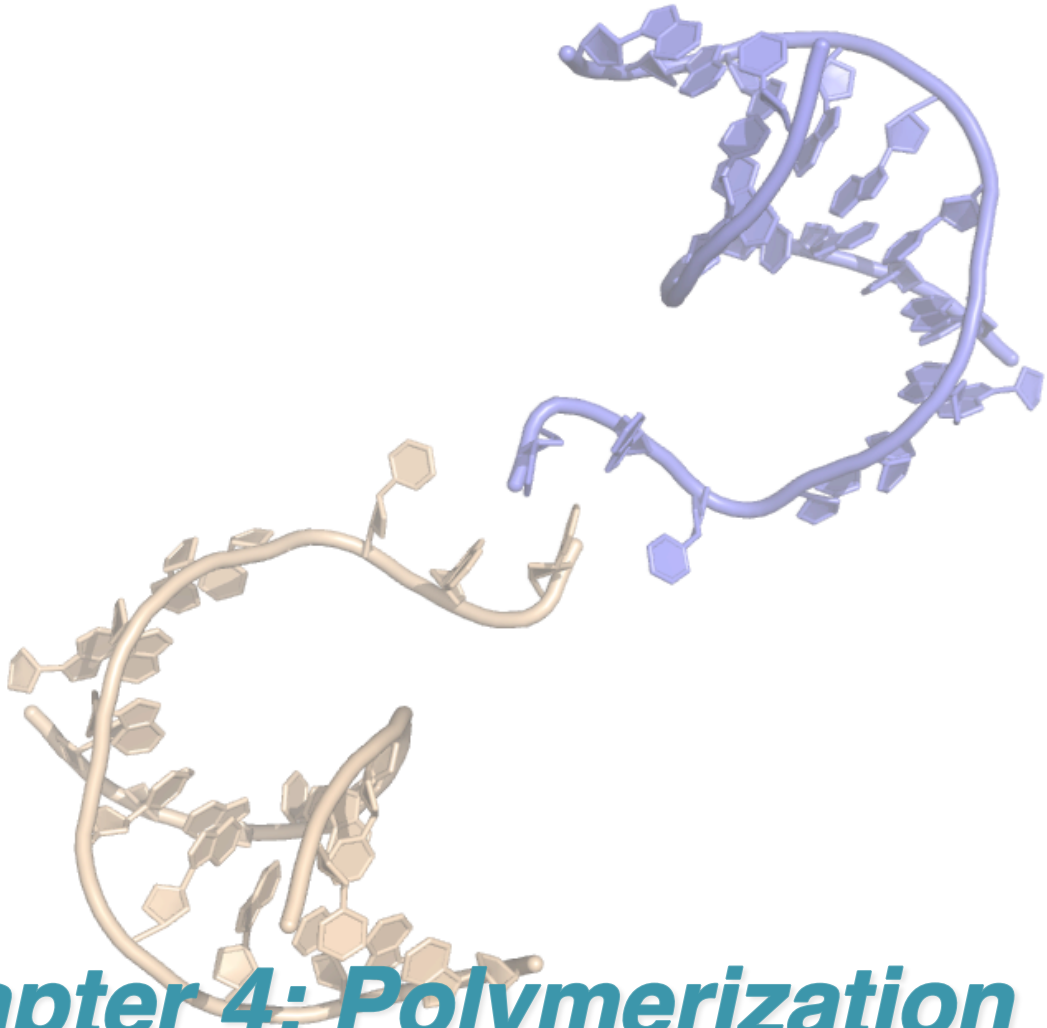

Chapter 4: Polymerization across discontinuous templates by PrimPol

Figure: Alignment of the protrusions of two dsDNA molecules (PDB ID 4X0Q)

PrimPol has the extraordinary capacity to realign primers ahead of unreadable lesions such as AP sites and UV lesions taking advantage of primer/template microhomologies beyond the damaged site (Martínez-Jiménez et al., 2015). Moreover, this capacity is highly related with the ability of PrimPol to efficiently tolerate distortions in both the primer and template strands during polymerization (Martínez-Jiménez et al., 2015). Interestingly, these properties of PrimPol, which are only mirrored by a few human polymerases, mainly Polθ and Polμ (Hogg et al., 2012; Kent et al., 2015; Martin et al., 2012), could suggest that PrimPol may also be capable to connect two non-complementary oligonucleotides by virtue of existing microhomologies to polymerize across these molecules. Hence, to gain further insight into DSB repair in human cells, in this chapter we have tested this hypothesis and we show that indeed, PrimPol has the capacity to polymerize across discontinuous DNA molecules, even with null complementarity, as it has been also described for another primase of the AEP family (Hu et al., 2012).

1.PrimPol can polymerize across discontinuous DNA templates

To evaluate the ability of PrimPol to connect separate DNA strands and polymerize across them, purified PrimPol was incubated independently with 3 different 5'-labelled ssDNA molecules of distinct length and sequence, together with either dNTPs or NTPs (Figure 39A). Remarkably, PrimPol was able to elongate any of the ssDNA molecules provided (Figure 39A, top 3 panels), demonstrating that PrimPol is endowed with the inherent property of transpolymerization across discontinuous ssDNA strands. As expected, PrimPol was much more efficient in all the cases using dNTPs compared to NTPs (Figure 39A, compare the top and bottom panels), demonstrating that PrimPol discriminates against NTPs during these reactions. On the other hand, the experiments shown in Figure 39A also indicated that nucleotide incorporation by PrimPol was more efficient when using the longer ssDNA, suggesting that a certain length is needed for optimal binding and/or to have more options for connection. The smallest ssDNA molecule used, 13-mer, has a sequence rich in Cs with only little microhomologies, and accordingly, when using this ssDNA, PrimPol could only catalyse incorporation of dGTP among the dNTPs provided individually (Figure 39A, top left panel); however the fact that the nucleotide of at the 3' end is not complementary to any other nucleotide of the ssDNA molecule suggests that PrimPol can likely tolerate mismatches even at the primer-terminus, especially those that are stable such as the T:G pair, during these kind of reactions. The size of the elongated product is compatible with the slippage-

mediated reiterative insertion of dGTP at the template tracks of Cs (Figure 39B), which was limited when the 4 dNTPs were provided. When using a longer ssDNA molecule (20-mer) with a different sequence (Figure 39A, central top panels), dGTP was again the only elongating dNTP, which was also repeatedly incorporated. In this case, there

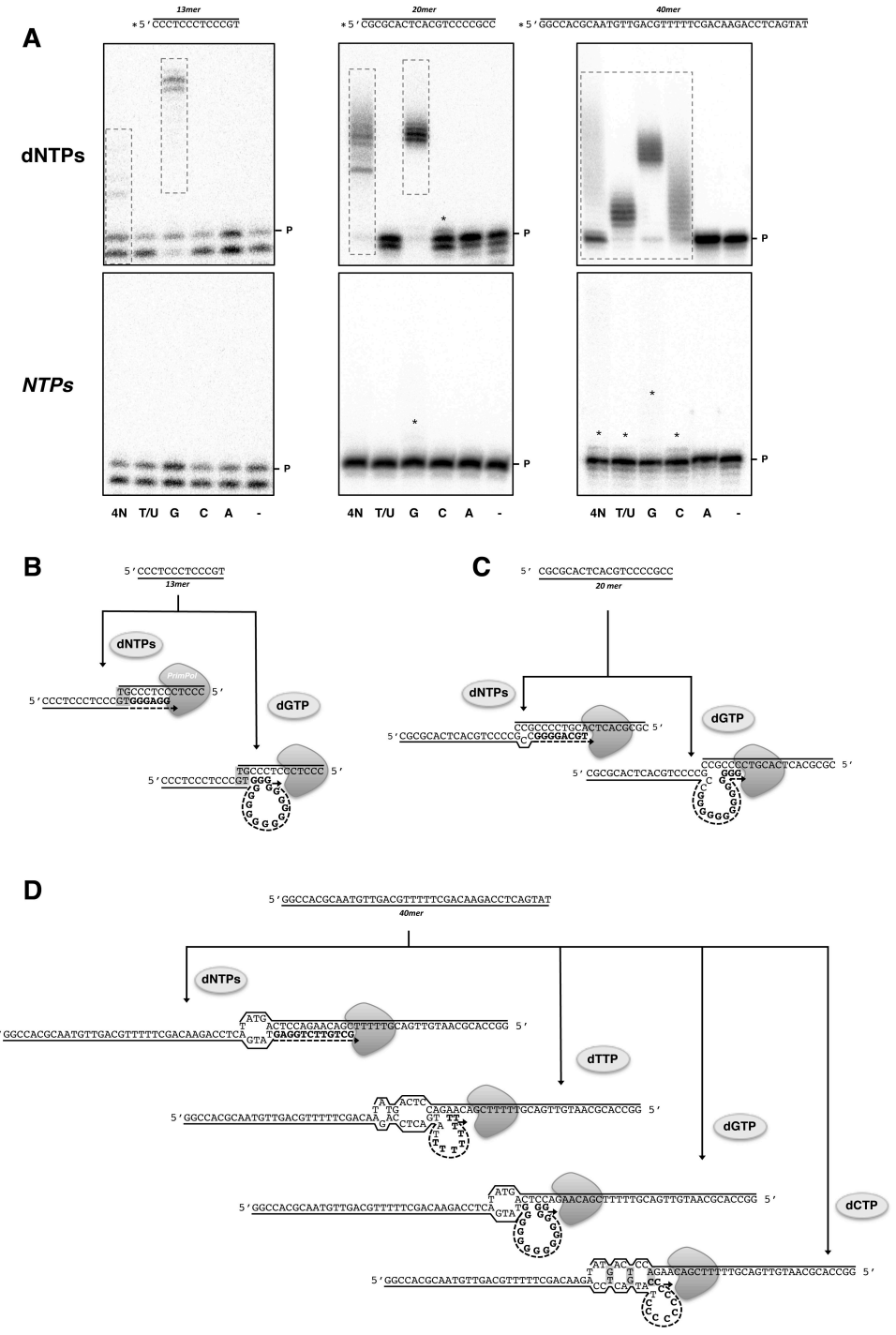

Figure 39. Sugar discrimination and sequence context influence on the polymerization across discontinuous templates by PrimPol. (A) Polymerization activity on a 5'-labelled 13-, 20- or 40-mer ssDNA oligonucleotides by purified PrimPol using the indicated dNTPs or NTPs as substrates. (B) Model depicting a plausible explanation of PrimPol-mediated DNA synthesis across the 13-mer ssDNA molecule. (C) Plausible model explaining for the DNA synthesis by PrimPol detected using the 20-mer molecule. (D) Model depicting the products of extension generated by PrimPol when incubated with the labelled 40-mer ssDNA molecule.

was more obvious nucleotide complementarity for connecting the 3' end of the 20-mer molecule to a second DNA molecule, allowing the prediction of a more stable alignment prior to catalysis by PrimPol (Figure 39C). Finally, when PrimPol was incubated with a longer ssDNA (40-mer) with a distinct sequence, PrimPol could also incorporate dTTP and dCTP among the individually provided nucleotides (Figure 39A top right panel), whose incorporation was barely detectable in the previous experiments (Figure 39A top left and central panels), which argues in favour of less evident microhomologies to mediate ssDNA bridging and nucleotide incorporation by PrimPol. Analysis of the sequence of this 40-mer molecule again suggests that PrimPol can efficiently tolerate mismatches close to the primer-terminus, and that iterative incorporation of individually provided nucleotides is likely facilitated by PrimPol-induced primer slippage (Figure 39D). Overall, it is worthy to note that in al these experiments presented in Figure 39A, extension by PrimPol was generally more limited when the 4 dNTPs were provided together, suggesting that in a physiological context, PrimPol-mediated synthesis on a discontinuous template could be more restricted, thus minimizing expansions.

Importantly, by using a homopolymeric ssDNA (poly-dT), we evaluated if PrimPol has an intrinsic terminal transferase activity that could facilitate connectivity of two non-complementary strands. As shown in Figure 40, PrimPol did not extend poly-dT neither with dC, dG nor dT, but only dATP (complementary to the poly-dT oligonucleotide) was repeatedly incorporated. That indicates that PrimPol has no terminal transferase activity, but is capable of connecting two ssDNA strands even when they are strictly non-complementary.

In summary, these data suggest that PrimPol-mediated can synthesize across a

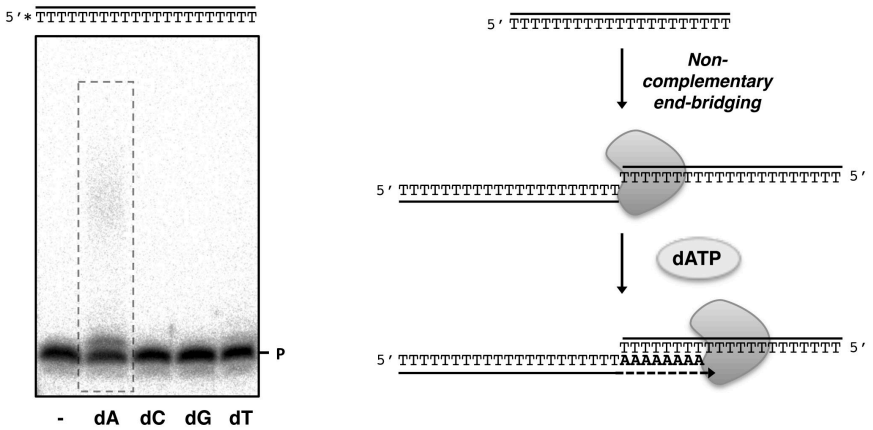

Figure 40. PrimPol promotes the synapsis of ssDNA molecules with null-complementarity. When incubated with a 5'-labelled homopolymer (poly-dT) as ssDNA, PrimPol could not incorporate of dC,dG or dT arguing against a conventional terminal transferase activity. Conversely, efficient and repetitive dAMP incorporation occurred, arguing in favour of a PrimPol-mediated non-complementary synapsis of two poly-dT molecules (see the scheme).

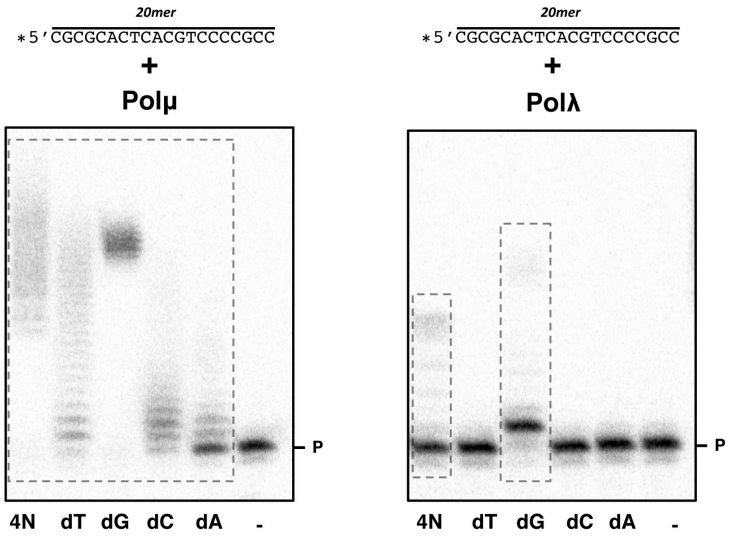

Figure 41. Polymerization across discontinuous ssDNA molecules by the NHEJ human polymerases Polμ and Polλ. 5 nM of 5' [^{32}P]-labelled 20 mer ssDNA molecule depicted in figure were incubated with 100 μM of the indicated dNTPs, 1X reaction buffer, 1 mM $MnCl_2$ and 400 nM of either purified human Polμ (A) or human Polλ (B) for 60 min at 30ºC. Samples were resolved and primer extension was analysed as described in the materials and methods section. Polμ could incorporate any of the four dNTPs thanks to its terminal transferase activity. However, similarly to PrimPol (Figure 1A, central panel), among the nucleotides provided individually, Polμ showed higher efficiency using dGTP suggesting that these nucleotide was incorporated, at least in part, in a template-dependent reiterative fashion via primer slipagge. This could indicate Polμ likely bridges the ssDNA molecules similarly to PrimPol (Figure 1C) and is in agreement with the high propensity of Polμ to induce expansions (Aza et al., 2013). Polλ only incorporated dGTP and the 4 dNTPs together, likewise PrimPol, consequent with the fact that it lacks template-independent activity, however with dGTP extension by Polλ was mainly limited to 1 insertion suggesting that it bridges the ssDNA differently from PrimPol (Figure 1C).

discontinuous templates even if they are not complementary, which could indicate a possible role in DSB repair. Interestingly, this activity of transpolymerization by PrimPol is stimulated by the use of dNTPs as substrates and by the presence of microhomologies to promote connectivity of the two ssDNA molecules. Additionally, this activity also seems to parallel that described for other enzymes of the AEP family (Hu et al., 2012), and also for human Polθ, which was recently demonstrated to be involved in the microhomology-mediated end joining (MMEJ) pathway of DSB repair (Hogg et al., 2012; Kent et al., 2015; Mateos-Gomez et al., 2015). As we also tested, the activity of PrimPol on this kind of substrates also paralleled that of the two human DNA polymerases involved in non-homologous end joining (NHEJ) of DSBs, Polλ and Polμ (Figure 41), again suggesting a potential role for PrimPol in alternative pathways of DSB repair.

2. PrimPol cannot polymerize across dsDNA molecules with short 3'-protruding ends

After evaluating the effect of sequence context and substrate selection on the polymerization across discontinuous ssDNA molecules, we sought to determine the

activity of PrimPol on DNA substrates mimicking other physiological DSB repair intermediates. First, PrimPol was incubated with the labelled 20-mer DNA molecule used in figure 39A but hybridized to a shorter DNA molecule to generate a dsDNA with a 3' protrusion of 4 nt (Figure 42A, see scheme), this way resembling a NHEJ intermediate. The 3' protrusion of this dsDNA molecule has low self-complementary, but the bridging of two of these molecules by PrimPol could be plausible if 2 of the last 3nt of the protrusion (GCC) were annealed, leading to the formation of two matches, one mismatch in the middle, and two 1nt gaps with a template dC flanking the annealed nucleotides. Under these conditions, PrimPol was mostly inactive, which could be due to the low self-complementarity of the 3' protruding sequence of the dsDNA or to the length of the protrusion being too short. Only a similar pattern of reiterative dGTP incorporation could be detected, which was probably catalysed by PrimPol using a minor fraction of the labelled ssDNA 20-mer that was not correctly hybridized. Interestingly, the low level of synthesis detected in this experiment confirmed that the previously detected activity using the 20 mer-ssDNA molecule (Figure 39A central panel), was indeed due to the ability of PrimPol to promote bridging of two molecules based on microhomologies. Next, we performed a similar experiment by adding to the mix an unlabelled ssDNA molecule with a 3' end complementary to the protruding sequence of the labelled dsDNA molecule (Figure 42B). Interestingly, PrimPol could barely extend the labelled dsDNA molecule in the presence of this unlabelled ssDNA molecule (Fig 42B). In addition to the background incorporation of dGTP, poor incorporation of a single dGTP was the only activity detected, which could have been inserted in a template-directed fashion after alignment of the molecules, since the first available template base would be a dC. However, the very low efficiency of this incorporation suggests that despite the presence of complementary sequences between the two molecules PrimPol can barely extend short protruding sequences, which are characteristic of the NHEJ pathway. Next, we performed a similar experiment, but this time the ssDNA unlabelled molecule was replaced in the mix with an unlabelled dsDNA molecule with a 3' protrusion partially complementary to the protrusion of the labelled dsDNA molecule (Figure 42C). This unlabelled dsDNA was generated by hybridization of the ssDNA molecule used in figure 42B with a shorter oligonucleotide. 3' end bridging of these two dsDNA molecules, if mediated by PrimPol, would generate two 1nt gaps with a template dC, highly resembling physiological NHEJ bridging intermediates. Likewise previously, PrimPol could barely extend the labelled dsDNA in this experiment (Figure 42C), as only similar inefficient incorporation of dGTP

was detected, suggesting again that PrimPol may not be able to efficiently bridge dsDNA molecules with short protrusions. This could also indicate that PrimPol may not be able to interact with the 5' end of a DNA molecule downstream of the primer, unlike some polymerases specialized in NHEJ. In this regard, the activity of most DNA polymerases from the X family specialized in NHEJ, such as Polλ, is clearly enhanced by the interaction with a 5' phosphate group flanking the gap (García-Díaz et al., 2002). When PrimPol was incubated with the two dsDNA molecules used previously in Figure 42C, but with a 5'P group flanking the protrusion of the unlabelled molecule, little or no activity was observed (Figure 42D), since again, only very poor incorporation of a single dGTP was observed, suggesting that PrimPol is not stimulated by the presence of 5'P, in contrast to most NHEJ polymerases. Altogether these results demonstrate that PrimPol cannot polymerize across discontinuous templates using dsDNA with short 3'-protrusions, suggesting that PrimPol may not be able to bridge these kinds of molecules and that PrimPol may not take part in the classical NHEJ pathway.

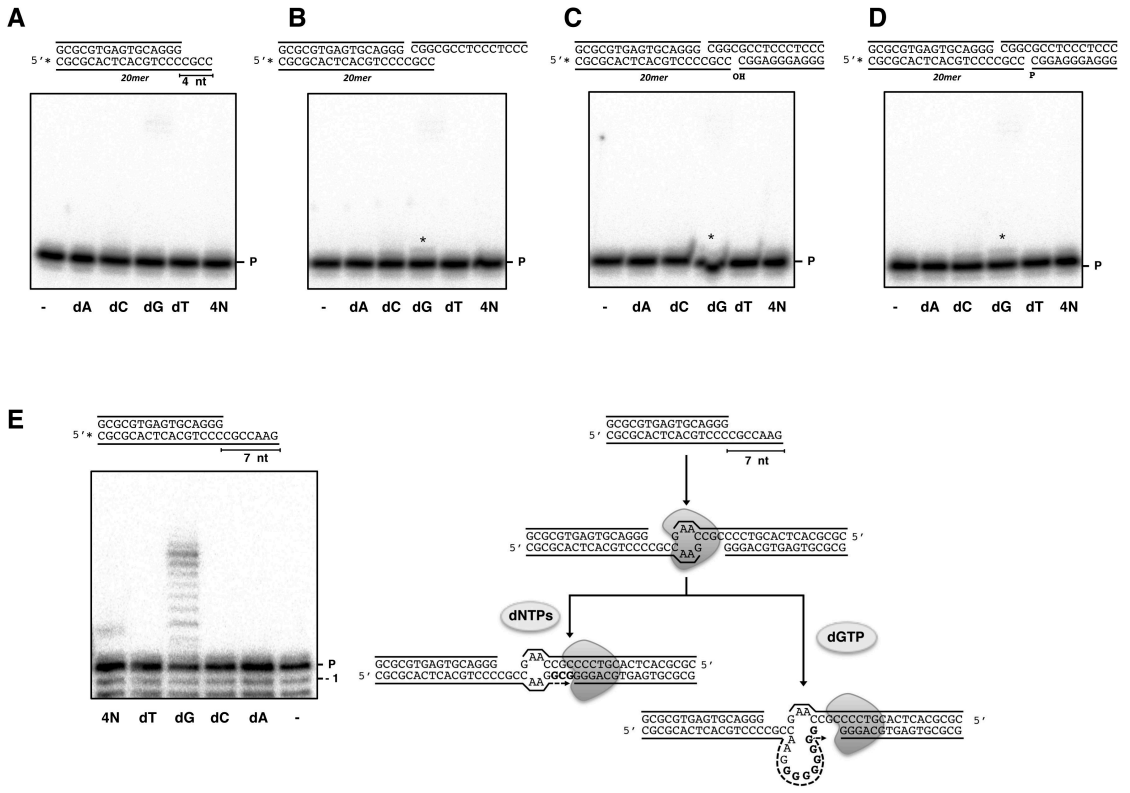

Figure 42. PrimPol-mediated DNA synthesis using dsDNA molecules with 3'-protrusions (A) Analysis of the ability of purified PrimPol to polymerize across a discontinuous template using a 5' labelled dsDNA with a 4nt 3'-protrusion and the indicated deoxynucleotides. (B-D) Same experiment as in (A) but adding to the mix an unlabelled oligonucleotide, either in ssDNA form (C) or hybridized to a shorter oligonucleotide generate a dsDNA molecule with a 3'-protusion, which in turn either lacked (C) or harboured a 5'P (D) flanking the protrusion. Note that the 3'end of these unlabelled molecules is complementary to the 3'-protruding end of the labelled dsDNA molecule. (E) *In vitro* DNA synthesis by PrimPol on a dsDNA molecule related to the one used in (A) but with a longer 3'-protruding end of 7nt.

Given that PrimPol was mostly inactive using DNA substrates with short protrusions (Figure 42A, B, C & D), we wanted to test its activity on dsDNA substrates with longer protrusions, which are characteristic of DSB repair pathways such as MMEJ (also known as alternative NHEJ, a-NHEJ) (Deriano and Roth, 2013; McVey and Lee, 2008). For this purpose, we devised a labelled dsDNA derived from the one used in figure 42A, but with a longer protrusion of 7 nt. Strikingly, when incubated with this molecule, PrimPol could efficiently extend the 3´-protruding strand, most likely by using the protrusion of a second DNA molecule as template (Figure 42E). Remarkably, the sequence of the 7 nt 3'-protrusion has limited self complementarity, which again suggests that PrimPol can proficiently tolerate mismatches during end-alignment. We speculate that in this scenario PrimPol can tolerate two A:A mismatches to align the ends by forming two G:C matches flanking the mismatches (Figure 42E see scheme). After this alignment PrimPol could initiate synthesis using dGTP, that can be either repeatedly incorporated via slippage, or which could be normally extended in the presence of the other dNTPs (Figure 42E). It is worthy to note that, when the 4 dNTPs were simultaneously present, PrimPol generated mainly a +3 product of extension, further suggesting that PrimPol can align two of these dsDNA molecules as we propose in the scheme in Figure 42E. Altogether, these results suggest that PrimPol can polymerize across discontinuous templates using dsDNA molecules with 3'-protruding ends of a certain length, necessarily longer than 4 nt. This was also confirmed using dsDNA with 10 nt or 13 nt protruding 3´ends (Figure 43), and could suggest a role for PrimPol in DSB repair. The fact that PrimPol can extend substrates

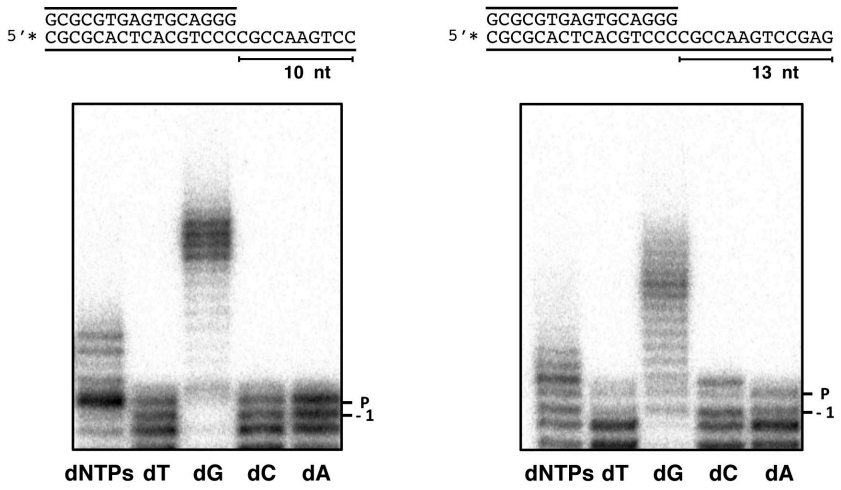

Figure 43. PrimPol-mediated DNA synthesis across dsDNA molecules with long 3'-protrusions. PrimPol can catalyse DNA synthesis across dsDNA with 3'-protrusions of 10 nt (*left*) and 13 nt (*right*). Reactions were performed as described in Materials and Methods by incubating purified PrimPol (400 nM) with the depicted labelled DNA molecules (5 nM) and dNTPs (100 μM), which were provided either individually or combined.

with this sort of 3'-protrusions, which are moderately long, could suggest a role in MMEJ. However, PrimPol can work with a minimal complementarity connecting the discontinuous strands, hence a role for PrimPol in classical NHEJ or different uncharacterized end-joining pathways cannot be discarded.

3. DNA synthesis across discontinuous templates by PrimPol strictly requires Mn^{2+}

PrimPol can catalyse DNA synthesis using either Mg^{2+} or Mn^{2+} as metal cofactors, although it displays marked higher efficiency using Mn^{2+} (García-Gómez et al., 2013; Martínez-Jiménez et al., 2015). Nevertheless, a recent study has demonstrated that Mg^{2+} stimulates error-free bypass of 8oxoG by PrimPol (Zafar et al., 2014), indicating a possible functional relevance of this ion as an alternative metal cofactor for PrimPol. Hence, we wanted to test the effect of Mn^{2+} and Mg^{2+}, by considering both their concentration and combination, in other PrimPol-mediated reactions such as the polymerization across discontinuous templates. For this purpose, we evaluated the effect of these ions on the incorporation of dGTP on the 20-mer ssDNA shown in the central panel of figure 39A. In that experiment, performed with 1 mM Mn^{2+}, PrimPol incorporated dGTP very efficiently, but also recurrently, probably by repetitive slippage at a track of Cs after annealing of two ssDNA molecules (Figure 39C), As shown in Figure 44A PrimPol could catalyse this reaction using various concentrations of Mn^{2+}, but was inactive when using using any of the concentrations of Mg^{2+} tested (Figure 44B), suggesting that PrimPol strictly requires Mn^{2+} for DNA synthesis across discontinuous templates. Furthermore, PrimPol displayed a similar polymerization pattern of multiple dGTP incorporation in the range of 250 to 1000 μM Mn^{2+}. Quite strikingly, at 100 μM Mn^{2+} DNA synthesis was restricted to a single dGTP

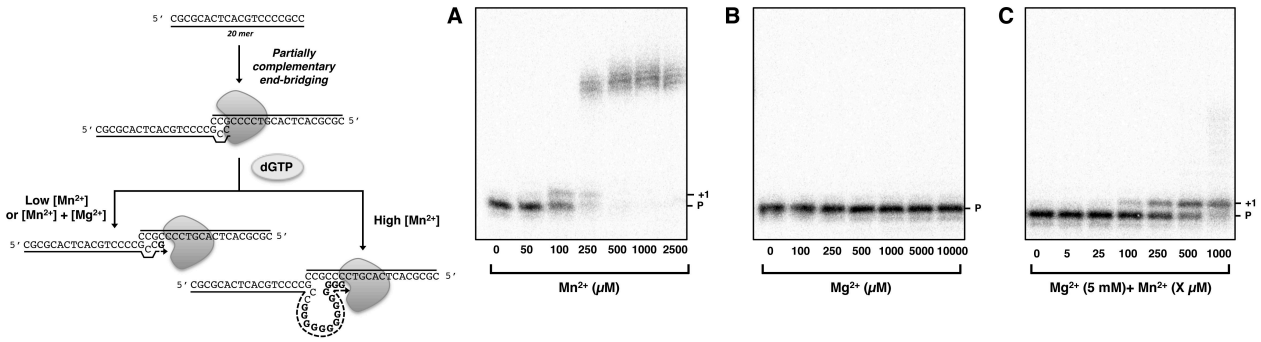

Figure 44. Mn^{2+} and Mg^{2+} modulate DNA synthesis across discontinuous templates by PrimPol. (A) Analysis of dGTP incorporation by purified PrimPol on a 5' labelled ssDNA 20-mer molecule using the indicated concentrations of Mn^{2+}. (B) Same as in (A) but using the indicated concentrations of Mg^{2+} as metal cofactor. (C) Same experiment as in (A) and (B) but using 5 mM Mg^{2+} combined with the indicated of Mn^{2+}.

incorporation, which could suggest that this concentration of Mn^{2+} could lead to a different positional bridging of the two molecules, or because is too low to drive translocation after the first (+1) dGTP addition (Figure 44 see scheme). In any case, these data indicate that low Mn^{2+} concentrations, close to the physiological range (Ash and Schramm, 1982), limit the activity of PrimPol during polymerization across discontinuous templates avoiding error-prone expansions: alternatively, PrimPol could be specialized in just initiating this kind of reactions and be subsequently replaced by a more faithful polymerase. Next, we further addressed the physiological context, by repeating the experiment using a unique concentration of Mg^{2+} (5 mM) mixed with variable concentrations of Mn^{2+} (Figure 44C). Similarly to the experiment in which Mn^{2+} was provided alone (Figure 44A), discontinous synthesis by PrimPol was detected when using a range of 100-1000 μM of Mn^{2+} in combination with 5 mM Mg^{2+} (Figure 44C). However, in stark contrast to the experiment with Mn^{2+} alone, when both metal ions were present, extension by PrimPol was mainly limited to a single and efficient incorporation of dGTP at any of the Mn^{2+} concentrations tested. This result suggests that the combination of Mg^{2+} and Mn^{2+} allows efficient synthesis across discontinuous DNA molecules by PrimPol but also that it pronouncedly limits extension by PrimPol, which could be useful to avoid expansions at homopolymeric DNA tracks. This piece of evidence could be particularly relevant since recent analysis of the fidelity of PrimPol indicate that it is highly prone to generate insertions/deletions at homopolymeric tracks as small as 2 nucleotides (Martínez-Jiménez et al., 2015).

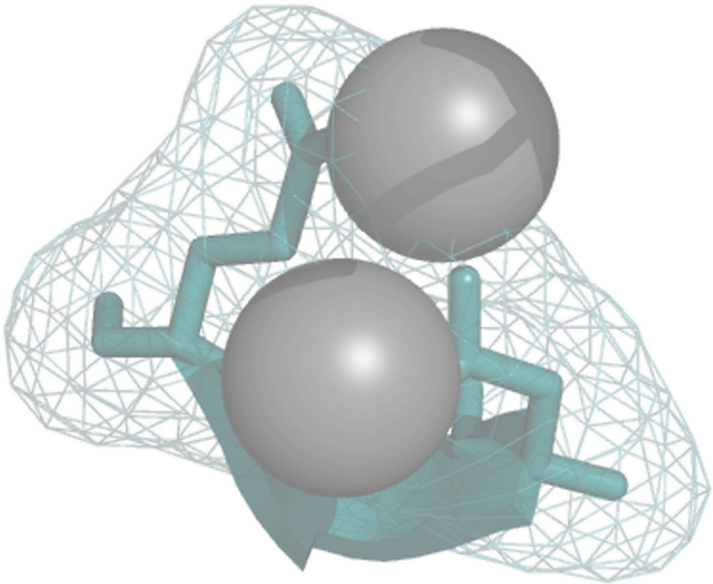

Chapter 5: The influence of distinct metal cofactors on PrimPol-mediated TLS

Figure: Model of human PrimPol structure depicting Asp^{114} and Glu^{116}

As explained in the introduction section, in spite of the high degree of specialization of the human DNA polymerases these enzymes have common characteristics including a two-metal ion mechanism of catalysis (Steitz, 1999). Mg^{2+} is considered the physiological metal cofactor of most DNA polymerases, however increasing evidence indicates that some polymerases are stimulated by Mn^{2+} (e.g. (Blanca et al., 2003; Frank and Woodgate, 2007; Martin et al., 2013a)). PrimPol can catalyse DNA synthesis using both Mg^{2+} and Mn^{2+}, although it shows a clear preference for the latter (García-Gómez et al., 2013; Martínez-Jiménez et al., 2015). As mentioned in the previous chapter, a recent study demonstrated that in contrast to Mn^{2+}, Mg^{2+} stimulated error-free bypass of 8oxoG by PrimPol (Zafar et al., 2014), however, the effect of the concentration and combination of both metal cofactors in this and other TLS reactions has never been considered. In this chapter we have evaluated the effect of the concentration and combination of both Mn^{2+} and Mg^{2+} in the efficiency and fidelity of PrimPol during TLS. For this purpose, we studied their effect on: 1) TLS across 8oxoG and 2) primer realignment reactions, promoted by PrimPol to dislocate the template and overcome unreadable lesions (Martínez-Jiménez et al., 2015).

1. PrimPol preferentially incorporates dNTPs opposite 8oxodG preferably despite NTPs higher physiological concentration of NTPs

Before studying the effect of the concentration and combination of Mn^{2+} and Mg^{2+} on PrimPol-mediated TLS of 8oxodG, we wanted to gain further insight into sugar discrimination by PrimPol during the reaction. It has already been described that PrimPol can incorporate both dNTPs (dATP and dCTP) and NTPs (ATP and CTP) opposite 8oxodG; beind dNTPS the preferred nucleotides to tolerate this lesion (García-Gómez et al., 2013). Nevertheless, the physiological concentration of NTPs is much higher than that of dNTPs (10- to 100-fold depending on the nucleotide and cell-cycle phase (Traut, 1994)) being the levels of ATP particularly elevated. That asymmetry could compensate the relatively low efficiency of incorporation of NTPs by PrimPol opposite 8oxodG, thereby competing with dNTPs *in vivo*. To test this idea we incubated purified PrimPol with a 5'-labelled template/primer DNA structure (having an 8oxodG in the 1+ template position) and physiological concentrations of dATP, dCTP, ATP and CTP, which are the dNTPs and NTPs that PrimPol can incorporate opposite the lesion, and that were added to the mix either alone or combined. Given the high levels of oxidative stress in mitochondria, we speculate that the large TLS capacity of PrimPol to deal with 8oxodG would be of a maximal importance in mitochondria; thus,

we used as reference the physiological concentrations of nucleotides described in this organelle (Pursell et al., 2008; Traut, 1994). This was not possible in the case of CTP since its concentration in mitochondria was not measured in parallel in those studies, hence we used its normal cellular concentration reported in (Traut, 1994), assuming that it might be similar to its concentration in mitochondria. Note that primer extension generated with NTPs was easily distinguishable from that generated with dNTPs due to the lower mobility of the former (Figure 45A, e.g. note the different mobility of products extended with CTP and dCTP in lanes 6 and 8, respectively). Interestingly, when PrimPol was incubated with physiological concentrations of ATP, CTP, dATP and dCTP together, no primer extension could be detected (Figure 45A, lane 1), which we speculate that could be due to a possibly inhibitory effect of the high concentration of nucleotides in the assay, especially of ATP. Hence, we also used diluted concentration of these nucleotides maintaining the physiological ratios. Under these conditions PrimPol could generate two products of extension (Figure 45A, lane 2): an upper band compatible with NTP incorporation and a lower band compatible with dNTP incorporation. However, in this experimental condition PrimPol showed low efficiency, possibly due to the low concentration of dNTPs. Given the low level incorporation of ATP alone despite its high concentration in mitochondria (Figure 45A, lane 5), we considered this substrate as the less preferred by PrimPol during the tolerance of 8oxodG and consequently it was discarded from the mix. In its absence, PrimPol displayed higher efficiency, thereby confirming its inhibitory effect, and generated the same two products of different mobility detected previously in lane 2, but this time the

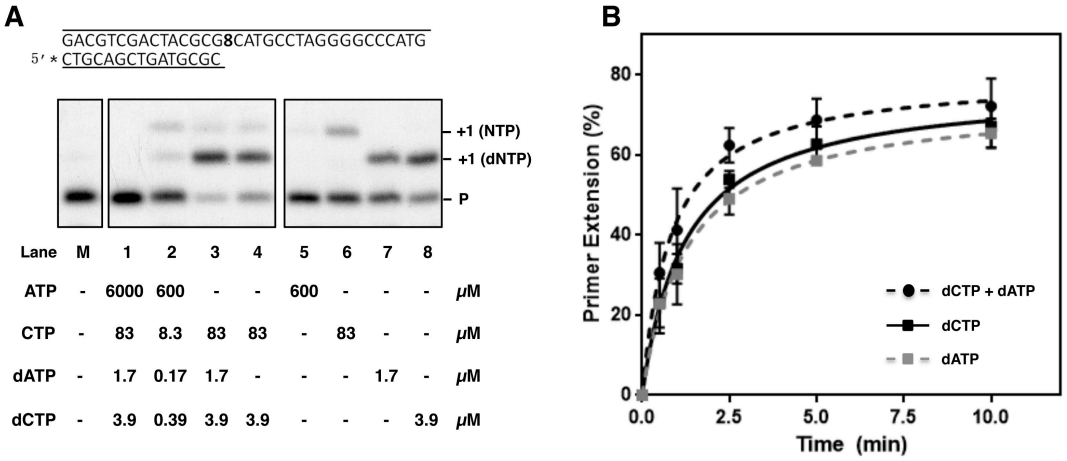

Figure 45. Tolerance of 8oxodG by human PrimPol using mitochondrial concentrations of nucleotides. (A) Competitive study of incorporation of the indicated physiological concentrations of ATP, CTP, dATP and dCTP by purified PrimPol opposite 8oxodG using the depicted DNA template/primer substrate. (B) Kinetics of the incorporation opposite 8oxodG by PrimPol (200 nM) using physiological nucleotide ratios: 39 μM dCTP, 17 μM dATP, 39 μM dCTP + 17 μM dATP. Data are the means of two independent experiments and the error bars correspond to the SD.

lower band (corresponding to an incorporated dNTP) showed much higher intensity than the upper band (Figure 45A, lane 3), suggesting that dNTPs are the preferred substrates for 8oxodG tolerance by PrimPol, which almost outcompete CTP completely despite its higher concentration. Next we sought to determine which could be the preferred dNTP inserted by PrimPol opposite 8oxodG, given that we could not discriminate between dATP and dCTP insertion due to their similar electrophoretic mobility. For this purpose dATP was removed from the mix, and under these conditions, PrimPol generated the same two products of extension detected previously (Figure 45A, lane 4), but the band of higher mobility, corresponding in this condition to dCTP insertion, was in this case less intense (Figure 45A, compare lanes 3&4), suggesting that PrimPol can incorporate either dATP or dCTP opposite 8oxodG if they are present together at their physiological concentrations. To further confirm this conclusion, physiological (mitochondrial) concentrations of dATP and dCTP were evaluated individually, showing a similar efficiency of incorporation opposite 8oxodG, slightly favouring the error-free (dCTP) incorporation (Figure 45A, compare lanes 7 &8). The kinetics of incorporation of both dATP and dCTP provided at physiological ratios (Figure 45B, 17 μM dATP (grey dotted line) and 39 μM dCTP (black line)), either alone or combined was also evaluated in a similar experiment. The experiment also demonstrated that PrimPol incorporates both nucleotides at a similar rate, although dCTP slightly more efficiently. When both dNTPs were present together, the efficiency of the reaction was slightly higher, confirming that PrimPol can incorporate both dATP and dCTP opposite 8oxodG if the are present together (Figure 45B, black dotted line).

Altogether these results demonstrate that PrimPol incorporates preferably dNTPs opposite 8oxodG despite the higher *in vivo* concentration of NTPs. However, PrimPol cannot discriminate efficiently between dATP and dCTP and it is likely to incorporate both opposite 8oxodG *in vivo*.

2. TLS of 8oxodG by PrimPol is alternatively modulated by Mn^{2+} and Mg^{2+}

Previous studies demonstrated that PrimPol bypasses 8oxodG very efficiently, in fact as efficiently as a regular dG, although it incorporates dATP slightly better than the error-free dCTP (García-Gómez et al., 2013). However, those first studies were conducted using Mn^{2+} (1 mM), and a recent work has demonstrated that Mg^{2+} (10 mM) favours dCTP over dATP incorporation opposite 8oxodG by PrimPol (Zafar et al., 2014). This metal-dependent outcome prompted us to study the effect of the concentration and combination of Mn^{2+} and Mg^{2+} in PrimPol-mediated bypass of

8oxodG. Since our data indicate that it incorporates dNTPs with much higher preference, even despite the higher physiological concentration of NTPs (Figure 45), we only considered the incorporation of dATP and dCTP for these analyses. First we incubated purified PrimPol with either dCTP or dATP, together with variable concentrations of Mn^{2+} and a primer/template DNA molecule with an 8oxodG in the +1 template position (Figure 46, see scheme). As expected at high concentrations of Mn^{2+}, close to 1000 μM, PrimPol incorporated dATP with higher efficiency than dCTP (Figure 46A), although at lower concentrations, below 250 μM, PrimPol incorporated both nucleotides similarly due to a more pronounced decrease in the efficiency of dATP incorporation (Figure 46A). As recently reported for 10 mM Mg^{2+} (Zafar et al., 2014), dCTP incorporation was favoured over dATP at all the Mg^{2+} concentrations tested, albeit as anticipated, with a pronounced decrease in the efficiency of PrimPol compared to its activation by Mn^{2+} (Figure 46B). These results confirmed that Mg^{2+} increases PrimPol fidelity during the bypass of 8oxodG although with the cost of lower overall efficiency. Next, to test the effect of the combination of both metal cofactors, we performed a similar experiment using variable concentrations of Mn^{2+} and a fixed concentration (5 mM) of Mg^{2+}. Under these conditions, PrimPol incorporated dCTP with higher efficiency than dATP at Mn^{2+} concentrations lower than 50 μM (Figure 46C), similarly to when Mg^{2+} was provided

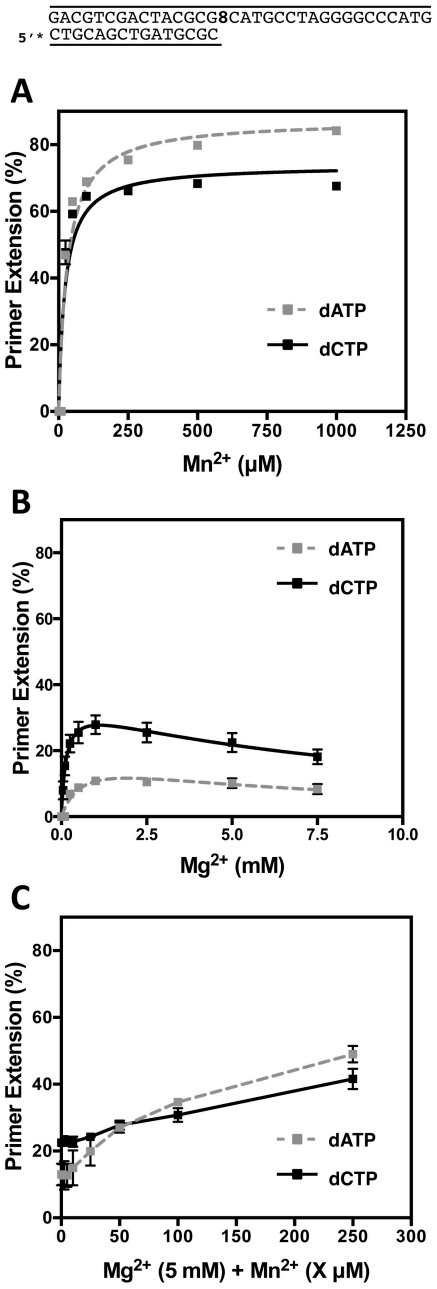

Figure 46. Effect of different metal cofactor conditions on 8oxodG tolerance by PrimPol. dATP (grey dotted line) and dCTP (black line) incorporation opposite 8oxodG by purified wild-type PrimPol using the depicted the labelled template/primer DNA molecule and the indicated concentrations of: (A) Mn^{2+}, (B) Mg^{2+} and (C) 5mM of Mg^{2+} and the indicated concentration of Mn^{2+}. Data are the means from at least 3 independent experiments and error bars correspond to the SD.

alone (Figure 46B & C). Interestingly, when the concentration of Mn^{2+} was higher than 50 μM, dATP incorporation opposite 8oxodG by PrimPol was progressively more efficient than dCTP insertion, although this was more clearly patent at the highest concentration used (250 μM) suggesting that at these metal concentrations Mn^{2+} may prevail during PrimPol-mediated bypass of 8oxodG.

Altogether these results demonstrate that Mn^{2+} and Mg^{2+} distinctively modulate TLS of 8oxodG by PrimPol. Mn^{2+} provides PrimPol with optimal efficiency although it favours the incorporation of dATP (Figure 46A). Conversely, Mg^{2+} favours the error-free bypass of 8oxodG although with the cost of lower efficiency (Figure 46B). The combination of both metal cofactors balanced the fidelity versus the efficiency of 8oxodG bypass by PrimPol, differently than each metal alone (Figure 46C), suggesting that *in vivo*, PrimPol discriminates poorly between dATP and dCTP during the tolerance of 8oxodG.

3. PrimPol Glu^{116} enhances dATP incorporation opposite 8oxodG

Most DNA polymerases require three amino acids for the coordination of the metal cofactors, which are essential for catalysis. These residues are generally carboxylates, and two of them localize close together in the primary sequence being separated by only one non-conserved amino acid. These two proximate metal ligands are aspartic acids in most cases and form a motif commonly referred to as motif A, with the consensus DxD. Interestingly, the DxD motif is present in most members of the AEP family including distantly related members such as the catalytic subunit of the human conventional primase Prim1, the polymerase domain of LigD from *Mycobacterium tuberculousis*, the vaccinia virus primase (Vaccinia/D5) and the herpes virus UL52 primase (HHV/UL52) (Figure 47A). In stark contrast to these enzymes, several PrimPols from the AEP family have an aspartic acid and a glutamic acid at these corresponding positions (Asp^{114} and Glu^{116} in the case of human PrimPol) that form a DxE variant motif of metal coordination (Figure 47A). PrimPol from *Thermus thermophilus* is an interesting exception since it harbours the DxD motif (Figure 47A), however our unpublished biochemical characterization of this PrimPol indicates that is less dependent upon Mn^{2+}, suggesting that the DxE motif might be optimized for the use of this cofactor. Interestingly, Glu^{116}, the distinctive amino acid from the DxE motif in human PrimPol, is highly conserved in other PrimPols from evolutionarily distant organisms suggesting its functional relevance (Figure 47B). Given the impact of alternative metal cofactors in 8oxodG tolerance by PrimPol, we sought to determine the

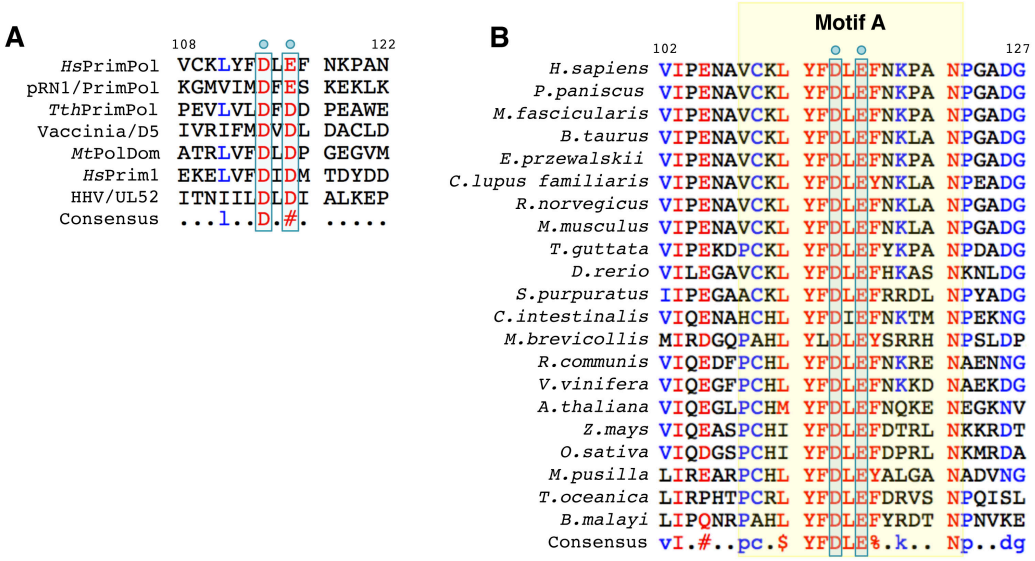

Figure 47. A DxE metal ligand motif is distinctive of eukaryotic/archaeal PrimPols and highly conserved through evolution. (A) Amino acid sequence alignment of several AEP family members including: *Hs*PrimPol, human PrimPol, pRN1/PrimPol, plasmid pRN1 ORF904 from *Sulfolobus islandicus*, *Tth*PrimPol, *Thermus thermophilus* PrimPol, PrimPol Vaccinia/D5, vaccinia virus primase, *Mt*PolDom, LigD polymerase domain from *Mycobacterium tuberculosis, Hs*Prim1, catalytic subunit of the human RNA primase and HHV/UL52, herpes virus UL52 primase. Blue arrows on the top indicate the metal binding residues. (B) Multiple amino acid sequence alignment of PrimPol orthologs showing that the DxE metal ligand motif of human PrimPol is highly conserved through evolution.

possible involvement of the metal ligand Glu^{116} in this effect and on PrimPol-mediated TLS of the lesion.

For this purpose we studied the E116D PrimPol mutant (previously developed in our laboratory), in which Glu^{116} has been replaced by the more conventional aspartic acid found in most AEP members. Interestingly, the E116D mutant incorporated dCTP and dATP with very similar efficiency at all the concentrations of Mn^{2+} tested (Figure 48A), in clear contrast to wild-type PrimPol (Figure 48A). In fact, compared to wild-type PrimPol, the E116D mutant had a decreased efficiency of dATP incorporation, although only moderately, but had little or no effect on dCTP incorporation opposite 8oxodG, suggesting that Glu^{116} contributes to the error-prone bypass of 8oxodG in the presence of Mn^{2+}. Likewise wild-type PrimPol, the E116D mutant preferably incorporated dCTP over dATP opposite 8oxodG at all tested concentrations of Mg^{2+} (Figure 48B), but in agreement with our previous results, Glu^{116} mutation to aspartic acid decreased the efficiency of dATP insertion while had little effect on dCTP incorporation, although this effect was only moderate and particularly patent at concentration of Mg^{2+} below 2.5 mM. The effect of the E116D mutation was very evident in the presence of both metal cofactors, as the mutant incorporated dCTP with higher efficiency than dATP (Figure 48C), at all the concentrations of Mn^{2+} tested in combination with 5 mM Mg^{2+}, except for the highest (250 μM), in clear contrast to wild-type PrimPol that only incorporated

this nucleotide preferably when Mn^{2+} concentration was lower than 50 μM. Altogether these results demonstrate that PrimPol Glu^{116} contributes to the error-prone tolerance of 8oxodG under all the metal cofactor conditions tested, more markedly in the presence of both Mg^{2+} and Mn^{2+} ions.

4. Mn^{2+} and Glu^{116} stimulate template dislocation by PrimPol

Unlike 8oxodG, certain DNA lesions such as AP sites and pyrimidine dimers cannot be "read" by PrimPol, and therefore nucleotides are not incorporated opposite these lesions. However, PrimPol can skip those lesions efficiently by taking advantage of microhomologies in the template sequence that serve to realign the primer in a downstream position beyond the damaged site (García-Gómez et al., 2013; Martínez-Jiménez et al., 2015). Although this sort of reaction could be beneficial *in vivo* to avoid fork stalling, they would also be highly error-prone as they would lead to significant deletions, hence it is tempting to speculate that primer realignment should be regulated to some extent. The effect that Mg^{2+}, Mn^{2+} and the E116D mutation had on the TLS of 8oxodG by PrimPol prompted us to test whether they can affect similarly the primer realignment ability of PrimPol.

To evaluate primer realignment by PrimPol, we used a labelled synthetic dsDNA molecule whose template strand has two trinucleotide repeats (TAC) (Figure 49 see

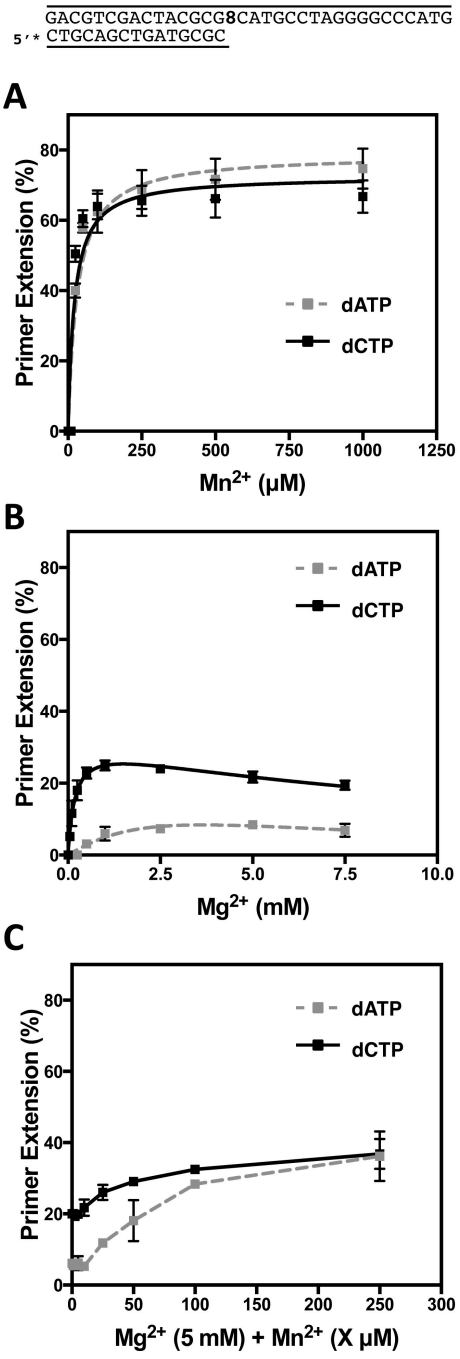

Figure 48. Effect of Mn^{2+} and Mg^{2+} concentration and combination on 8oxodG tolerance by the PrimPol E116D mutant. Incorporation of dATP (grey dotted line) and dCTP (black line) opposite 8oxodG opposite 8oxodG in a 5' labelled template/primer DNA structure using the indicated concentration of: (A) Mn^{2+}, (B) Mg^{2+} and (C) 5mM of Mg^{2+} and the indicated concentrations of Mn^{2+}. dATP (grey dotted line). Data are means of at least 2 independent experiments and the error bars represent the SD.

scheme and note the underlined nucleotides) separated by other 3 nucleotides (TTG). One of the repeats is paired to the 3'end of the primer, whereas the other is found in ssDNA form, downstream of the primer. This DNA template/primer configuration allows PrimPol to normally extend the primer by 2 nt when dATP is provided (Figure 49, see scheme); however, if dCTP is the only nucleotide provided, the primer is extended by 1nt after its repositioning at the downstream trinucleotide repeat (Figure 49, see scheme). Therefore, by using this molecule we could comparatively study the effect of Mg^{2+} and Mn^{2+} on regular primer extension, measured by dATP insertion, and on primer realignment, monitored by dCTP insertion.

When using Mn^{2+}, PrimPol incorporated dATP much more efficiently than dCTP (Figure 49A), at all the concentrations of Mn^{2+} evaluated. In fact, dCTP could only be

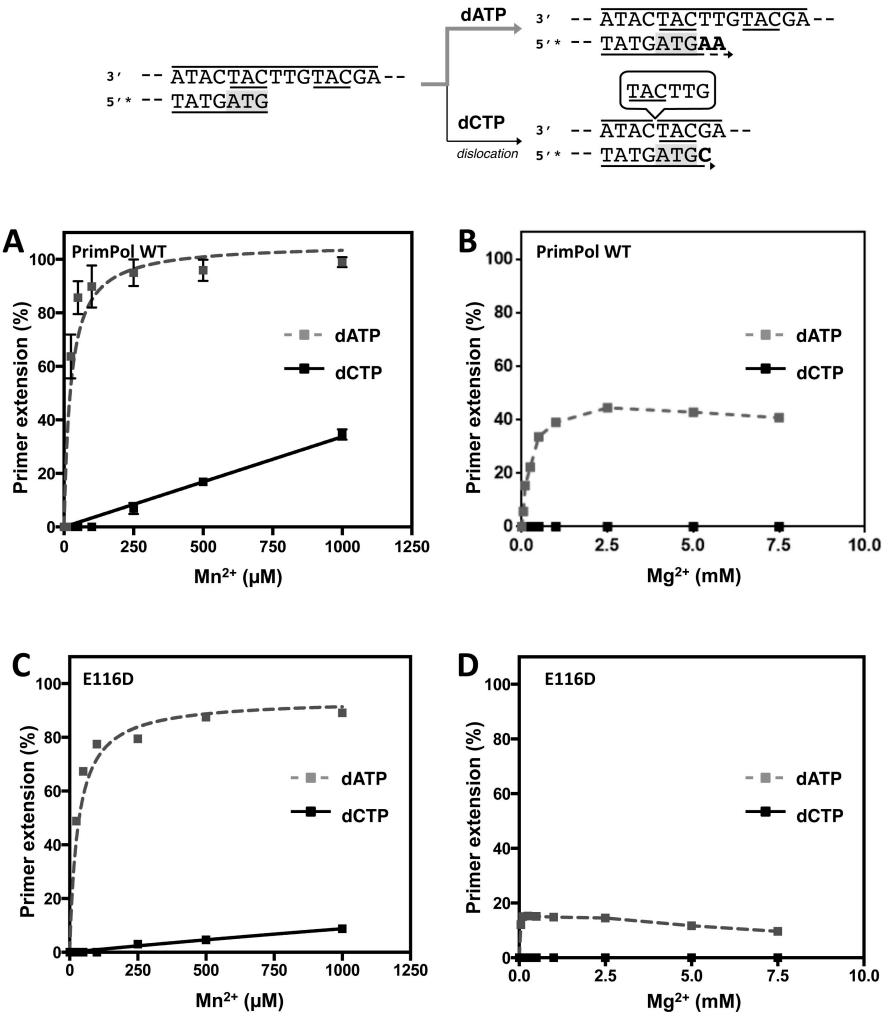

Figure 49. Primer realignment by PrimPol wild-type and the E116D mutant under different metal cofactor conditions. Primer realignment and normal primer extension were comparatively studied by evaluating dCTP (black line) and dATP (grey dotted line) insertion by PrimPol in the presence of the indicated concentrations of either Mn^{2+} (A) or Mg^{2+} (B). The same experiments were carried out using the PrimPol E116D mutant together with either Mn^{2+} (C) or Mg^{2+} (D).

incorporated with Mn^{2+} concentrations higher than 250 μM, demonstrating that although PrimPol can promote primer realignment, it is kinetically challenging. As expected, PrimPol incorporated dATP less efficiently in the presence of Mg^{2+}, but remarkably, PrimPol could not incorporate dCTP at any of the concentrations tested, thus demonstrating that PrimPol strictly requires Mn^{2+} for primer realignment reactions. Likely, Mg^{2+} does not provide PrimPol with enough efficiency to overcome the challenge imposed by this reaction. Remarkably, the E116D mutant could also catalyse primer realignment, and likewise wild-type PrimPol much less efficiently than regular primer extension (Figure 49C) and strictly requiring Mn^{2+} (Figure 49D). Interestingly the E116D mutant catalysed dATP incorporation less efficiently than wild-type PrimPol, especially in the presence of Mg^{2+} (Figure 49 B & D), suggesting that Glu^{116} may be necessary for optimal PrimPol activity. Remarkably, Glu^{116} mutation to aspartic acid also reduced the efficiency of dCTP incorporation in the presence of Mn^{2+} by 3-fold, compared to wild-type PrimPol (Figure 49A & C), more markedly than the effect of the mutation on regular primer extension (dA incorporation), suggesting that this residue could be required for Mn^{+2}-driven primer realignments by PrimPol. Altogether these results demonstrate that PrimPol strictly requires Mn^{2+} to realign primers, although these events are only catalysed *in vitro* at high concentrations of $Mn^{2+,}$ distant from the physiological levels (Ash and Schramm, 1982). Nevertheless, it would be worth considering whether the efficiency of this reaction could be boosted by the presence of an unreadable lesion in the template, or facilitated by interaction with protein partners, as RPA or mtSSB. Our data also shows that Glu^{116} is required for optimal efficiency during the realignment of the primers, yet in this experiments its mutation to aspartic acid also decreased the overall efficiency of the enzyme, suggesting that the role of this residue in primer realignment might be indirect.

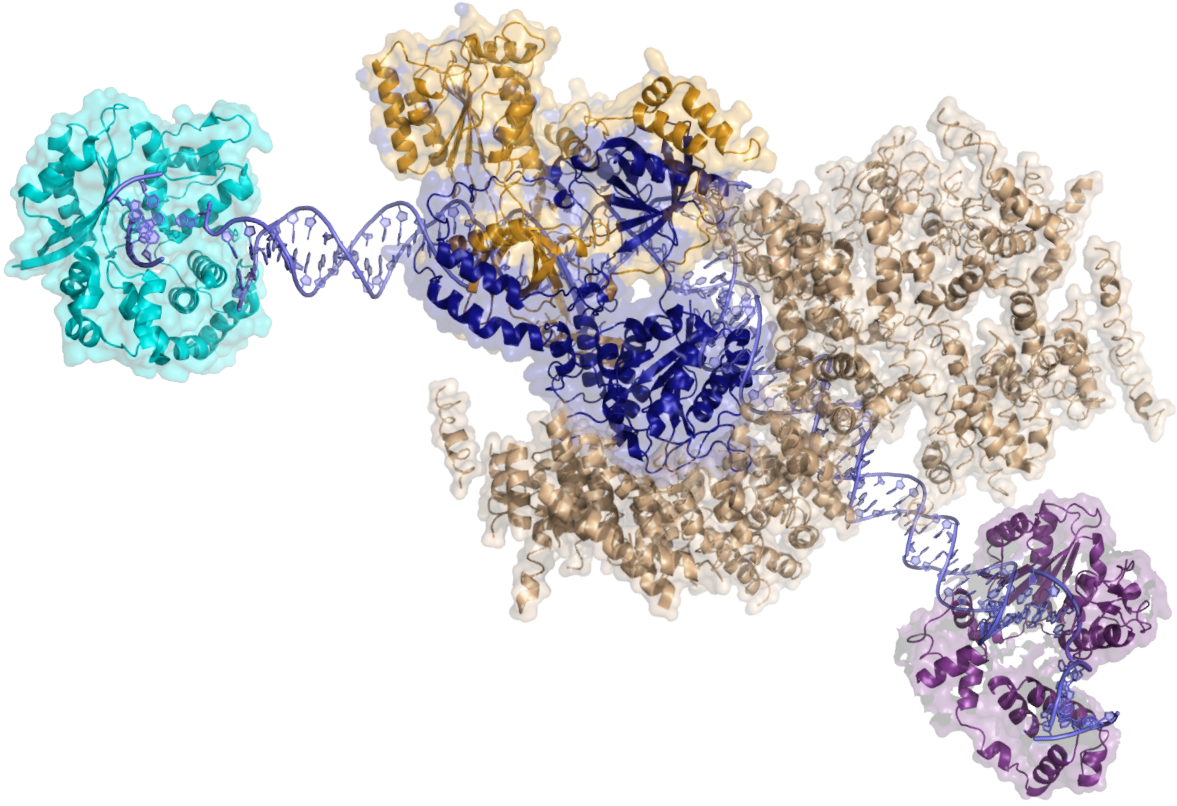

Discussion

1. Ribonucleotides: useful substrates for damage tolerance and DNA repair?

From a chemical standpoint ribonucleotides are almost identical to deoxynucleotides except for the hydroxyl group present in the 2' position of the ribose, which sets riboses apart from deoxyriboses. However, that small difference has big implications as it renders ribonucleotides much more prone to hydrolysis (Li and Breaker, 1999), something that in turn has significantly impacted life and evolution, being one of the reasons why most organisms store their genetic information in the form of the more stable DNA. Hence, it is generally assumed that ribonucleotide incorporation to the DNA is undesirable given that they are a potential source of SSBs. Moreover, replicative polymerases such as Polε cannot efficiently copy template ribonucleotides and can be potentially stalled during the process (Nick McElhinny et al., 2010), which is also another reason why ribonucleotides incorporation to the DNA is generally considered undesirable, and overall, another reason why ribonucleotides embedded in the DNA are considered by some as "damage".

The fact that replicative polymerases can efficiently discriminate between ribo- and deoxynucleotides to incorporate the latter almost exclusively also reflects the hazardous potential of ribonucleotide incorporation to the DNA. DNA polymerases that can efficiently discriminate against ribonucleotides, such as those specialized in DNA replication, are commonly endowed with a bulky residue within their active sites that locates where the 2' hydroxyl group would be positioned, thereby leading to an steric hindrance that prevents binding of the ribonucleotides. This residue, usually referred to as the "steric gate", is commonly aromatic (Brown and Suo, 2011). However, in spite of this, since the concentration of ribonucleotides in much higher tan that of deoxynucleotides (10- to 100-fold) (Traut, 1994), misincorporation of ribonucleotides by replicative DNA polymerases has a significant frequency (Nick McElhinny et al., 2010), estimated to be of around 2 ribonucleotide incorporations per 1 kilobase (kb) of DNA. This makes ribonucleotides probably the most abundant potential damage in the DNA (Sparks et al., 2012), and replicative polymerases arguably the most relevant source for accumulation of single ribonucleotides embedded in the DNA. Realization of these and other evidence prompted the discovery of the ribonucleotide excision repair pathway, a mechanism present in eukaryotic cells specialized in removing these single ribonucleotides embedded in the DNA (Sparks et al., 2012). This pathway was reconstituted *in vitro* with purified proteins from *S. cerevisiae* and is initiated by RNase H2 that incises the DNA in 5' of the ribonucleotide. Although to our knowledge, the conservation of this exact mechanism of RER has not been formally demonstrated in

higher eukaryotes, the severe phenotype displayed by RNase H2 deficient mice argues in favor of its conservation and clearly indicates that ribonucleotide incorporation to the DNA is a common event in mammals and that their removal from the DNA is essential for life (Reijns et al., 2012). Furthermore, defects in RNase H2 have been linked to the Aicardi-Goutières syndrome (Crow et al., 2006), a severe neurological disorder that can lead to death in early childhood, which also emphasizes the relevance of RNase H2 function in human cells. Importantly, all these data drew important attention to the study of ribonucleotides incorporation to the DNA, leading to significant advances in the field, but most of this work has focused on the downside of ribonucleotide incorporation to the DNA.

On the contrary, the work presented on this Doctoral Thesis supports the idea that ribonucleotide incorporation to the DNA may also have positive aspects in certain circumstances. This is not such a novel idea as ribonucleotide incorporation to the DNA is a physiological event, since for instance, DNA replication is initiated with short tracks of ribonucleotides that are synthesized by primases. Our work using *Sp*Pol4 as model suggests that likewise in the DNA replication scenario, ribonucleotides can be useful substrates for PolX-mediated DNA repair not only due to their abundance, which leads to efficient gap-filling and nucleotide incorporation required for NHEJ, but also because they can be safely removed and replaced by DNA via the RER pathway. Our study is thus remarkable, especially because it is the first demonstration that RNase H2 can initiate the repair of ribonucleotides paired to 8oxodG, being one of the first reported links between safe ribonucleotide incorporation and damage tolerance.

8oxodG is a hazardous DNA lesion due to its high abundance and to its capacity to stably match with adenine leading to the frequent misincorporation of dATP opposite the lesion and eventually to transversion mutations (Moriya, 1993; Moriya et al., 1991). It arises in the DNA upon guanine oxidation (Figure 50A), and is mainly repaired by BER, in a process initiated by OGG1 (homolog of MutM in *E. coli*). The absence of an OGG1 homologue in *S. pombe* suggests that 8oxodG:dC base pairs could be left unrepaired, thus promoting misincorporation of dATP most likely during DNA replication with a potential impact in mutagenesis (Figure 50A). However, most of these errors should be eliminated by MutY, conserved in fission yeast (*Sp*MYH), by excising the adenine from 8oxodG:dA base pairs (Lu and Fawcett, 1998) (Figure 50A). Coupled to the action of MutY homologs (MYH), a specialized polymerase able to copy 8oxodG in an error-free manner is considered indispensable to avoid mutagenesis, as replicative DNA polymerases display a reduced efficiency and fidelity when tolerating this lesion.

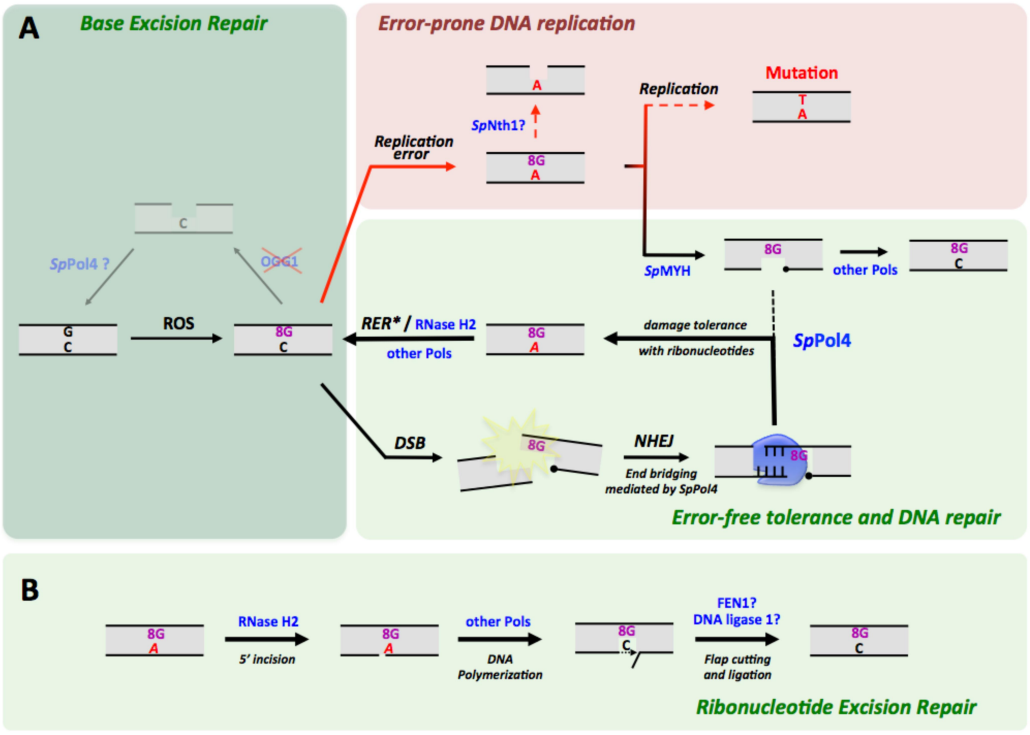

Figure 50. Model for *Sp*Pol4 contribution to *S. pombe* GO system. (A) Reactive oxygen species (ROS) can oxidize guanines in the genome of *S. pombe*. The absence of a OGG1 homolog in fission yeast suggests that the premutagenic 8oxodG:dC base pair could be persist in the DNA, prompting the incorporation of dATP during DNA replication. *S. pombe* MutY homolog (*Sp*MYH) can remove the wrong dAMP from the 8oxodG:dAMP base pair, and other polymerases (not *Sp*Pol4) can directly reconstitute a 8oxodG:dCMP base pair. *Sp*Pol4 can tolerate 8oxodG, mainly during NHEJ, using preferably the abundant ATP. That inserted ribonucleotide is then removed by a specialized RER mechanism (*the enzymatic reactions are shown in detail in (B)). (B) Insertion of ATP by *Sp*Pol4 would not be harmful as RNase H2 can recognize 8oxodG:AMP base pairs to initiate RER, thus triggering the error-free bypass of 8oxodG coupled to strand displacement, and preventing mutagenesis.

Some DNA polymerases from family X, specialized in performing short polymerization reactions associated to BER and NHEJ, are also well suited to participate in the MutY-dependent conversion of 8oxodG:dA into 8oxodG:dC base pairs, thus having a translesion synthesis (TLS) function. Polλ is particularly relevant in this scenario, being critical for the 8oxodG repair in humans, acting downstream MYH and incorporating the error-free dCTP almost exclusively (Maga et al., 2007; van Loon and Hubscher, 2009). Here we have shown that the unique PolX in *S. pombe* is not an ortholog of Polλ in this regard, but other endogenous polymerases have this potential.

Conversely, we have demonstrated that unlike human Polλ, *Sp*Pol4 tolerates 8oxodG by preferably incorporating ATP not only during gap-filling, but also during NHEJ (the main function of *Sp*Pol4), and that this ability is not significantly influenced by other repair factors present in the cell extracts. It has been recently shown that ribonucleotides can be valuable substrates for DNA repair, being used by human Pol*μ* during NHEJ, potentiating its fidelity without decreasing its efficiency (Martin et al., 2013a). That is particularly relevant given that, as mentioned earlier, their physiological

concentrations substantially exceed that of dNTPs (Traut, 1994). Thus, even though we can not discard that *Sp*Pol4 may incorporate ATP following *Sp*MYH activity, *Sp*Pol4 is more likely specialized in tolerating 8oxodG during NHEJ, taking advantage of the highly abundant ATP as a valid substrate to promote efficient repair of the most hazardous lesion for cell viability: DSBs (Figure 50A). Our *in vivo* analyses suggest that *Δpol4* cells are only mildly sensitive to oxidative damage (Figure 51), which would support that *Sp*Pol4 could be specialized in the repair of clustered damage, perhaps incorporating ATP during infrequent events caused by 8oxodG persistence and DSB formation.

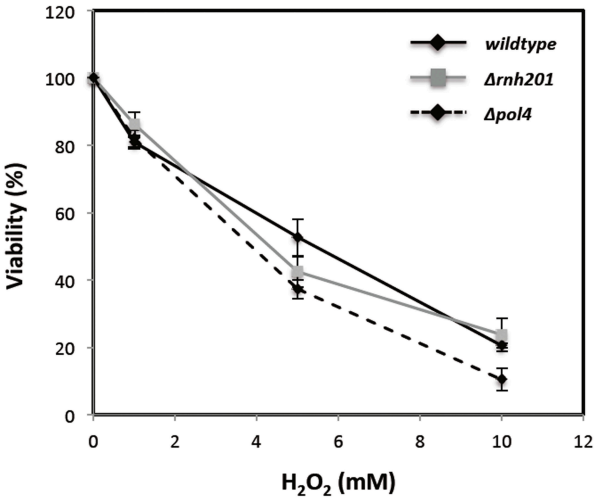

Figure 51. *Δpol4* cells are moderately sensitive to H_2O_2. To evaluate whether *pol4* (*h⁻ Δpol4:hphMX)* or *rnh201* (*h⁻ Δrnh201:kanMX) strains (obtained in this work)* are more sensitive to oxidative damage than a wild-type (*h⁻ 972*) strain, cells were grown to mid-logarithmic phase and subsequently treated with 0, 1, 5 and 10 mM of H_2O_2 for 3h at 30 °C. After treatment, 500 cells were plated in YES medium and incubated for 3 days at 30 °C. Colonies were counted and viability was calculated relative to the 0 mM plate. Data with standard deviations from two independent experiments are presented. The experiment shows that *Δpol4* cells are sensitive to H_2O_2, but this phenotype is not pronounced. Moreover, *rnh201* deletion did not sensitize cells to oxidative damage, which was somewhat expected, since *rnh201* deletion in budding yeast has not been associated with any clear phenotype and does not sensitize cells to hydroxyurea (Williams et al., 2013); remarkably, this study also showed that the *rnh201* deletion was problematic only when vast ribonucleotide insertion was provoked by mutating the sugar steric gate of the replicative polymerase Pol2. We suggest that the accumulation of ribonucleotides by *Sp*Pol4 during 8oxodG tolerance is probably not sufficient to drive cell death if *rnh201* is depleted. Likewise, the mild sensitivity caused by *pol4* deletion is also not surprising because we expect *Sp*Pol4 role in tolerating 8oxodG to be associated primarily with clustered damage, after 8oxodG persistence indirectly leads to DSBs. Therefore, we suggest that there are probably other pathways of 8oxodG tolerance in *S. pombe* that are compensating for the lack of *pol4*. This is in line with the fact that depletion of relevant genes for 8oxodG tolerance in mammals causes mild phenotypes, as for instance the case of *ogg1* deletion in mice (Osterod et al., 2001).

What is the consequence of this specialization? Remarkably, ATP incorporation opposite 8oxodG leads to the accumulation of two different "damages" (base and sugar) within a single base pair, which is in principle undesirable as ribonucleotides increase the probability of chromosomal strand breakage (Li and Breaker, 1999). However, as mentioned earlier, we have demonstrated that the insertion of ATP opposite 8oxodG may not be problematic, as 8oxodG:AMP base pairs were efficiently recognized by RNase H2 (Figure 50B). Strikingly, incision at the 5´-side of AMP was specifically coupled to the incorporation of dCTP opposite 8oxodG, which is *Sp*Pol4-independent (Figure 50B). The identity of the DNA polymerase involved in this "mismatch repair" reaction remains to be determined, and Polδ could be a good candidate given its association to RER in *S. cerevisiae* (Sparks et al., 2012).

These data emphasize the relevant role of NTPs for damage tolerance and suggest that ATP incorporation opposite 8oxodG by *Sp*Pol4 could be an intermediate step that triggers a subsequent error-free bypass of the lesion (Figure 50A). *Sp*Pol4 is closely related to human Pol*μ*, which also incorporates ribonucleotides to DNA very efficiently (Martin et al., 2013a; Nick McElhinny and Ramsden, 2003; Ruiz et al., 2003), and tolerates 8oxodG preferably in an error-prone manner (Zhang et al., 2002). Therefore, it is tempting to speculate that this mechanism may be conserved in human cells during NHEJ coupled to 8oxodG tolerance, and that it may involve a first step of Pol*μ*-mediated ATP incorporation, followed by RER and Polλ-mediated insertion of dCTP. This would be in agreement with the important role of RNase H2 in maintaining genomic stability in mammalian cells (48).

Another source of 8oxodG/8oxoG accumulation in the genome is the incorporation of the 8oxo-dGTP and 8oxo-GTP from the cellular pool of nucleotides, which could be a relevant scenario in *S. pombe*, as homologs for MutT/MTH1 have not been identified. Our results using fission yeast extracts demonstrate that the endogenous DNA polymerases of *S. pombe* are able to misincorporate 8oxo-dGTP opposite dA, but *Sp*Pol4 contribution was undetectable. Accordingly, the only enzyme capable of removing an incorporated 8oxodG in *S. pombe*, *Sp*NTH1, operates when the lesion is paired to dA (Yonekura et al., 2007), as a specialized mismatch repair probably associated to DNA replication. Remarkably, *Sp*NTH1 activity could interfere with *Sp*MYH, removing a templating 8oxodG from 8oxodG:dA mispairs, but this would be inconvenient and lead directly to mutagenesis (Figure 50A). *Sp*Pol4 could incorporate 8oxo-dGTP/8oxo-GTP during in vitro DNA polymerization and was the only polymerase present in extracts capable of incorporating 8oxo-dGTP opposite dC and 8oxo-GTP opposite either dA or dC. However, these oxidized nucleotides are incorporated very inefficiently by *Sp*Pol4 in comparison with undamaged nucleotides, requiring a significantly higher concentration than dTTP/UTP and dGTP/GTP for similar efficiency *in vitro*. 8oxo-dGTP concentration is relevant in mammalian mitochondria, which are exposed to high levels of oxidative stress, as it matches dTTP concentration in some tissues, but being only a fraction of the dGTP pool (Pursell et al., 2008). 8oxo-dGTP/8oxo-GTP levels have not been determined in *S. pombe* but are likely to be significant, possibly resembling the situation of mammalian mitochondria; however, *Sp*Pol4 marked preference for undamaged nucleotides suggests that in a physiological context, the oxidized nucleotides will be probably outcompeted by dGTP/GTP and dTTP/UTP. These results contrast with *Sp*Pol4 ability to tolerate 8oxodG as efficiently

as undamaged DNA, and suggests that its active site has been adapted to efficiently tolerate this lesion in a template, but to avoid its incorporation as a dNTP/NTP, which is in line with the absence of a MutT homolog. A recent study of *Thermus thermophillus* PolX (TthPolX) suggested that the absence of an specific asparagine, relatively conserved among PolXs, could be an adaptation of the active site to avoid 8oxo-dGTP incorporation opposite dA in organisms where the GO system does not sanitize this oxidized nucleotide, although it hampers pyrimidine incorporation (Garrido et al., 2014). This residue is Asn^{279} in Polβ and its mutation to alanine was shown to revert Polβ's preference for incorporation of 8oxo-dGTP opposite template dA, favouring the template dC (Miller et al., 2000). That residue is absent in *Sp*Pol4, which is in agreement with its preference for purines over pyrimidines (González-Barrera et al., 2005), and further suggests and adaptation to avoid 8oxodGTP/8oxoGTP accumulation in the genome.

In summary, our data suggest that *Sp*Pol4 takes part in the tolerance of 8oxodG in *S. pombe*, most likely during NHEJ. *Sp*Pol4 incorporates preferably ATP opposite 8oxodG, but this error-prone event is just an intermediate step that recruits RNase H2 and other RER enzymes that eliminate the ribonucleotide and triggers dCTP incorporation. Nevertheless, in spite of these compelling evidence, further analyses are required to understand the relevance of ribonucleotides for DNA repair and damage tolerance. In this regard, although ribonucleotide incorporation was detected using cell extracts, one limitation of the work we present is that it does not provide actual evidence on incorporation of ribonucleotides in response to damage *in vivo*. In the case of *Sp*Pol4, this could be evaluated by analyzing the sensitivity to alkali of purified genomic DNA of *S. pombe* after treatment with damaging agents. Ribonucleotide incorporation would increase genomic DNA sensitivity to alkali due to their higher propensity to hydrolysis. This analysis should be performed in RNase H2-deficient background to avoid prompt removal of the ribonucleotides, and one would anticipate that genomic DNA from *Sp*Pol4 deficient strains should be less sensitive to alkali, consequent with having less incorporated ribonucleotides. However, it is quite likely that this approach could fail to address *Sp*Pol4-mediated ribonucleotide incorporation *in vivo*, since one would also expect these *Sp*Pol4-mediated incorporations to be negligible compared to ribonucleotide insertion mediated by replicative DNA polymerases, which could obscure any difference between *Sp*Pol4 deficient and proficient cells.

2. Regulation by phosphorylation of DNA polymerases specialized in NHEJ

Realization that both human Polλ and Polμ were adapted to NHEJ suggested functional redundancy, but exhaustive research demonstrated that on the contrary, these polymerases have complementary roles in this pathway. In fact, recent evidence has clearly demonstrated that they are adapted the repair broken ends of different complementarity and to fill gaps of different size *in vivo* (Pryor et al., 2015). However, it could be anticipated that there are certain kinds of broken ends in which both polymerases could be operative, such as those ends with little complementarity whose alignment would generate short gaps. Additionally, due to the hazardous nature of DSBs, in order to allow rapid DNA synthesis and repair it could also be expected that the recruitment of Polλ and Polμ to the DSB could not be simply mediated by their affinity to the DNA ends. Therefore, after the elucidation of Polμ and Polλ's unique roles in NHEJ, determination of how their activity is regulated in this pathway is essential to address the adaptation of these DNA polymerases to NHEJ, which would explain how they are recruited to the damaged site and how superfluous competition between the two could be avoided.

However, since the discovery of Polλ and Polμ their possible regulation in response to DNA damage also remained largely unknown. In the past years, some studies have demonstrated that both Polλ and Polμ are regulated through phosphorylation by CDK-cyclin complexes during the cell-cycle although in these studies there is no clear link to NHEJ, their major role. In the case of Polλ this phosphorylation was demonstrated to stabilize the protein in the S-phase, preventing proteasome-mediated degradation (Frouin et al., 2005; Wimmer et al., 2008) and it is thought to be related to the function of Polλ in 8oxodG tolerance (Markkanen et al., 2012). Conversely phosphorylation of Polμ by CDK-cyclin complexes did not affect its stability but led to a marked decrease of its activity *in vitro* (Esteban et al., 2013), although likewise in the case of Polλ, this regulation does not appear to be directly linked to NHEJ. DNA-PK is a kinase considered to be essential for regulation of the NHEJ pathway through phosphorylation by its kinase subunit, thereby regulating the access of other factors to the DSB (Lieber, 2008). Although little is known about how DNA-PK might modulate the function of other proteins during NHEJ, if Polμ and Polλ are regulated during this pathway, DNA-PK-mediated phosphorylation of these polymerases could be anticipated as the most likely mechanism.

In this Doctoral Thesis, we have addressed this question by evaluating the regulation of Polλ by DNA-PK-mediated phosphorylation. We have demonstrated that

indeed, DNA-PKcs efficiently phosphorylates Polλ, providing the first evidence of how its activity could be directly regulated during NHEJ. We show that phosphorylation stimulates the activity of Polλ during NHEJ *in vivo* (Figure 27), by enhancing its interaction with Ku80 after DNA damage (Figure 29). Surprisingly, we have observed that Polλ stably interacts with Ku80 in the absence of DNA damage, when it is not phosphorylated by DNA-PKcs (Figure 28 & 29). This could be in agreement with several studies that detected interaction between these proteins irrespectively of the phosphorylation status of Polλ (Ma et al., 2004; Mueller et al., 2008) and it is tempting to speculate that this DNA damage-independent interaction could function to keep these two NHEJ factors localizing in close proximity to allow a more rapid response to a DSB. Interestingly, we have observed that phosphorylation of Polλ is triggered by DNA damage and is required for the interaction between Ku80 and Polλ only after DNA damage induction. Remarkably, in these conditions, the interaction is not increased compared to the no-damage context, but it is clearly diminished in a phosphodead mutant (T204A) (Figure 29). This is somehow surprising and may be unintuitive, but it could be possibly related to the fact that during the first steps of NHEJ Ku80, together with Ku70, forms a complex with the DNA-PKcs thereby generating the DNA-PK complex itself (Davis and Chen, 2013). This would indicate that after the generation of the DSB, the nature of the interaction between Ku80 and Polλ is different because the former would be in complex with the DNA-PKcs, and could explain why it only relies on phosphorylation of Polλ only after the DSB is formed.

In this regard, the efficient interaction that we detected between Ku80 and Polλ in the absence of DNA damage is intriguing but could be somehow expected given that this interaction was demonstrated to be mediated by the BRCT domain of Polλ (Ma et al., 2004; Mueller et al., 2008; Nick McElhinny et al., 2005), and also since Thr^{204}, the residue that we have identified as the main target for DNA-PKcs-dependent phosphorylation of Polλ, is located in an S/P-rich intermediate domain. Therefore, on the basis of Thr^{204} localization in the S/P-rich domain, we speculate that DNA-PKcs-mediated phosphorylation of this residue stimulates the interaction of Polλ and Ku80 indirectly, by affecting the global conformation of Polλ. Our Thermal shift and partial proteolysis assays comparing wild-type Polλ and a phospho-mimetic T204E mutant protein support this idea, as they suggest that the phosphorylation of Thr^{204} could lead to a different and more open conformation of Polλ (Figure 30). Additionally, it is worth noting that our data is in agreement with the previous suggestion that the S/P-rich intermediate domain of Polλ could function as a regulatory domain (García-Díaz et al.,

2000). Despite the structure of human Polλ has been solved multiple times (first resolution in (Garcia-Diaz et al., 2004)), the structure of the S/P-rich domain remains unknown, indicating that it is highly flexible. This is in line with the fact that DNA-PKcs phosphorylation sites are commonly present in unstructured and/or highly flexible regions (Harris et al., 2004; Neal et al., 2014; Zhang et al., 2004), which is probably a consequence of the fact that this flexibility allows easier access to the active site of the large DNA-PKcs.

Remarkably our work also poses the intriguing question of whether Thr^{204} phosphorylation could play a role in the selection of Polμ vs Polλ during NHEJ. To determine this, future studies should also focus on whether Polμ could also be regulated through phosphorylation by the DNA-PK complex. Taking into account the aforementioned distinct substrate specificity of Polμ and Polλ, some regulation mechanism could be anticipated that would discriminate between them according to substrate structure. In fact, one would speculate that this possible regulation of Polμ could be somehow complementary to the one we describe for Polλ. Hence, it is tempting to speculate that the selection of Polμ vs Polλ could be at least partly determined by distinct post-translational modifications, to avoid competition at those substrates where both polymerases could be active. According to our data, the fact that Ku80 and Polλ interact in non-damage conditions, could suggest that Polλ is the preferred polymerase, chosen constitutively due to its lower error-proneness compared to Polμ. Next, if Polλ is not suited to repair the broken ends due to their low complementarity, some signal, possibly a phosphorylation, could trigger a swith between Polλ and Polμ. In this model Ku80 could play facilitate the selection of the specific polymerase required, which could be in agreement with the fact that interaction of Ku80 protein in human cells seems more specific of Polλ compared to Pol*μ* (Xing et al., 2015).

In this thesis we have also evaluated phosphorylation in response to DNA damage of *Sc*Pol4, the only PolX found in the budding yeast *S. cerevisiae*. We have demonstrated that *Sc*Pol4 is phosphorylated by the Tel1, the yeast homolog of ATM. ATM is arguably the most relevant kinase in human cells that mediates the overall response to DSBs (Jackson, 2002), and since DNA-PK is not conserved in yeast, it may be more directly involved in NHEJ in this *S. cerevisiae.* We show that Tel1/ATM phosphorylates *Sc*Pol4 Thr^{540}, and importantly, these data contributed to the demonstration that this phosphorylation stimulates *Sc*Pol4 activity in NHEJ ((Ruiz et al., 2013), see the articles attached in this Thesis). These data, in a way, resembles the

role of DNA-PK-mediated phosphorylation of Polλ in human cells, which is consequent with the close evolutionary relationship of *Sc*Pol4 and Polλ. Importantly, it was also demonstrated that *Sc*Pol4 phosphorylation impacts chromosomal translocations in yeast ((Ruiz et al., 2013), see the articles attached in this Thesis). Although Tel1 functions to enhance NHEJ partly by phosphorylating *Sc*Pol4, this also moderately enhances DSB repair *in trans*, because chromosomal translocations can be induced by conventional NHEJ and rely on filling of small gaps by phosphorylated *Sc*Pol4. Chromosomal translocations are extremely hazardous events whereby after a chromosome breaks either the entire molecule or just a part of it reattaches to a different chromosome (Roukos and Misteli, 2014). The study of the molecular events leading to chromosomal translocations is particularly relevant because very little is known about their biogenesis and also since these events are highly related to tumourigenesis (Mitelman et al., 2007). Given the potentially severe consequences of chromosomal translocations, the involvement of *Sc*Pol4 in these events in budding yeast, and the similarities between the mechanism of regulation by phosphorylation in response to DNA damage of *Sc*Pol4 and human Polλ, it would be worth to assess the possible involvement of the latter, or of the other human PolXs in chromosomal translocations in human cells.

3. Characterization of tumour variants: reverse engineering approach for structure-function analysis of DNA polymerases

Most lines of evidence indicate that tumourigenesis is a highly complex process whereby a succession of genetic changes, each conferring a survival advantage, must take place in order to lead to a progressive transformation of a normal cell into a cancer cell (Hanahan and Weinberg, 2000). These genetic changes allow cancer cells to overcome the anti-cancer barriers present in normal cells, and provide cancer cells with several distinctive capabilities including limitless replicative potential (Hanahan and Weinberg, 2000). Interestingly, the genetic alterations leading to the transformation of a normal cell into a cancer cell are commonly point mutations (*e.g.* insertion, deletions, single base modifications), and due to the role of DNA polymerases as DNA synthesizers, one would expect that alteration of the function and fidelity of these enzymes could contribute somehow to the accumulation of these mutations, and in turn to the tumourigenesis process (nicely reviewed in (Lange et al., 2011)). In this regard, several evidence argue in favour of this idea. For instance, Polδ and Polε exonuclease-deficient mice have shorter lifespans and highly increased frequency of carcinogenesis

(Albertson et al., 2009; Goldsby et al., 2002; Uchimura et al., 2009), clearly suggesting that altered function of replicative polymerases can drive cancer. Another relevant example of this is Polη, a DNA polymerase whose deficiency is known to cause in humans a variant form of *xeroderma pigmentosum* (XP-V), which renders the patients highly prone to sunlight-induced skin cancer (Johnson et al., 1999; Masutani et al., 1999). Finally, Telomerase, a very peculiar DNA polymerase specialized in telomere maintenance, is also a relevant example because it is probably the DNA polymerase more directly related with cancer, since its reactivation avoids telomere shortening, an essential requisite for the growth of cancers (Shay and Wright, 2011).

However, in spite of this compelling evidence, in the case of most DNA polymerases, whether they may contribute to tumourigenesis is not well understood. Since tumourigenesis is indeed a complex process, several aspects, such as gene expression and point mutations, should be considered to address whether altered function of some DNA polymerases contribute to this process. Additionally, the study of DNA polymerase function in cancer is particularly relevant, given that they could be interesting therapeutic targets (Lange et al., 2011). In fact, inhibition of certain DNA polymerases could sensitize tumours to chemotherapeutic agents. Some published data argue in favour of this idea, as for instance, tumours with decreased levels of Rev1 and Polζ are more sensitive to cisplatin and cyclophosphamide (Xie et al., 2010).

The contribution of the DNA polymerases from the X family to tumourigenesis is also not fully understood. Polβ is the better studied PolX in this context as some tumour-associated point mutants of Polβ have been characterized demonstrating that they induce mutations (Dalal et al., 2005; Lang et al., 2004) and that their expression leads to cellular transformation (Sweasy et al., 2005). Additionally, a tumour-associated single point mutant of Polλ has also been characterized and shown to be associated to colorectal cancer (Terrados et al., 2009). The mutant variant has a reduced fidelity, and leads to increased genomic instability, a common characteristic of cancer cells. From our perspective, overall, these data are particularly relevant for two reasons: 1) It helps to understand whether the altered function of these polymerases could contribute to tumourigenesis and 2) from a structural and functional standpoint, it allows the identification of point mutations that alter the properties of polymerases and in turn of residues critical for their specific function.

Inspired by this, we have characterized two tumour-associated Polμ point mutants, G174S and R175H, previously associated with two different tumour samples (Bell et al., 2011; Durinck et al., 2011). We have demonstrated that these mutations impact

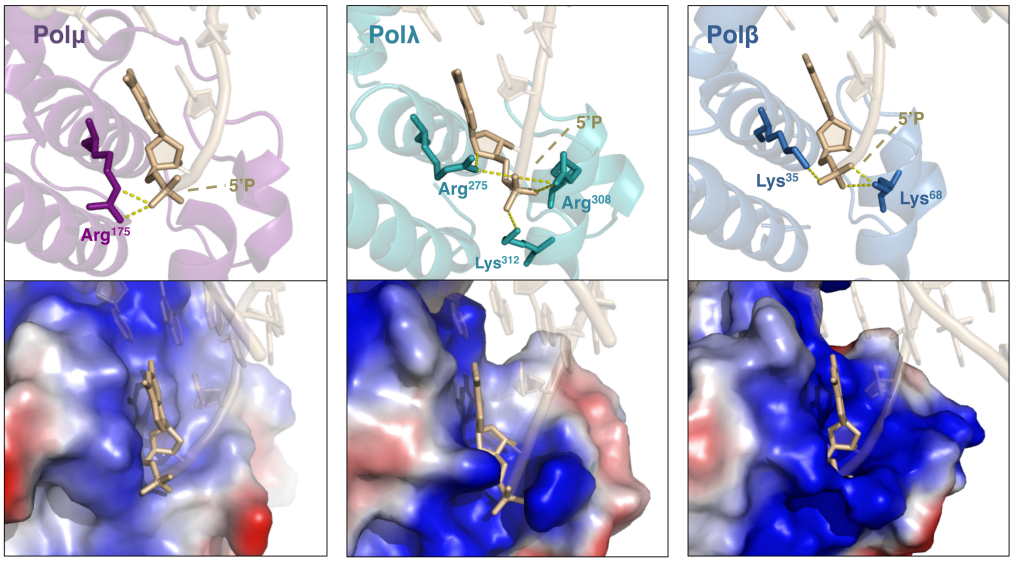

Figure 52. 5'P binding pocket of three human PolXs. The top panels show the positively charged residues at physiological pH that directly bind the 5'P group in human Polμ (left panel, PDB ID 4M04), human Polλ (central panel, PDB ID 1XSN) and human Polβ (right panel, PDB ID 1BPY). The lower panels show the electrostatic surface surrounding the 5'P group of human human Polμ (left panel), human Polλ (central panel) or human Polβ (right panel). The colour blue represents positively charged surfaces whereas the colour red represents negatively charged surfaces.

similarly the activity of Polμ during NHEJ decreasing both its efficiency and fidelity, due to the fact that they lead to an impaired incorporation of template-directed nucleotides (Figure 34). As we show, bona-fide NHEJ reactions by Polμ require the presence of a 5'P group flanking the template base, which enhances both the fidelity and efficiency of these reactions (Figure 35). In fact, the absence of this group leads to the random incorporation of nucleotides at DSBs by Polμ, a natural consequence of its inherent terminal transferase activity (Figure 35). Remarkably, the G174S and R175H mutants were as proficient as wild-type Polμ in these terminal-transferase events, but in contrast to their wild-type counterpart, their activity did not respond to the presence of the 5'P flanking the template base (Figure 35C), suggesting that their defective activity is somehow related to an impaired recognition of the 5'P during NHEJ. Arg^{175} is a ligand of the 5'P group itself, hence the effect of the R175H mutation is not surprising, especially taking into account the previously reported effect of Arg^{175} mutation to alanine, shown to hamper binding to the DNA, bridging of broken ends, and overall, the activity of Polμ on any DNA substrate harbouring that group (Davis et al., 2008). Arg^{175} mutation to histidine, although detrimental, was not as dramatic as mutation to alanine since the R175H mutant retained normal activity 1n-gapped substrates (Figure 34A). Interaction with 5'P group has already been reported to be essential for the activity of most of the studied template-directed polymerases from the X-family (e.g., (García-Díaz et al., 2002; González-Barrera et al., 2005; Prasad et al., 1994; Singhal and

Wilson, 1993)) and the study of R175H further supports the idea. In line with this, it is interesting to note that other template-directed PolXs, such as Polβ and Polλ, harbour similar or equivalent residues at the corresponding position of Arg^{175}, and also that this residue is not conserved in TdT, a template independent polymerases that displays no positively charged residues interacting with the 5'P within the 8 kDa domain. Moreover, this positively charged pocket of the 8 kDa domain, absent in TdT and that includes Arg^{175} in Polμ, is less developed in Polμ than in Polβ and Polλ (Figure 52), the latter two lacking template-independent activity. This could suggest that interaction with the 5'P limits terminal transferase activity, as was previously shown for Polμ (Andrade et al., 2009). Moreover, this could also suggest that mutation of the interactors of the 5'P in Polμ, as in the case of the R175H mutant, can limit template-directed nucleotide insertions at DSBs.

Analysis of the R175H mutant also lead to another relevant conclusion: interaction with the 5'P flanking the gap is essential for the efficiency of Polμ on 2nt gaps. Several studies have demonstrated that when Polμ faces a 2 nt gap it preferably copies the second template base, which is the one closer to the 5' end of the downstream DNA, this way skipping the first available template base (Ruiz et al., 2004; Juárez et al., 2006; Martin et al., 2012; Moon et al., 2015; Pryor et al., 2015). This error-prone

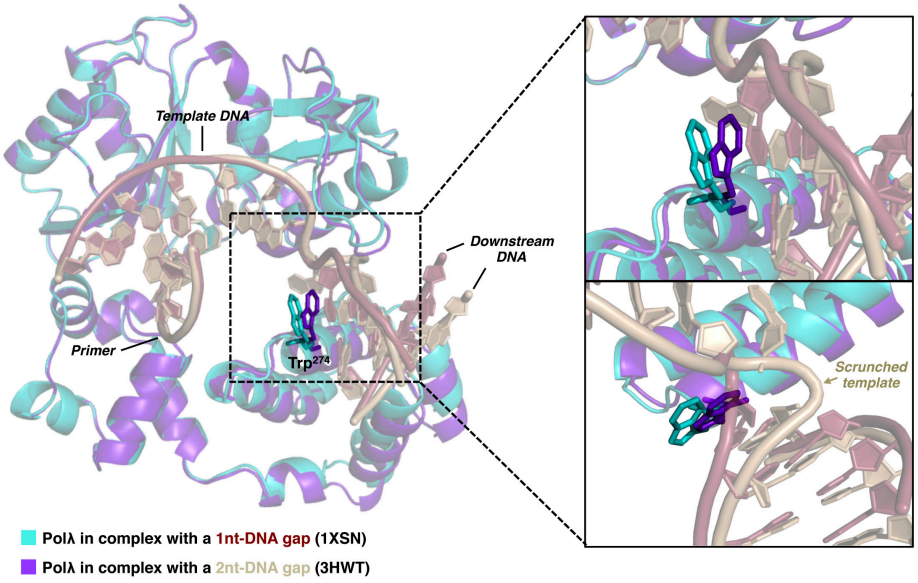

Figure 53. Possible involvement of human Polλ Trp^{274} in template scrunching at 2nt gaps. In clear contrast to human Polμ Gly^{174}, the equivalent residue of human Polλ, Trp^{274}, performs stacking interactions with the adjacent template base 5' of the gap. Given the effect of the G174S on 2nt gap-filling by Polμ (see Figure 37), we speculate that the position of these residues, Gly^{174} and Trp^{274}, could be relevant for 2nt gap-filling reactions mediated by the members of the PolX family. Analysis of the structures of human Polλ in complex with a 1nt gap and with a 2nt gap indicates that Trp^{274} is placed very close to the site where the template of the 2nt-gapped DNA is scrunched. Moreover, when the DNA is scrunched, Trp^{274} moves accordingly, which could suggest that it is involved in this reaction. The 3D structural images in this figure were created using the structure of human Polλ in complex with a 1nt-gapped DNA and ddTTP (PDB ID 1XSN) (Garcia-Diaz et al., 2005) and the structure of the ternary complex of human Polλ bound to a 2nt-gapped substrate with a scrunched dA (PDB ID 3HWT) (Garcia-Diaz et al., 2009).

behaviour is a stark difference between Polμ and Polλ, since the latter was shown to correctly fill 2nt gaps *in vivo* (Pryor et al., 2015), thanks to its unique template scrunching ability (Garcia-Diaz et al., 2009). Interestingly, our work also indicates that, although the G174S and R175H mutations caused a similar defect in NHEJ, this was not the case in 2nt gap-filling reactions, possibly indicating that they affect NHEJ differently. In fact, the G174S mutation was not deleterious for 2nt gap-filling, as it stimulated nucleotide incorporation opposite the first template base, decreasing –but not reverting- the preference of Polμ for the skipping ahead reaction. As mentioned earlier, Polλ harbours at the corresponding position of Gly^{174} a tryptophan (Trp^{274}), a bulky residue that performs stacking interaction with the template DNA 5' of the gap. This stark difference was noticed as soon as the structure of Polμ was solved (Moon et al., 2007b), although this has never been understood. Given the stimulating effect of Gly^{174} on skipping ahead during 2nt gap-filling by Polμ, it is temping to speculate that stacking interactions with the template DNA proximal to the gap may limit skipping ahead at 2nt gaps in the case of Polλ. Comparison of the structures of Polλ bound to a 1nt gap and to a 2nt gap reveals that Trp^{274} is placed in close proximity to where the DNA is scrunched by Polλ in a 2nt gap (Figure 53), and that in fact, it moves accordingly to the template DNA when the it is scrunched (Figure 53), suggesting that it may contribute to this process. In any case, the dramatic effect that the G174S mutation had on NHEJ by Polμ, both *in vivo* and *in vitro*, suggests that, in contrast to Polλ, Polμ requires a small, flexible and non-polar residue at that position to perform NHEJ efficiently, although with the cost of enhanced error-proneness at 2nt gaps. The fact that R175H and G174S showed similar defectiveness during NHEJ, but that only the latter was effective in 2nt gaps may indicate that the defect caused by the G174S mutation in NHEJ may proceed via inappropriate orientation of the DNA, and not be caused by defective binding of the DNA. Different position of the DNA by the G174S mutant could explain why it incorporates nucleotides opposite the first template base of a DNA gap more efficiently than wild-type Polμ. Moreover unaffected binding in this mutant would also be in agreement with the fact that Gly^{174} is not a ligand of the 5'P group, unlike Arg^{175}. Our EMSA experiments support this idea since they showed that only the R175H bound defectively to the DNA. Hence, one would speculate that Gly^{174}, being such a small and flexible residue, could allow maximal movement of the templating base so that Polμ can correctly orientate it for catalysis. This could be particularly relevant for NHEJ, especially of non-complementary ends where the primer and primer and template are not physically connected.

Overall, we believe that our characterization of the G174S and R175H mutants validates the study of tumour-associated variants of DNA polymerase to further address the relationship between the structure and function of DNA polymerase and to anticipate to some a certain extent whether they could contribute to tumourigenesis. However, we must emphasize that our work does not establish a direct link between Polμ and the tumourigenesis process itself. Given that some consider that an early tumourigenesis step may be the mutation of genes that modulate the fidelity of DNA repair to increase the frequency of mutagenesis (Loeb, 2001), it is tempting to speculate that the G174S and R175H could contribute to the process, due to their increased error-proneness during NHEJ *in vitro*. Although we have no explicit measurement of their fidelity of synthesis *in vivo*, the *in vitro* data could suggest that they could lead to mutation accumulations *in vivo* in response to DSBs. Furthermore, even if these mutants do not display increased error-proneness *in vivo*, defective Polμ activity *in vivo* could lead to remodelling of the DNA ends, implying end resection and loss of genetic information, so that they become compatible with repair by Polλ-mediated NHEJ. Analysis of cellular transformation after stable expression of the variants in primary cells, similarly to what was performed in the case of Polβ (Sweasy et al., 2005), would be a nice experimental approach to gain further insight in this regard. However, the fact that both mutations, G174S and R175H have been identified only in one tumour sample casts doubt on their involvement in tumourigenesis, and therefore, the real impact of the G174S and R175H on tumour development, if any, remains yet to be determined.

4. New perspectives on human PrimPol: the least specialized human DNA polymerase?

NHEJ and HR have been traditionally considered to be the two major pathways of DSB repair in mammalian cells (Chapman et al., 2012), nonetheless, it is now clear the existence of an additional pathway termed MMEJ (Deriano and Roth, 2013; McVey and Lee, 2008), which can operate in NHEJ-proficient cells (Deriano and Roth, 2013), contrary to what was initially expected. These three pathways have different mechanisms of action; in fact, an early divergent step that separates NHEJ from MMEJ and HR is resection of the breaks, which is highly limited in the case of NHEJ. MMEJ and HR intermediates have longer protruding ends, but in the case of HR template discontinuity is circumvented by invasion of the sister chromatid allowing replicative polymerases to take part in this pathway (Holmes and Haber, 1999). Recently, human

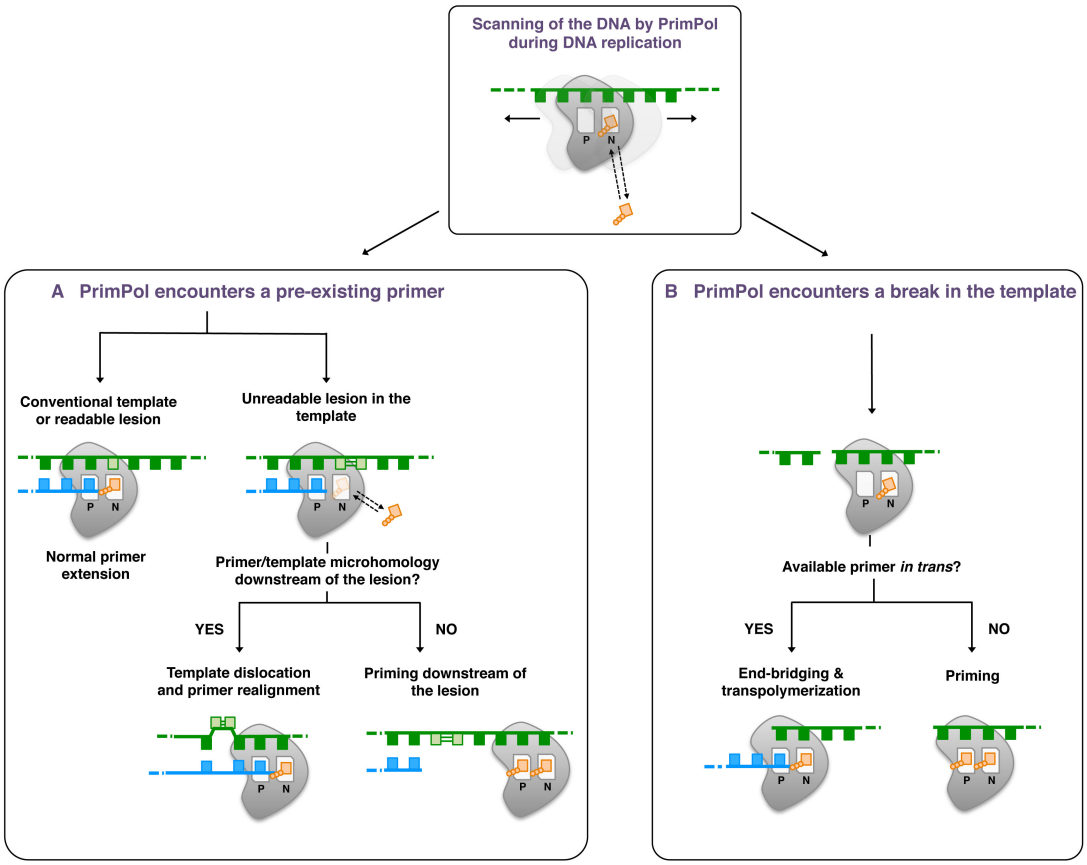

Figure 54. Model for the influence of the DNA context on PrimPol activity. PrimPol is recruited to ssDNA where it scans this molecule. (A) Upon encountering a damaged site, PrimPol can extend the primer at a stalled fork across "readable" lesions (*left*). If the lesion is "unreadable" PrimPol can realign the primer beyond the damaged site taking advantage of primer/template microhomologies (*right*). Ultimately, if this is impossible, PrimPol can initiate synthesis *de novo* (*right*). (B) If PrimPol encounters a SSB, it can preform transpolymerization, which we speculate to be mediated first by the formation of pre-ternary complex at one of the ends, and second by the bridging of a primer *in trans* (*left*). Likewise previously, if this is not possible, PrimPol can initiate synthesis *de novo* (*right*).

Polθ has been linked to MMEJ, and some of the most compelling pieces of evidence that support this idea is the ability of Polθ to synthesize DNA across dsDNA with relatively long protrusions *in vitro* (≥ 6nt) (Hogg et al., 2012; Kent et al., 2015). In this work we show that PrimPol activity somehow parallels that of Polθ, as it is highly efficient in bridging and polymerizing across long ssDNA molecules, requiring for this relatively long protrusions, necessarily longer that 4 nt (Figure 42). This evidence could suggest a role for PrimPol in MMEJ, although the participation of PrimPol in other pathways should not be discarded, as for instance the single-strand annealing subpathway of HR operates similarly to MMEJ. In this regard, it is tempting to speculate whether PrimPol could be involved in HR, in particular due to its ability to realign primers, which is way resembles strand invasion and that is probably related to its capacity to bridge ssDNA ends.

In this sense, it is likely that that all the activities and biochemical properties that PrimPol displays are highly related and selectively triggered depending on the DNA context. In fact, we suggest that PrimPol is constituvely recruited to ssDNA, in agreement with its interactions with mtSSB and RPA (Guilliam et al., 2015; Wan et al., 2013), where it scans the DNA, occasionally forming transient pre-ternary complexes with a dNTP (Figure 54), as we speculate most primases to do, given that they normally bind first the dNTP in the 3' position prior priming (Frick and Richardson, 2001). At this stage, normal primer extension across lesions at stalled forks would likely be the preferred option for PrimPol (Figure 54A), since it is the less challenging form a kinetic standpoint. Conversely, if PrimPol cannot read the lesion, it will realign the primer at a downstream position, and ultimately if this is impossible, it may re-prime ahead of the damage (Figure 54A), which according to the published data, is probably the most frequent PrimPol-mediated transaction in nuclear DNA (Mourón et al., 2013). Remarkably, according to the work presented herein, we also propose that if while scanning the template DNA PrimPol encounters a break, it can also overcome this challenge. In fact, we also suggest that it will face this challenge in a primase-like fashion, by first forming a pre-ternary complex with a dNTP in the ssDNA template and the searching for available primer *in trans* (Figure 54B), similarly to what was described for a bacterial AEP member specialized in NHEJ (Brissett et al., 2011). This way, if PrimPol fails to encounter the primer, it will bind another dNTP at the primer position (in a 5' position within the active site) and then initiate synthesis *de novo* (Figure 54B). Nonetheless, understanding pre-ternary complex formation by PrimPol would be essential to validate this hypothesis. On the other hand, this transpolymerization activity of PrimPol could be particularly relevant to tolerate single-strand breaks (SSB) in the template DNA during DNA replication, and hence, PrimPol could not be specialized in DSB repair *per se*, especially taking into account that SSBs can be overcome during DNA replication through the generation of intermediates with protruding ends (Caldecott, 2008).

Overall, our data supports the idea that PrimPol harbours a unique amalgam of biochemical properties amongst human DNA polymerases, clearly indicating that it is a polyvalent enzyme, less specialized than other polymerases or primases, especially those operating in the nucleus. We believe that this is consequent with the fact that it functions in the mitochondria, where PrimPol and Polγ are the only polymerases known to localize and thus, we speculate that if PrimPol is involved in DSB repair, this function is likely to be associated to mitochondria. Interestingly, this could be in line with a

possible role of PrimPol in MMEJ since this mechanism has been recently shown to prevail over NHEJ in mitochondria (Tadi et al., 2016), but in any case the exact role of PrimPol in DSB repair, if any, remains to be elucidated. In this regard, to gain further insight it would be pertinent to evaluate the sensitivity of PrimPol deficient cells to DSB-inducing agents and also to identify with precision PrimPol interacting partners by immunoprecipitation studies after DSB induction, which could indicate in what pathway is PrimPol involved, although recents studies indicate that PrimPol deficient cells are not sentsitve to camptothecin, a DSB inducing agent (Kobayashi et al., 2016).

Remarkably, our data also show that PrimPol synthesizes across the discontinuous templates and tolerates 8oxodG preferably using dNTPs over NTPs (Figure 41 A and Figure 42). As mentioned before, ribonucleotides can be useful substrates for repair and damage tolerance due to their high abundance (Traut, 1994), and also since their removal from the DNA can be efficiently initiated by RNase H1 and RNase H2 (Cerritelli and Crouch, 2009). The fact that PrimPol discriminates against NTPs would also be in line with a possible role in mtDNA metabolism given that RNase H2, the enzyme that can initiate the removal of single embedded ribonucleotides in the DNA, does not operate in mitochondria. However, mtDNA is a really intriguing scenario to study ribonucleotide incorporation since ribonucleotides are thought to be involved in the replication mechanism of this molecule and thus to abound in mtDNA (Holt, 2009). In fact, some analyses have demonstrated frequent and biased ribonucleotide incorporation throughout the lagging-strand (RITOLS) during mtDNA replication (Yang et al., 2002), and further studies have shown processed transcripts as the possible source of those ribonucleotides (Reyes et al., 2013). However, in spite of this, there is little or no evidence regarding whether ribonucleotides could also be relevant in the tolerance of lesions and the in the repair of mtDNA, and, although RNase H2 absence in mitochondria argues against this idea, it would be interesting to explore this possibility. In fact, RNase H1, the enzyme that initiates the removal of short tracks of RNA embedded in the DNA, does localize in mitochondria, which could support that ribonucleotides could mediate repair and/or tolerance in the mtDNA in a different fashion to what we have observed in the case of nuclear genomic DNA.

Additionally, we have demonstrated that the efficiency and fidelity of PrimPol-mediated TLS of 8oxodG is regulated by the presence and concentration of Mg^{2+} and Mn^{2+}. It is generally assumed that Mg^{2+} is the physiological cofactor for most DNA polymerases, however, several studies have shown that some DNA polymerases, including Polλ (Blanca et al., 2003), Polι (Frank and Woodgate, 2007), Polμ (Martin et

al., 2013a) and PrimPol (García-Gómez et al., 2013) preferentially utilize Mn^{2+} *in vitro*. In this work we confirm that, as demonstrated in (Zafar et al., 2014), Mg^{2+} favours the incorporation of dCTP opposite 8oxodG, although with the cost of lower efficiency compared to Mn^{2+}. However, combination with Mn^{2+} counteracts this effect, clearly enhancing the efficiency of 8oxodG tolerance although rendering the incorporation of dATP similar or even more efficient than dCTP; this effect was more patent when the concentration of Mn^{2+} was higher than 50 μM, and considering that its physiological concentration is generally lower, the effect of Mg^{2+} on PrimPol-mediated tolerance of 8oxodG might be relevant *in vivo*. Importantly, despite the alternative modulation induced by these metal cofactors, in most conditions PrimPol still generally discriminates poorly between dATP and dCTP during the tolerance of 8oxodG, especially when both cofactors were simultaneously present. Considering this and the fact that the physiological concentration of dATP and dCTP is similar in mitochondria (Pursell et al., 2008), the organelle where PrimPol-mediated tolerance of 8oxodG could be more relevant, our work indicates that PrimPol is likely to incorporate either dATP or dCTP opposite 8oxodG *in vivo*. Given that PrimPol tolerates 8oxodG more efficiently than Polγ, we speculate that it may assist mtDNA replication whenever Polγ encounters this lesion. PrimPol low discrimination between dATP and dCTP would support this role since fork stalling is more hazardous than misincorporation of dAMP opposite the lesion. Moreover, misincorporated dAMPs opposite 8oxodG could be later removed in mitochondria, as the glycosylase that initiates their removal in human cells, MYH, is known to localize in this organelle (Alexeyev et al., 2013).

We also demonstrate that Mn^{2+} and Mg^{2+} regulate the activity of PrimPol during other reactions including polymerization across discontinuous templates. In this case, PrimPol strictly required Mn^{2+} to be able to catalyse these events, being completely inactive with Mg^{2+}, although when using Mn^{2+} PrimPol was highly prone to incorporate nucleotides uncontrollably, by sliding back the primer at homopolymeric tracks, a process that could lead to expansions and that was limited by the presence of the 4 dNTPs (Figure 41). Strikingly, although PrimPol was inactive with Mg^{2+} in this scenario, its combination with Mn^{2+} limited primer extension by PrimPol to a single incorporation of the dNTP that was inserted uncontrollably by PrimPol with Mn^{2+} (Figure 44). This stark difference again suggests that Mg^{2+} limits error-prone DNA synthesis by PrimPol likewise in the case of 8oxodG. PrimPol also strictly required Mn^{2+} to promote primer realignment (Figure 49), an event required by PrimPol to skip unreadable lesions such as pyrimidine dimers (Martínez-Jiménez et al., 2015). Nucleotide excision repair is the

pathway responsible for the repair of bulky lesions such as pyrimidine dimers (Marteijn et al., 2014), but it has not been demonstrated to function in mitochondria, suggesting that in this organelle primer realignment by PrimPol might be relevant. Nevertheless, PrimPol required high concentrations of Mn^{2+} (higher than 250 μM) to catalyse primer realignment, which are distant from those physiological (Ash and Schramm, 1982), suggesting that the possible relevance or PrimPol-mediated primer realignment *in vivo* is still unclear and should be further addressed. In any case, these data showed clear differences in PrimPol activity when both Mg^{2+} and Mn^{2+} where combined compared to when they were provided alone. This could suggest that both cofactors may be simultaneously present in the active site of PrimPol, something that has never been described for any DNA polymerase.

PrimPol is endowed with a characteristic DxE metal binding motif (motif A) compared to other AEP members, which is highly conserved through evolution (Figure 47), suggesting functional relevance. By analysing a mutant in which Glu^{116}, the distinctive residue in the motif, was replaced by an aspartic acid, we have demonstrated that Glu^{116} contributes specifically to the error-prone tolerance of 8oxodG by PrimPol (Figure 48). Possibly this residue is an adaptation to tolerate 8oxodG as efficiently as possible with the cost of lower fidelity. Nevertheless, to further understand this, it would be worth evaluating the effect Glu^{116} in the overall fidelity of PrimPol. Interestingly, we have also observed that Glu^{116} contributes to primer realignment (Figure 49), although in these experiments its mutation to aspartic acid also decreased the efficiency of regular primer extension, suggesting that the effect on primer realignment might be indirect. Overall, we have demonstrated that Glu^{116} is more relevant for those reactions that are more dependent upon Mn^{2+}, which was evident in the case of primer realignment and even more in the case of the TLS of 8oxodG, where Mn^{2+} increased more pronouncedly the incorporation of dATP than dCTP, an en event also enhanced by Glu^{116}. Hence it very likely that Glu^{116} is an adaptation to stabilize Mn^{2+} at the active site of PrimPol, in order to use this metal cofactor as efficiently as possible to thereby promote efficient TLS with the cost of increased error-proneness.

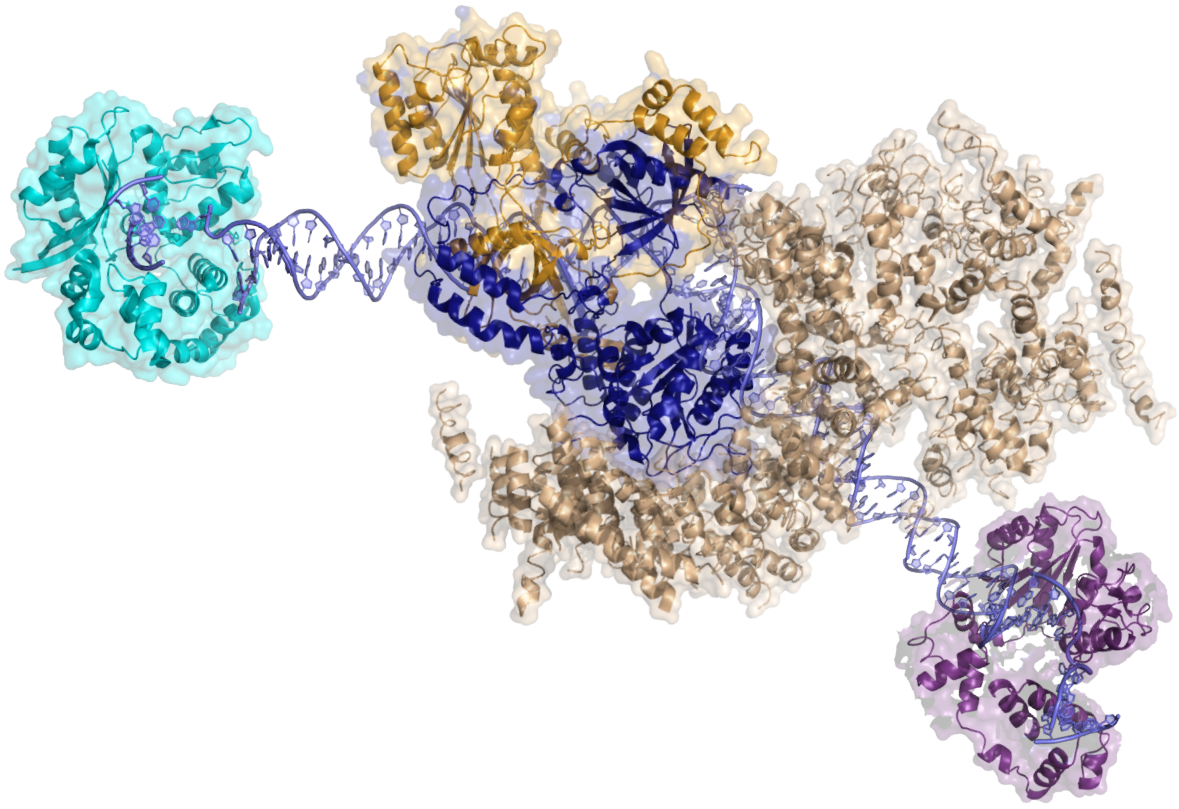

Conclusiones

1. *Sp*Pol4 tolera la lesión oxidativa 8oxodG con mucha eficiencia pero preferentemente de manera propensa al error. Debido a esto y la mayor concentración fisiológica de los ribonucleótidos, *Sp*Pol4 tolera el 8oxodG incorporando el ribonucleótido más abundante, ATP, de manera exclusiva durante reacciones de relleno de *gaps* en el DNA y durante la reparación de dobles roturas por el mecanismo de NHEJ.

2. La incorporación de ATP frente a 8oxodG por *Sp*Pol4 no es una actividad problemática puesto que la RNase H2 es capaz de reconocer ribonucleótidos apareados frente a 8oxodG en el DNA e iniciar su reparación. Además, en el caso de las riboadenosinas apareadas a 8oxodG, la incisión de este par de bases iniciada por la RNase H2 está específicamente acoplada a la incorporación del nucleótido correcto, dCTP, frente a la lesión en extractos totales de *S. pombe*, previniendo así mutaciones de transversión.

3. *Sp*Pol4 es capaz de incorporar al DNA los nucleótidos oxidados 8oxo-dGTP y 8oxo-GTP frente a las bases dA y dC, pero incorpora estos sustratos de manera poco eficiente en comparación con los nucleótidos competidores no dañados.

4. La quinasa Tel1/ATM fosforila a la polimerasa *Sc*Pol4 de *S. cerevisiae* en el residuo Thr^{540} tanto *in vitro* como *in vivo* en respuesta a daño en el DNA. De manera similar, la polimerasa humana Polλ es fosforilada en el residuo Thr^{204} tanto *in vitro* como *in vivo* en respuesta a daño en el DNA por DNA-PKcs, la quinasa reguladora de la vía de NHEJ.

5. La fosforilación en el residuo Thr^{204} estimula la actividad de Polλ durante NHEJ *in vivo*. En concordancia con su localización en el dominio S/P de Polλ, el residuo Thr^{204} no está involucrado directamente en la catálisis pero su fosforilación mejora la actividad de Polλ en NHEJ *in vivo* estimulando la interacción con el factor Ku80 después de la inducción del daño en el DNA. Presumiblemente, la fosforilación del residuo Thr^{204} mejora la interacción con Ku80 mediante la modificación de la conformación de Polλ.

6. Las variantes tumorales G174S y R175H de la polimerasa humana Polμ disminuyen su eficiencia durante NHEJ *in vitro*, más pronunciadamente en el caso de las roturas de extremos no complementarios, y también *in vivo*. Estas mutaciones causan a su vez una disminución en la fidelidad de Polμ durante NHEJ puesto que disminuyen selectivamente la capacidad de incorporación de nucleótidos complementarios al molde.

7. El defecto de las mutaciones G174S y R175H en NHEJ *in vitro* está causado únicamente en el caso del mutante R175H por una unión defectuosa al DNA. Esto sugiere que el mutante G174S no puede orientar bien las bases moldes del DNA y se traduce en que cada mutación afecta de manera diferente al relleno de *gaps* de 2nt mediado por Polμ. Mientras que la mutación R175H disminuye la eficiencia en estas reacciones *in vitro*, la mutación G174S modula la fidelidad de Polμ en este contexto.

8. PrimPol humana posee capacidad de transpolimerización a través de moldes discontinuos *in vitro*. Esta actividad requiere extremos de DNA con protrusiones 3' relativamente largas, la presencia de Mn^{2+} como cofactor, y aunque PrimPol no requiere estrictamente homología entre molde e iniciador, su presencia estimula la eficiencia de estás reacciones.

9. La combinación y concentración de los cofactores metálicos Mn^{2+} y Mg^{2+} modula la eficiencia y fidelidad de PrimPol humana durante la síntesis translesión a través del 8oxodG y durante las dislocaciones de moldes de DNA. La combinación de ambos cofactores proporciona un buen balance entre eficiencia y fidelidad: mientras que Mn^{2+} proporciona a PrimPol una eficiencia óptima, el Mg^{2+} mejora la fidelidad de esas reacciones aunque supone una reducción de la eficiencia.

10. El residuo Glu^{116} del motivo de unión de metales de PrimPol humana optimiza el uso de Mn^{2+} como cofactor para la catálisis. La mutación de este residuo a ácido aspártico reduce la eficiencia de manera más acusada en aquellas reacciones mediadas por PrimPol más dependientes de Mn^{2+}, como la incorporación de dATP frente a 8oxodG o la dislocación de moldes de DNA.

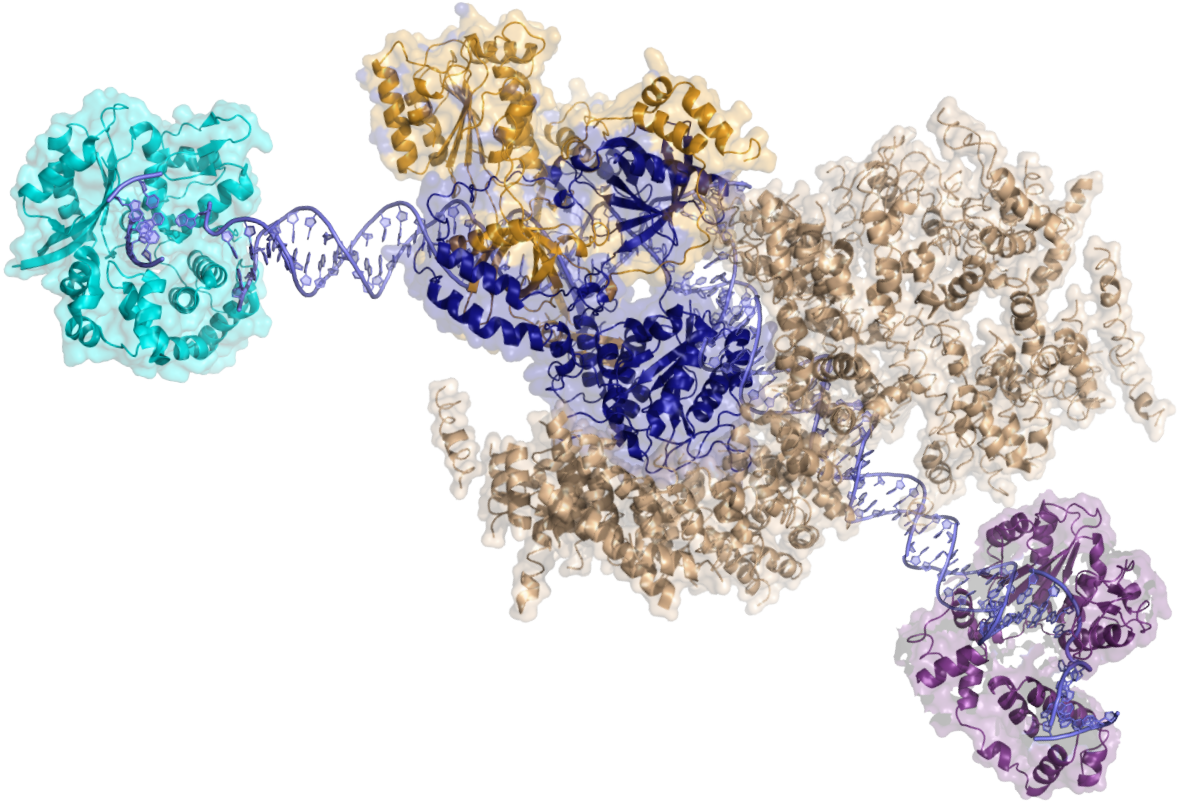

Conclusions

1. *Sp*Pol4 tolerates the oxidative lesion 8oxodG with high efficiency although preferably in an error-prone fashion. Due to this fact and to the higher physiological concentration of ribonucleotides, *Sp*Pol4 tolerates 8oxodG by incorporating the most abundant ribonucleotide, ATP, almost exclusively, during DNA gap-filling reactions and during DSB repair by the NHEJ mechanism.

2. ATP incorporation opposite 8oxodG by *Sp*Pol4 is not a problematic activity given that RNase H2 can recognize ribonucleotides paired opposite 8oxodG in the DNA and initiate their repair. Furthermore, in the case of riboadenosines paired to 8oxodG, incision of this base pair initiated by RNase H2 is specifically coupled to the incorporation of the correct nucleotide, dCTP, opposite this lesion, thus preventing transversion mutations.

3. *Sp*Pol4 can incorporate the oxidized nucleotides 8oxo-dGTP and 8oxo-GTP to the DNA opposite templates dA and dC, although it incorporates these substrates with low efficiency compared to undamaged nucleotides.

4. The Tel1/ATM kinase phosphorylates the *Sc*Pol4 polymerase from *S. cerevisiae* in residue Thr^{540} both *in vitro* and *in vivo* in response to DNA damage. Similarly, human Polλ is phosphorylated in the Thr^{204} residue both *in vitro* and *in vivo* in response to DNA damage by the DNA-PKcs kinase, the main regulator of the NHEJ pathway.

5. Phosphorylation of the Thr^{204} residue stimulates the activity of Polλ during NHEJ *in vivo*. In agreement with its localization in the S/P domain of Polλ, the Thr^{204} residue is not directly involved in catalysis, but its phosphorylation improves the activity of Polλ during NHEJ *in vivo* by stimulating the interaction with the Ku80 factor after induction of DNA damage. Presumably, the phosphorylation of the Thr^{204} residue improves the interaction with Ku80 by modifying the conformation of Polλ.

6. The tumour variants G174S and R175H of the human polymerase Polμ diminish its efficiency during NHEJ *in vitro*, more pronouncedly in the case of broken ends with no complementarity, and also *in vivo*. These mutations in turn cause a decrease in the fidelity of Polμ during NHEJ given that they selectively diminish its ability to incorporate nucleotides complementary to the template.

7. The defect induced by the G174S and R175H mutations in NHEJ *in vitro* is caused by defective DNA binding only in the case of the R175H mutant. This suggests that the G174S mutant cannot correctly orientate templates bases in a DSB and

translates into the fact that each mutation affects differently 2nt gap-filing by Polμ. Whereas the R175H mutation decreases the efficiency of these reactions *in vitro*, the G174S mutation modulates the fidelity of Polμ in this context.

8. Human PrimPol can perform transpolymerization across discontinuous templates *in vitro*. This activity requires relatively long 3'-protruding DNA ends, the presence of Mn^{2+} as cofactor and although PrimPol does not strictly require homology between primer and template, its presence stimulates the efficiency of these reactions.

9. The combination and concentration of the metal cofactors Mn^{2+} and Mg^{2+} modulates the efficiency and fidelity of human PrimPol during translesion synthesis across 8oxodG and during the dislocation of DNA templates. The combination of both cofactors leads to a good balance between fidelity and efficiency: whereas Mn^{2+} provides PrimPol with optimal efficiency, Mg^{2+} improves the fidelity of those reactions, although with the cost of reduced efficiency.

10. Residue Glu^{116}, forming the metal binding motif A of human PrimPol, optimizes the use of Mn^{2+} as metal cofactor for catalysis. The mutation of this residue to the consensus aspartic acid reduces the efficiency of those PrimPol-mediated reactions that are more dependent upon Mn^{2+}, such as the incorporation of dATP opposite 8oxodG or the dislocation of DNA templates.

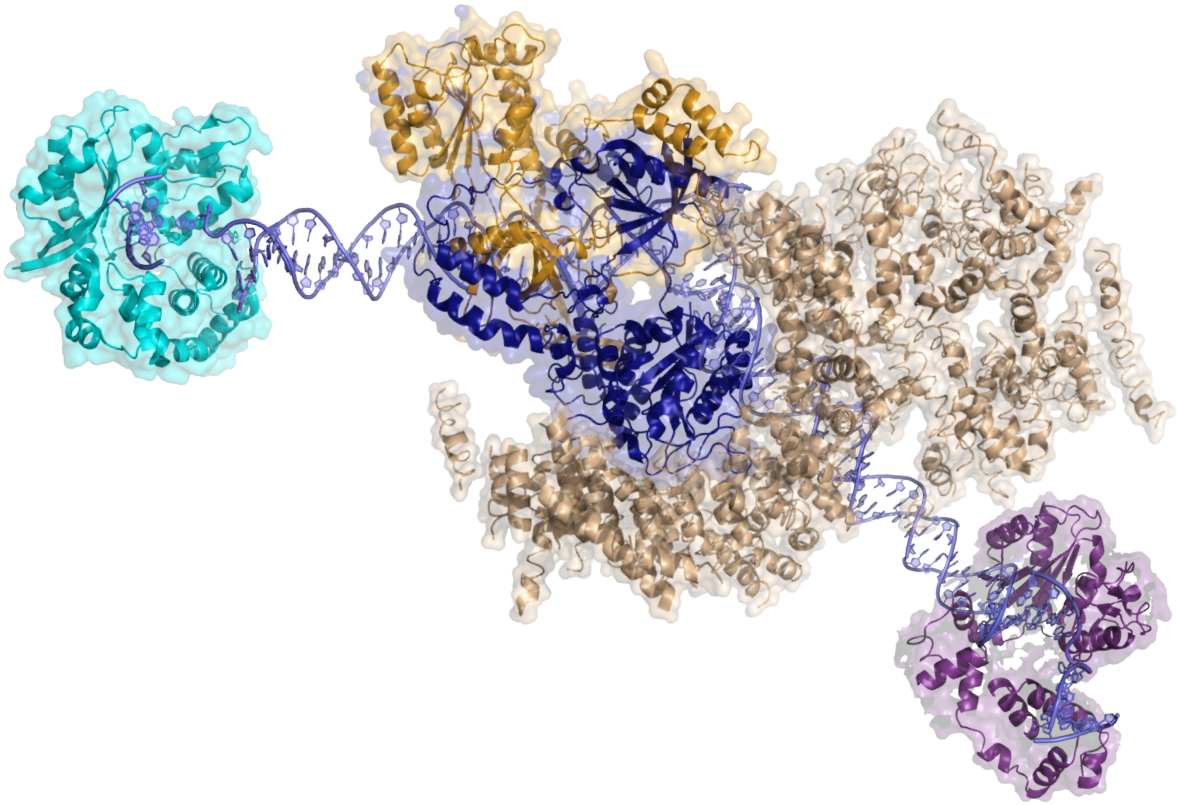

Bibliography

Albertson, T.M., Ogawa, M., Bugni, J.M., Hays, L.E., Chen, Y., Wang, Y., Treuting, P.M., Heddle, J. a, Goldsby, R.E., Preston, B.D., 2009. DNA polymerase epsilon and delta proofreading suppress discrete mutator and cancer phenotypes in mice. Proc. Natl. Acad. Sci. U. S. A. 106, 17101–4.

Alexeyev, M., Shokolenko, I., Wilson, G., LeDoux, S., 2013. The maintenance of mitochondrial DNA integrity--critical analysis and update. Cold Spring Harb. Perspect. Biol. 5, a012641.

Ames, B.N., 1983. Dietary carcinogens and anticarcinogens. Oxygen radicals and degenerative diseases. Science 221, 1256–64.

Andrade, P., Martín, M.J., Juárez, R., López de Saro, F., Blanco, L., 2009. Limited terminal transferase in human DNA polymerase mu defines the required balance between accuracy and efficiency in NHEJ. Proc. Natl. Acad. Sci. U. S. A. 106, 16203–8.

Arnold, K., Bordoli, L., Kopp, J., Schwede, T., 2006. The SWISS-MODEL workspace: a web-based environment for protein structure homology modelling. Bioinformatics 22, 195–201.

Arzumanov, A.A., Victorova, L.S., Jasko, M. V, Yesipov, D.S., Krayevsky, A.A., 2000. Terminal deoxynucleotidyl transferase catalyzes the reaction of DNA phosphorylation. Nucleic Acids Res. 28, 1276–81.

Ash, D.E., Schramm, V.L., 1982. Determination of free and bound manganese(II) in hepatocytes from fed and fasted rats. J. Biol. Chem. 257, 9261–4.

Autexier, C., Lue, N.F., 2006. The structure and function of telomerase reverse transcriptase. Annu. Rev. Biochem. 75, 493–517.

Avkin, S., Goldsmith, M., Velasco-Miguel, S., Geacintov, N., Friedberg, E.C., Livneh, Z., 2004. Quantitative analysis of translesion DNA synthesis across a benzo[a]pyrene-guanine adduct in mammalian cells: the role of DNA polymerase kappa. J. Biol. Chem. 279, 53298–305.

Aza, A., Martin, M.J., Juarez, R., Blanco, L., Terrados, G., 2013. DNA expansions generated by human Pol on iterative sequences. Nucleic Acids Res. 41, 253–263.

Bassing, C.H., Swat, W., Alt, F.W., 2002. The mechanism and regulation of chromosomal V(D)J recombination. Cell 109 Suppl, S45–55.

Bebenek, K., Garcia-Diaz, M., Blanco, L., Kunkel, T.A., 2003. The frameshift infidelity of human DNA polymerase lambda. Implications for function. J. Biol. Chem. 278, 34685–90.

Bebenek, K., Garcia-Diaz, M., Patishall, S.R., Kunkel, T.A., 2005. Biochemical properties of Saccharomyces cerevisiae DNA polymerase IV. J. Biol. Chem. 280, 20051–8.

Bebenek, K., Kunkel, T.A., 2004. Functions of DNA polymerases. Adv. Protein Chem. 69, 137–65.

Beckman, K.B., Ames, B.N., 1997. Oxidative decay of DNA. J. Biol. Chem. 272, 19633–6.

Bell, D., Berchuck, A., Birrer, M., Chien, J., Cramer, D.W., Dao, F., Dhir, R., DiSaia, P., Gabra, H., Glenn, P., et al., 2011. Integrated genomic analyses of ovarian carcinoma. Nature 474, 609–615.

Bell, S.P., Dutta, A., 2002. DNA replication in eukaryotic cells. Annu. Rev. Biochem. 71,

333–74.

Bemark, M., Khamlichi, A.A., Davies, S.L., Neuberger, M.S., 2000. Disruption of mouse polymerase zeta (Rev3) leads to embryonic lethality and impairs blastocyst development in vitro. Curr. Biol. 10, 1213–6.

Bertocci, B., De Smet, A., Berek, C., Weill, J.-C., Reynaud, C.-A., 2003. Immunoglobulin kappa light chain gene rearrangement is impaired in mice deficient for DNA polymerase mu. Immunity 19, 203–11.

Bertocci, B., De Smet, A., Weill, J.-C., Reynaud, C.-A., 2006. Nonoverlapping functions of DNA polymerases mu, lambda, and terminal deoxynucleotidyltransferase during immunoglobulin V(D)J recombination in vivo. Immunity 25, 31–41.

Blanca, G., Shevelev, I., Ramadan, K., Villani, G., Spadari, S., Hübscher, U., Maga, G., 2003. Human DNA polymerase lambda diverged in evolution from DNA polymerase beta toward specific Mn(++) dependence: a kinetic and thermodynamic study. Biochemistry 42, 7467–76.

Bocquier, A.A., Liu, L., Cann, I.K., Komori, K., Kohda, D., Ishino, Y., 2001. Archaeal primase: bridging the gap between RNA and DNA polymerases. Curr. Biol. 11, 452–6.

Boiteux, S., Gellon, L., Guibourt, N., 2002. Repair of 8-oxoguanine in Saccharomyces cerevisiae: interplay of DNA repair and replication mechanisms. Free Radic. Biol. Med. 32, 1244–53.

Boulé, J.B., Rougeon, F., Papanicolaou, C., 2001. Terminal deoxynucleotidyl transferase indiscriminately incorporates ribonucleotides and deoxyribonucleotides. J. Biol. Chem. 276, 31388–93.

Boulton, S.J., Jackson, S.P., 1996. Saccharomyces cerevisiae Ku70 potentiates illegitimate DNA double-strand break repair and serves as a barrier to error-prone DNA repair pathways. EMBO J. 15, 5093–103.

Braithwaite, E.K., Kedar, P.S., Stumpo, D.J., Bertocci, B., Freedman, J.H., Samson, L.D., Wilson, S.H., 2010. DNA polymerases beta and lambda mediate overlapping and independent roles in base excision repair in mouse embryonic fibroblasts. PLoS One 5, e12229.

Braithwaite, E.K., Prasad, R., Shock, D.D., Hou, E.W., Beard, W.A., Wilson, S.H., 2005. DNA polymerase lambda mediates a back-up base excision repair activity in extracts of mouse embryonic fibroblasts. J. Biol. Chem. 280, 18469–75.

Brissett, N.C., Martin, M.J., Pitcher, R.S., Bianchi, J., Juarez, R., Green, A.J., Fox, G.C., Blanco, L., Doherty, A.J., 2011. Structure of a preternary complex involving a prokaryotic NHEJ DNA polymerase. Mol. Cell 41, 221–31.

Brissett, N.C., Pitcher, R.S., Juarez, R., Picher, A.J., Green, A.J., Dafforn, T.R., Fox, G.C., Blanco, L., Doherty, A.J., 2007. Structure of a NHEJ Polymerase-Mediated DNA Synaptic Complex. Science (80-.). 318, 456–459.

Brown, J.A., Suo, Z., 2011. Unlocking the sugar “steric gate” of DNA polymerases. Biochemistry 50, 1135–42.

Burgers, P.M., Koonin, E. V., Bruford, E., Blanco, L., Burtis, K.C., Christman, M.F., Copeland, W.C., Friedberg, E.C., Hanaoka, F., Hinkle, D.C., et al., 2001. Eukaryotic DNA polymerases: proposal for a revised nomenclature. J. Biol. Chem. 276, 43487–90.

Byrnes, J.J., Downey, K.M., Black, V.L., So, A.G., 1976. A new mammalian DNA

polymerase with 3’ to 5' exonuclease activity: DNA polymerase delta. Biochemistry 15, 2817–23.

Caldecott, K.W., 2008. Single-strand break repair and genetic disease. Nat. Rev. Genet. 9, 619–31.

Capp, J.-P., Boudsocq, F., Bertrand, P., Laroche-Clary, A., Pourquier, P., Lopez, B.S., Cazaux, C., Hoffmann, J.-S., Canitrot, Y., 2006. The DNA polymerase lambda is required for the repair of non-compatible DNA double strand breaks by NHEJ in mammalian cells. Nucleic Acids Res. 34, 2998–3007.

Ceccaldi, R., Rondinelli, B., D’Andrea, A.D., 2016. Repair Pathway Choices and Consequences at the Double-Strand Break. Trends Cell Biol. 26, 52–64.

Cerritelli, S.M., Crouch, R.J., 2009. Ribonuclease H: the enzymes in eukaryotes. FEBS J. 276, 1494–505.

Chapman, J.R., Taylor, M.R.G., Boulton, S.J., 2012. Playing the end game: DNA double-strand break repair pathway choice. Mol. Cell 47, 497–510.

Chayot, R., Danckaert, A., Montagne, B., Ricchetti, M., 2010. Lack of DNA polymerase μ affects the kinetics of DNA double-strand break repair and impacts on cellular senescence. DNA Repair (Amst). 9, 1187–99.

Clayton, D.A., 1991. Replication and transcription of vertebrate mitochondrial DNA. Annu. Rev. Cell Biol. 7, 453–78.

Conaway, R.C., Lehman, I.R., 1982. A DNA primase activity associated with DNA polymerase alpha from Drosophila melanogaster embryos. Proc. Natl. Acad. Sci. U. S. A. 79, 2523–7.

Corpet, F., 1988. Multiple sequence alignment with hierarchical clustering. Nucleic Acids Res. 16, 10881–90.

Creighton, S., Bloom, L.B., Goodman, M.F., 1995. Gel fidelity assay measuring nucleotide misinsertion, exonucleolytic proofreading, and lesion bypass efficiencies. Methods Enzymol. 262, 232–56.

Crow, Y.J., Leitch, A., Hayward, B.E., Garner, A., Parmar, R., Griffith, E., Ali, M., Semple, C., Aicardi, J., Babul-Hirji, R., et al., 2006. Mutations in genes encoding ribonuclease H2 subunits cause Aicardi-Goutières syndrome and mimic congenital viral brain infection. Nat. Genet. 38, 910–6.

Dalal, S., Hile, S., Eckert, K.A., Sun, K., Starcevic, D., Sweasy, J.B., 2005. Prostate-Cancer-Associated I260M Variant of DNA Polymerase β Is a Sequence-Specific Mutator †. Biochemistry 44, 15664–15673.

Davis, A.J., Chen, D.J., 2013. DNA double strand break repair via non-homologous end-joining. Transl. Cancer Res. 2, 130–143.

Davis, B.J., Havener, J.M., Ramsden, D.A., 2008. End-bridging is required for pol to efficiently promote repair of noncomplementary ends by nonhomologous end joining. Nucleic Acids Res. 36, 3085–3094.

Decottignies, A., 2007. Microhomology-mediated end joining in fission yeast is repressed by pku70 and relies on genes involved in homologous recombination. Genetics 176, 1403–15.

Deriano, L., Roth, D.B., 2013. Modernizing the nonhomologous end-joining repertoire: alternative and classical NHEJ share the stage. Annu. Rev. Genet. 47, 433–55.

Desiderio, S. V, Yancopoulos, G.D., Paskind, M., Thomas, E., Boss, M.A., Landau, N.,

Alt, F.W., Baltimore, D., 1984. Insertion of N regions into heavy-chain genes is correlated with expression of terminal deoxytransferase in B cells. Nature 311, 752–5.

Dianov, G.L., Hübscher, U., 2013. Mammalian base excision repair: the forgotten archangel. Nucleic Acids Res. 41, 3483–90.

Domínguez, O., Ruiz, J.F., Laín de Lera, T., García-Díaz, M., González, M. A., Kirchhoff, T., Martínez-A, C., Bernad, A., Blanco, L., 2000. DNA polymerase mu (Pol μ), homologous to TdT, could act as a DNA mutator in eukaryotic cells. EMBO J. 19, 1731–42.

Durinck, S., Ho, C., Wang, N.J., Liao, W., Jakkula, L.R., Collisson, E.A., Pons, J., Chan, S.-W., Lam, E.T., Chu, C.,et al., 2011. Temporal Dissection of Tumorigenesis in Primary Cancers. Cancer Discov. 1, 137–143.

Esposito, G., Godindagger, I., Klein, U., Yaspo, M.L., Cumano, A., Rajewsky, K., 2000. Disruption of the Rev3l-encoded catalytic subunit of polymerase zeta in mice results in early embryonic lethality. Curr. Biol. 10, 1221–4.

Esteban, V., Martin, M.J., Blanco, L., 2013. The BRCT domain and the specific loop 1 of human Polμ are targets of Cdk2/cyclin A phosphorylation. DNA Repair (Amst). 12, 824–34.

Falkenberg, M., Larsson, N.-G., Gustafsson, C.M., 2007. DNA replication and transcription in mammalian mitochondria. Annu. Rev. Biochem. 76, 679–99.

Fan, W., Wu, X., 2004. DNA polymerase lambda can elongate on DNA substrates mimicking non-homologous end joining and interact with XRCC4-ligase IV complex. Biochem. Biophys. Res. Commun. 323, 1328–33.

Ferreira, M.G., Cooper, J.P., 2004. Two modes of DNA double-strand break repair are reciprocally regulated through the fission yeast cell cycle. Genes Dev. 18, 2249–54.

Fleck, O., Vejrup-Hansen, R., Watson, A., Carr, A.M., Nielsen, O., Holmberg, C., 2013. Spd1 accumulation causes genome instability independently of ribonucleotide reductase activity but functions to protect the genome when deoxynucleotide pools are elevated. J. Cell Sci. 126, 4985–94.

Forbes, S.A., Bhamra, G., Bamford, S., Dawson, E., Kok, C., Clements, J., Menzies, A., Teague, J.W., Futreal, P.A., Stratton, M.R., 2008. The Catalogue of Somatic Mutations in Cancer (COSMIC). Curr. Protoc. Hum. Genet. Chapter 10, Unit 10.11.

Foury, F., 1989. Cloning and sequencing of the nuclear gene MIP1 encoding the catalytic subunit of the yeast mitochondrial DNA polymerase. J. Biol. Chem. 264, 20552–60.

Frank, E.G., Woodgate, R., 2007. Increased catalytic activity and altered fidelity of human DNA polymerase iota in the presence of manganese. J. Biol. Chem. 282, 24689–96.

Frick, D.N., Richardson, C.C., 2001. DNA PRIMASES. Annu. Rev. Biochem. 70, 39–80.

Friedberg, E.C., 2005. Suffering in silence: the tolerance of DNA damage. Nat. Rev. Mol. Cell Biol. 6, 943–53.

Frouin, I., Toueille, M., Ferrari, E., Shevelev, I., Hübscher, U., 2005. Phosphorylation of human DNA polymerase lambda by the cyclin-dependent kinase Cdk2/cyclin A

complex is modulated by its association with proliferating cell nuclear antigen. Nucleic Acids Res. 33, 5354–61.

Garcia-Diaz, M., Bebenek, K., 2007. Multiple functions of DNA polymerases. CRC. Crit. Rev. Plant Sci. 26, 105–122.

Garcia-Diaz, M., Bebenek, K., Krahn, J.M., Blanco, L., Kunkel, T.A., Pedersen, L.C., 2004. A Structural Solution for the DNA Polymerase λ-Dependent Repair of DNA Gaps with Minimal Homology. Mol. Cell 13, 561–572.

Garcia-Diaz, M., Bebenek, K., Krahn, J.M., Kunkel, T.A., Pedersen, L.C., 2005. A closed conformation for the Pol lambda catalytic cycle. Nat. Struct. Mol. Biol. 12, 97–8.

Garcia-Diaz, M., Bebenek, K., Krahn, J.M., Pedersen, L.C., Kunkel, T.A., 2006. Structural analysis of strand misalignment during DNA synthesis by a human DNA polymerase. Cell 124, 331–42.

García-Díaz, M., Bebenek, K., Kunkel, T.A., Blanco, L., 2001. Identification of an intrinsic 5'-deoxyribose-5-phosphate lyase activity in human DNA polymerase lambda: a possible role in base excision repair. J. Biol. Chem. 276, 34659–63.

Garcia-Diaz, M., Bebenek, K., Larrea, A.A., Havener, J.M., Perera, L., Krahn, J.M., Pedersen, L.C., Ramsden, D.A., Kunkel, T.A., 2009. Template strand scrunching during DNA gap repair synthesis by human polymerase lambda. Nat. Struct. Mol. Biol. 16, 967–72.

García-Díaz, M., Bebenek, K., Sabariegos, R., Domínguez, O., Rodríguez, J., Kirchhoff, T., García-Palomero, E., Picher, A.J., Juárez, R., Ruiz, J.F., et al., 2002. DNA polymerase lambda, a novel DNA repair enzyme in human cells. J. Biol. Chem. 277, 13184–91.

García-Díaz, M., Domínguez, O., López-Fernández, L.A., de Lera, L.T., Saníger, M.L., Ruiz, J.F., Párraga, M., García-Ortiz, M.J., Kirchhoff, T., del Mazo, J., et al., 2000. DNA polymerase lambda (Pol lambda), a novel eukaryotic DNA polymerase with a potential role in meiosis. J. Mol. Biol. 301, 851–67.

García-Gómez, S., Reyes, A., Martínez-Jiménez, M.I., Chocrón, E.S., Mourón, S., Terrados, G., Powell, C., Salido, E., Méndez, J., Holt, I.J., Blanco, L., 2013. PrimPol, an Archaic Primase/Polymerase Operating in Human Cells. Mol. Cell 52, 541–553.

Garrido, P., Mejia, E., Garcia-Diaz, M., Blanco, L., Picher, A.J., 2014. The active site of TthPolX is adapted to prevent 8-oxo-dGTP misincorporation. Nucleic Acids Res. 42, 534–43.

Gibbs, P.E.M., McDonald, J., Woodgate, R., Lawrence, C.W., 2005. The relative roles in vivo of Saccharomyces cerevisiae Pol eta, Pol zeta, Rev1 protein and Pol32 in the bypass and mutation induction of an abasic site, T-T (6-4) photoadduct and T-T cis-syn cyclobutane dimer. Genetics 169, 575–82.

Gilfillan, S., Dierich, A., Lemeur, M., Benoist, C., Mathis, D., 1993. Mice lacking TdT: mature animals with an immature lymphocyte repertoire. Science 261, 1175–8.

Goldsby, R.E., Hays, L.E., Chen, X., Olmsted, E. a, Slayton, W.B., Spangrude, G.J., Preston, B.D., 2002. High incidence of epithelial cancers in mice deficient for DNA polymerase delta proofreading. Proc. Natl. Acad. Sci. U. S. A. 99, 15560–5.

González-Barrera, S., Sánchez, A., Ruiz, J.F., Juárez, R., Picher, A.J., Terrados, G., Andrade, P., Blanco, L., 2005. Characterization of SpPol4, a unique X-family DNA

polymerase in Schizosaccharomyces pombe. Nucleic Acids Res. 33, 4762–74.

Gozalbo-López, B., Andrade, P., Terrados, G., de Andrés, B., Serrano, N., Cortegano, I., Palacios, B., Bernad, A., Blanco, L., Marcos, M. a R., Gaspar, M.L., 2009. A role for DNA polymerase mu in the emerging DJH rearrangements of the postgastrulation mouse embryo. Mol. Cell. Biol. 29, 1266–75.

Guilliam, T.A., Jozwiakowski, S.K., Ehlinger, A., Barnes, R.P., Rudd, S.G., Bailey, L.J., Skehel, J.M., Eckert, K.A., Chazin, W.J., Doherty, A.J., 2015. Human PrimPol is a highly error-prone polymerase regulated by single-stranded DNA binding proteins. Nucleic Acids Res. 43, 1056–1068.

Håkansson, P., Dahl, L., Chilkova, O., Domkin, V., Thelander, L., 2006. The Schizosaccharomyces pombe replication inhibitor Spd1 regulates ribonucleotide reductase activity and dNTPs by binding to the large Cdc22 subunit. J. Biol. Chem. 281, 1778–83.

Hanahan, D., Weinberg, R. a, 2000. The hallmarks of cancer. Cell 100, 57–70.

Harman, D., 1981. The aging process. Proc. Natl. Acad. Sci. U. S. A. 78, 7124–8.

Harris, R., Esposito, D., Sankar, A., Maman, J.D., Hinks, J.A., Pearl, L.H., Driscoll, P.C., 2004. The 3D Solution Structure of the C-terminal Region of Ku86 (Ku86CTR). J. Mol. Biol. 335, 573–582.

Harrison, L., Hatahet, Z., Wallace, S.S., 1999. In vitro repair of synthetic ionizing radiation-induced multiply damaged DNA sites. J. Mol. Biol. 290, 667–84.

Helbock, H.J., Beckman, K.B., Shigenaga, M.K., Walter, P.B., Woodall, a a, Yeo, H.C., Ames, B.N., 1998. DNA oxidation matters: The HPLC-electrochemical detection assay of 8-oxo-deoxyguanosine and 8-oxo-guanine. Proc. Natl. Acad. Sci. 95, 288–293.

Hogg, M., Sauer-Eriksson, A.E., Johansson, E., 2012. Promiscuous DNA synthesis by human DNA polymerase θ. Nucleic Acids Res. 40, 2611–22.

Holmes, A.M., Haber, J.E., 1999. Double-strand break repair in yeast requires both leading and lagging strand DNA polymerases. Cell 96, 415–24.

Holt, I.J., 2009. Mitochondrial DNA replication and repair: all a flap. Trends Biochem. Sci. 34, 358–65.

Hu, J., Guo, L., Wu, K., Liu, B., Lang, S., Huang, L., 2012. Template-dependent polymerization across discontinuous templates by the heterodimeric primase from the hyperthermophilic archaeon Sulfolobus solfataricus. Nucleic Acids Res. 40, 3470–3483.

Hübscher, U., 1983. The mammalian primase is part of a high molecular weight DNA polymerase alpha polypeptide. EMBO J. 2, 133–6.

Iyer, L.M., Koonin, E. V., Leipe, D.D., Aravind, L., 2005. Origin and evolution of the archaeo-eukaryotic primase superfamily and related palm-domain proteins: structural insights and new members. Nucleic Acids Res. 33, 3875–96.

Jackson, S.P., 2002. Sensing and repairing DNA double-strand breaks. Carcinogenesis 23, 687–696.

Jang, Y.H., Goddard, W. a, Noyes, K.T., Sowers, L.C., Hwang, S., Chung, D.S., 2002. First principles calculations of the tautomers and pK(a) values of 8-oxoguanine: implications for mutagenicity and repair. Chem. Res. Toxicol. 15, 1023–35.

Jansen, J.G., Langerak, P., Tsaalbi-Shtylik, A., van den Berk, P., Jacobs, H., de Wind,

N., 2006. Strand-biased defect in C/G transversions in hypermutating immunoglobulin genes in Rev1-deficient mice. J. Exp. Med. 203, 319–23.

Jarosz, D.F., Godoy, V.G., Delaney, J.C., Essigmann, J.M., Walker, G.C., 2006. A single amino acid governs enhanced activity of DinB DNA polymerases on damaged templates. Nature 439, 225–8.

Jiricny, J., 2006. The multifaceted mismatch-repair system. Nat. Rev. Mol. Cell Biol. 7, 335–46.

Johnson, K.A., 2008. Role of induced fit in enzyme specificity: a molecular forward/reverse switch. J. Biol. Chem. 283, 26297–301.

Johnson, K.A., 2010. The kinetic and chemical mechanism of high-fidelity DNA polymerases. Biochim. Biophys. Acta 1804, 1041–8.

Johnson, R.E., Kondratick, C.M., Prakash, S., Prakash, L., 1999. hRAD30 mutations in the variant form of xeroderma pigmentosum. Science 285, 263–5.

Juárez, R., Ruiz, J.F., Nick McElhinny, S.A., Ramsden, D., Blanco, L., 2006. A specific loop in human DNA polymerase mu allows switching between creative and DNA-instructed synthesis. Nucleic Acids Res. 34, 4572–82.

Karanam, K., Kafri, R., Loewer, A., Lahav, G., 2012. Quantitative live cell imaging reveals a gradual shift between DNA repair mechanisms and a maximal use of HR in mid S phase. Mol. Cell 47, 320–9.

Kato, K.I., Gonçalves, J.M., Houts, G.E., Bollum, F.J., 1967. Deoxynucleotide-polymerizing enzymes of calf thymus gland. II. Properties of the terminal deoxynucleotidyltransferase. J. Biol. Chem. 242, 2780–9.

Kaufmann, G., Falk, H.H., 1982. An oligoribonucleotide polymerase from SV40-infected cells with properties of a primase. Nucleic Acids Res. 10, 2309–21.

Kent, T., Chandramouly, G., McDevitt, S.M., Ozdemir, A.Y., Pomerantz, R.T., 2015. Mechanism of microhomology-mediated end-joining promoted by human DNA polymerase θ. Nat. Struct. Mol. Biol. 22, 230–237.

Khanna, K.K., Jackson, S.P., 2001. DNA double-strand breaks: signaling, repair and the cancer connection. Nat. Genet. 27, 247–54.

Kinoshita, E., 2005. Phosphate-binding Tag, a New Tool to Visualize Phosphorylated Proteins. Mol. Cell. Proteomics 5, 749–757.

Klungland, A., Lindahl, T., 1997. Second pathway for completion of human DNA base excision-repair: reconstitution with purified proteins and requirement for DNase IV (FEN1). EMBO J. 16, 3341–8.

Kobayashi, K., Guilliam, T.A., Tsuda, M., Yamamoto, J., Bailey, L.J., Iwai, S., Takeda, S., Doherty, A.J., Hirota, K., 2016. Repriming by PrimPol is critical for DNA replication restart downstream of lesions and chain-terminating nucleosides. Cell Cycle 4101, 1–12.

Kouchakdjian, M., Bodepudi, V., Shibutani, S., Eisenberg, M., Johnson, F., Grollman, A.P., Patel, D.J., 1991. NMR structural studies of the ionizing radiation adduct 7-hydro-8-oxodeoxyguanosine (8-oxo-7H-dG) opposite deoxyadenosine in a DNA duplex. 8-Oxo-7H-dG(syn).dA(anti) alignment at lesion site. Biochemistry 30, 1403–12.

Krejci, L., Altmannova, V., Spirek, M., Zhao, X., 2012. Homologous recombination and its regulation. Nucleic Acids Res. 40, 5795–818.

Krokan, H.E., Standal, R., Slupphaug, G., 1997. DNA glycosylases in the base excision repair of DNA. Biochem. J. 325 (Pt 1, 1–16.

Kuchta, R.D., Stengel, G., 2010. Mechanism and evolution of DNA primases. Biochim. Biophys. Acta 1804, 1180–9.

Lai, J.S., Herr, W., 1992. Ethidium bromide provides a simple tool for identifying genuine DNA-independent protein associations. Proc. Natl. Acad. Sci. 89, 6958–6962.

Lang, T., Maitra, M., Starcevic, D., Li, S.-X., Sweasy, J.B., 2004. A DNA polymerase beta mutant from colon cancer cells induces mutations. Proc. Natl. Acad. Sci. U. S. A. 101, 6074–9.

Lange, S.S., Takata, K., Wood, R.D., 2011. DNA polymerases and cancer. Nat. Rev. Cancer 11, 96–110.

Lee, J.W., Blanco, L., Zhou, T., Garcia-Diaz, M., Bebenek, K., Kunkel, T.A., Wang, Z., Povirk, L.F., 2004. Implication of DNA polymerase lambda in alignment-based gap filling for nonhomologous DNA end joining in human nuclear extracts. J. Biol. Chem. 279, 805–11.

Lee, K., Lee, S.E., 2007. Saccharomyces cerevisiae Sae2- and Tel1-dependent single-strand DNA formation at DNA break promotes microhomology-mediated end joining. Genetics 176, 2003–14.

Lehman, I.R., Bessman, M.J., Simms, E.S., Kornberg, A., 1958. Enzymatic synthesis of deoxyribonucleic acid. I. Preparation of substrates and partial purification of an enzyme from Escherichia coli. J. Biol. Chem. 233, 163–70.

Lehmann, A.R., Niimi, A., Ogi, T., Brown, S., Sabbioneda, S., Wing, J.F., Kannouche, P.L., Green, C.M., 2007. Translesion synthesis: Y-family polymerases and the polymerase switch. DNA Repair (Amst). 6, 891–9.

Li, P., Li, J., Li, M., Dou, K., Zhang, M.-J., Suo, F., Du, L.-L., 2012. Multiple end joining mechanisms repair a chromosomal DNA break in fission yeast. DNA Repair (Amst). 11, 120–30.

Li, Y., Breaker, R.R., 1999. Kinetics of RNA Degradation by Specific Base Catalysis of Transesterification Involving the 2 ′ -Hydroxyl Group. J. Am. Chem. Soc. 121, 5364–5372.

Liang, F., Jasin, M., 1996. Ku80-deficient cells exhibit excess degradation of extrachromosomal DNA. J. Biol. Chem. 271, 14405–11.

Lieber, M.R., 2008. The Mechanism of Human Nonhomologous DNA End Joining. J. Biol. Chem. 283, 1–5.

Lieber, M.R., 2010. The mechanism of double-strand DNA break repair by the nonhomologous DNA end-joining pathway. Annu. Rev. Biochem. 79, 181–211.

Lindahl, T., 1993. Instability and decay of the primary structure of DNA. Nature 362, 709–15.

Loeb, L.A., 2001. A mutator phenotype in cancer. Cancer Res. 61, 3230–9.

Lu, A.L., Fawcett, W.P., 1998. Characterization of the recombinant MutY homolog, an adenine DNA glycosylase, from yeast Schizosaccharomyces pombe. J. Biol. Chem. 273, 25098–105.

Lucas, D., Delgado-García, J.M., Escudero, B., Albo, C., Aza, A., Acín-Pérez, R., Torres, Y., Moreno, P., Enríquez, J.A., Samper, E., et al., 2013. Increased

learning and brain long-term potentiation in aged mice lacking DNA polymerase μ. PLoS One 8, e53243.

Lucas, D., Escudero, B., Ligos, J.M., Segovia, J.C., Estrada, J.C., Terrados, G., Blanco, L., Samper, E., Bernad, A., 2009. Altered Hematopoiesis in Mice Lacking DNA Polymerase μ Is Due to Inefficient Double-Strand Break Repair. PLoS Genet. 5, e1000389.

Ma, Y., Lu, H., Tippin, B., Goodman, M.F., Shimazaki, N., Koiwai, O., Hsieh, C.-L., Schwarz, K., Lieber, M.R., 2004. A Biochemically Defined System for Mammalian Nonhomologous DNA End Joining. Mol. Cell 16, 701–713.

Maga, G., Villani, G., Crespan, E., Wimmer, U., Ferrari, E., Bertocci, B., Hübscher, U., 2007. 8-oxo-guanine bypass by human DNA polymerases in the presence of auxiliary proteins. Nature 447, 606–8.

Mahajan, K.N., Nick McElhinny, S. a, Mitchell, B.S., Ramsden, D.A., 2002. Association of DNA polymerase mu (pol mu) with Ku and ligase IV: role for pol mu in end-joining double-strand break repair. Mol. Cell. Biol. 22, 5194–202.

Mahaney, B.L., Meek, K., Lees-Miller, S.P., 2009. Repair of ionizing radiation-induced DNA double-strand breaks by non-homologous end-joining. Biochem. J. 417, 639–50.

Mallory, J.C., Petes, T.D., 2000. Protein kinase activity of Tel1p and Mec1p, two Saccharomyces cerevisiae proteins related to the human ATM protein kinase. Proc. Natl. Acad. Sci. U. S. A. 97, 13749–54.

Markkanen, E., van Loon, B., Ferrari, E., Parsons, J.L., Dianov, G.L., Hubscher, U., 2012. Regulation of oxidative DNA damage repair by DNA polymerase and MutYH by cross-talk of phosphorylation and ubiquitination. Proc. Natl. Acad. Sci. 109, 437–442.

Marteijn, J. A., Lans, H., Vermeulen, W., Hoeijmakers, J.H.J., 2014. Understanding nucleotide excision repair and its roles in cancer and ageing. Nat. Rev. Mol. Cell Biol. 15, 465–81.

Martin, M.J., Garcia-Ortiz, M. V., Esteban, V., Blanco, L., 2013a. Ribonucleotides and manganese ions improve non-homologous end joining by human Polμ. Nucleic Acids Res. 41, 2428–36.

Martin, M.J., Garcia-Ortiz, M.V., Gomez-Bedoya, A., Esteban, V., Guerra, S., Blanco, L., 2013b. A specific N-terminal extension of the 8 kDa domain is required for DNA end-bridging by human Polμ and Polλ. Nucleic Acids Res. 41, 9105–16.

Martin, M.J., Juarez, R., Blanco, L., 2012. DNA-binding determinants promoting NHEJ by human Polμ. Nucleic Acids Res. 40, 11389–403.

Martínez-Jiménez, M.I., García-Gómez, S., Bebenek, K., Sastre-Moreno, G., Calvo, P., Diaz-Talavera, A., Kunkel, T.A., Blanco, L., 2015. Alternative solutions and new scenarios for translesion DNA synthesis by human PrimPol. DNA Repair (Amst). 29, 127–38.

Masai, H., Matsumoto, S., You, Z., Yoshizawa-Sugata, N., Oda, M., 2010. Eukaryotic chromosome DNA replication: where, when, and how? Annu. Rev. Biochem. 79, 89–130.

Masutani, C., 2000. Mechanisms of accurate translesion synthesis by human DNA polymerase eta. EMBO J. 19, 3100–3109.

Masutani, C., Kusumoto, R., Yamada, A., Dohmae, N., Yokoi, M., Yuasa, M., Araki, M.,

Iwai, S., Takio, K., Hanaoka, F., 1999. The XPV (xeroderma pigmentosum variant) gene encodes human DNA polymerase eta. Nature 399, 700–4.

Mateos-Gomez, P.A., Gong, F., Nair, N., Miller, K.M., Lazzerini-Denchi, E., Sfeir, A., 2015. Mammalian polymerase θ promotes alternative NHEJ and suppresses recombination. Nature 518, 254–257.

Matsumoto, Y., Kim, K., 1995. Excision of deoxyribose phosphate residues by DNA polymerase beta during DNA repair. Science 269, 699–702.

McCulloch, S.D., Kokoska, R.J., Masutani, C., Iwai, S., Hanaoka, F., Kunkel, T.A., 2004. Preferential cis-syn thymine dimer bypass by DNA polymerase eta occurs with biased fidelity. Nature 428, 97–100.

McDonald, J.P., Frank, E.G., Plosky, B.S., Rogozin, I.B., Masutani, C., Hanaoka, F., Woodgate, R., Gearhart, P.J., 2003. 129-derived strains of mice are deficient in DNA polymerase iota and have normal immunoglobulin hypermutation. J. Exp. Med. 198, 635–43.

McKinnon, P.J., 2009. DNA repair deficiency and neurological disease. Nat. Rev. Neurosci. 10, 100–12.

McVey, M., Lee, S.E., 2008. MMEJ repair of double-strand breaks (director's cut): deleted sequences and alternative endings. Trends Genet. 24, 529–38.

Mehta, A., Haber, J.E., 2014. Sources of DNA Double-Strand Breaks and Models of Recombinational DNA Repair. Cold Spring Harb. Perspect. Biol. 6, a016428–a016428.

Michaels, M.L., Miller, J.H., 1992. The GO system protects organisms from the mutagenic effect of the spontaneous lesion 8-hydroxyguanine (7,8-dihydro-8-oxoguanine). J. Bacteriol. 174, 6321–5.

Miller, H., Prasad, R., Wilson, S.H., Johnson, F., Grollman, A.P., 2000. 8-oxodGTP incorporation by DNA polymerase beta is modified by active-site residue Asn279. Biochemistry 39, 1029–33.

Mitelman, F., Johansson, B., Mertens, F., 2007. The impact of translocations and gene fusions on cancer causation. Nat. Rev. Cancer 7, 233–245.

Miyabe, I., Kunkel, T.A., Carr, A.M., 2011. The major roles of DNA polymerases epsilon and delta at the eukaryotic replication fork are evolutionarily conserved. PLoS Genet. 7, e1002407.

Mo, J.Y., Maki, H., Sekiguchi, M., 1992. Hydrolytic elimination of a mutagenic nucleotide, 8-oxodGTP, by human 18-kilodalton protein: sanitization of nucleotide pool. Proc. Natl. Acad. Sci. U. S. A. 89, 11021–5.

Moldovan, G.-L., Pfander, B., Jentsch, S., 2007. PCNA, the maestro of the replication fork. Cell 129, 665–79.

Moon, A.F., Garcia-Diaz, M., Batra, V.K., Beard, W.A., Bebenek, K., Kunkel, T.A., Wilson, S.H., Pedersen, L.C., 2007a. The X family portrait: structural insights into biological functions of X family polymerases. DNA Repair (Amst). 6, 1709–25.

Moon, A.F., Garcia-Diaz, M., Bebenek, K., Davis, B.J., Zhong, X., Ramsden, D.A., Kunkel, T.A., Pedersen, L.C., 2007b. Structural insight into the substrate specificity of DNA Polymerase mu. Nat. Struct. Mol. Biol. 14, 45–53.

Moon, A.F., Gosavi, R.A., Kunkel, T.A., Pedersen, L.C., Bebenek, K., 2015. Creative template-dependent synthesis by human polymerase mu. Proc. Natl. Acad. Sci. U.

S. A. 112, E4530–6.

Moon, A.F., Pryor, J.M., Ramsden, D.A., Kunkel, T.A., Bebenek, K., Pedersen, L.C., 2014. Sustained active site rigidity during synthesis by human DNA polymerase μ. Nat. Struct. Mol. Biol. 21, 253–60.

Moreno, S., Klar, A., Nurse, P., 1991. Molecular genetic analysis of fission yeast Schizosaccharomyces pombe. Methods Enzymol. 194, 795–823.

Moriya, M., 1993. Single-stranded shuttle phagemid for mutagenesis studies in mammalian cells: 8-oxoguanine in DNA induces targeted G.C-->T.A transversions in simian kidney cells. Proc. Natl. Acad. Sci. U. S. A. 90, 1122–6.

Moriya, M., Ou, C., Bodepudi, V., Johnson, F., Takeshita, M., Grollman, A.P., 1991. Site-specific mutagenesis using a gapped duplex vector: A study of translesion synthesis past 8-oxodeoxyguanosine in E. coli. Mutat. Res. Repair 254, 281–288.

Mourón, S., Rodriguez-Acebes, S., Martínez-Jiménez, M.I., García-Gómez, S., Chocrón, S., Blanco, L., Méndez, J., 2013. Repriming of DNA synthesis at stalled replication forks by human PrimPol. Nat. Struct. Mol. Biol. 20, 1383–1389.

Mueller, G.A., Moon, A.F., DeRose, E.F., Havener, J.M., Ramsden, D.A., Pedersen, L.C., London, R.E., 2008. A comparison of BRCT domains involved in nonhomologous end-joining: Introducing the solution structure of the BRCT domain of polymerase lambda. DNA Repair (Amst). 7, 1340–1351.

Nakajima, S., Lan, L., Kanno, S., Takao, M., Yamamoto, K., Eker, A.P.M., Yasui, A., 2004. UV light-induced DNA damage and tolerance for the survival of nucleotide excision repair-deficient human cells. J. Biol. Chem. 279, 46674–7.

Neal, J.A., Sugiman-Marangos, S., VanderVere-Carozza, P., Wagner, M., Turchi, J., Lees-Miller, S.P., Junop, M.S., Meek, K., 2014. Unraveling the complexities of DNA-dependent protein kinase autophosphorylation. Mol. Cell. Biol. 34, 2162–75.

Nelson, J.R., Gibbs, P.E., Nowicka, A.M., Hinkle, D.C., Lawrence, C.W., 2000. Evidence for a second function for Saccharomyces cerevisiae Rev1p. Mol. Microbiol. 37, 549–54.

Nick McElhinny, S. A., Watts, B.E., Kumar, D., Watt, D.L., Lundström, E.-B., Burgers, P.M.J., Johansson, E., Chabes, A., Kunkel, T.A., 2010. Abundant ribonucleotide incorporation into DNA by yeast replicative polymerases. Proc. Natl. Acad. Sci. U. S. A. 107, 4949–54.

Nick McElhinny, S.A., Gordenin, D.A., Stith, C.M., Burgers, P.M.J., Kunkel, T.A., 2008. Division of labor at the eukaryotic replication fork. Mol. Cell 30, 137–44.

Nick McElhinny, S.A., Havener, J.M., Garcia-Diaz, M., Juárez, R., Bebenek, K., Kee, B.L., Blanco, L., Kunkel, T.A., Ramsden, D.A., 2005. A gradient of template dependence defines distinct biological roles for family X polymerases in nonhomologous end joining. Mol. Cell 19, 357–66.

Nick McElhinny, S.A., Ramsden, D.A., 2003. Polymerase mu is a DNA-directed DNA/RNA polymerase. Mol. Cell. Biol. 23, 2309–15.

Norbury, C., Moreno, S., 1997. Cloning cell cycle regulatory genes by transcomplementation in yeast. Methods Enzymol. 283, 44–59.

Obenauer, J.C., Cantley, L.C., Yaffe, M.B., 2003. Scansite 2.0: Proteome-wide prediction of cell signaling interactions using short sequence motifs. Nucleic Acids Res. 31, 3635–41.

Oda, Y., Uesugi, S., Ikehara, M., Nishimura, S., Kawase, Y., Ishikawa, H., Inoue, H., Ohtsuka, E., 1991. NMR studies of a DNA containing 8-hydroxydeoxyguanosine. Nucleic Acids Res. 19, 1407–12.

Ogi, T., Shinkai, Y., Tanaka, K., Ohmori, H., 2002. Polkappa protects mammalian cells against the lethal and mutagenic effects of benzo[a]pyrene. Proc. Natl. Acad. Sci. U. S. A. 99, 15548–53.

Ollis, D.L., Brick, P., Hamlin, R., Xuong, N.G., Steitz, T.A., 1985. Structure of large fragment of Escherichia coli DNA polymerase I complexed with dTMP. Nature 313, 762–6.

Osterod, M., Hollenbach, S., Hengstler, J.G., Barnes, D.E., Lindahl, T., Epe, B., 2001. Age-related and tissue-specific accumulation of oxidative DNA base damage in 7,8-dihydro-8-oxoguanine-DNA glycosylase (Ogg1) deficient mice. Carcinogenesis 22, 1459–63.

Otsuka, C., Kunitomi, N., Iwai, S., Loakes, D., Negishi, K., 2005. Roles of the polymerase and BRCT domains of Rev1 protein in translesion DNA synthesis in yeast in vivo. Mutat. Res. 578, 79–87.

Panier, S., Boulton, S.J., 2014. Double-strand break repair: 53BP1 comes into focus. Nat. Rev. Mol. Cell Biol. 15, 7–18.

Pelletier, H., Sawaya, M.R., Kumar, A., Wilson, S.H., Kraut, J., 1994. Structures of ternary complexes of rat DNA polymerase beta, a DNA template-primer, and ddCTP. Science 264, 1891–903.

Peña-Diaz, J., Jiricny, J., 2012. Mammalian mismatch repair: error-free or error-prone? Trends Biochem. Sci. 37, 206–214.

Picher, A.J., Blanco, L., 2007. Human DNA polymerase lambda is a proficient extender of primer ends paired to 7,8-dihydro-8-oxoguanine. DNA Repair (Amst). 6, 1749–56.

Pitcher, R.S., Brissett, N.C., Picher, A.J., Andrade, P., Juarez, R., Thompson, D., Fox, G.C., Blanco, L., Doherty, A.J., 2007. Structure and function of a mycobacterial NHEJ DNA repair polymerase. J. Mol. Biol. 366, 391–405.

Podlutsky, A.J., Dianova, I.I., Podust, V.N., Bohr, V.A., Dianov, G.L., 2001. Human DNA polymerase beta initiates DNA synthesis during long-patch repair of reduced AP sites in DNA. EMBO J. 20, 1477–82.

Prasad, R., Beard, W.A., Wilson, S.H., 1994. Studies of gapped DNA substrate binding by mammalian DNA polymerase beta. Dependence on 5'-phosphate group. J. Biol. Chem. 269, 18096–101.

Pryor, J.M., Waters, C.A., Aza, A., Asagoshi, K., Strom, C., Mieczkowski, P.A., Blanco, L., Ramsden, D.A., 2015. Essential role for polymerase specialization in cellular nonhomologous end joining. Proc. Natl. Acad. Sci. 112, E4537–E4545.

Pursell, Z.F., McDonald, J.T., Mathews, C.K., Kunkel, T.A., 2008. Trace amounts of 8-oxo-dGTP in mitochondrial dNTP pools reduce DNA polymerase gamma replication fidelity. Nucleic Acids Res. 36, 2174–81.

Radak, Z., Zhao, Z., Goto, S., Koltai, E., 2011. Age-associated neurodegeneration and oxidative damage to lipids, proteins and DNA. Mol. Aspects Med. 32, 305–315.

Ramsden, D.A., 2011. Polymerases in nonhomologous end joining: building a bridge over broken chromosomes. Antioxid. Redox Signal. 14, 2509–19.

Ramsden, D.A., Asagoshi, K., 2012. DNA polymerases in nonhomologous end joining: are there any benefits to standing out from the crowd? Environ. Mol. Mutagen. 53, 741–51.

Reijns, M.A.M., Rabe, B., Rigby, R.E., Mill, P., Astell, K.R., Lettice, L.A., Boyle, S., Leitch, A., Keighren, M., Kilanowski, F., Devenney, P.S., Sexton, D., Grimes, G., Holt, I.J., Hill, R.E., Taylor, M.S., Lawson, K.A., Dorin, J.R., Jackson, A.P., 2012. Enzymatic Removal of Ribonucleotides from DNA Is Essential for Mammalian Genome Integrity and Development. Cell 149, 1008–1022.

Reyes, A., Kazak, L., Wood, S.R., Yasukawa, T., Jacobs, H.T., Holt, I.J., 2013. Mitochondrial DNA replication proceeds via a "bootlace" mechanism involving the incorporation of processed transcripts. Nucleic Acids Res. 41, 5837–50.

Robertson, A.B., Klungland, A., Rognes, T., Leiros, I., 2009. DNA repair in mammalian cells: Base excision repair: the long and short of it. Cell. Mol. Life Sci. 66, 981–93.

Romain, F., Barbosa, I., Gouge, J., Rougeon, F., Delarue, M., 2009. Conferring a template-dependent polymerase activity to terminal deoxynucleotidyltransferase by mutations in the Loop1 region. Nucleic Acids Res. 37, 4642–56.

Ropp, P. a, Copeland, W.C., 1996. Cloning and characterization of the human mitochondrial DNA polymerase, DNA polymerase gamma. Genomics 36, 449–58.

Roukos, V., Misteli, T., 2014. The biogenesis of chromosome translocations. Nat. Cell Biol. 16, 293–300.

Ruiz, J.F., Juárez, R., García-Díaz, M., Terrados, G., Picher, A.J., González-Barrera, S., Fernández de Henestrosa, A.R., Blanco, L., 2003. Lack of sugar discrimination by human Pol mu requires a single glycine residue. Nucleic Acids Res. 31, 4441–9.

Ruiz, J.F., Lucas, D., García-Palomero, E., Saez, A.I., González, M.A., Piris, M.A., Bernad, A., Blanco, L., 2004. Overexpression of human DNA polymerase mu (Pol mu) in a Burkitt's lymphoma cell line affects the somatic hypermutation rate. Nucleic Acids Res. 32, 5861–73.

Ruiz, J.F., Pardo, B., Sastre-Moreno, G., Aguilera, A., Blanco, L., 2013. Yeast Pol4 Promotes Tel1-Regulated Chromosomal Translocations. PLoS Genet. 9, e1003656.

Russo, M.T., De Luca, G., Degan, P., Bignami, M., 2007. Different DNA repair strategies to combat the threat from 8-oxoguanine. Mutat. Res. Mol. Mech. Mutagen. 614, 69–76.

Sale, J.E., Lehmann, A.R., Woodgate, R., 2012. Y-family DNA polymerases and their role in tolerance of cellular DNA damage. Nat. Rev. Mol. Cell Biol. 13, 141–52.

Sanchez-Berrondo, J., Mesa, P., Ibarra, A., Martínez-Jiménez, M.I., Blanco, L., Méndez, J., Boskovic, J., Montoya, G., 2012. Molecular architecture of a multifunctional MCM complex. Nucleic Acids Res. 40, 1366–80.

Sawaya, M.R., Prasad, R., Wilson, S.H., Kraut, J., Pelletier, H., 1997. Crystal structures of human DNA polymerase beta complexed with gapped and nicked DNA: evidence for an induced fit mechanism. Biochemistry 36, 11205–15.

Schatz, D.G., Ji, Y., 2011. Recombination centres and the orchestration of V(D)J recombination. Nat. Rev. Immunol. 11, 251–63.

Schipler, A., Iliakis, G., 2013. DNA double-strand-break complexity levels and their possible contributions to the probability for error-prone processing and repair

pathway choice. Nucleic Acids Res. 41, 7589–7605.

Shay, J.W., Wright, W.E., 2011. Role of telomeres and telomerase in cancer. Semin. Cancer Biol. 21, 349–353.

Shiloh, Y., 2003. ATM and related protein kinases: safeguarding genome integrity. Nat. Rev. Cancer 3, 155–68.

Singhal, R.K., Wilson, S.H., 1993. Short gap-filling synthesis by DNA polymerase beta is processive. J. Biol. Chem. 268, 15906–11.

Sobol, R.W., Prasad, R., Evenski, A., Baker, A., Yang, X.P., Horton, J.K., Wilson, S.H., 2000. The lyase activity of the DNA repair protein beta-polymerase protects from DNA-damage-induced cytotoxicity. Nature 405, 807–10.

Sparks, J.L., Chon, H., Cerritelli, S.M., Kunkel, T.A., Johansson, E., Crouch, R.J., Burgers, P.M., 2012. RNase H2-Initiated Ribonucleotide Excision Repair. Mol. Cell 47, 980–986.

Steitz, T.A., 1999. DNA polymerases: structural diversity and common mechanisms. J. Biol. Chem. 274, 17395–8.

Sugo, N., Aratani, Y., Nagashima, Y., Kubota, Y., Koyama, H., 2000. Neonatal lethality with abnormal neurogenesis in mice deficient in DNA polymerase beta. EMBO J. 19, 1397–404.

Sung, P., Klein, H., 2006. Mechanism of homologous recombination: mediators and helicases take on regulatory functions. Nat. Rev. Mol. Cell Biol. 7, 739–50.

Swanson, P.C., 2004. The bounty of RAGs: recombination signal complexes and reaction outcomes. Immunol. Rev. 200, 90–114.

Sweasy, J.B., Lang, T., Starcevic, D., Sun, K.-W., Lai, C.-C., Dimaio, D., Dalal, S., 2005. Expression of DNA polymerase β cancer-associated variants in mouse cells results in cellular transformation. Proc. Natl. Acad. Sci. U. S. A. 102, 14350–5.

Tadi, S.K., Sebastian, R., Dahal, S., Babu, R.K., Choudhary, B., Raghavan, S.C., 2016. Microhomology-mediated end joining is the principal mediator of double-strand break repair during mitochondrial DNA lesions. Mol. Biol. Cell 27, 223–35.

Tano, K., Nakamura, J., Asagoshi, K., Arakawa, H., Sonoda, E., Braithwaite, E.K., Prasad, R., Buerstedde, J.-M., Takeda, S., Watanabe, M., Wilson, S.H., 2007. Interplay between DNA polymerases beta and lambda in repair of oxidation DNA damage in chicken DT40 cells. DNA Repair (Amst). 6, 869–75.

Terrados, G., Capp, J.-P., Canitrot, Y., García-Díaz, M., Bebenek, K., Kirchhoff, T., Villanueva, A., Boudsocq, F., Bergoglio, V., Cazaux, C., Kunkel, T.A., Hoffmann, J.-S., Blanco, L., 2009. Characterization of a Natural Mutator Variant of Human DNA Polymerase λ which Promotes Chromosomal Instability by Compromising NHEJ. PLoS One 4, e7290.

Tissier, a, McDonald, J.P., Frank, E.G., Woodgate, R., 2000. poliota, a remarkably error-prone human DNA polymerase. Genes Dev. 14, 1642–50.

Traut, T.W., 1994. Physiological concentrations of purines and pyrimidines. Mol. Cell. Biochem. 140, 1–22.

Tseng, H.-M., Tomkinson, A.E., 2002. A physical and functional interaction between yeast Pol4 and Dnl4-Lif1 links DNA synthesis and ligation in nonhomologous end joining. J. Biol. Chem. 277, 45630–7.

Uchimura, A., Hidaka, Y., Hirabayashi, T., Hirabayashi, M., Yagi, T., 2009. DNA

Polymerase δ Is Required for Early Mammalian Embryogenesis. PLoS One 4, e4184.

Uchiyama, Y., Takeuchi, R., Kodera, H., Sakaguchi, K., 2009. Distribution and roles of X-family DNA polymerases in eukaryotes. Biochimie 91, 165–70.

Valko, M., Izakovic, M., Mazur, M., Rhodes, C.J., Telser, J., 2004. Role of oxygen radicals in DNA damage and cancer incidence. Mol. Cell. Biochem. 266, 37–56.

van Loon, B., Hubscher, U., 2009. An 8-oxo-guanine repair pathway coordinated by MUTYH glycosylase and DNA polymerase. Proc. Natl. Acad. Sci. 106, 18201–18206.

Vermeulen, C., Bertocci, B., Begg, A.C., Vens, C., 2007. Ionizing radiation sensitivity of DNA polymerase lambda-deficient cells. Radiat. Res. 168, 683–8.

Wan, L., Lou, J., Xia, Y., Su, B., Liu, T., Cui, J., Sun, Y., Lou, H., Huang, J., 2013. hPrimpol1/CCDC111 is a human DNA primase-polymerase required for the maintenance of genome integrity. EMBO Rep. 14, 1104–12.

Waters, C.A., Strande, N.T., Wyatt, D.W., Pryor, J.M., Ramsden, D.A., 2014. Nonhomologous end joining: a good solution for bad ends. DNA Repair (Amst). 17, 39–51.

Williams, J.S., Smith, D.J., Marjavaara, L., Lujan, S.A., Chabes, A., Kunkel, T.A., 2013. Topoisomerase 1-Mediated Removal of Ribonucleotides from Nascent Leading-Strand DNA. Mol. Cell 49, 1010–1015.

Wilson, T.E., Lieber, M.R., 1999. Efficient processing of DNA ends during yeast nonhomologous end joining. Evidence for a DNA polymerase beta (Pol4)-dependent pathway. J. Biol. Chem. 274, 23599–609.

Wimmer, U., Ferrari, E., Hunziker, P., Hübscher, U., 2008. Control of DNA polymerase λ stability by phosphorylation and ubiquitination during the cell cycle. EMBO Rep. 9, 1027–1033.

Wintersberger, U., Wintersberger, E., 1970. Studies on deoxyribonucleic acid polymerases from yeast. 2. Partial purification and characterization of mitochondrial DNA polymerase from wild type and respiration-deficient yeast cells. Eur. J. Biochem. 13, 20–7.

Wittschieben, J., Shivji, M.K., Lalani, E., Jacobs, M.A., Marini, F., Gearhart, P.J., Rosewell, I., Stamp, G., Wood, R.D., 2000. Disruption of the developmentally regulated Rev3l gene causes embryonic lethality. Curr. Biol. 10, 1217–20.

Xie, K., Doles, J., Hemann, M.T., Walker, G.C., 2010. Error-prone translesion synthesis mediates acquired chemoresistance. Proc. Natl. Acad. Sci. 107, 20792–20797.

Xing, M., Yang, M., Huo, W., Feng, F., Wei, L., Jiang, W., Ning, S., Yan, Z., Li, W., Wang, Q., et al., 2015. Interactome analysis identifies a new paralogue of XRCC4 in non-homologous end joining DNA repair pathway. Nat. Commun. 6, 6233.

Yagura, T., Kozu, T., Seno, T., 1982. Mouse DNA replicase. DNA polymerase associated with a novel RNA polymerase activity to synthesize initiator RNA of strict size. J. Biol. Chem. 257, 11121–7.

Yang, M.Y., Bowmaker, M., Reyes, A., Vergani, L., Angeli, P., Gringeri, E., Jacobs, H.T., Holt, I.J., 2002. Biased Incorporation of Ribonucleotides on the Mitochondrial L-Strand Accounts for Apparent Strand-Asymmetric DNA Replication. Cell 111, 495–505.

Yonekura, S.-I., Nakamura, N., Doi, T., Sugiyama, H., Yamamoto, K., Yonei, S., Zhang, Q.-M., 2007. Recombinant Schizosaccharomyces pombe Nth1 protein exhibits DNA glycosylase activities for 8-oxo-7,8-dihydroguanine and thymine residues oxidized in the methyl group. J. Radiat. Res. 48, 417–24.

Zafar, M.K., Ketkar, A., Lodeiro, M.F., Cameron, C.E., Eoff, R.L., 2014. Kinetic analysis of human PrimPol DNA polymerase activity reveals a generally error-prone enzyme capable of accurately bypassing 7,8-dihydro-8-oxo-2'-deoxyguanosine. Biochemistry 53, 6584–94.

Zahn, K.E., Averill, A.M., Aller, P., Wood, R.D., Doublié, S., 2015. Human DNA polymerase θ grasps the primer terminus to mediate DNA repair. Nat. Struct. Mol. Biol. 22, 304–311.

Zhang, Y., Wu, X., Guo, D., Rechkoblit, O., Taylor, J.-S., Geacintov, N.E., Wang, Z., 2002. Lesion bypass activities of human DNA polymerase mu. J. Biol. Chem. 277, 44582–7.

Zhang, Y., Wu, X., Yuan, F., Xie, Z., Wang, Z., 2001. Highly frequent frameshift DNA synthesis by human DNA polymerase mu. Mol. Cell. Biol. 21, 7995–8006.

Zhang, Z., Hu, W., Cano, L., Lee, T.D., Chen, D.J., Chen, Y., 2004. Solution Structure of the C-Terminal Domain of Ku80 Suggests Important Sites for Protein-Protein Interactions. Structure 12, 495–502.